JECAM
Joint Experiment for Crop Assessment and Monitoring

GEO GROUP ON EARTH OBSERVATIONS

# GEO Joint Experiment for Crop Assessment and Monitoring (JECAM):

# 2015 Progress Report

April 2015

**This page intentionally left blank**

## Executive Summary

This report shows the progress that GEO JECAM (Joint Experiment for Crop Assessment and Monitoring) test sites have made since JECAM started in 2011, with the focus on 2014. The amount and types of Earth Observation (EO) data received are also reported, along with in situ data, analytical results, and future plans. JECAM is the foundation of the Research & Development (R&D) portion of the GEOGLAM (GEO Global Agricultural Monitoring) initiative, and so the R&D results are important for the development and sharing of 'best practices' in agricultural monitoring.

A historical background of JECAM is provided, showing how the concept evolved, and how the providers of EO data were engaged to support the initiative.

We have instituted an annual report process to obtain information on JECAM research progress, EO data usage and collaboration activities. The progress of several JECAM sites to February 2015 is presented in this document. There are currently thirty-four JECAM test sites, of which a few appear to be dormant, and a few have just started. Twenty-two sites submitted progress reports this year. This participation rate is very encouraging.

Our website (www.jecam.org) was launched in 2012. Content from the annual reports will be used to keep the site 'fresh', accurate and current.

The data acquisition planning with CEOS Space Agencies and commercial providers went fairly well and most JECAM sites are receiving data. The types of EO data used at each JECAM test site (that reported this year) are shown in Table 1. The entries of this table show the number of images for each sensor, where the sites reported them. (Where the use of a sensor was reported without a number of images, an 'x' appears.) The figures in this table give an idea of relative volume of data. However, a word of caution when reading these figures. Clearly, the area of one image in $km^2$ varies widely from sensor to sensor. Also, large numbers should not be interpreted as necessarily more important than small numbers; sometimes a few images can bring immense benefit to a research team.

The JECAM sites are looking at a common range of monitoring needs over a very diverse range of landscape conditions and cropping systems, including:

- Crop identification and acreage estimation
- Yield prediction
- Near Real Time Crop condition
- Land management
- Soil moisture.

Many of the JECAM sites reported having produced numerous papers (peer reviewed and other), presentations and other documents with the research results.

### Table 1 Types of EO Data Used at Each JECAM Test Site

| | Low/ Moderate Optical | | | | | | | | Moderate SAR | | | Fine/ Very Fine Optical | | | | | |
|---|---|---|---|---|---|---|---|---|---|---|---|---|---|---|---|---|---|
| **JECAM Site** | **Terra/Aqua** | **Landsat** | **AWIFS** | **Hyperion** | **HJ-1** | **UK-DMC-ii** | **Deimos** | **Proba-V** | **RADARSAT-2** | **TerraSAR-X** | **Sentinel-1** | **Rapideye** | **SPOT** | **Pléiades** | **Formosat-2** | GF-1&ZY03 | **Chris** |
| Argentina | | | | | | 8 | 4 | x | 20 | 1 | | | | | | | |
| Belgium | | | | | | | | | | 7 | | | | | | | |
| Brazil – São Paulo | | 5 | | | | | 3 | | | | | | | | | | |
| Brazil – Tapajos | | | | | | | | | | | | | | | | | |
| Burkina Faso | | 12 | | | | | 4 | | | | | 7 | | 3 | | | |
| Canada CFIA – Ottawa | | 6 | | | | | | | 9 | | | 9 | | | | | 4 |
| Canada/Red River | | x | | | | | | | x | | | x | | | | | |
| Canada/South Nation | | | | | | | | | | | | 20 | | | | | |
| China/Anhui | | | | | | | | | 7 | | | | | | | | |
| China/ Guangdong (Leizhou) | | | | | | | | | 7 | | | | | | | | |
| China/ Shandong | 46 | | | | 12 | | | 57 | | | | 4 | | | | 8 | |
| France | | 11 | | | | | 10 | | | x | x | | 4 | 3 | 18 | | |
| Italy Apulian Tavoliere | | 2 | | | | | | | | | x | | | | | | |
| Madagascar | | 11 | | | | | 3 | | | | | | 26 | 9 | | | |
| Morocco | 4 | 2 | | | | | | | | | | | | | | | |
| Russia/ Stavropol | x | x | | | | | x | | | | | | | | | | |
| Russia/ Tula | x | x | | 2 | | | | | | | | | | | | | |
| Senegal | | | | | | | | | | | | | | 3 | | | |
| South Africa | x | 3 | | | | | | x | | | | | 54 + | | | | |
| Tunisia | | 29 | | | | | | | | 5 | | | 7 | | | | |
| Ukraine | | 6 | | | | | | 7 | | | | | | | | | |
| U.S.A. | | | 5 | | | | | | | | | | | | | | |

JECAM will continue to be responsive to GEOGLAM "R&D towards monitoring enhancements", and the GEOGLAM needs will define the JECAM community activities. To this end, JECAM intends to support enhanced collaboration between sites. The collaboration will support the

development of standards and practices that inform the GEOGLAM “system of systems” for agricultural monitoring. JECAM sites will also participate in the validation of new sensors as opportunities arise.

An important JECAM Science Meeting was held in Ottawa, Canada in July 2014. A significant event was the presentation of proposed guidelines for minimum data sets (MDS) for all JECAM sites to use for collection of both EO and ground in-situ data. The objective of the JECAM minimum data set requirements is to build a common data set of satellite and in situ observations to support research and methods benchmarking activities across JECAM sites. The JECAM network facilitates data sharing and collaborative research among its partners to develop crop assessment and agricultural monitoring methods for a large variety of agriculture systems. The enhanced coordination will facilitate a high level of bi-lateral and multi-lateral collaboration.

The most active JECAM sites were invited to joint the MDS experiment, and share data and results with other PIs (principal investigators). Multi-user licences are being pursued with a number of EO data suppliers (space agencies and commercial data suppliers), to allow sharing of EO data. NASA is developing a “cloud” prototype to enhance data sharing and provide mechanisms for enforcement of the multi-user licences.

This is a rich set of scientific results, produced by expert teams around the world, in a wide variety of geographic settings and cropping systems, available for sharing and definition of ‘best practices’. It provides clear indication of the impact of CEOS support.

**This page intentionally left blank**

**Table of Contents**

**List of Figures**

**List of Tables**

# 1. Introduction

This report shows the progress that GEO JECAM (Joint Experiment for Crop Assessment and Monitoring) test sites have made since JECAM started in 2011, with the focus on progress made in 2014. The amount and types of Earth Observation (EO) data received are also reported, along with in situ data, analytical results, and future plans. JECAM is the foundation of the Research & Development (R&D) portion of the GEOGLAM (GEO Global Agricultural Monitoring) initiative, and so the R&D results are important for the development and sharing of 'best practices' in agricultural monitoring.

# 2. Background

In November 2009, the first JECAM meeting was held at the SAR for Agricultural Monitoring Workshop, in Kananaskis, Alberta, Canada. In December 2009, at the request of the GEO Agricultural Community of Practice, Canada took on JECAM coordination. In January 2010, a call was issued to the international community to provide standardized documentation of research sites. In September 2010, a JECAM meeting was held in Hong Kong to focus on Asian sites and data sharing issues. In-situ data sharing protocols were developed. In October 2010, a meeting took place in Brussels, concentrating Europe and Africa. In May 2011, a meeting in Brazil focused on South America.

In order for JECAM to succeed, collaboration with CEOS (Committee on Earth Observation Satellites) is needed to ensure access to and sharing of EO data of the test sites around the world. Without coordinated acquisition of EO data of the test sites, JECAM will be unable to develop the agricultural monitoring system of systems. The world's space agencies have collaborated for the benefit of the international community before; examples of coordinated acquisition of data to support scientific efforts include (but are not limited to) the International Polar Year (2007 – 2009) and the GEO Forest Carbon Tracking task.

An international meeting of the JECAM secretariat was held with the space agencies and commercial data providers in Ottawa, Canada in June 2011 to discuss this question. Several data providers once again agreed to marshal their resources to provide coordinated EO data for this task which can be instrumental in addressing food security.

The benefits for CEOS and the space agencies are visible demonstrations of support to the international community on a matter of such high priority as food security. These demonstrations have the potential to translate into public support for CEOS programs. In the examples of the International Polar Year and the GEO Forest Carbon Tracking task, these benefits have been realized. Further benefits include validation of the usefulness of the data from each EO sensor for agricultural monitoring, and dissemination of the research results.

The overarching purpose of JECAM is to compare data and methods for crop area, condition monitoring and yield estimation, with the aim of establishing 'best practices' for different agricultural systems. The goal of the JECAM experiments is to facilitate the inter-comparison of monitoring and modeling methods, product accuracy assessments, data fusion, and product integration for agricultural monitoring. These international shared experiments are being undertaken at a series of sites which represent the world's main cropping systems and agricultural practices. The approach is to collect and share i) time-series datasets from a variety of Earth observing satellites useful for agricultural monitoring and ii) in-situ crop and meteorological measurements for each site.

Synthesis of the results from JECAM will enable the following outcomes:

(i) Development of international standards for agricultural monitoring and reporting protocols;

(ii) A convergence of the approaches to define best monitoring practices for different agricultural systems;

(iii) Identification of requirements for future EO systems for agricultural monitoring.

The JECAM sites are looking at a common range of monitoring needs over a very diverse range of landscape conditions and cropping systems, including:

- Crop identification and acreage estimation
- Yield prediction
- Near Real Time Crop condition / Crop stress
- Land management
- Soil moisture.

The Guide to Interacting with Space Agencies and Commercial Data Providers has been provided to each JECAM test site, so that they could access EO data by contacting the space agencies and commercial data providers directly, rather than via the JECAM Secretariat.

We have instituted an annual report process to obtain information on JECAM research progress, EO data usage and collaboration activities. The JECAM web site, www.jecam.org, was launched in 2012. Content from the annual reports will be used to keep the site 'fresh', accurate and current.

An important JECAM Science Meeting was held in Ottawa, Canada in July 2014. A significant event was the presentation of proposed guidelines for minimum data sets (MDS) for all JECAM sites to use for collection of both EO and ground in-situ data. The objective of the JECAM minimum data set requirements is to build a common data set of satellite and in situ

observations to support research and methods benchmarking activities across JECAM sites. The JECAM network facilitates data sharing and collaborative research among its partners to develop crop assessment and agricultural monitoring methods for a large variety of agriculture systems. The enhanced coordination will facilitate a high level of bi-lateral and multi-lateral collaboration.

The most active JECAM sites were invited to joint the MDS experiment, and share data and results with other PIs (principal investigators). Multi-user licences are being pursued with a number of EO data suppliers (space agencies and commercial data suppliers), to allow sharing of EO data.

There are currently thirty-four JECAM sites in the following countries:

- Argentina
- Australia
- Belgium
- Brazil (2)
- Burkina Faso
- Canada (3)
- China (6)
- France
- Italy Apulian Tavoliere
- Madagascar
- Mali
- Mexico
- Morocco
- Paraguay
- Russia (2)
- Saudi Arabia
- Senegal
- South Africa
- Taiwan
- Tanzania
- Tunisia
- Ukraine
- Uruguay
- USA (2).

JECAM collaborates with the Asia-RiCE (Asian Rice Crop Estimation & Monitoring) activity led by Japan, with a number of Asian countries participating. Asia-RiCE is directed by an ad hoc team of stakeholders with an interest in the development of Asia-RiCE as a component of the GEOGLAM initiative. It is a regional cooperative framework for monitoring of the rice crop, which is the staple food for more than half of humanity, with 90% of the world crop grown and consumed in Asia. The objectives of Asia-RiCE are:

- To ensure that Asian countries receive the full potential benefits of GEOGLAM, and that they are suitably engaged and prepared to do so;
- To ensure that rice crop monitoring issues are given suitable priority and attention within the scope of the full GEOGLAM initiative, including in the development of the observing requirements; and
- To establish a framework for the coordination necessary to engage, manage and support the various stakeholders.

The NASA CEOS Systems Engineering Office (SEO) will provide a secure portal with Amazon cloud-based hosting services for this JECAM initiative and Asia-RiCE team activity. This portal will receive shared EO data (among them, RADARSAT-2). Approved users will have controlled (via login and password) access to datasets, analysis applications and processing tools. The portal traffic will be monitored by NASA with reports to be made available to licence sponsors on demand.

The following sections provide a progress report for the JECAM test sites up to February 2015.

We wish to thank the JECAM site teams for their impressive contributions to this work.

## 3. Argentina

Team Leader and Members: Diego de Abelleyra, Santiago Verón, Carlos di Bella

Project Objectives

The original objectives for the site have changed.

- Crop identification and Crop Area Estimation. We are testing several classification methods using optical images, RADAR images, and combinations. Field observations of land use and crop type are carried out several times during a year to calibrate and validate our classification results. During the 2014-2015 campaign, we began collecting additional field data from a minimum dataset area of 20x20 Km. Furthermore, an inter-comparison of methodologies with other JECAM/SIGMA sites (China, Russia, Ukraine, Brazil) is being performed.
- Crop Rotations. From the crop type maps produced yearly since 2010, we are characterizing crop rotation at field level. In addition, we are analyzing the spatial patterns of different rotations and trying to identify the environmental and socio-economic drivers. In parallel, we plan to assess the environmental impacts of this management practice.
- Yield Prediction and Forecasting. We incorporated information from yield monitors to improve the spatial description of the within field yield variability. Our proposed methodology is mainly based on MODIS BRDF corrected daily at 250 m red and NIR reflectance. During 2014, we requested the acquisition and processing of Proba-V 100 m data to test if the addition of these images to our yield prediction methodology could improve results.

Site Description

- Location: San Antonio de Areco, Buenos Aires, Argentina

| | |
|---|---|
| **Centroid** | Latitude: 34° 7'18.69"S<br>Longitude: 59°35'53.05"O |
| **Top left** | Latitude: 33°41'55.45"S<br>Longitude: 60°11'51.70"W |
| **Bottom right** | Latitude: 34°34'11.67"S<br>Longitude: 59° 2'55.13"W |

- Topography: gentle slopes less than 3%
- Soils: Mostly Mollisols. Silt loam / Silty clay loam textured.
- Drainage class/irrigation: Well drained soils / Mostly rain fed fields
- Crop calendar

Main grain crops are soybean, maize and wheat. Early wheat is planted in June/July while late wheat is planted at the end of July and August. Wheat heading occurs in mid October and its harvest takes place at the beginning of December. After a wheat crop, a late soybean crop is commonly planted in December, and is harvested in April. Also, a late maize crop can be planted after a winter crop. Soybean and maize are mostly planted as one season crop. In these cases, soybean is planted in November and harvested in March/April and maize is planted in October and harvested in March.

- Field size: Typical field size is 20 ha but there is high variability in plot size.
- Climate and weather: The climatic type is humid temperate. The mean annual precipitation amounts to about 1000 mm falling mainly in summer (mean monthly precipitation: 100-120 mm) and to a lesser extent in winter months (mean monthly precipitation: 40-50 mm). The mean annual temperature is 17C ranging from 24C in January and 10C in July.
- Agricultural methods used: Since the diffusion of no-tillage systems and genetically modified crops in the 1990's, and the more recent increases in international prices of soybeans, there has been an intensification of agriculture. This intensification was characterized by the replacement of mixed cattle and crop systems by continuous cropping. According to the archives of the Ministerio de Agricultura Ganaderia y Pesca from Argentina (SIIA), soy, maize and wheat are the most important crops. Over the last 3 years, late maize has been increasingly sown.

<u>EO Data Received during 2014</u>

RADARSAT-2

- Supplier: CSA
- SAR
- Number of scenes: 20
- Range of dates: October 2010 – February 2012
- Beam modes/ incidence angles/ spatial resolutions: Fine Quad Pol mode. FQ17 – FQ21
- Processing level: Single Look Complex

TerraSAR-X:

- Space agency or Supplier: German Space Agency (DLR)
- SAR
- Number of scenes: 1
- Range of dates: Feb 2014
- Beam modes/ incidence angles/ spatial resolutions:
    - ScanSAR. Polarization VV. Incidence angle: 27.3/36.5. Resolution 20 m.
- Processing level: Single Look Complex
- Challenges, if any, in ordering and acquiring the data

With this last image, we finished our quota of 30 images in total. The acquisition planning tool for Terrasar-X (EOWEB next generation) is excellent. It is easy to know the area and the date of each future scene. All images requested were acquired with success. The processing for Scansar SLC mode is quite tedious using open source software (e.g. NEST). Manual geo-referencing had to be performed.

DMCii:

- Space agency or Supplier: DMC International Imaging Ltd
- Optical
- Number of scenes: 8
- Range of dates: April 2014 – Dec 2014

Images were very useful to supplement other optical images that were not available because of cloudiness. If we have the possibility to obtain orthorectified images, it will improve significantly the time required for image processing that in general requires manual geo-referencing.

Deimos:

- Space agency or Supplier: DMC International Imaging Ltd
- Optical
- Number of scenes: 4
- Range of dates: Feb 2014 – Jun 2014

Images were very useful to supplement other optical images that were not available because of cloudiness.

Proba-V

- Space agency or Supplier: VITO
- Optical
- Beam modes/ incidence angles/ spatial resolutions:
  100 m product
- Number of scenes: all available from March 2014.

**Figure 1 Soybean Field - Argentina**

In situ Data

Regional surveys were performed during key crop developing stages by visual identification:

- Land use: Agriculture / Livestock
- Crop type: Wheat, early and late soybean, early and late maize.
- Tillage system.

For the 2014-2015 agricultural campaign, a new area of 25x25 Km is being intensively surveyed according to the new JECAM minimum dataset protocol.

Measurements at maturity of soybean crops were performed (dry biomass and yield) to validate our methodology for yield estimation. Crop monitor data is also being used to obtain more information on the spatial distribution of yield within each field.

**Figure 2 Dry Weight of Soybeans**

Collaboration

We started an inter-comparison study among other JECAM sites: Ukraine, Russia, China and Brazil. The objective of the study is to test methodologies developed at each site in other regions using the field data collected at each site. Classes to be tested are cropland and no cropland. A common area size of 60x60 Km was defined. Each site carries on the application of its methodology with the other sites considered.

We are participating in the Kyoto & Carbon Initiative (KC-4) project "Asia-RiCE: Rice Crop Estimation and Monitoring," in collaboration with the Asia-Rice sites.

We joined the Multi-User Request Form (MURF) to access RADARSAT-2 data together with a group of JECAM and Asia-Rice sites.

Results

*Crop Type Maps*

Our main results in this activity are:

1) the development of a classification methodology implemented in R language and

2) the generation of the study area crop rotation map for the 2010-2014 period.

The methodology accounts for the bias that can be introduced by the specific ground truth data assigned to calibration or validation stages. Additionally it provides a proxy for the spatial variability of the classification accuracy by assigning each pixel to a class based on majority (or weighted) voting from 5 classifiers (maximum likelihood, logistic regressions, neural networks, support vector machines and random forests). Each of the classifiers is run 5 times with different cal-val datasets. Using this methodology, we achieved general accuracies higher than 90% for each of the 4 classifications. Lastly, together with a decision tree, we characterized rotations by, for example, the number of soy crops (or consecutive soy crops) in the 4-year period in each pixel. We plan to finish this task in the near future. These results partially fulfill two of SIGMA's objectives: the characterization of agricultural systems and the assessment of the environmental impacts of crop rotations in the Pampas.

*Multitemporal Analysis of X and C band SAR over Soybean fields*

Here we found a moderate ability of TerraSAR-X to estimate the amount of biomass of soybean crops and soil moisture compared to RADARSAT-2 ability. For the former, the coefficient of determination between sigma HH or HV and soil moisture or the vegetation water content as

well as dry or wet soybean biomass did not exceed 0.53. In contrast, for RADARSAT-2, sigma HH, VV, and HV the coefficients of determinations for the same dependent variables ranged between 0.62 and 0.84, except for soil moisture which were considerably lower (~0.21). The sign and shape of the relationships were always positive and non-linear with different saturation thresholds as can be seen in Figure 3.

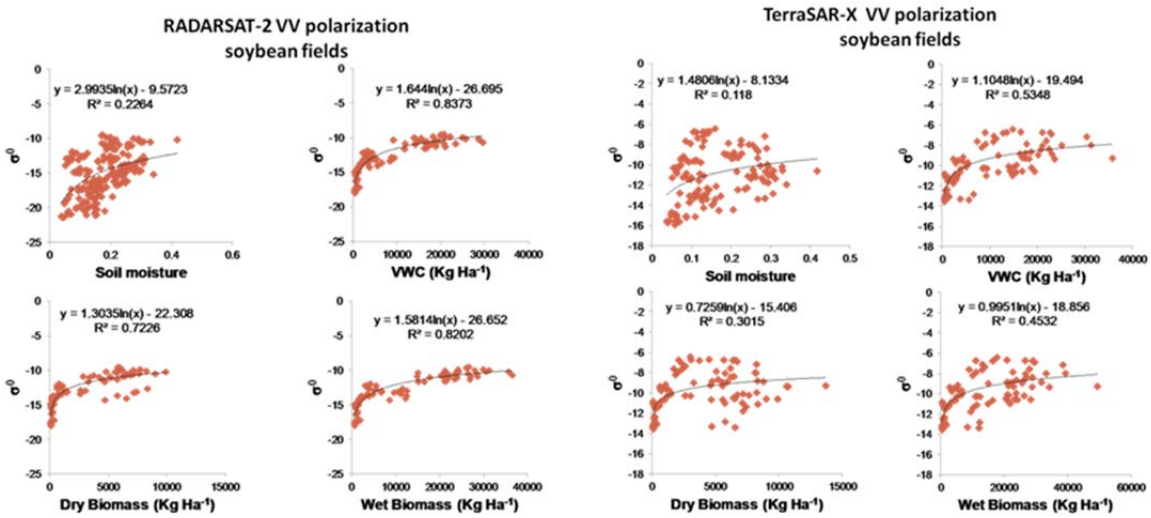


**Figure 3 Comparison of Results between RADARSAT-2 and TerraSAR-X**

*Comparison of "Simultaneous" Acquisitions of X and C band SAR over Maize and Bare Soil Fields*

From field measurements of maize height, wet and dry biomass and soil moisture performed simultaneously with a RADARSAT-2 and TerraSAR-X acquisitions, we found the following results (see Table 2). In this table, the independent variables are described in the column called 'Radar index'; vegetation variables are in the left side of the table, and soil variables are in the right side of the table. RADARSAT-2 showed high correlation to soybean vegetation water content but saturation was observed near 10Tn $Ha^{-1}$. Information derived from both platforms was quite sensitive to soil moisture, especially over bare soils. We concluded that while vegetation water content (VWC) is the main structural variable that we could accurately estimate from SAR, further research should be conducted to improve the estimation of maize dry weight, which is the most useful variable for yield estimation. Shannon entropy seems to be a good starting point to address these needs.

**Table 2 Coefficients of Determination of Relationships between Independent Variables, Vegetation and Soil Variables**

| Satellite | Radar index | Crop Height | Dry Weight | VWC |
|---|---|---|---|---|
| TerraSAR-X | $\sigma^0$ HH | 0.14 | 0.12 | 0.13 |
| | $\sigma^0$ VV | 0.16 | 0.12 | 0.19 |
| | Alpha | 0.00 | 0.00 | 0.00 |
| | Anisotropy | 0.01 | 0.00 | 0.00 |
| | Cloude Entropy | 0.01 | 0.00 | 0.00 |
| | Shannon Entropy | 0.18 | 0.16 | 0.23 |
| | number of observations | 39 | 40 | 40 |
| RADARSAT-2 | $\sigma^0$ HH | 0.05 | 0.03 | 0.05 |
| | $\sigma^0$ VH | 0.05 | 0.06 | 0.05 |
| | $\sigma^0$ VV | 0.18 | 0.16 | 0.25 |
| | Alpha | 0.01 | 0.01 | 0.00 |
| | Anisotropy | 0.00 | 0.00 | 0.00 |
| | Cloude Entropy | 0.12 | 0.11 | 0.13 |
| | Shannon Entropy | 0.16 | 0.15 | 0.23 |
| | Freeman-Durden Surface | 0.02 | 0.03 | 0.01 |
| | Freeman-Durden Volumetric | 0.15 | 0.15 | 0.16 |
| | Freeman-Durden Double Bounce | 0.02 | 0.01 | 0.01 |
| | Number of observations | 39 | 40 | 40 |

| Satellite | Radar index | Bare soil | Maize |
|---|---|---|---|
| TerraSAR-X | $\sigma^0$ HH | 0.35 | 0.34 |
| | $\sigma^0$ VV | 0.42 | 0.21 |
| | Alpha | 0.03 | 0.00 |
| | Anisotropy | 0.00 | 0.00 |
| | Cloude Entropy | 0.00 | 0.00 |
| | Shannon Entropy | 0.62 | 0.48 |
| | number of observations | 34 | 40 |
| RADARSAT-2 | $\sigma^0$ HH | 0.55 | 0.12 |
| | $\sigma^0$ VH | 0.38 | 0.06 |
| | $\sigma^0$ VV | 0.55 | 0.28 |
| | Alpha | 0.08 | 0.00 |
| | Anisotropy | 0.00 | 0.00 |
| | Cloude Entropy | 0.10 | 0.05 |
| | Shannon Entropy | 0.80 | 0.50 |
| | Freeman Durden Surface | 0.70 | 0.04 |
| | Freeman Durden Volumetric | 0.54 | 0.29 |
| | Freeman Durden Double Bounce | 0.31 | 0.01 |
| | Number of observations | 34 | 40 |

## Plans for Next Growing Season

For this year, we plan to continue performing field surveys of land use to generate cropland and crop type maps. This will allow the improvement and the update of crop rotations maps. We also plan to test our methodology for crop classification in other regions and years. In order to accomplish this activity, we expect to get access to ground truth data collected by other research groups in other locations and/or growing seasons. If accessed, these data will allow the testing whether the classifiers used in one site/growing season can be apply at another location and/or year, thus removing (or downplaying) the importance of one of the most important constraints to scale from local to regional land use classifications: the need for ground truth data. Finally and related to yield estimation, we plan to continue with the analysis of yield monitors data to validate and improve our approach.

Next year, we will change the EO data that we order. We still require high resolution optical images (20-30 m) at key points in the growing season for crop type discrimination. The

acquisition of images from several platforms (LANDSAT, DMCii, DEIMOS) is necessary to increase the probability of having cloud free images at these key stages.

SAR images are requested in SCANSAR mode to test its ability for crop type discrimination (particularly for summer crops maize and soybean).

Publications since last year's report

Peer reviewed papers:

De Abelleyra D, Verón S. 2014. Comparison of different BRDF correction methods to generate daily normalized MODIS 250m time series. *Remote Sensing of Environment*, 140: 46-59.

Verón SR, de Abelleyra D. 2014. Comparison of X and C band satellite RADAR images to characterize irrigated agricultural fields. Proceedings of the International Geoscience and Remote Sensing Symposium IGARSS 2014. Quebec, Canada. pp: 2106-2109.

Presentations:

De Abelleyra D, Verón S. 2014. JECAM Argentina "San Antonio de Areco". JECAM Science Meeting. Agriculture and Agrifood Canadá, Ottawa, Canadá. 21-23 July, 2014.

De Abelleyra D, Verón S. 2014. The use of SAR images for agricultural applications in Argentina. JECAM Science Meeting. Agriculture and Agrifood Canadá, Ottawa, Canadá. 21-23 July, 2014.

## 4. Australia

No report received.

# 5. Belgium

Team Leader and Members: Pierre Defourny, Aline Léonard and François Waldner.

Project Objectives

The original objectives for the site have not changed.

- Crop identification and Crop Area Estimation Cropped Land: developing a method to support crop area estimation on a field with resolution (minimum mapping unit) Nuts 3; Mapping Frequency: 2 maps / year; 1 for winter wheat mapping, 1 maize mapping.
- Crop Condition/Stress: improve estimation of biophysical variables retrieval for crop growth monitoring; methodology development for winter wheat Leaf Area Index (LAI) estimation from optical and SAR data in an operational perspective.

Site Description

- Location: Belgium, Centroid: Latitude 49.75° N, Longitude 3.75° E
- Topography: Elevation varies between 20 and 200 meters, the topography is generally flat or slightly undulating.
- Soils: soil texture is loam.
- Drainage class/irrigation: soil drainage is moderately well-drained and irrigation infrastructure is not frequent.
- Crop calendar: Crop types are wheat, barley, potatoes, sugar beets, maize, alfalfa, etc. The crop calendar is: Wheat / barley: March-August; Maize: April - September.
- Field size : from 3 to 15 ha.
- Climate and weather: Climate at the site is moderately humid, with annual rainfall of about 780 mm which is relatively well distributed over the year.

EO Data Received/Used

Mission/sensor: TerraSAR-X

- Space agency or Supplier: German Aerospace Center (DLR)
- SAR
- Number of scenes: 7
- Range of dates: from April 2014 to August 2014
- Beam modes/ incidence angles/ spatial resolutions: Stripmap
- Processing level: MGD products
- Challenges, if any, in ordering and acquiring the data: due to conflicts, it was difficult to have images acquired every 2 weeks at high incidence angle
- Challenges, if any, in processing and using the data: no.

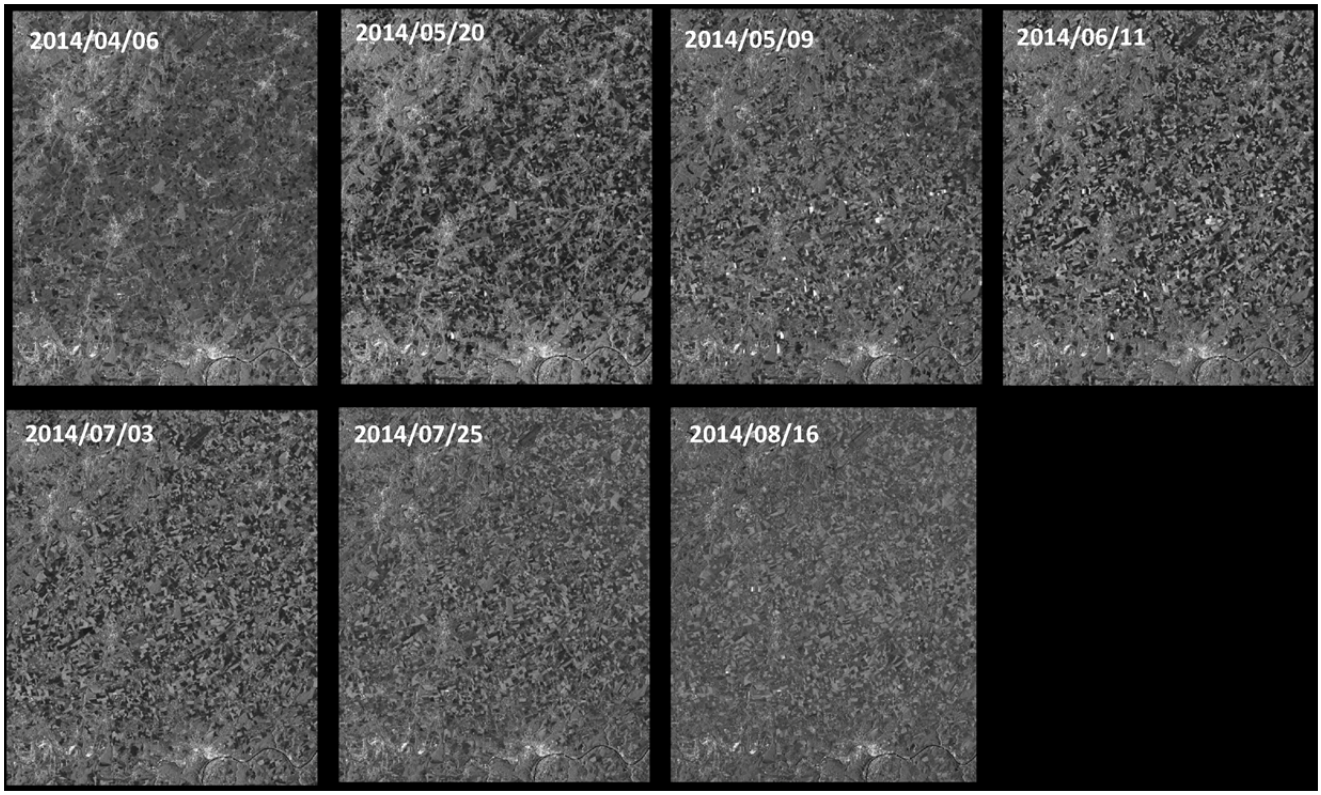


**Figure 4 TerraSAR-X over Belgium site from April to August 2014**

In situ Data

A field campaign was carried out during the 2014 growth season in a sample of 15 winter wheat fields located in the Loamy Region in Belgium. The aim of the campaign was to collect a data set for the validation of retrieval of biophysical variables. Each field was visited between 4 and 8 times and, each time, plant height, phenological stage and the Leaf Area Index (LAI) were measured. LAI is defined as the one-sided green leaf area per unit of ground surface area ($m^2/m^2$) (Chen and Black, 1992). A non-destructive method for the measurement of the LAI is based on hemispherical pictures processed in the image analysis software CAN-EYE (www4.paca.inra.fr/can-eye). A NIKON PowerShot A590 IS camera equipped with a super wide fish-eye 0.25x with macro is used to take pictures from above the canopy, facing towards the soil (Figure 5).

Figure 5 Hemispherical Picture Taken in a Wheat Field

Depending on the date, between 8 and 12 photographs were taken in an area of 400 m² within the field. An example of a series of 4 hemispherical pictures taken at 4 different dates is shown in Figure 6.

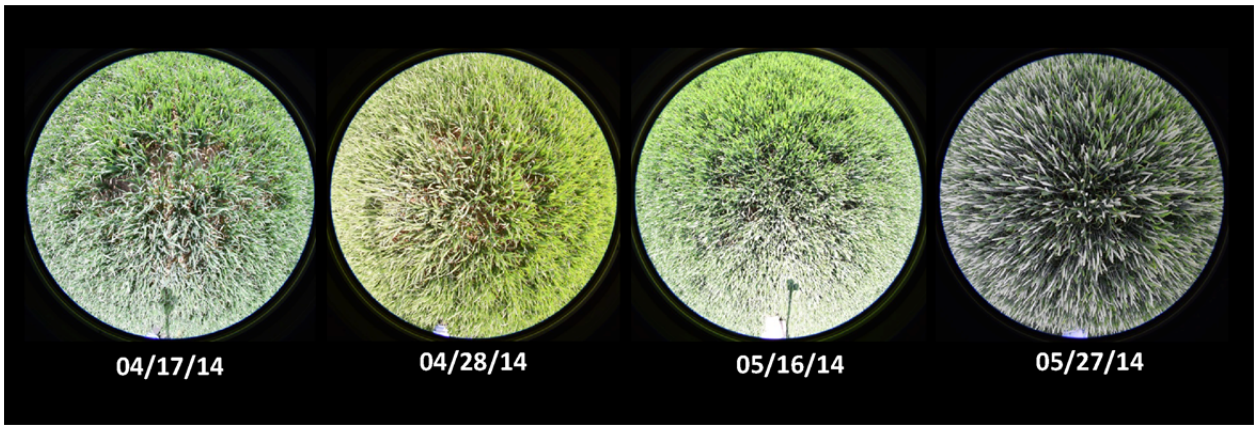


Figure 6 Time Series of In situ Fisheye Pictures taken in a Winter Wheat Field (Field 7)

In the CAN-EYE software, all pixels of each image are classified as vegetation or soil (according to their respective colour). From the result, the model computes the gap fraction in concentric circle around the centre of the image, giving the proportion of green vegetation for different inclination angles which allows to implement the leaf area index (LAI) (Weiss and Baret, 2010). In the case of crops such as winter wheat, all main aerial plant organs (leaves, stems...) are green, it is therefore more appropriate to use the term of GAI, instead of LAI, to refer to the biophysical parameter retrieved from the CAN-EYE process (Duveiller et al., 2011). Cover fraction (fCOVER), which is defined as the fraction of the soil covered by the vegetation viewed in the nadir direction, can be also derived from these pictures. Due to the characteristics of hemispherical images, it is not possible to get a value in the exact nadir direction, therefore the

cover fraction must be integrated over a range of zenith angles which is also done in the CAN-EYE software.

Collaboration

In the framework of the FP-7 and ESA funded projects, several collaborations have been established. The main research topics are crop mapping and retrieval of bio-physical variables.

A major goal of SIGMA (Stimulating Innovation for Global Monitoring of Agriculture and its Impact on the Environment in support of GEOGLAM) is to support GEOGLAM partly by coordinating JECAM activities. The consortium includes several JECAM site partners, including Stravopol (Russia), Kyev (Ukraine), Shandong (China), San Antonio (Argentina) and Sao Paolo (Brazil). A standardized field data collection protocol for crop type classification will be provided to the sites. In addition, efforts will be made to gather and pre-process a minimum standardized data set for each site. Research activities will focus on multi-sensor cropland and crop type mapping while encouraging cross-site experiments.

The ESA project Sen2Agri (Sentinel-2 Agriculture) will develop products relevant for agriculture monitoring as preparation for the future exploitation of the satellite Sentinel-2. The goal is to promote to key agriculture monitoring stakeholders and facilitate ownership of the proposed solution based on Sentinel-2 and the open source tool box, through a specific relationship with the JECAM network. The representative user group includes the EU MARS project and the GEOGLAM partners.

Results

We do not yet have results for 2014. TerraSAR-X images and field data are still being processed.

# 6. Brazil

## 6.1 São Paulo

Team Leader and Members: Guerric le Maire, CIRAD; Yann Nouvellon, CIRAD; Jean-Paul Laclau, CIRAD; José-Luiz Stape, IPEF and UNESP; Stéphane Dupuy, CIRAD.

Project Objectives

The project objectives for the site are:

- Crop identification and Crop Area Estimation.

Site Description

- Location: Latitude -22.9677, Longitude -48.7274.
- Topography: slope <5% in centroid area.
- Soils: Ferralsols, 20% Clay (in centroid area).
- Drainage class/irrigation: Moderately to well drained, high water consumption for Eucalyptus stands, cropland sometimes irrigated.
- Crop calendar: Eucalyptus: 6 year rotations; Other crops and sugarcane: monitoring started in December 2014, but mainly sugarcane monoculture and orange tree orchards.
- Field size: 40 ha for Eucalyptus field, large fields for other crop classes.
- Climate and weather: Humid Tropical (Aw Koppen), weather stations.

**Figure 7 Sugarcane**

**Figure 8 Soybean Fields**

Figure 9 Young Eucalyptus

Figure 10 Orange Tree Orchards

EO Data Received/Used

Mission/sensor: Landsat-5

- Space agency or Supplier: NASA
- Optical
- Number of scenes: 5
- Range of dates: 08/09/2013; 11/11/2013; 30/01/2014;11/09/2014;29/10/2014
- Beam modes/ incidence angles/ spatial resolutions: , 30 m MS + 15 m PAN
- Processing level: TOA reflectance
- Challenges, if any, in ordering and acquiring the data
- Challenges, if any, in processing and using the data

Mission/sensor: DEIMOS

- Space agency or Supplier: Deimos Imaging
- Optical
- Number of scenes: 3
- Range of dates: 13/11/2013;05/04/2014;19/07/2014;
- Beam modes/ incidence angles/ spatial resolutions: 20 m
- Processing level: TOA reflectance
- Challenges, if any, in ordering and acquiring the data
- Challenges, if any, in processing and using the data

**Figure 11 DEIMOS and Landsat Images of São Paulo Site**

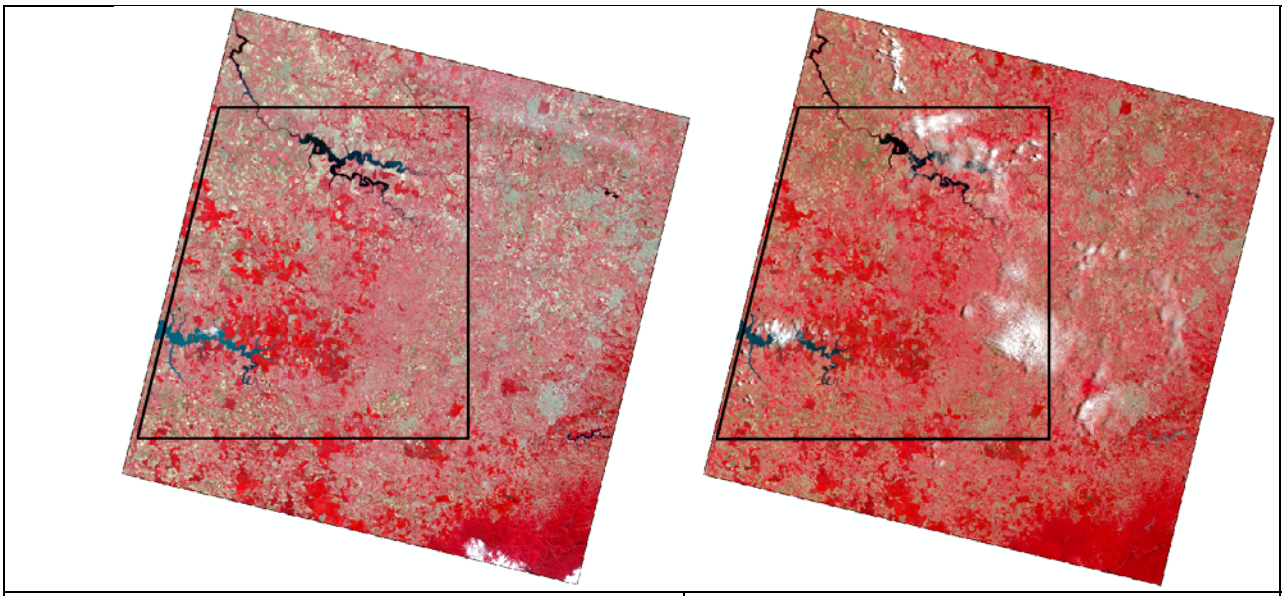

| 2013 09 08 Landsat | 2013 11 11 Landsat |
|---|---|

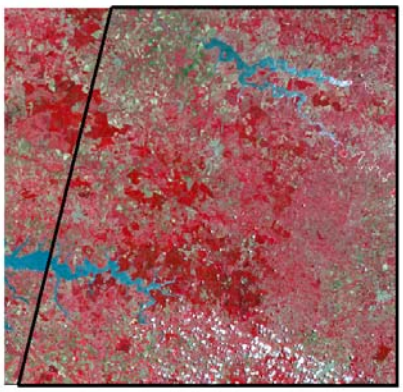

2013 11 13 Deimos

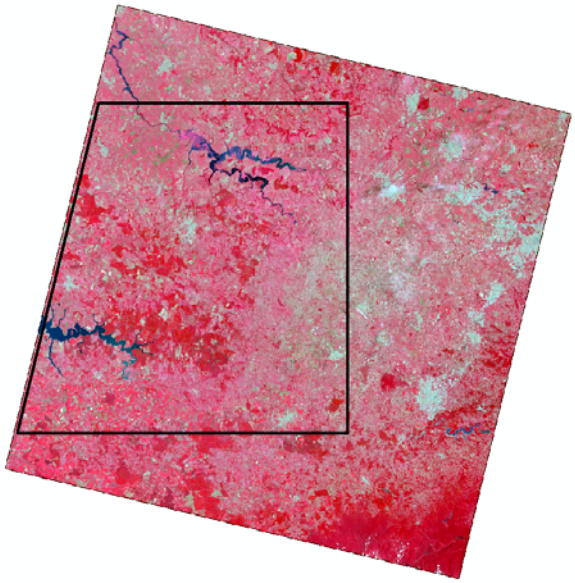

2014 01 30 Landsat

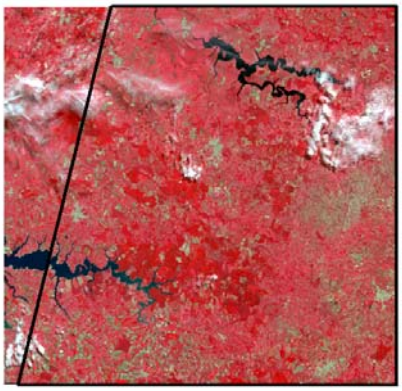

2014 04 05 Deimos

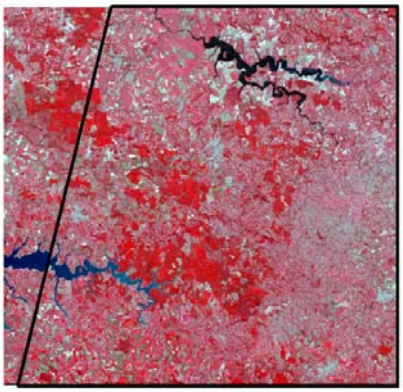

2014 07 19 Deimos

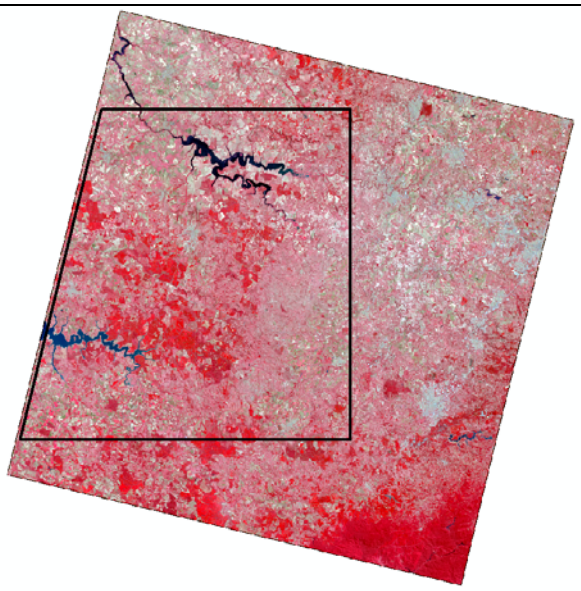

2014 09 11 Landsat

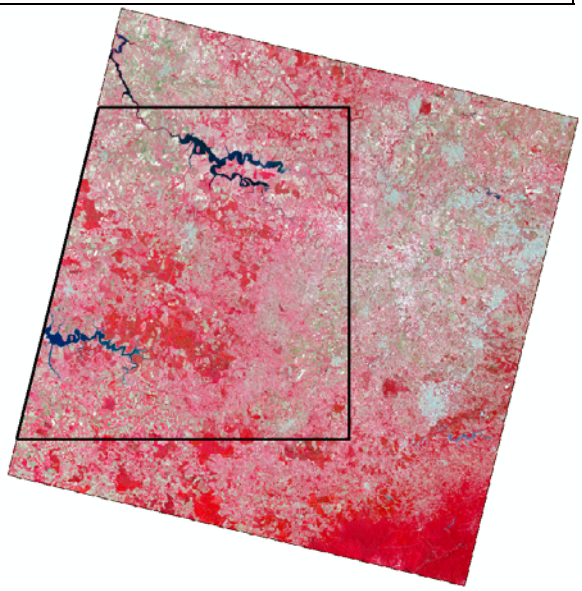

2014 10 29 Landsat

In situ Data

We collected 847 GPS point in the field in December 2014, following the JECAM protocol and updated nomenclature for our site specificities. GPS points were chosen along roads to cover most parts of the JECAM area (see Figure 12). GPS points were afterwards converted to polygons based on the images. The minimum homogeneous polygon of the 8 images described above was chosen.

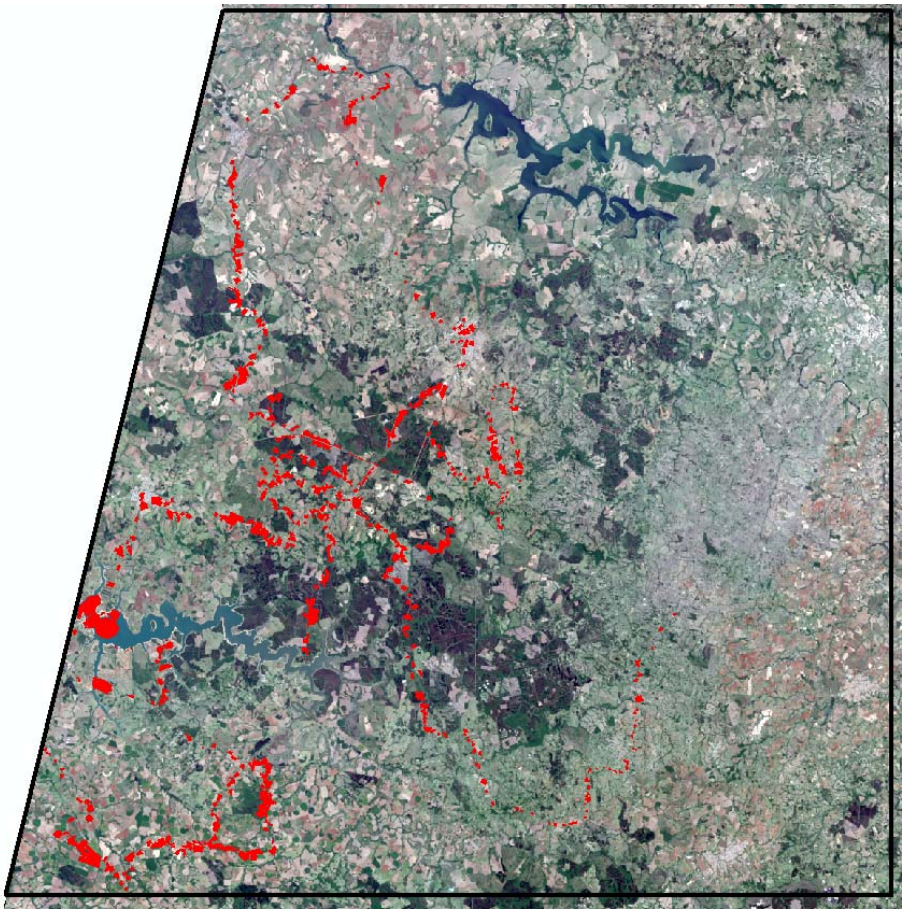

**Figure 12 Illustration of the 847 Polygons of the Classified Area**

The number of polygons for each class is given in Table 3.

**Table 3 Number of Polygons for each Class**

| Class | # polygons |
|---|---|
| Banana plantation | 3 |
| Built-up | 53 |
| Coffee plantation | 14 |
| Corn | 30 |
| Eucalypts plantation | 160 |
| Fallow | 7 |
| Forest | 36 |
| Orange tree plantation | 63 |
| Other | 30 |
| Pasture | 127 |
| Pines plantation | 47 |
| Rocks | 11 |
| Soybean | 91 |
| Sugarcane | 154 |
| Water | 21 |

Collaboration

Our work is part of the SIGMA - JECAM experiment on medium to large field size agrosystems.

The main objective of this project is to test and compare classification methods for cropland area estimations based on MODIS data, and applied in different contrasted sites. These sites were selected within JECAM for their large field size agrosystems. The nature of the collaboration for the Brazil-SP site relies on data preparation and share, field expertise, review of the results obtained in this experiment, complementary measurements if necessary, etc.

Results

We used the 8 images shown above to produce a land cover map of our JECAM site for December 2014. A brief description of the method we used follows. First, a polygon segmentation of the images was performed under Trimble eCognition software. Then, 240 variables were computed for each polygon: we used all the band reflectances of all images, and computed several vegetation indices. The Random Forest algorithm was then used under R. The model was calibrated on the field data, and afterward applied on the entire image, giving the final landcover map. Some interesting outputs were also computed, such as the classification stability, based on the membership probability. A confusion matrix is shown in Table 4. The result is very good for sugarcane, eucalyptus, pines, forests, pastures and water bodies. The classification error is high for coffee plantations, maize and orange tree orchards.

## Table 4 Confusion Matrix

| | Banana | Build-up surface | Coffee | Eucalyptus | Maize | Natural forest | Orange tree | Other | Pasture | Pinnus | Soya beans | Sugar cane | Water bodies | Young fallow | class error |
|---|---|---|---|---|---|---|---|---|---|---|---|---|---|---|---|
| Banana | **0** | 0 | 1 | 1 | 0 | 0 | 1 | 0 | 0 | 0 | 0 | 0 | 0 | 0 | 100% |
| Build-up surface | 0 | **12** | 0 | 0 | 0 | 0 | 0 | 0 | 0 | 0 | 0 | 1 | 0 | 0 | 8% |
| Coffee | 0 | 0 | **6** | 1 | 0 | 0 | 4 | 0 | 3 | 0 | 0 | 0 | 0 | 0 | 57% |
| Eucalyptus | 0 | 0 | 1 | **137** | 0 | 1 | 0 | 0 | 2 | 0 | 0 | 1 | 0 | 0 | 4% |
| Maize | 0 | 0 | 0 | 1 | **4** | 0 | 0 | 0 | 4 | 0 | 17 | 5 | 0 | 0 | 87% |
| Natural forest | 0 | 0 | 0 | 3 | 0 | **33** | 0 | 0 | 0 | 0 | 0 | 0 | 0 | 0 | 8% |
| Orange tree | 0 | 0 | 1 | 1 | 0 | 1 | **16** | 0 | 8 | 0 | 1 | 0 | 0 | 0 | 43% |
| Other | 0 | 0 | 0 | 0 | 0 | 0 | 0 | **0** | 1 | 0 | 10 | 11 | 0 | 0 | 100% |
| Pasture | 0 | 0 | 0 | 1 | 0 | 0 | 0 | 0 | **110** | 0 | 5 | 9 | 0 | 0 | 12% |
| Pinnus | 0 | 0 | 0 | 0 | 0 | 0 | 0 | 0 | 0 | **6** | 0 | 0 | 0 | 0 | 0% |
| Soya beans | 0 | 0 | 0 | 1 | 3 | 0 | 0 | 1 | 3 | 0 | **73** | 11 | 0 | 0 | 21% |
| Sugar cane | 0 | 0 | 0 | 0 | 0 | 0 | 0 | 0 | 3 | 0 | 2 | **149** | 0 | 0 | 3% |
| Water bodies | 0 | 0 | 0 | 0 | 0 | 0 | 0 | 0 | 0 | 0 | 0 | 0 | **9** | 0 | 0% |
| Young fallow | 0 | 0 | 0 | 0 | 0 | 0 | 0 | 0 | 1 | 0 | 0 | 7 | 0 | **0** | 100% |

The classified surfaces of the JECAM site for December 2014 are given in Table 5. Some results are still unrealistic, like the coffee plantation, orange trees and maize area, but it is possible that the next field campaigns will help to constrain these classes.

**Table 5 Classified Surfaces in December 2014**

| Class | area (ha) | % of the total area |
|---|---|---|
| Banana | 130.40 | 0.008% |
| Build-up surface | 39 656.73 | 2.454% |
| Coffee | 81 163.27 | 5.023% |
| Eucalyptus | 180 609.11 | 11.177% |
| Maize | 2 025.74 | 0.125% |
| Natural forest | 175 723.77 | 10.875% |
| Orange tree | 86 593.38 | 5.359% |
| Other | 1 137.54 | 0.070% |
| Pasture | 513 740.70 | 31.793% |
| Pines | 22 603.40 | 1.399% |
| Rocks | 2 200.99 | 0.136% |
| Soybeans | 95 522.29 | 5.911% |
| Sugarcane | 365 820.20 | 22.639% |
| Water bodies | 48 899.04 | 3.026% |
| Young fallow | 89.85 | 0.006% |
| | 1 615 916.42 | |

The resulting land cover map is shown in Figure 13. The classification stability based on membership probability is shown in Figure 14. The better results are those close to 1. This reflects the fact that croplands (South-West and East) are classified with lower membership probability.

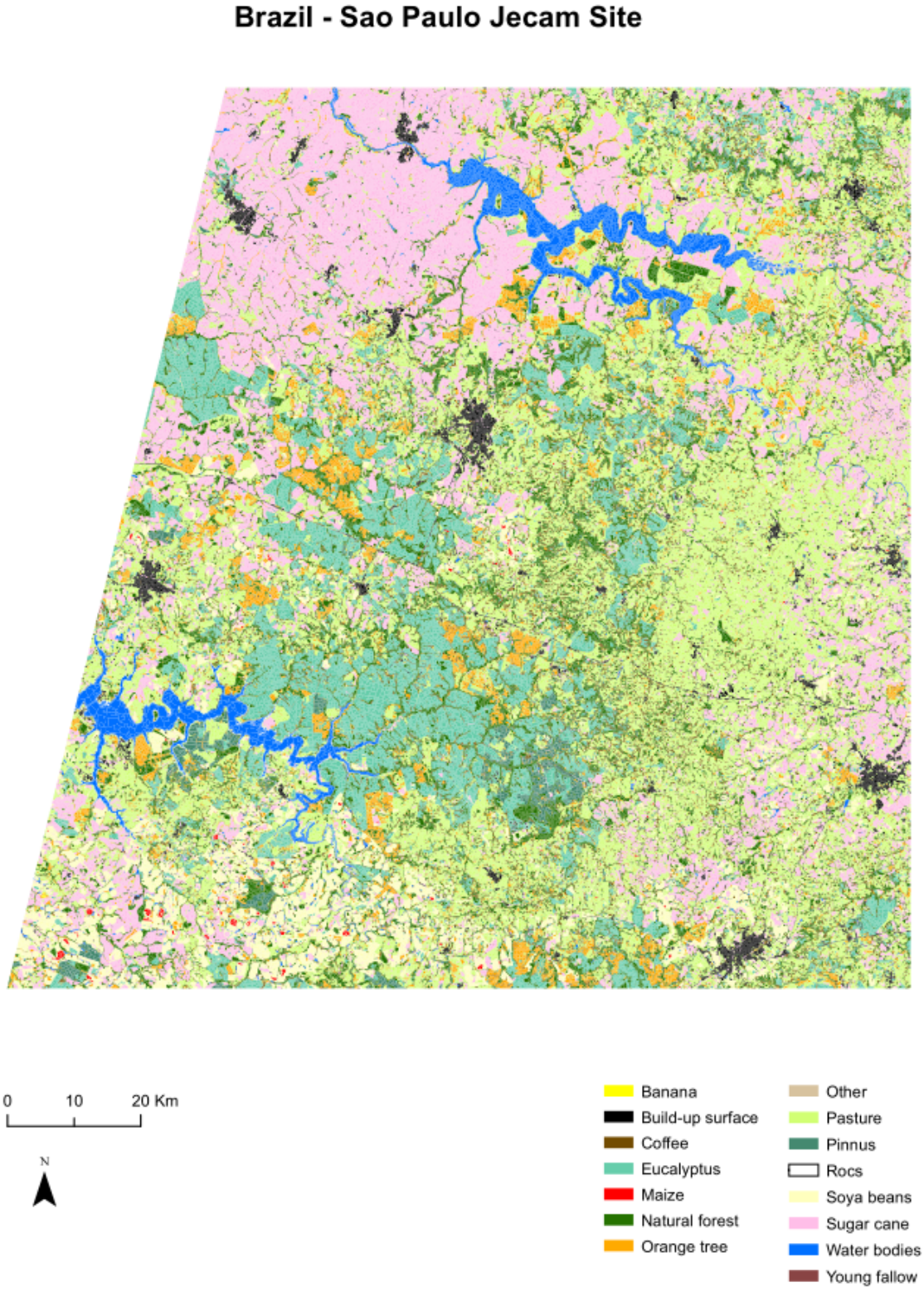


**Figure 13 December 2014 Classification of Brazil - São Paulo JECAM Site**

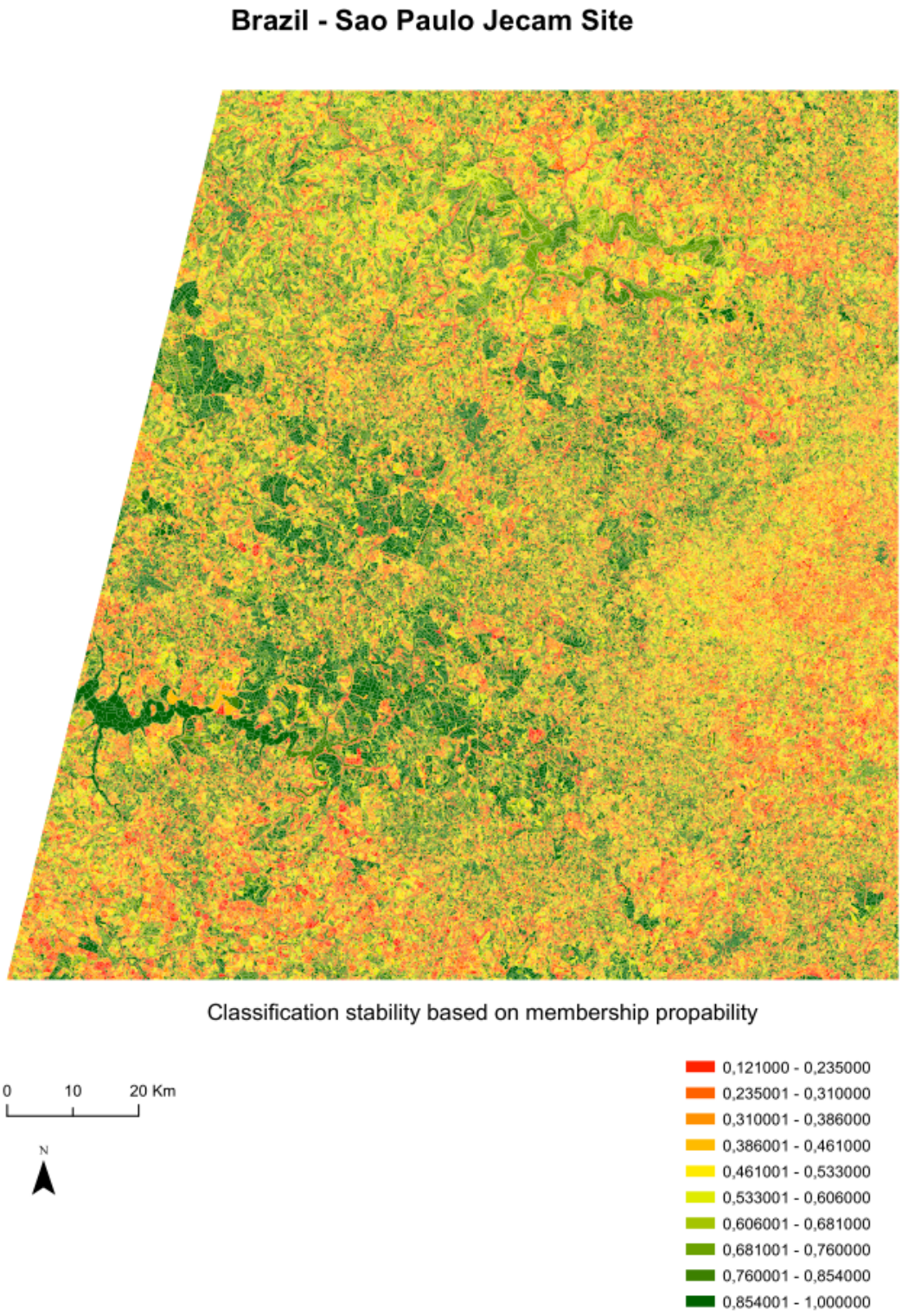


**Figure 14 Classification Stability based on Membership Probability**

The project objectives have been met for the moment. We will continue to improve the map by adding new training polygons by photointerpretation, and with new field campaigns. The method seems well adapted for the main class, but we see difficulties for classes with small a number of samples, as expected. One issue is the “other” class, which groups all land use that were met only several times in the field visit. The question of adding this “other” class in the classification algorithm is still controversial.

One major difficulty is cropland classes since there is not a common “regional” calendar (e.g some soybean fields are just sown when others are harvested). Therefore, we will increase the frequency of field visits in 2015, with measurements expected every 2.5 months. The Random Forest method needs also further exploration when images are partly covered by clouds. Use of textural variables computed on the panchromatic channels may also enhance some results, especially in row-structured fields such as orange tree orchards. While the algorithm is in theory able to handle a large number of variables, it could be useful to keep only the more important ones (e.g. through a PCA analysis for instance).

Can this approach be called ‘best practice’? Even if some aspects could be enhanced (see above), this method seems reliable enough. More investigations for improving the classification and the validation will be necessary.

## Plans for Next Growing Season

We will maintain the current approach, by doing field inventories every 2.5-3 months on the south-western part of the JECAM area, mainly covered by croplands. Image acquisitions are also planned this year (in particular SPOT images).

We anticipate ordering the same type/quantity of EO data next year, including DEIMOS data if possible. We could acquire radar images if other JECAM partners are interested.

## Publications

le Maire, G., Dupuy, S., Nouvellon, Y., Loos, R.A., & Hakamada, R. (2014). Mapping short-rotation plantations at regional scale using MODIS time series: Case of eucalypt plantations in Brazil. Remote Sensing of Environment, 152, 136-149.

## 6.2 Brazil – Tapajos

No report received.

# 7. Burkina Faso

Team Leader: Stéphane Dupuy, Maison de la Télédétection

Team Members: Patrice SANOU, ISESTEL Ouagadougou; Jacques IMBERNON, Montpellier; Mamy SOUMARE, IER, Bamako; Eric VALL, CIRDES, Bobodioulasso; Audrey JOLIVOT, CIRAD, Montpellier; Agnès BÉGUÉ, CIRAD, Montpellier

## Project Objectives

The original project objectives have not changed. They are:

- Crop identification and crop area estimation
- Yield prediction and forecasting.

## Site Description

The county of Koumbia is located in the southwest of Burkina Faso in the province of Tuy, in the Hauts-Basins.

| | |
|---|---|
| Site Extent | Centroid: lat: 11°10.596 / long: -3°39.830 |
| Top left: lat: 11°24.54 / long: -3°53.089 | Bottom Right: lat: 11°4.301 / long: -3°26.086 |

- Soils: Mostly sandy
- Drainage class/irrigation: No
- Crop calendar: June to November
- Field size: ≤ 3ha (Cotton and Maize/Sorghum)
- Climate and weather: Tropical dry.

## EO Data Received/Used

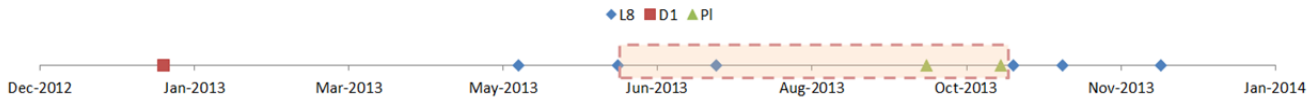


**Figure 15 EO Images Received in 2013**

The EO images received in 2013 are shown in Figure 15 and those received in 2014 are shown in Figure 16. The red dots correspond to the Pleiades images. The crop calendar is highlighted.

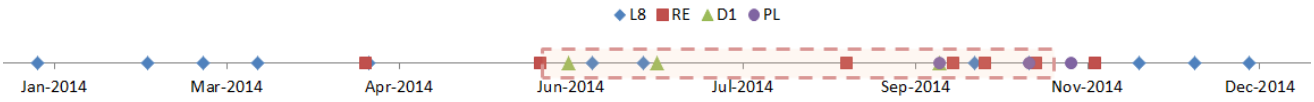


**Figure 16 EO Images Received in 2014**

Pléiades

- Space agency or Supplier : Airbus Defence and Space (ex Astrium services)
- Optical
- Number of scenes: 3
- Range of dates: 2014/09/25 – 2014/10/21 – 2014/11/02
- Beam modes/ incidence angles/ spatial resolutions: pansharpened (4 spectral bands) 0.5m
- Processing level: ortho

The 2014 Pléiades mosaic is shown in Figure 17.

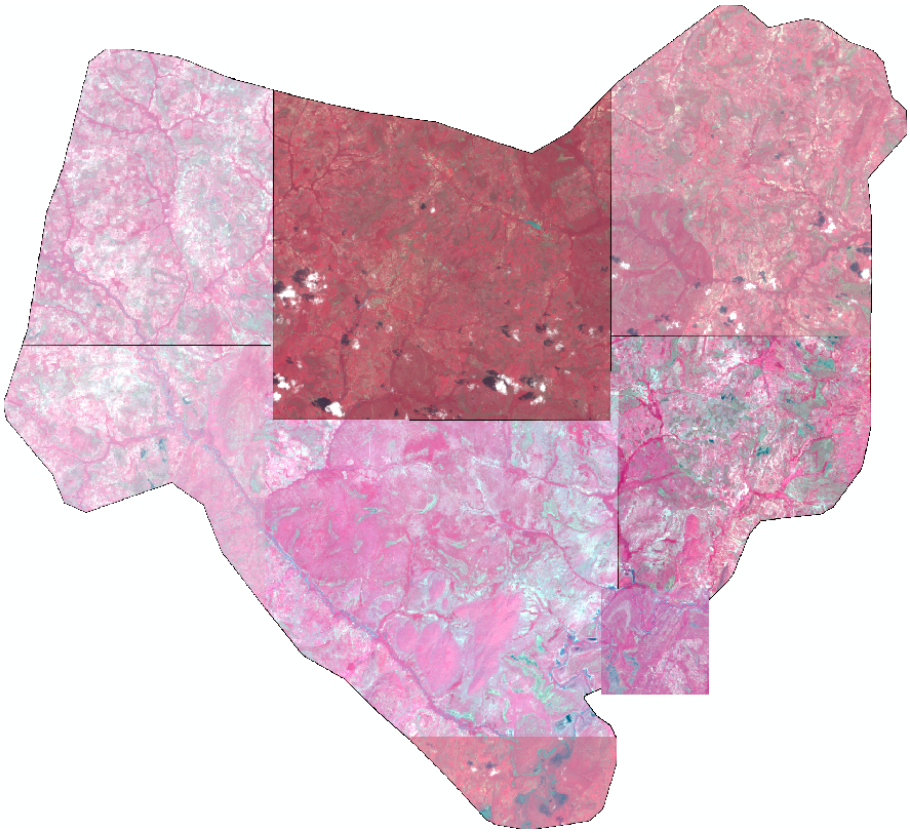

**Figure 17 Pleiades Mosaic for 2014**

Deimos 1

- Space agency or Supplier: DEIMOS Imaging
- Optical
- Number of scenes : 4
- Range of dates : 2014/06/09 – 20140705 – 2014/08/07 - 2014/09/25
- Beam modes/ incidence angles/ spatial resolutions : 20m
- Processing level : ortho

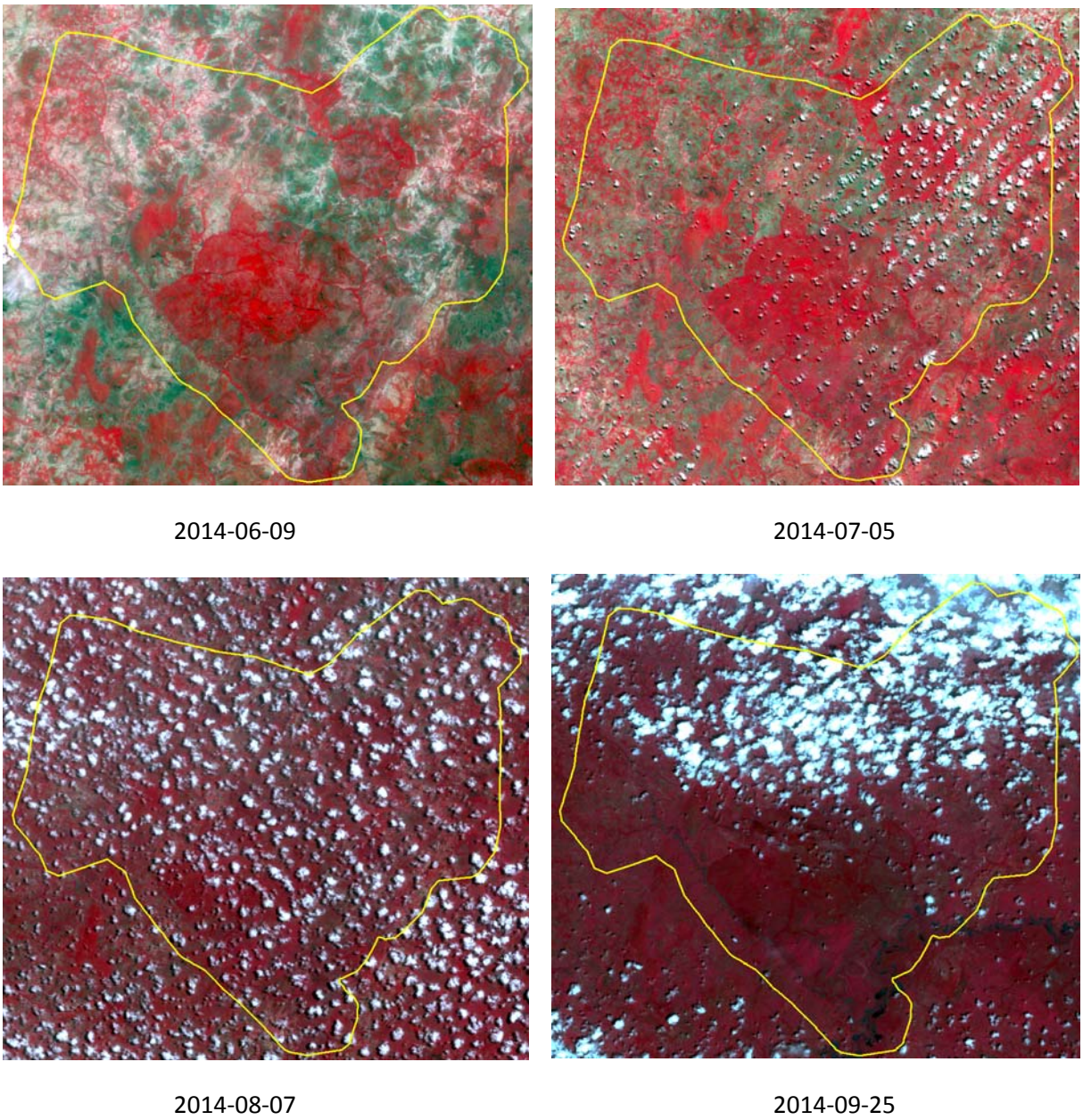


**Figure 18 DEIMOS Images in 2014**

RapidEye

- Space agency or Supplier: Blackbridge
- Optical
- Number of scenes: 14
    - 7 without clouds / with some clouds / partial coverage of the site
    - 7 unusable due to heavy cloud cover

- Range of dates: 2014/04/11 – 2014/06/01 – 2014/08/29 – 2014/09/29 – 2014/10/08 – 2014/10/23 – 2014/11/09
- Beam modes/ incidence angles/ spatial resolutions: 6m with 5 spectral bands
- Processing level

**Figure 19 RapidEye Images in 2014**

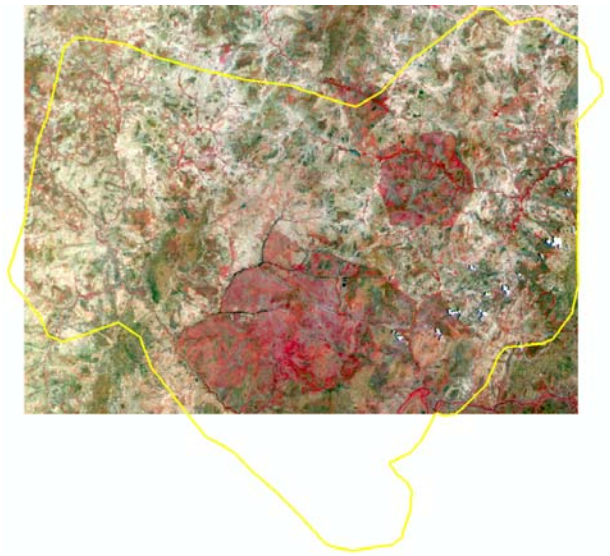

2014-04-11

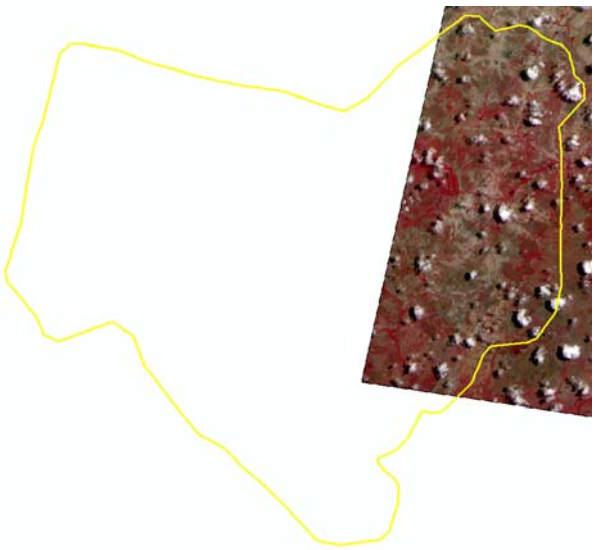

2014-06-01

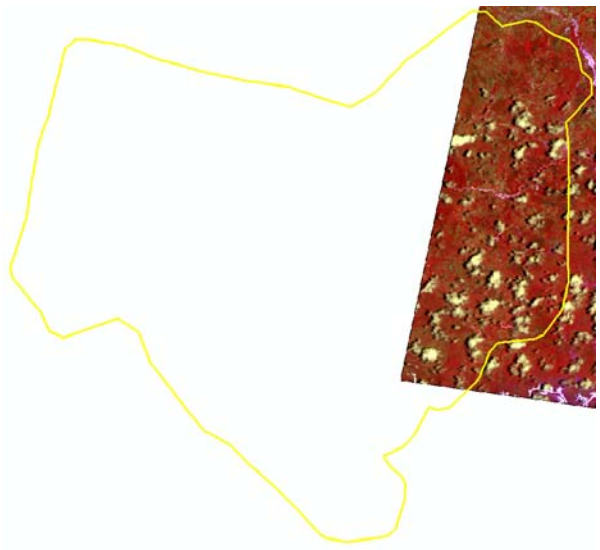

2014-08-29

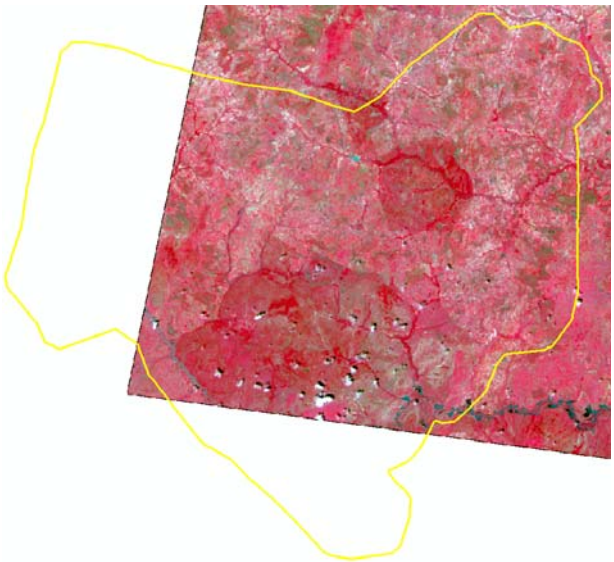

2014-09-29

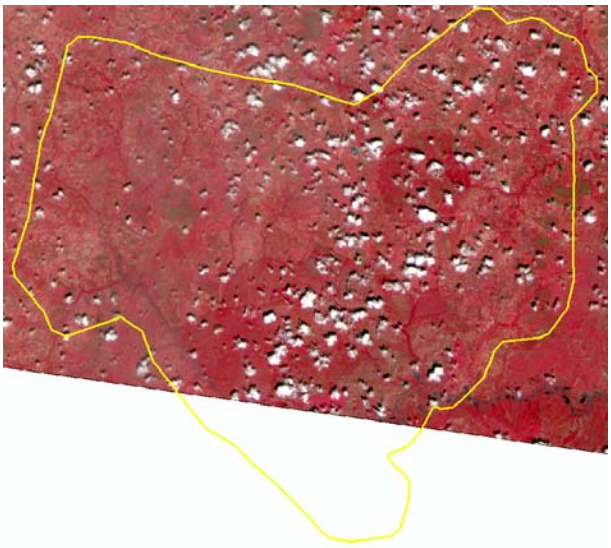

2014-10-08

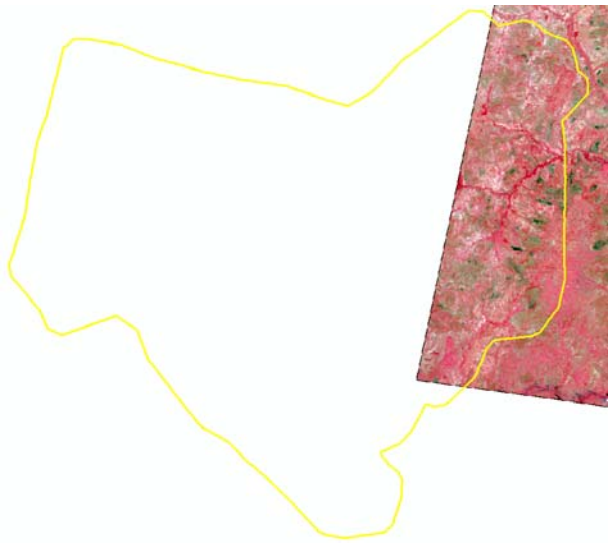

2014-10-23

2014-11-09

Landsat-8

- Space agency or Supplier : USGS
- Optical
- Number of scenes: 21
    - 12 without clouds / with some clouds
    - 9 unusable due to heavy cloud cover
- Range of dates : 2014/01/06 – 2014/02/07 – 2014/02/23 - 2014/03/11 – 2014/04/12 – 2014/06/16 – 2014/07/01 – 2014/10/05 – 2014/10/21 – 2014/11/22 – 2014/12/08 – 2014/12/24

- Beam modes/ incidence angles/ spatial resolutions : 7 spectrals bands (30m) and one panchromatic band (15m)
- Processing level : ortho

In situ Data

The points in red in Figure 20 are plots selected for yield prediction and forecasting. Parcels in yellow are field surveys conducted in October 2014.

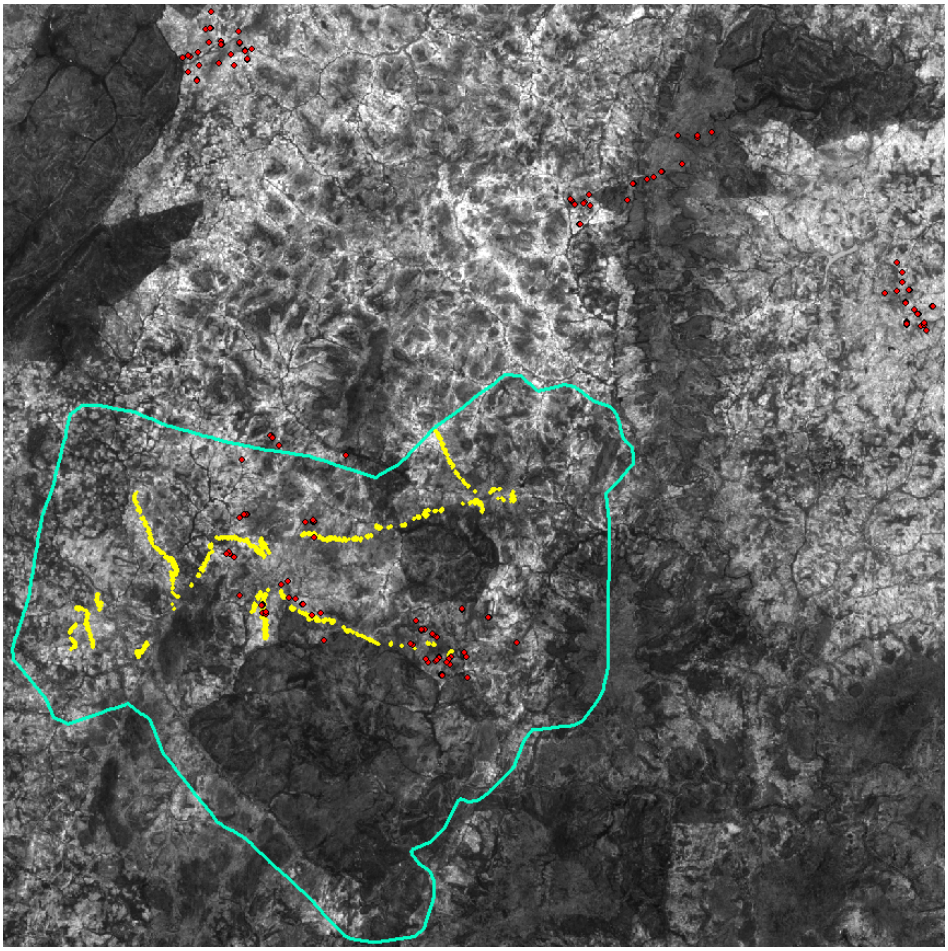

**Figure 20 Plots selected for Yield Prediction and Forecasting, and Field Surveys**

Field surveys were conducted on agricultural plots in October 2014. 640 GPS waypoints were collected. Points were manually converted to polygons (surface data) with Pleiades image. The points were selected on a tablet with Pleiades image on the screen. Parcels were identified

along roads and tracks at the end of the rainy season. We applied the procedures recommended by JECAM in the “JECAM Guidelines for Field Data Collection_v1 0”.

**Figure 21 Photos Taken during the Field Survey in October 2014**

Sesame

Cotton and Maize

Groundnuts

Herbaceous Savannah

Maize

Sorghum

Cow Peas

Young Fallow

In order to gather in situ data of yield, the main crop systems of the site were described and evaluated: crop varieties, crop rotation, use of inputs, tillage, fallow, use of plough or tractors. Secondly, the yield variability was obtained from the farmers and the link with climate variability was evaluated.

Methods: Six villages were selected according to their spatial distribution, their accessibility, the studies already carried out, and the remote sensing image footprints. In agreement with the farmers and peasant organizations, thirty plots were chosen in each village, to carry out two types of survey:

- A survey with the farmer, concerning the plot monitored: crop status for the three previous years, crop management techniques, area cultivated, production obtained, crop residues.
- Concerning the crop monitoring on the plot for the season 2014:

- Ten days crop monitoring
- The weighing of grains and biomass for three quadrants by plot.
- The daily measurement of rainfall, with three rain gauges put in each village (total of eighteen rain gauges).

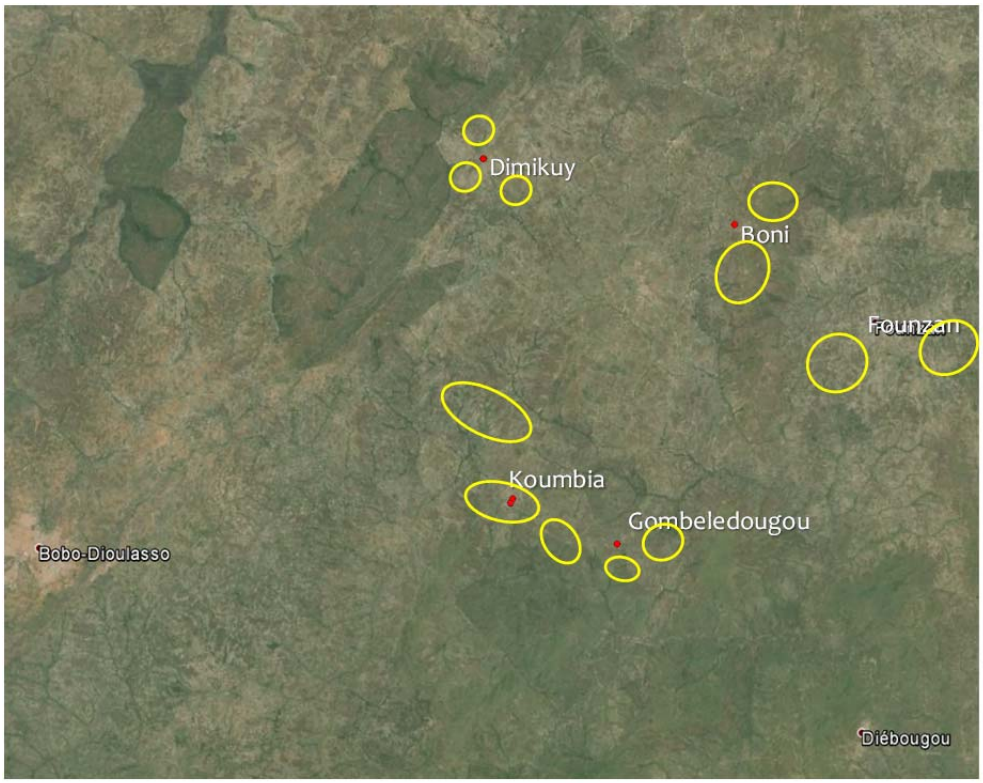


**Figure 22 Villages and Areas with Monitored Plots**

On the 137 plots monitored, 81 are cultivated with maize, 43 with sorghum and 13 with millet. This represents the general proportions of those crops in the zone. The following figures show some of the survey results.

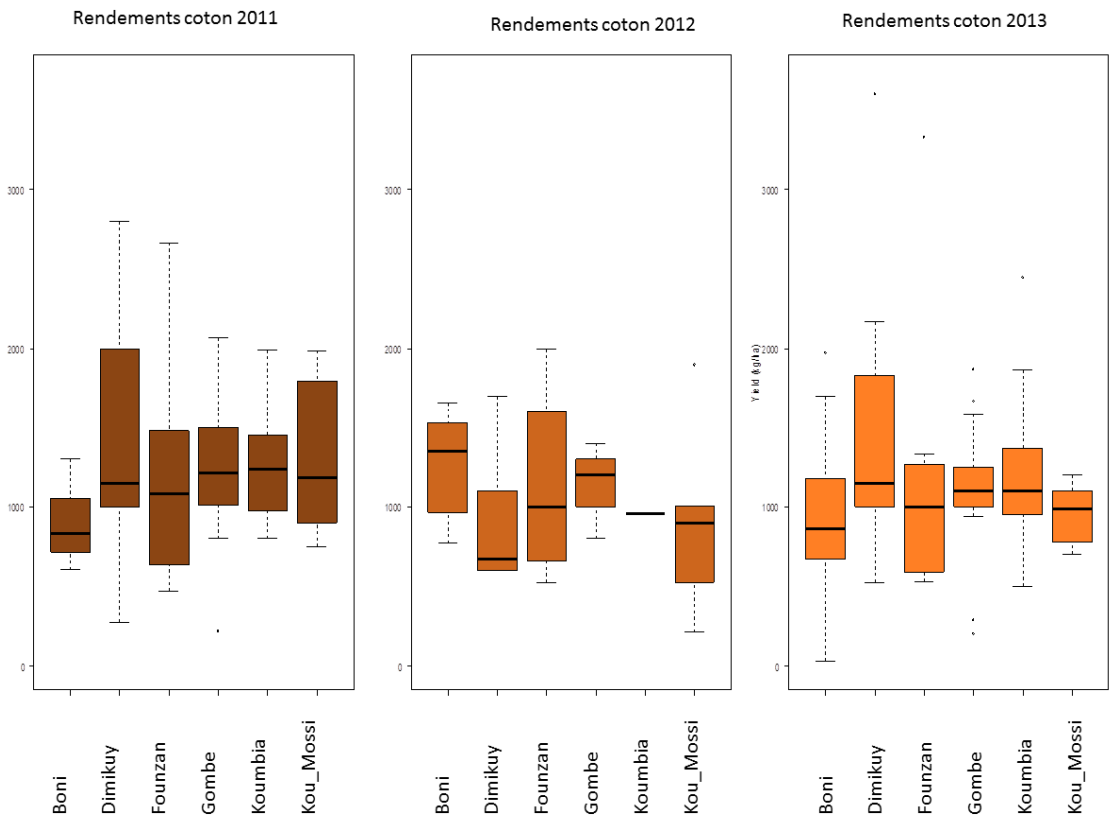


**Figure 23 Cotton Yields for each Village, 2011 - 2013**

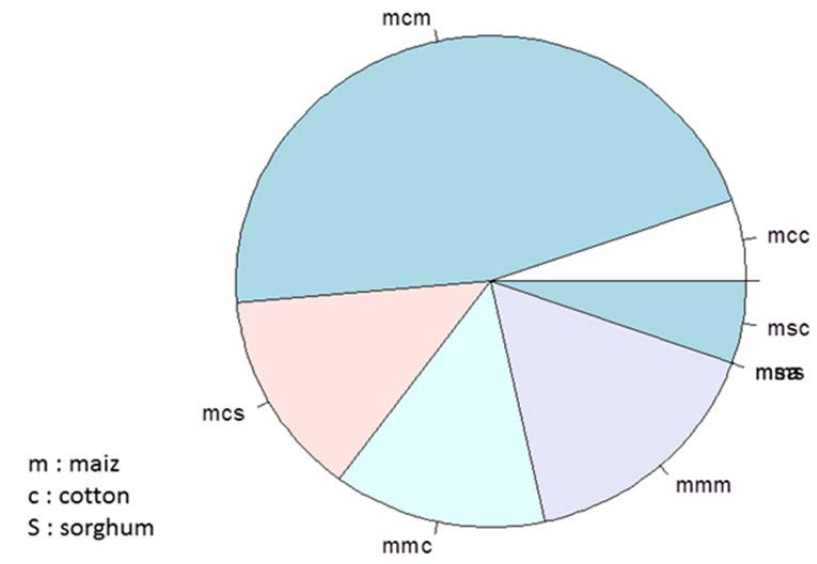


**Figure 24 Crop Rotation with Maize 2009-2011**

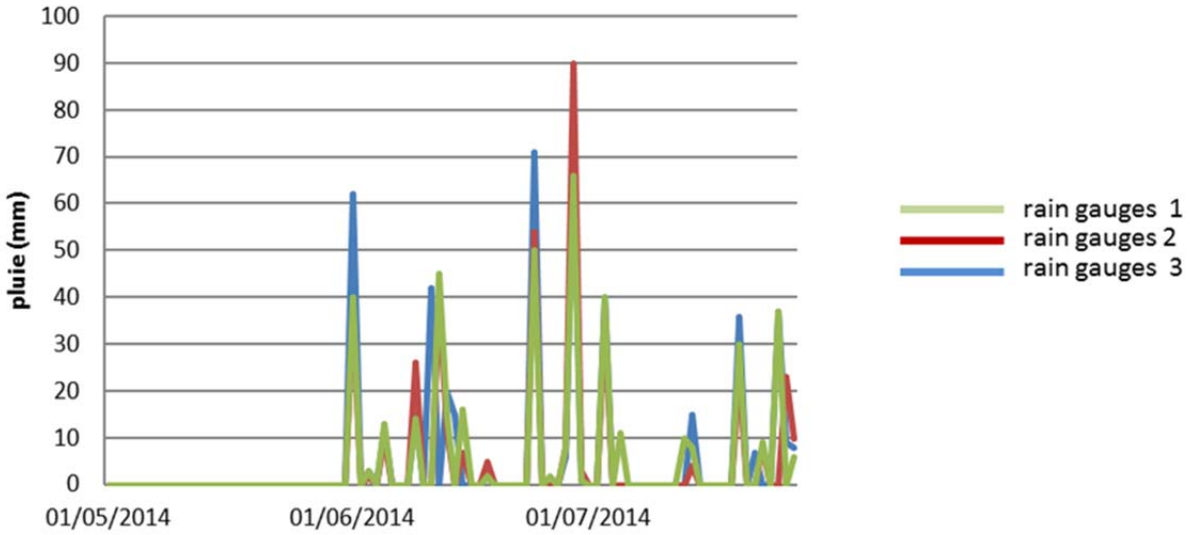


**Figure 25 Rainfall at the 3 rain guages in Boni Village, 2014**

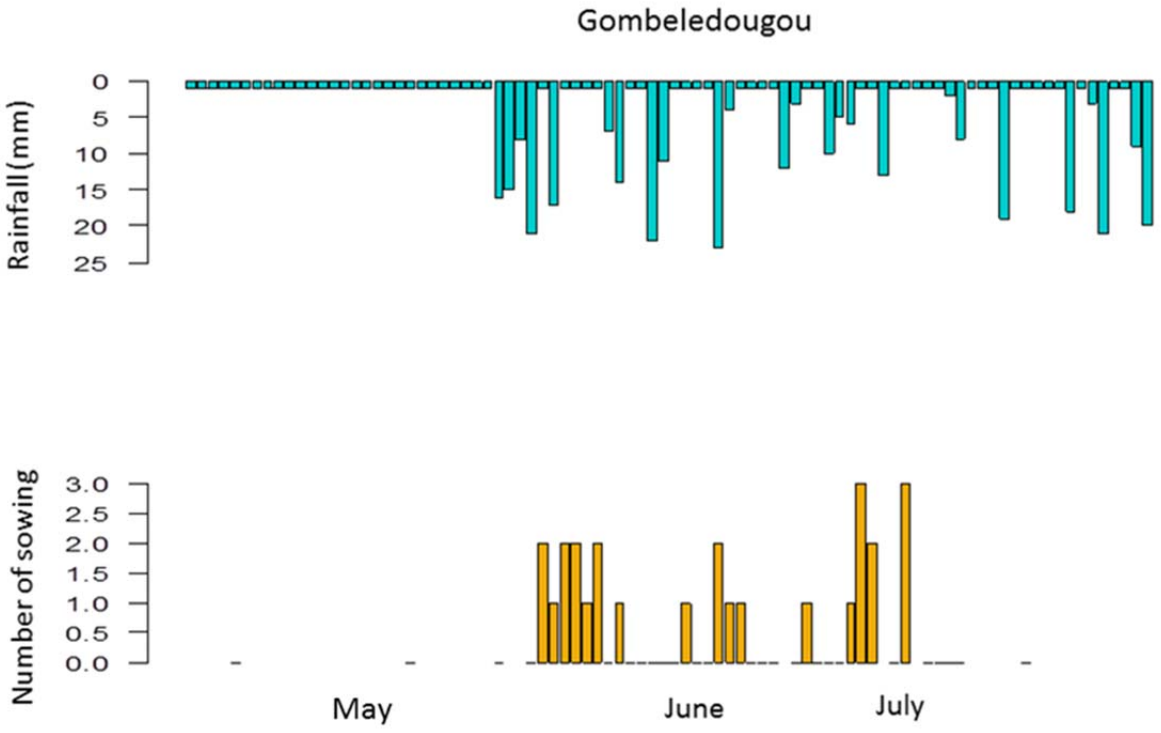


**Figure 26 Sowing Related to Recorded Rainfall in Gombeledougou, 2014**

Collaboration

We have collaborated with the Brazil Sao Paulo site and the Madagascar Antsirabe site. At these three sites, we have established a classification procedure based on Object Based Image Analysis (OBIA) approach and the use of the Random Forest algorithm.

Results

We have developed a method based on (i) the use of a THRS image for object extraction (using Object Based Image Analysis) and texture index extraction and (ii) the use of HR images for multi-temporal information. The classification is performed on the objects with the Random Forest (RF) algorithm for each level of JECAM nomenclature. RF uses the plots to define the decisions of rules for each class. The processing of the 2013 data are currently in progress. The 2014 data will be processed soon.

The preliminary results for 2013 follow. The RF algorithm conducts an evaluation of the results based on 1/3 of the training fields. We want to achieve a more robust validation based on validation segments. These segments are obtained with field work and photo-interpretation made by local staff. The results of the RF validation are given here. The 4 levels corresponding to the levels in the "JECAM guide for field data collection" are shown in Table 6.

| Level 1 | Level 2 | Level 3 | Level 4 |
|---|---|---|---|
| 89 % | 67 % | 61 % | 61.5 % |

**Table 6 Results of RF Validation, Overall Accuracy**

| | | Classification | | | | | | |
|---|---|---|---|---|---|---|---|---|
| | | Annual cropland | Build-up surface | Fallows | Ligneous crop | Natural spaces | Water bodies | class.error |
| Terrain | Annual cropland | **98%** | 0% | 0% | 0% | 2% | 0% | 2% |
| | Build-up surface | 9% | **85%** | 0% | 0% | 5% | 2% | 23% |
| | Fallows | 84% | 0% | **0%** | 0% | 16% | 0% | 65% |
| | Ligneous crop | 67% | 0% | 17% | **0%** | 17% | 0% | 71% |
| | Natural spaces | 16% | 1% | 0% | 0% | **83%** | 0% | 21% |
| | Water bodies | 6% | 0% | 0% | 0% | 6% | **89%** | 20% |

**Table 7 Confusion Matrix for Level 1**

| Terrain \ Classification | Build-up surface | Cash crops | Cereals | Fruit crops | Grassland | Leguminous | Natural forest | Oilseed crops | Old fallow | Roads | Rocs | Shrub land | Timber crops | Water bodies | Young fallow | class.error |
|---|---|---|---|---|---|---|---|---|---|---|---|---|---|---|---|---|
| Build-up surface | **42%** | 0% | 0% | 0% | 0% | 4% | 0% | 0% | 0% | 46% | 8% | 0% | 0% | 0% | 0% | 58% |
| Cash crops | 0% | **77%** | 19% | 0% | 1% | 1% | 0% | 1% | 0% | 0% | 0% | 1% | 0% | 0% | 0% | 23% |
| Cereals | 0% | 5% | **88%** | 0% | 1% | 2% | 0% | 2% | 0% | 0% | 0% | 2% | 0% | 0% | 0% | 12% |
| Fruit crops | 0% | 20% | 20% | **0%** | 20% | 0% | 20% | 0% | 0% | 0% | 0% | 0% | 0% | 0% | 20% | 100% |
| Grassland | 1% | 0% | 19% | 0% | **74%** | 0% | 0% | 0% | 0% | 0% | 3% | 3% | 0% | 0% | 0% | 26% |
| Leguminous | 0% | 8% | 45% | 0% | 1% | **26%** | 0% | 16% | 0% | 4% | 0% | 0% | 0% | 0% | 0% | 74% |
| Natural forest | 0% | 0% | 2% | 0% | 0% | 0% | **91%** | 0% | 0% | 0% | 0% | 7% | 0% | 0% | 0% | 9% |
| Oilseed crops | 0% | 7% | 43% | 0% | 0% | 21% | 0% | **22%** | 0% | 1% | 1% | 4% | 0% | 0% | 0% | 78% |
| Old fallow | 0% | 14% | 43% | 0% | 0% | 29% | 0% | 0% | **0%** | 0% | 0% | 0% | 0% | 0% | 14% | 100% |
| Roads | 7% | 0% | 0% | 0% | 2% | 2% | 0% | 0% | 0% | **83%** | 2% | 0% | 0% | 2% | 0% | 17% |
| Rocs | 0% | 0% | 0% | 0% | 0% | 0% | 0% | 4% | 0% | 0% | **96%** | 0% | 0% | 0% | 0% | 4% |
| Shrub land | 0% | 0% | 12% | 0% | 5% | 0% | 10% | 2% | 0% | 0% | 0% | **69%** | 0% | 0% | 2% | 31% |
| Timber crops | 0% | 0% | 100% | 0% | 0% | 0% | 0% | 0% | 0% | 0% | 0% | 0% | **0%** | 0% | 0% | 100% |
| Water bodies | 0% | 0% | 0% | 0% | 0% | 0% | 0% | 0% | 0% | 6% | 6% | 0% | 0% | **89%** | 0% | 11% |
| Young fallow | 0% | 23% | 42% | 0% | 16% | 0% | 0% | 6% | 0% | 0% | 0% | 10% | 0% | 0% | **3%** | 97% |

**Table 8 Confusion Matrix for Level 2**

The overall accuracy for Level 1 is very good. For other levels the results are less good. This is normal given the low spectral differences observed between some crops (Cow peas and groundnuts for example).

For the year 2013, we did not have enough images acquired during the growing season: only one image was acquired in July at the beginning of the rainy season.

To improve the results, we will combine some classes (cow peas and groundnuts for example), based on the confusion matrix produced by RF. Other classes with very small number of training plots (4 plots for orchards for instance) will be deleted.

Concerning the biomass and yield data at plot scale, the data have been collected, but not yet received, although it is expected shortly.

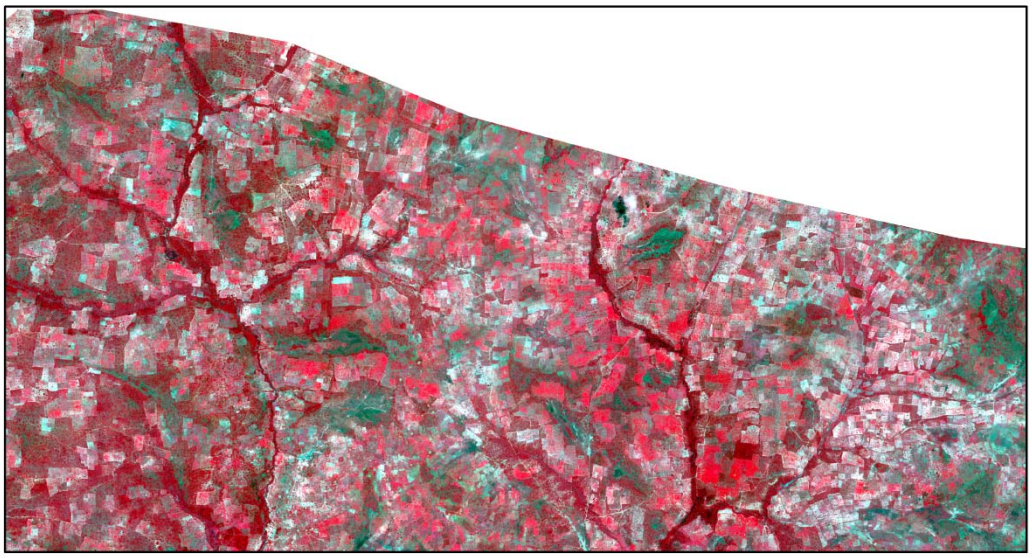

Pléiades image acquire on 2013/09/20

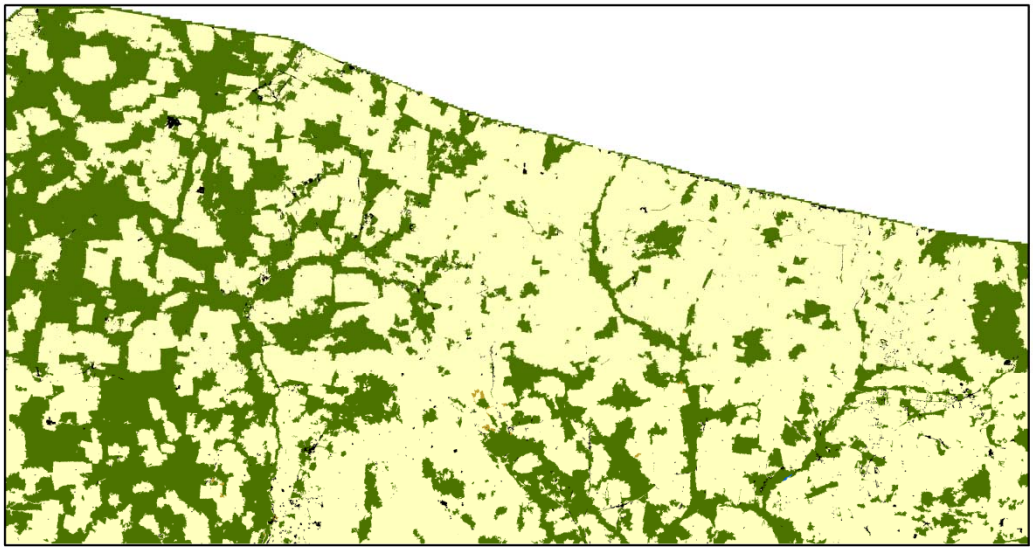

Land use map : Level 1

0 1 2 Km

Annual cropland
Build-up surface
Fallows
Natural spaces
Water bodies

**Figure 27 Classification Result for Level 1 in 2013**

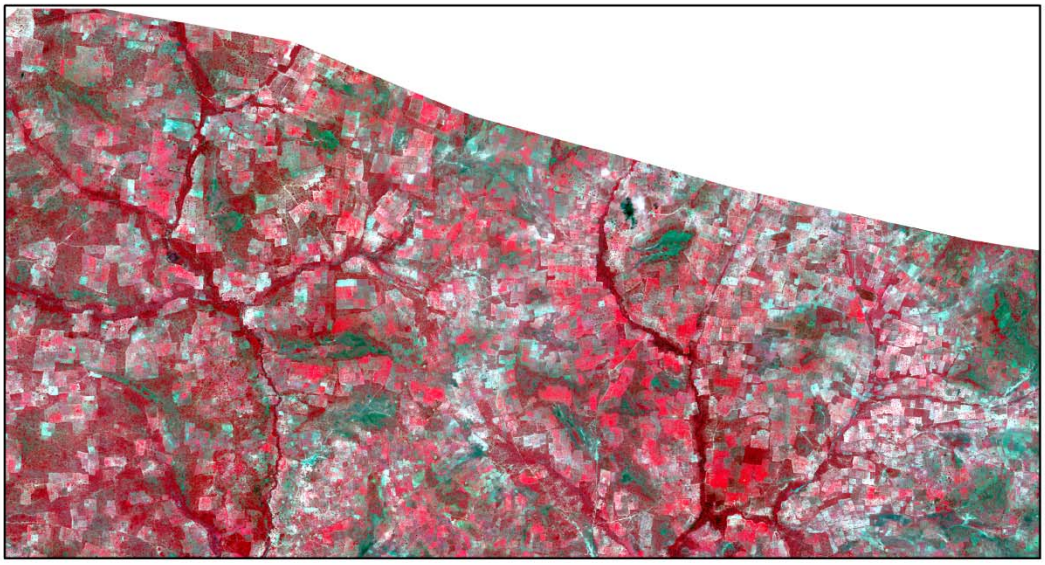

Pléiades image acquire on 2013/09/20

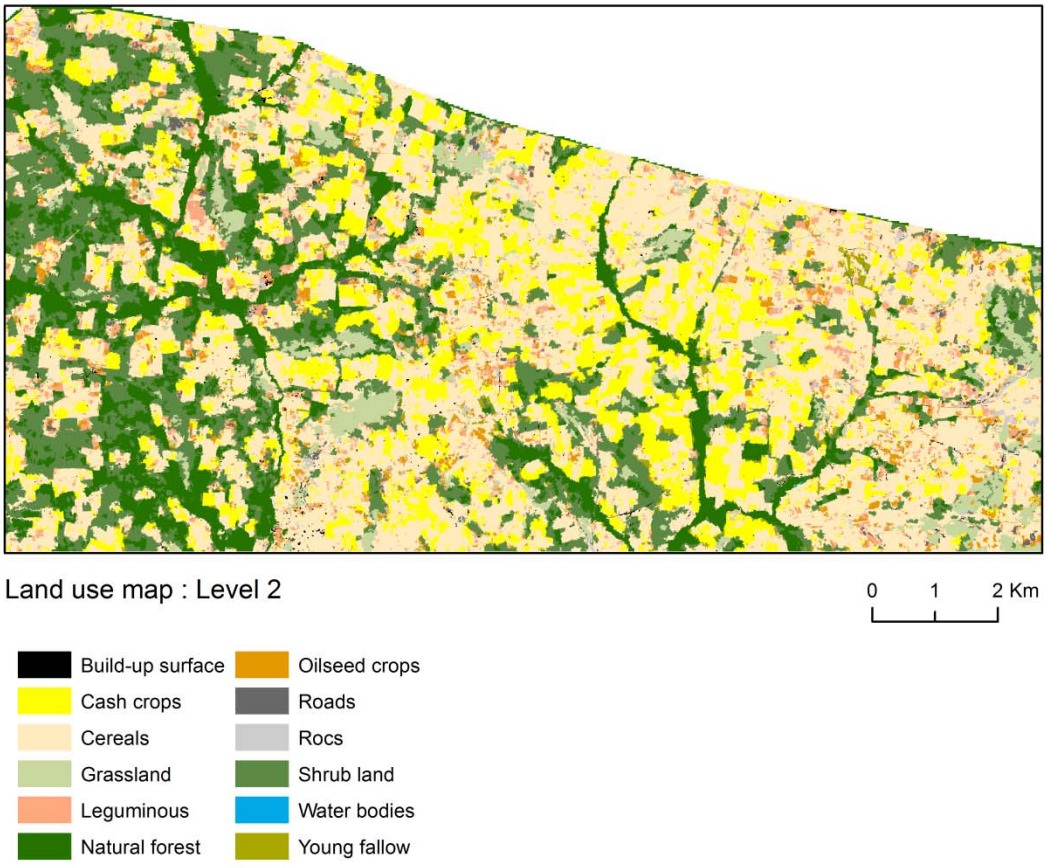


**Figure 28 Classification Result for Level 2 in 2013**

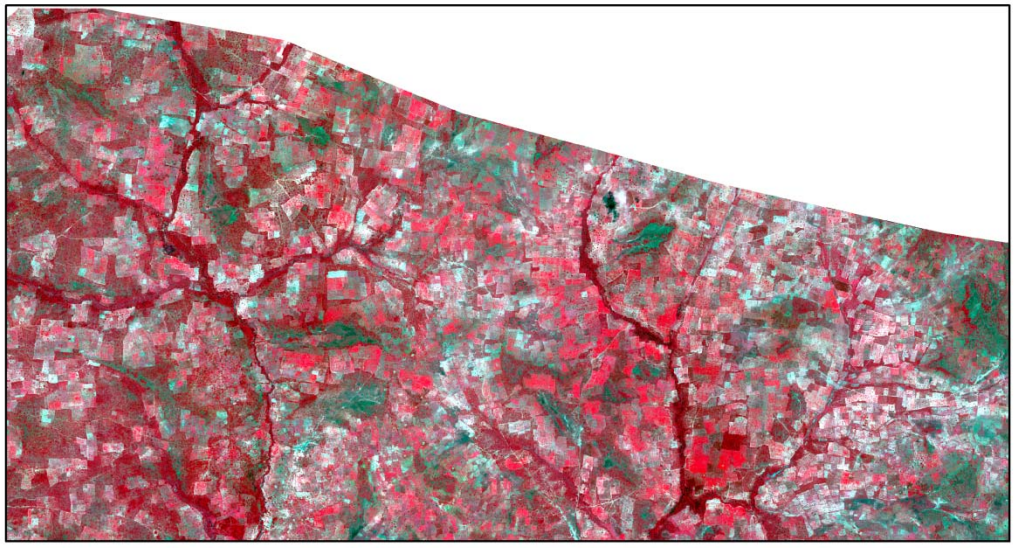

Pléiades image acquire on 2013/09/20

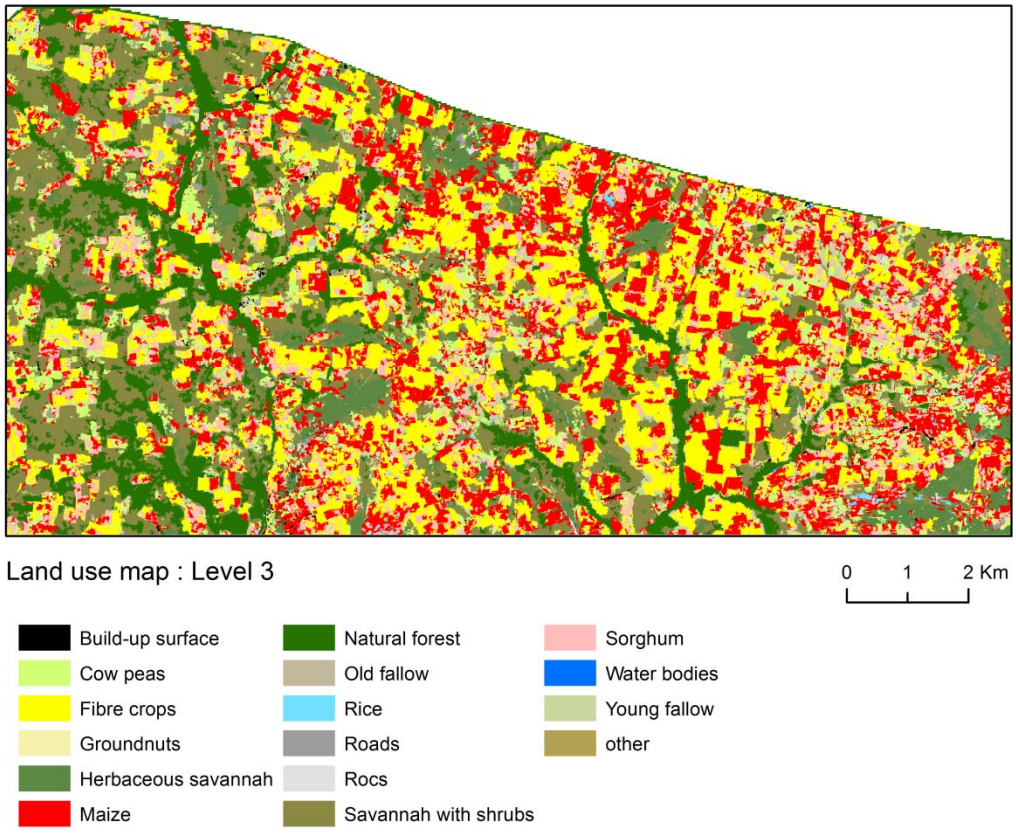


**Figure 29 Classification Result for Level 3 in 2013**

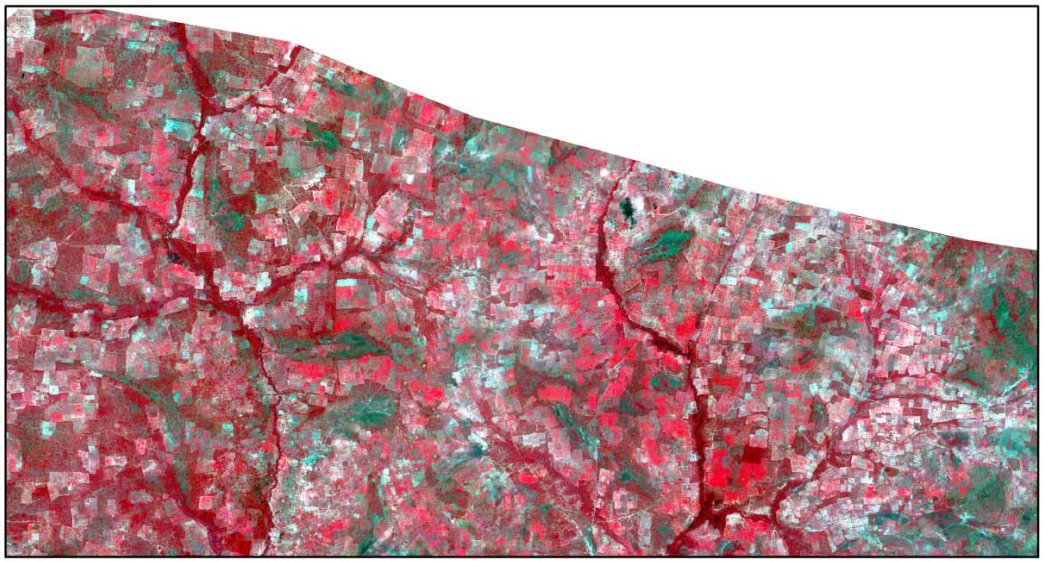

Pléiades image acquire on 2013/09/20

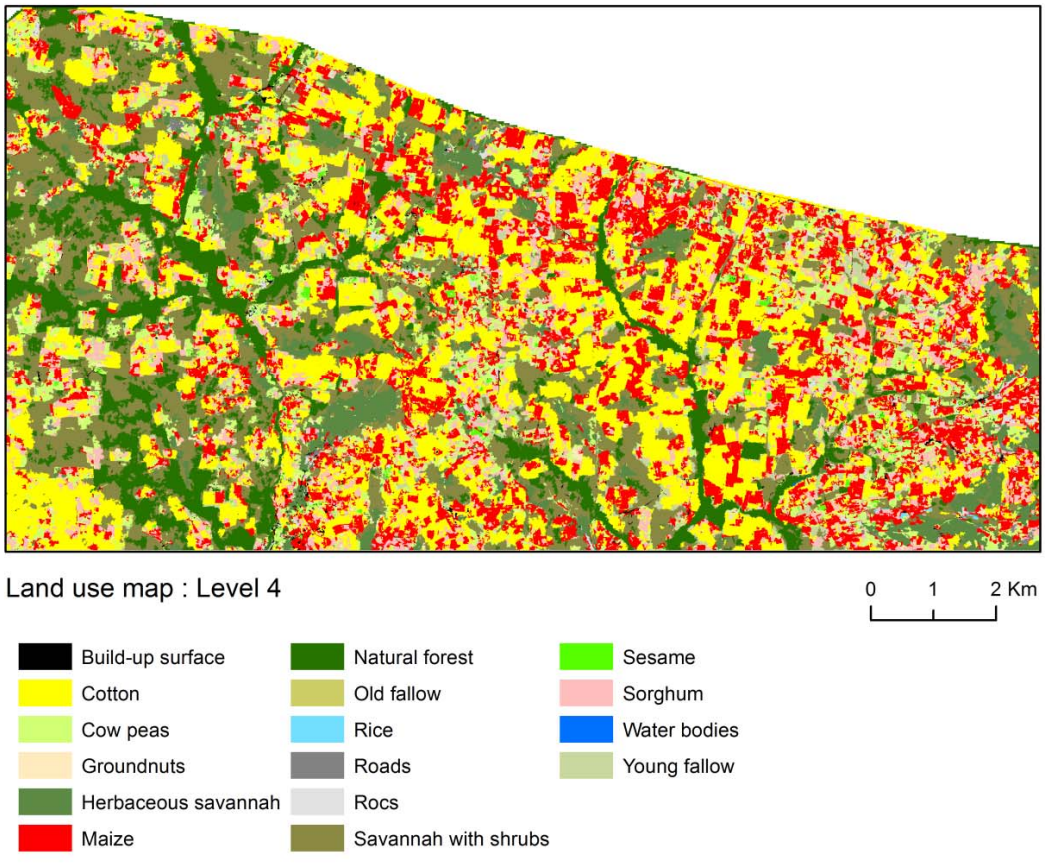


**Figure 30 Classification Result for Level 4 in 2013**

The project objectives are progressing well, but the work is still in progress. We followed the recommendations of the "JECAM guides" for the acquisition of field data. However, we have adapted to the nomenclature cultures present on our site.

We modified the project objectives in the sense that we added the study of Yield Prediction and Forecasting.

Plans for Next Growing Season

Next growing season, we will maintain the same approach. The EO data to be acquired will change as follows:

- We hope to renew field surveys: this will depend on the security conditions for the mission organization.
- Remote sensing data:
    - We will request Pleiades images of the area. The vesting period will be the same.
    - We hope to order SPOT 6-7 (one in the dry season and one in the end of rainy season).
    - We hope that this site will be selected for the "Sentinel 2 Agri" project for coverage with the first Sentinel-2 images.
    - We hope that this site will be selected for the image acquisition by the VENUS satellite (spatial resolution: 5m / temporal repetitiveness 2 days)
    - Landsat-8 images: every 16 days
    - RapidEye images: every month during dry season.

Publications

None yet.

# 8. Canada

## 8.1 CFIA (Canadian Food Inspection Agency)

Team Leader and Members: Drs. E. Pattey & G. Jégo

Co-App.: A. Vanderzaag, J. Liu, B.Qian, W. Smith, X. Geng

Coll.: F. Baret, N. Beaudoin, R. Desjardins, R. Fernandes, I. Jarvis, T Huffman, R. Lacaze, J. Sheng, H. McNairn, et al.

Project Objectives

The original objectives of the project have not changed. They are:

- Crop identification and Crop Area Estimation
- **Crop Condition/Stress**
- Soil Moisture
- **Yield Prediction** and Forecasting
- Crop Residue, Tillage and Crop Cover Mapping
- **Soil properties**.

Project title: "From fields to regions: Improving crop model predictions, using remote sensing-derived biophysical descriptors and climate data, to evaluate the impact of climate variations on crop production and environmental performance."

Objectives:

- Validation of LAI and fAPAR from Sentinel computation chain
- Assimilation techniques (re-initialization, forcing)
- Yield Prediction
- LAI, evapotranspiration, RUE, N2O fluxes
- Crop Condition/Stress
- The project needs Crop Cover Mapping and site can serve for training/validation.

Site Description

- Location: The centroid is at latitude 45° 18' 00"N, longitude 75° 46' 00"W. CFIA Ottawa Laboratory 3851 Fallowfield Road, Ottawa, Ontario, Canada.
- Topography: flat to gently sloping, < 0.5% Gradient.
- Soils: Modified marine sediments with a fine texture and neutral composition. Layers of silty sediments interspersed in the upper 2 meters. Clay loam is the dominant texture.

- Drainage class/irrigation: Tile Drainage and Precipitation Fed Field.
- Crop calendar: May 1 to end of October; spring crops: corn soybean, wheat canola.
- Field size: 15-75 ha fields.
- Climate and weather: Humid continental climate. Average of 732 mm of rain $yr^{-1}$ and 236 mm of snow $yr^{-1}$ and temperature averages from 13.4 °C- 20.9 °C from May-August (Environment Canada, Government of Canada 2014).
- Agricultural methods used: Tillage, synthetic fertilizer, seeding, harvest when grains are dry enough.

**Figure 31 CFIA-Ottawa Field Equipment**

As shown in Figure 31, $CO_2$, $H_2O$ and sensible heat flux is measured in two fields using 3 eddy covariance towers. Nitrous oxide fluxes are measured using 2 flux gradient towers. Destructive biomass, LAI, soil sampling, and yield mapping and non-destructive PAI, lChl (Dualex, SPAD), crop cover (nadir photos) soil moisture & T, intercepted PAR are performed. Other data are obtained from the weather station.

EO Data Received/Used

The EO data used in 2014 are shown in Table 9. The following figures provide examples.

## Table 9 EO Data Collected for CFIA in 2014

| Data | Supplier | Sensor | # scenes | Range of dates | Mode/ resolution | Processing level | Challenges |
|---|---|---|---|---|---|---|---|
| RapidEye | BlackBridge | Optical | 18 (9 good) | May 11 - Sept 19 | | 1B | Cloud |
| Landsat-8 | USGS | Optical | 6 | Apr 24 – Sep 15 | | Radiance | Cloud/long revising cycle |
| CHRIS | ESA | Optical | 4 | May 7 – Aug 11 | | Radiance | Cloud/long revising cycle |
| RADARSAT-2 | CSA | SAR | 7 | May 8 – Sept 29 | Fine Quad | polarization | Conflict |
| RADARSAT-2 | CSA | SAR | 2 | June 29, Jul 2 | Wide standard | polarization | Conflict |

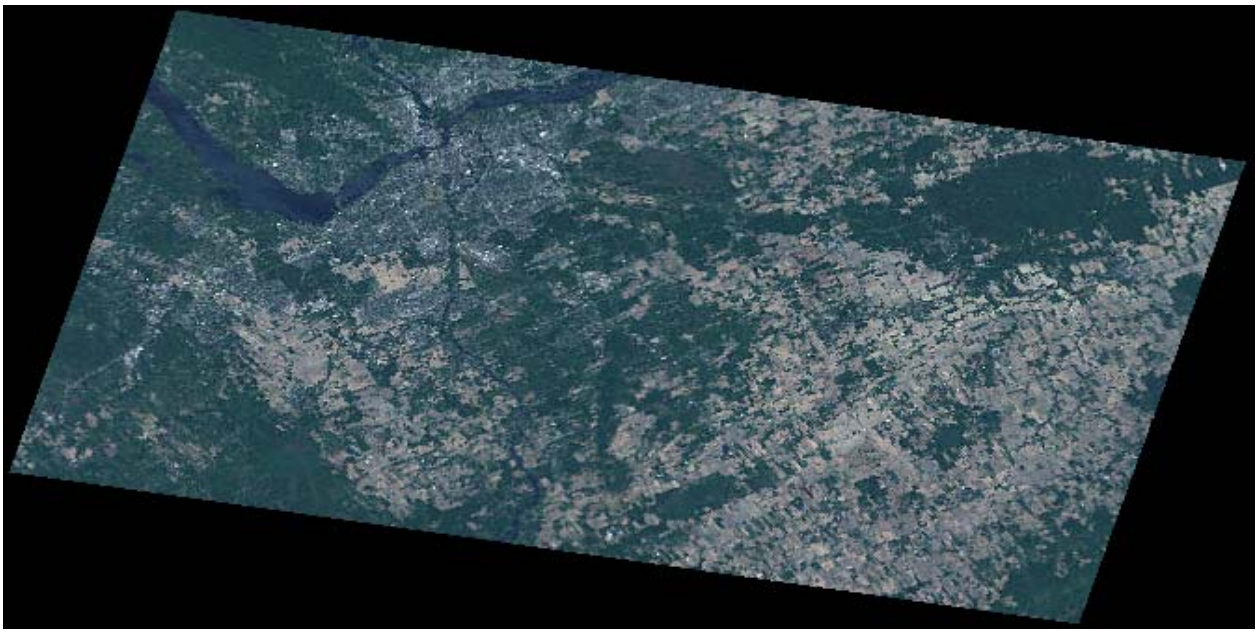

## Figure 32 RapidEye Image Acquired over CFIA, 7 June 2014

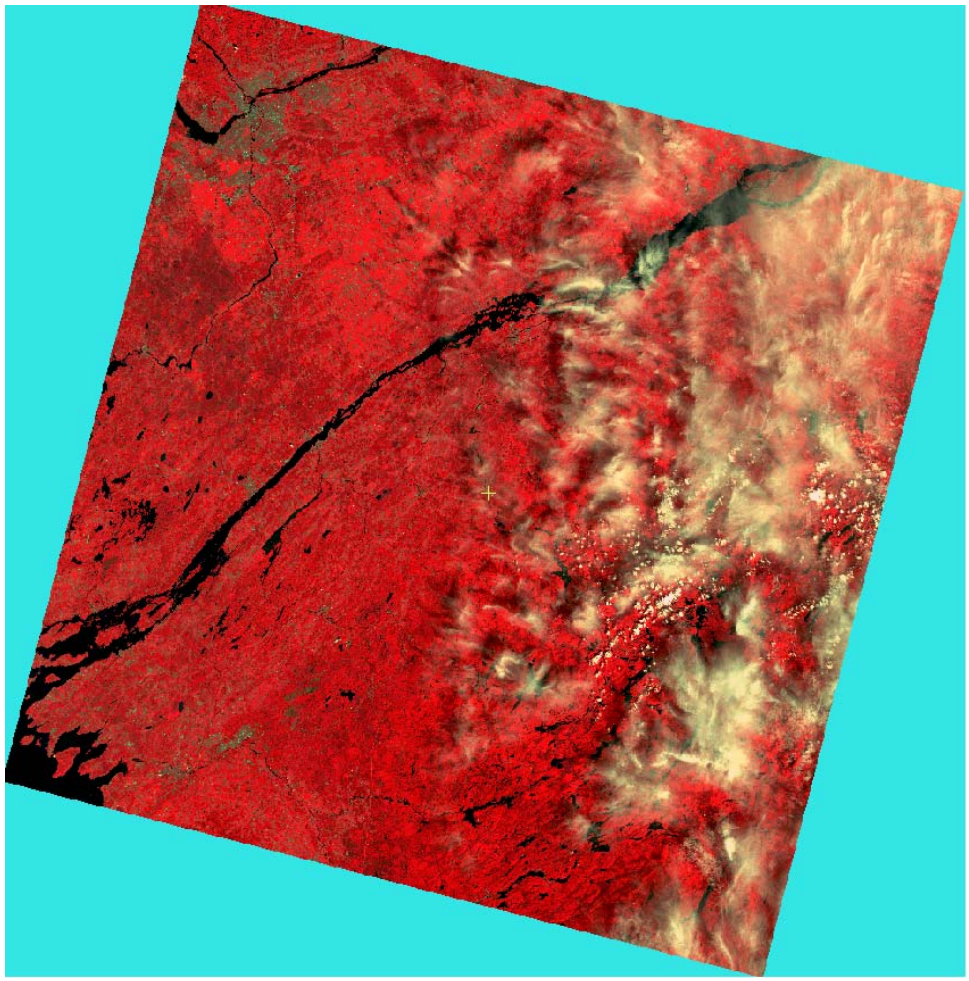

**Figure 33 Landsat-8 Image Acquired on 26 July 2014**

**Figure 34 CHRIS Image Acquired on 18 July 2014**

In situ Data

The following in situ data was collected:

- Eddy covariance fluxes (ET, sensible heat & $CO_2$ fluxes)
- Soil respiration (discrete & automated chambers)
- Crop cover (photography)
- PAI (DH photography, PASTIS-57 sensors)
- APAR (using 1-m long integrated PAR bars)
- Soil moisture (continuous soil profiles & soil sampling)
- Soil fertility sampling
- Destructive biomass & LAI, and yield mapping
- Non-destructive Leaf chlorophyll (SPAD, Dualex)
- Meteorological stations (rain gauge, net radiometers, PAR,
    - anemometers, soil T& moisture profiles)
- Flux gradient N2O fluxes (using tunable diode lasers).

Figure 35 shows an ultrasonic anemometer installed on the flux tower for measuring $CO_2$, latent and sensible heat fluxes using the eddy covariance technique. Figure 36 shows an automated soil respiration chamber to measure $CO_2$ efflux from the field surface (LI-COR, Lincoln, NE).

Figure 35 Ultrasonic Anemometer

Figure 36 Automated Soil Respiration Chamber

Volumetric soil moisture was measured of several profiles (up to 1m) using the Time Domain Reflectometry (6050X1 Trase system, SOILMOISTURE EQUIPMENT CORP, Goleta, CA). Figure 37 shows digital photo analyses for determining green plant area index and cover fraction.

**Figure 37 Digital Photo Analyses for Determining Green Plant Area Index and Cover Fraction**

Collaboration

We are collaborating with the following colleagues through the IMAGINES program:

- Roselyne Lacaze, Hygeos and Fred Baret, INRA
- Ferdinand Camacho (EOLAB) with flux data, FAPAR, LAI
- Fred Baret/Marie Weiss (INRA) (provided Pastis 57 sensors for deployment on the site).

Results

Soybean was the dominant crop planted by the private producers at CFIA for the 2014 growing season (Figure 38). The four following crops were monitored: spring wheat (Field 14), canola (Field 14NE), corn and soybean. Several PASTIS 57 units were deployed as illustrated in Figure 38 (with red triangles labelled P57_xxx). Fields were selected to cover a range of seeding dates. Rainfall was evenly distributed over the season.


**Figure 38 Layout of Crops Planted in 2014 at CFIA-Ottawa**

The delay in seeding and the absence of N application was well reflected in the dry biomass of spring wheat in field 14 (see Figure 39 and Figure 40).

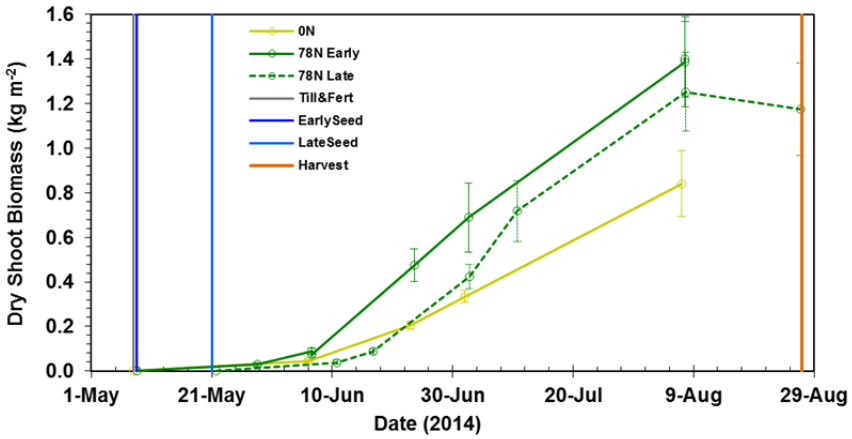


**Figure 39 Dry Shoot Biomass of Spring Wheat in 2014**

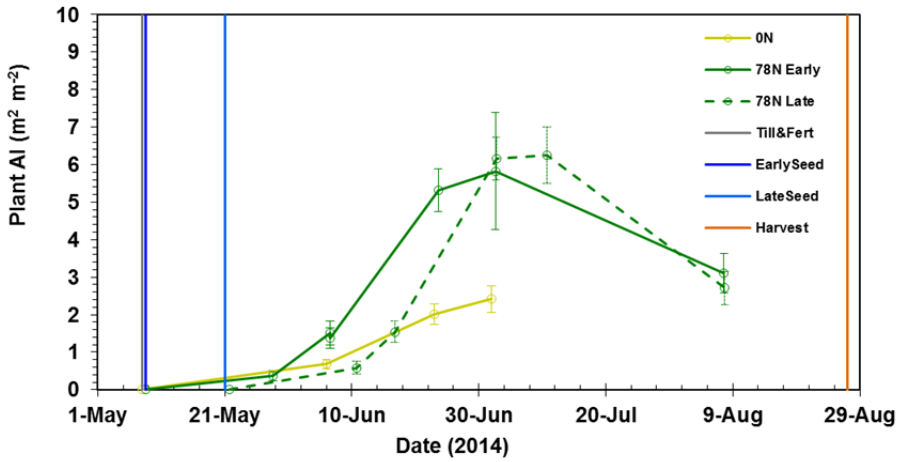


Figure 40 Plant Area Index of Spring Wheat in 2014

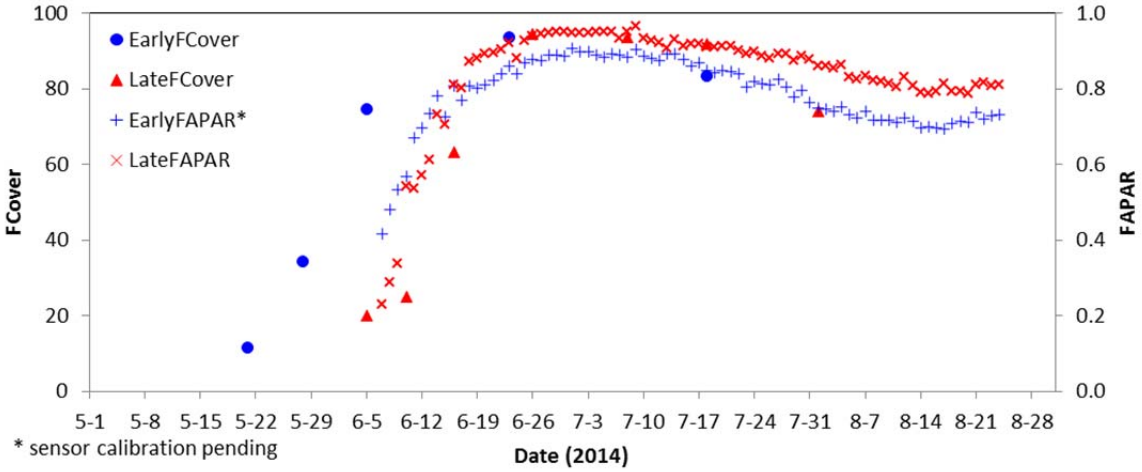


Figure 41 Cover Fraction and Fraction of Absorbed PAR

The cover fraction and fraction of absorbed PAR were measured in two contrasting sites of the wheat field (see Figure 41.)

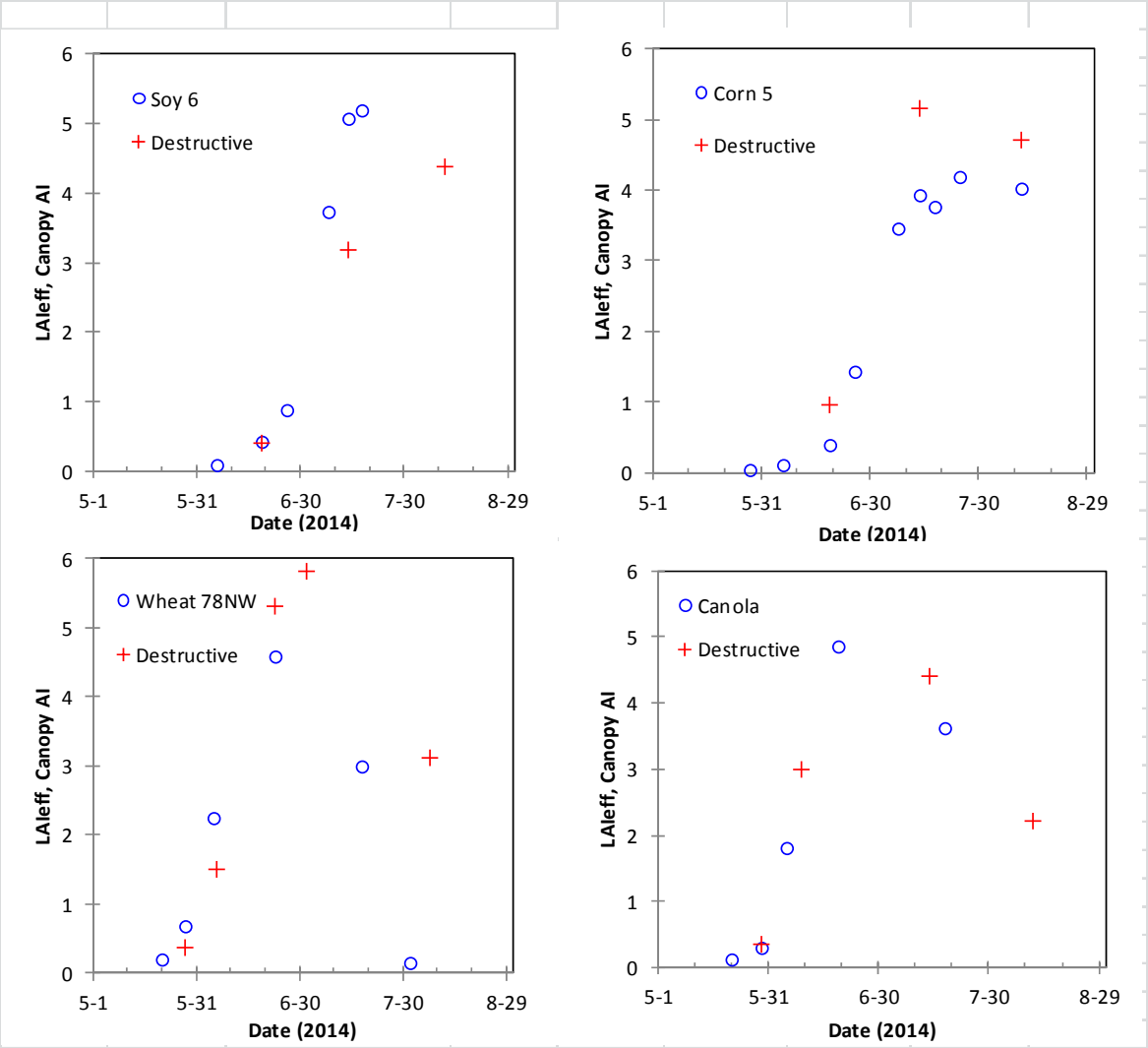


**Figure 42 Plant/Leaf Area Index of Selected Field Computed from Destructive Measurements and Photos**

The Plant Area Index was measured in all crops, but maximum leaf area was not always captured by the photos and destructive methods. All PASTIS 57 datasets were sent to INRA-Avignon last fall, and we are still waiting for the processed data.

Eddy covariance measuring systems were recording fluxes throughout the growing season. Fluxes are not yet converted to daily values. Similarly the yield data processing is not completed and the yield data from the private producers were not received yet although they were requested several times.

Can this approach be called 'best practice'? With a limited field crew (3 coop students and 2 research employees, who also maintain the experimental setup and process the data) the additional ground coverage is limited.

We are acquiring PASTIS PAR to monitor continuously 7 sites in addition to the PASTIS 57 sites. Additional long bars were also ordered to continuously record FAPAR for the 4 crops. This summer, the team of Dr Jiali Shang will contribute to the intensive field campaigns.

Plans for Next Growing Season

Next growing season, we will use the same approach. The main experimental site will be planted in Canola, and the second instrumented field will be planted in spring wheat. We anticipate to sample also corn and soybean fields.

As mentioned, we should be able to install PASTIS PAR sensors in addition to PASTIS 57.5 sensors. We will have additional fAPAR sites. We anticipate ordering the same type/quantity of EO data next year.

Publications

Liu, J., Pattey, E. and Admiral, S., 2013. Assessment of in situ crop LAI measurement using unidirectional view digital Photography. *Agric. For. Meteorol.* 169: 25-34.

Sansoulet, J., Pattey, E., Kroebel, R., Grant, B., Smith, W.N., Jego, G., Desjardins, R.L., Tremblay, N., Tremblay, G. 2014. Comparing the performance of STICS, DNDC and DayCent models for predicting N uptake and biomass of spring wheat in Eastern Canada. Field Crops Res. 156(1): 135-150.

Pattey, E., Liu, J., Admiral S., 2013. Performance of unidirectional view digital photography to retrieve crop LAI using GreenCropTracker software. American Society of Agronomy annual meeting, Tampa FL, Nov. 2013.

Camacho F., Baret F., Weiss M., Lacaze R., Di Bella C., Demarez V., Merhez Z., Rudiger C., De la Cruz F., Pat G.M.., Tapela M., Pattey E., Mattar C., Rojas J., Erena M., Chirima G.J.., Barcza Z., Waldner F. 2014. FAPAR in situ measurements network of sites within the IMAGINES project. First Workshop CEOS LPV FAPAR sub-group. Ispra, Italy, 23-24 January 2014

Pattey, E.; Jégo, G.; Mesbah, S. M.; Liu, J.; Hagolle, O. 2014. Impact of LAI Assimilation Approach on STICS Crop Model Performance to Predict Yield and Biomass of Field Crops. SENTINEL -2 for Science Workshop. ESRIN, Frascati, Italy, 20-22 May 2014.

Pattey, E., Jégo, G., Vanderzaag, A., Liu, J., Qian, B., Smith, W., Geng, X., Baret, F., Beaudoin, N., Desjardins, R., Fernandes, R., Jarvis, I., Huffman, T., Lacaze, R., McNairn, H.,2014. JECAM CFIA-Ottawa. JECAM/GEOGLAM Science Meeting. Ottawa, Canada, 21-23 July 2014.

## 8.2 South Nation Watershed

Team Leader and members: Dr. Heather McNairn, Dr. David Lapen, Dr. Angela Kross

Project Objectives

The original project objectives have not changed. This JECAM site is being used as a test bed for the use of SAR sensors for crop identification and crop area estimation. As well, optical and SAR data are being collected to determine if these sensors are capable of measuring crop condition and crop stress in response to controlled tile drainage (CTD) practices. Research on soil moisture using SAR is conducted in an area within the South Nation Watershed, that is adjacent to the area used for intense biophysical measurements in the Little Castor sub-watershed.

Site Description

Locations

South Nation Watershed

| | | | |
|---|---|---|---|
| Site Extent | | Centroid: | 45.332, -75.050 |
| Top left: | 45.416, -75.214 | Bottom Right: | 45.249, -74.886 |

WEBs Sub-Watershed

| | | | |
|---|---|---|---|
| Site Extent | | Centroid: | 45.265, -75.176 |
| Top left: | 45.268, -75.214 | Bottom Right: | 45.248, -75.142 |

The overall extent of the South Nation watershed is approximately 3,900 km², with a centroid at coordinates 45º 11’ 53.4”N, 75º 15’ 39.6”W. Nestled within the greater watershed are two smaller study basins of focused study and research, namely WEBs (centroid of 45º 15’ 49.1”N, 75º 10’ 41.9”W, approximately) and Casselman.

**Drainage:**

The WEBs (Watershed evaluation of Beneficial Management Practices) study basin comprises a sub-‘tileshed’ (tile drained watershed, see area in orange in Figure 43) area of approximately 950 hectares. Mean field sizes within the WEBs basin are 4.75 hectares, with the largest reaching over 24 hectares.

**Crop Calendar and Agriculture Methods:**

Livestock and cash crops in the watershed consist of corn, soybean, wheat (Triticum spp.) and forages. Field crop rotations can vary. For cropland without hay planting, crop rotations follow a

three year sequence: cereals-corn-soybean. Cropland with hay has a six year cycle: cereals-corn-soybean, and the following three years in hay. However, rotations can be heavily impacted by market conditions, and repetitive sequences of crops have been observed (for example corn).

Farms located within the WEBs basin are generally dedicated to dairy production. Manure spreading is normally done in either late summer or early fall. Conventional tillage, which is the dominant tillage practice in the study area, typically consists of spring cultivation and fall ploughing.

Just less than 50% of the WEBs study area receives liquid or solid bovine manure as a fertilizer amendment in spring and/or fall. Chemical fertilizer application rate varies according to the type of crop grown.

**Climate and Weather:**

Situated in a cool temperate humid continental climate in eastern Ontario Canada, mean yearly air temperatures are approximately 6.2ºC, total yearly precipitation is approximately 963 mm, and total yearly rainfalls are approximately 771.

**Soils:**

Dominant soils at the WEBs site are Bainsville silt loams, characterized by layered silt and fine sand, overlying clayey deposits, with poor natural drainage. The lower hydraulic conductivity clayey soils lie beneath top soils at approximately 1.0–1.5m depth.

**Topography:**

Local slope of the study area is generally <1%.

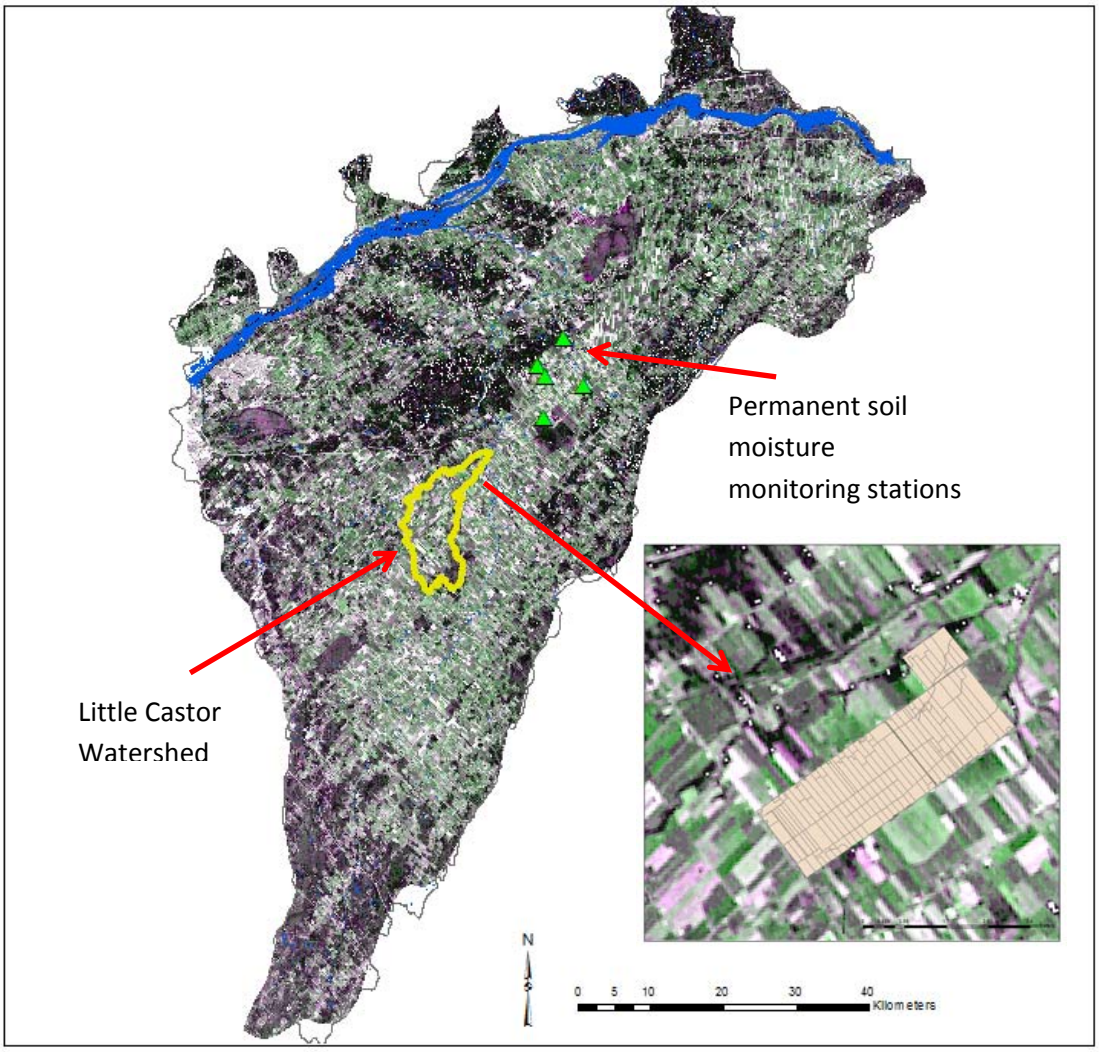


**Figure 43 South Nation Watershed JECAM Site**

EO Data Received/Used

**Table 10 Summary of South Nation Data Acquisitions**

| Supplier | Satellite Sensor | Number of scenes used | Range of dates | Processing level |
|---|---|---|---|---|
| Blackbridge | RapidEye (RE1 – RE5) | 20 | May 06th – September 26th | Basic product Level 1B |

In situ Data

During the 2014 growing season, a variety of crop production variables were collected at weekly intervals including: leaf area index using hemispherical photos (Figure 44), reflectance (using Cropscan), crop height, and phenology (Figure 45) and plant biomass. Measurements were done at corn, soybean and forage fields under controlled and uncontrolled drainage management. There are currently five permanent soil moisture monitoring stations (Figure 46), weather stations as well as field collected measurements of leaf chemistry and soil carbon flux.

a) b)

**Figure 44 Hemispherical Photos of Corn and Soybeans in: a) June (downward photos) and b) July (upward photos)**

a) b)

**Figure 45 Determination of Phenological Phases of Corn: a) Vegetative Phases and b) Reproductive Phases**

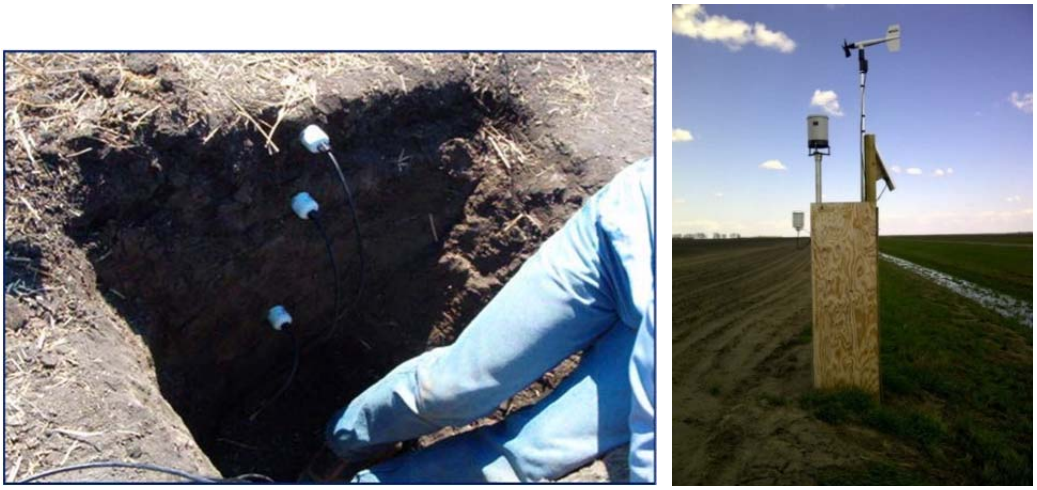

**Figure 46 Soil Moisture Station**

Collaboration

We have not been approached to participate in a collaborative project with other sites.

Results

This section presents findings from multiple years of data, not only 2014. A variety of vegetation indices were derived from the RapidEye imagery, including the: NDVI, simple ratio (SR), red edge normalized difference vegetation (NDVIre), red edge simple ratio (SRre), modified triangular vegetaton index (MTVI2), and red edge triangular vegetation index (RTVI). Landsat and SPOT4/5 images were used to derive the land surface water index (LSWI) and the moisture stress index (MSI). TerraSAR-X and RADARSAT-2 images were used to derive backscatter and ratio indices.

The relationships between the vegetation indices and ground measured LAI and biomass were established (based on data from 2011 to 2013, Figure 47 and Figure 48). (In all panels of Figure 47, dots represents soybean, triangles represent corn. The solid line is the best-fit function for the combined crops. All LAI sampling site observations were used to illustrate the relationships. In Figure 48, all total biomass sampling site observations were used to illustrate the relationships.) These relationships were used to create LAI maps for 2005 to 2013, which enabled the assessment of the response of crops to controlled and uncontrolled tile drainage at the field level (Figure 49)).

The results showed that Corn LAI from CTD fields was maintained or significantly higher relative to the LAI from UCTD fields, in 13 of the 14 site-years (over 7 years); corn biomass from CTD fields was also maintained or significantly higher in all 3 site-years of the study. For soybean, LAI from CTD fields was maintained or significantly higher in 4 of the 6 site-years (over 5 years); biomass from CTD fields was maintained in all 3 site years. For both crops, July and growing season (May to August) rainfall were potentially important variables for predicting crop responses to the drainage practices. The CTD practice was especially beneficial in drought years, and a more aggressive management of the CTD system, especially in the months July and August could improve the performance of the practice in the context of corn and soybean development.

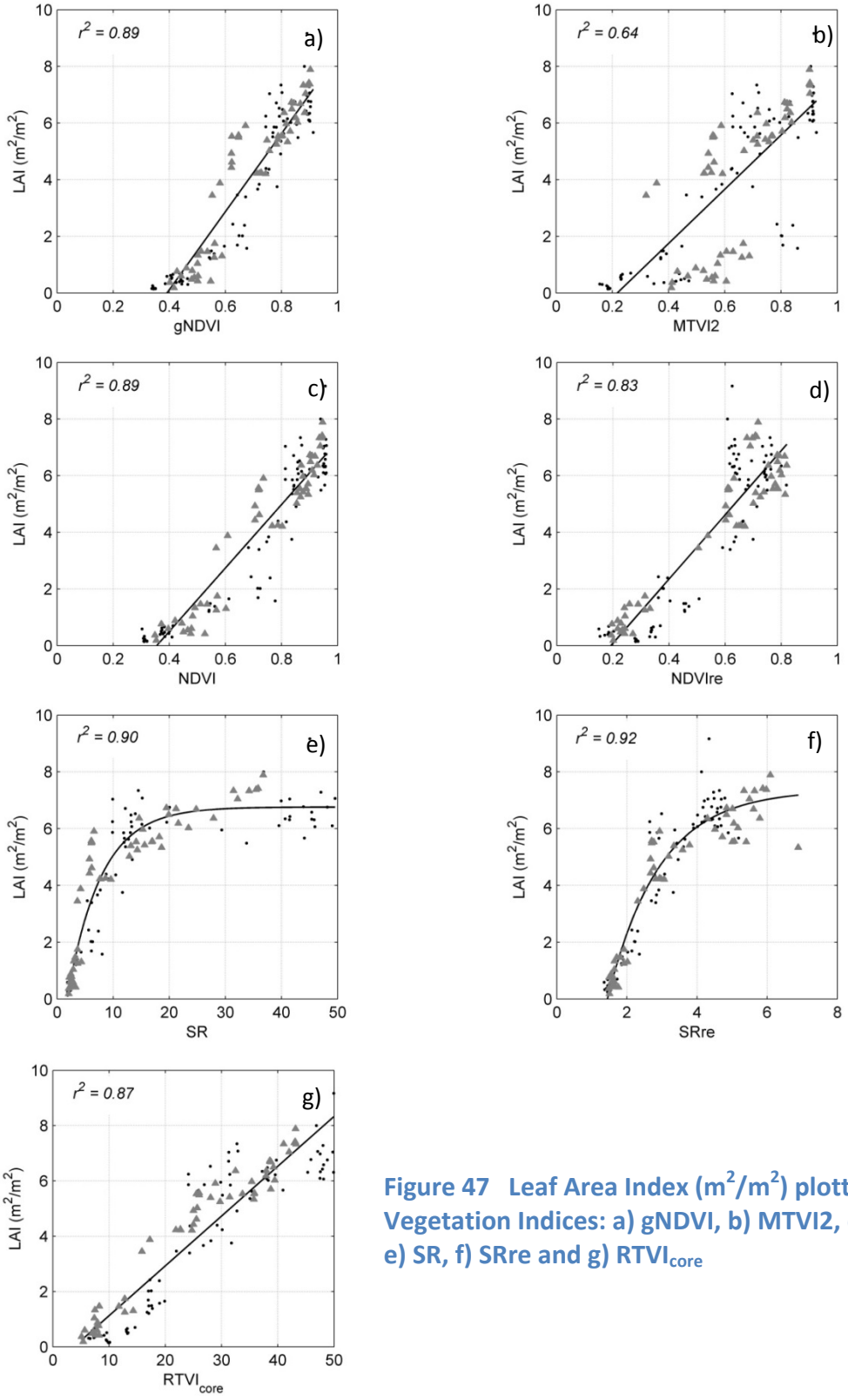


**Figure 47 Leaf Area Index ($m^2/m^2$) plotted against Vegetation Indices: a) gNDVI, b) MTVI2, c) NDVI, d) NDVIre, e) SR, f) SRre and g) $RTVI_{core}$**

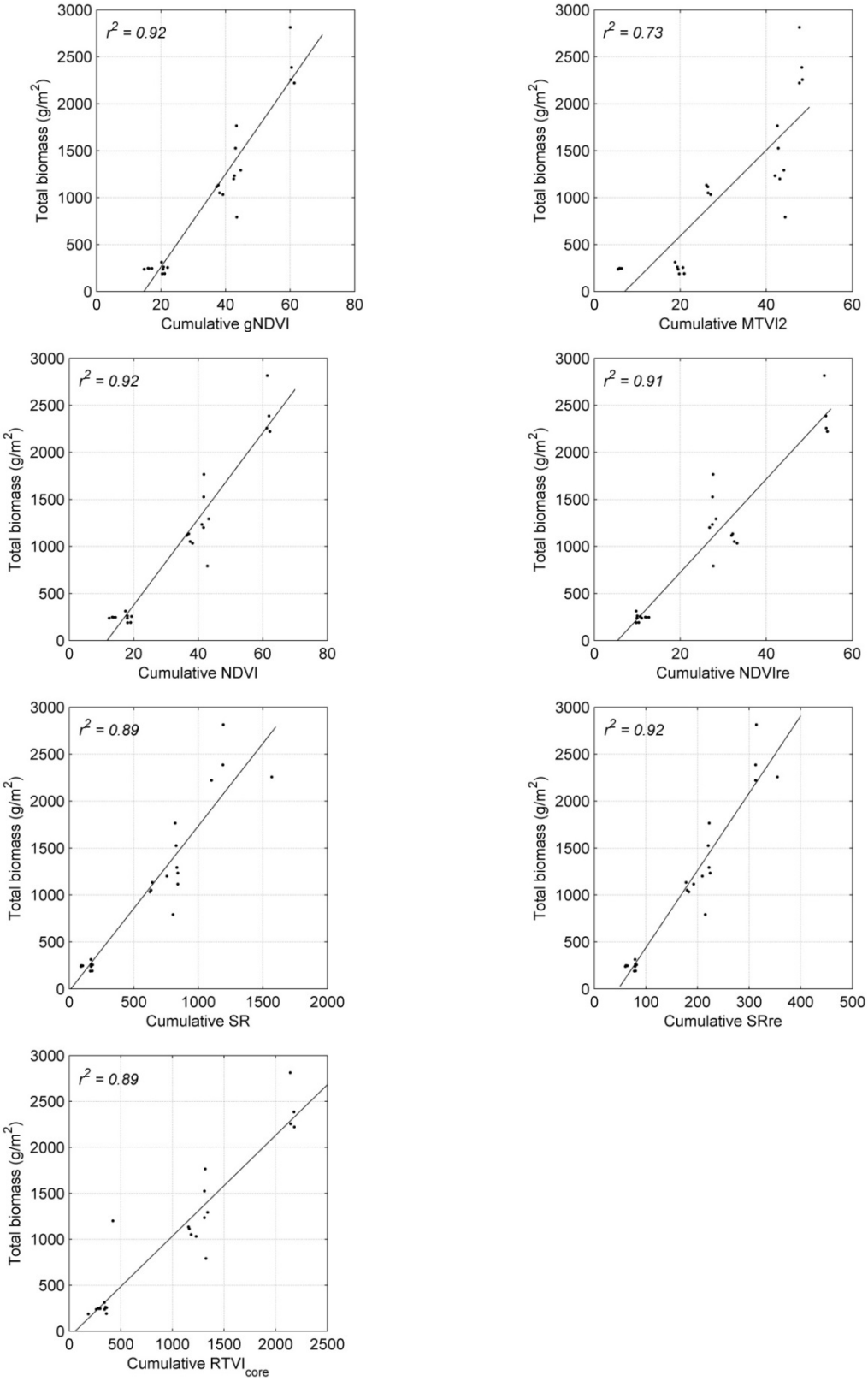


**Figure 48 Relationships between Cumulative Vegetation Indices and Total Dry Corn Biomass**

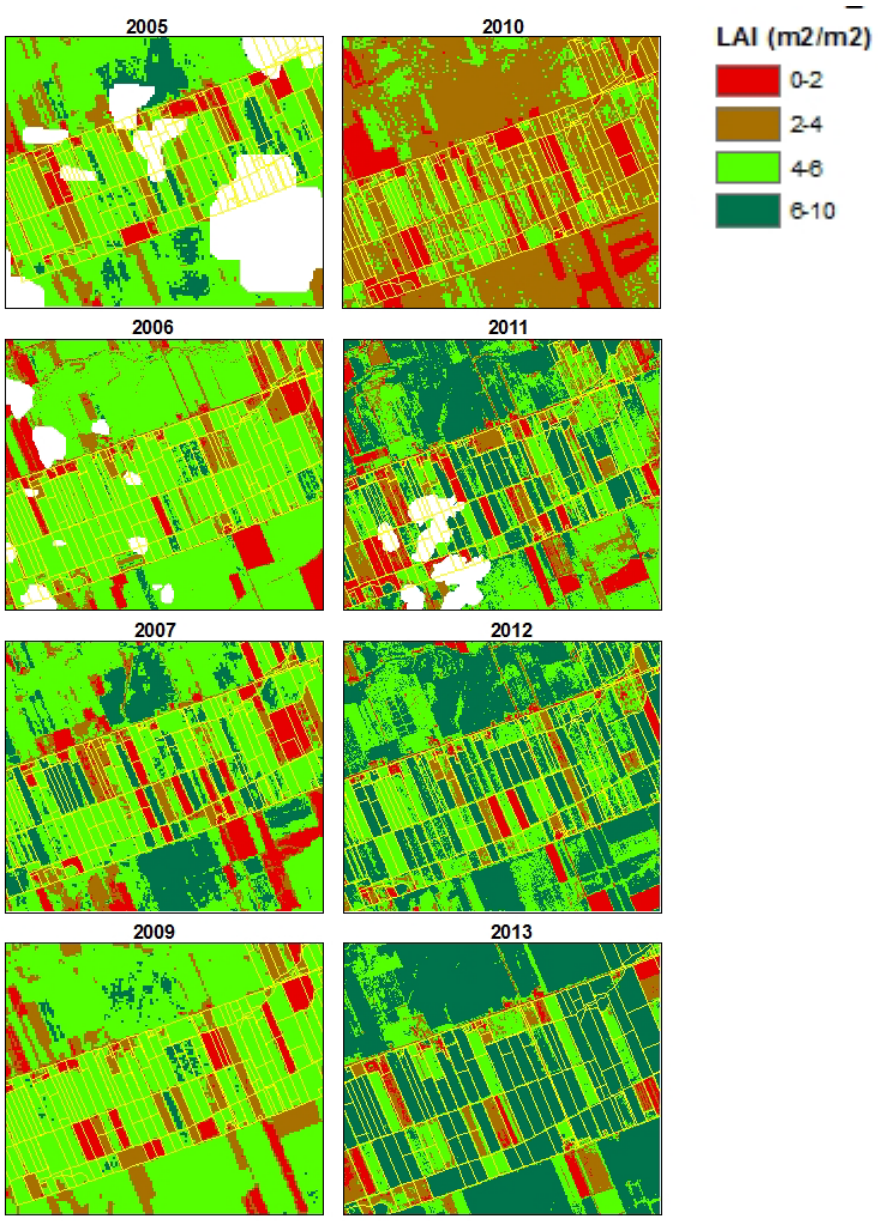


**Figure 49 Maps of Leaf Area Index between 2005 and 2013**

To evaluate the potential of SAR to deliver early season crop classification, we used a supervised decision tree classifier with TerraSAR-X (VV, VH) and RADARSAT-2 (HH, VV, HV/VH). Either the C-Band or X-Band data were capable of delivering highly accurate maps of corn and soybeans at the end of the growing season. Accuracies far exceeded 90% (Figure 50). Of particular interest was the finding that with three early season TerraSAR-X images, corn could be accurately identified by the end of June, a mere six weeks after planting and at a V6 vegetative growth stage (where the 6th leaf collar is visible).

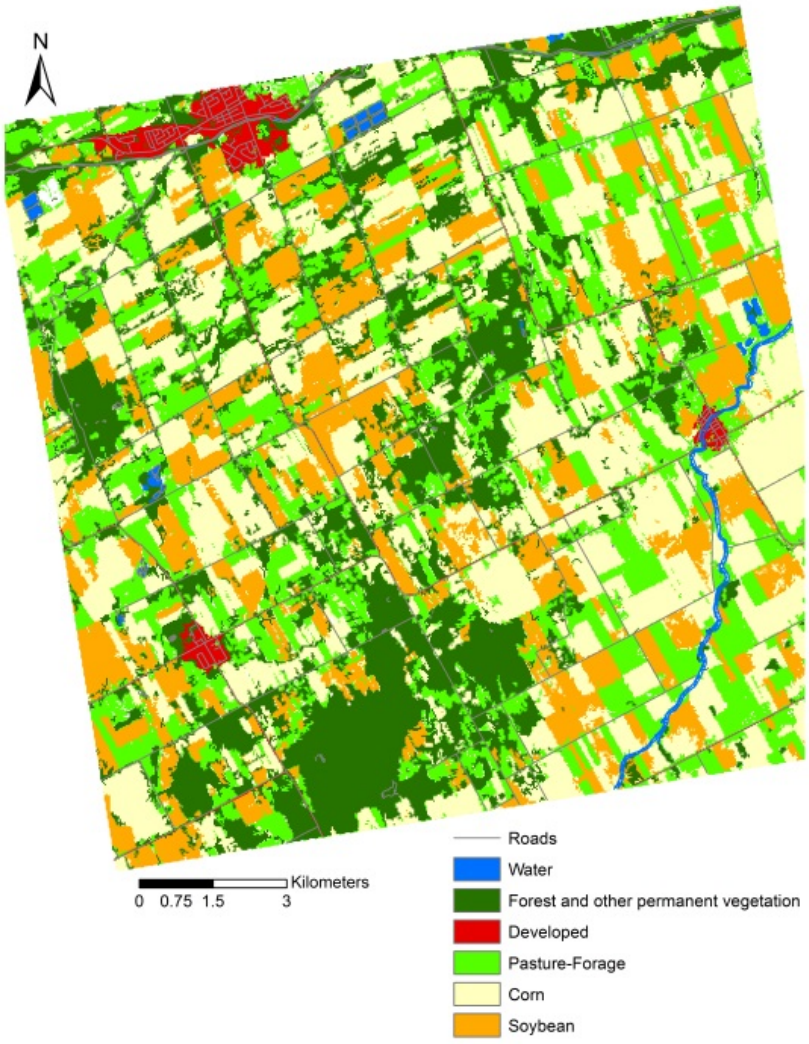


**Figure 50 An End-of-season Classification Map derived from TerraSAR-X (overall accuracy of 97.2%) (taken from McNairn et al. 2014)**

Identification this early in the season would assist in forecasting corn production. Soybeans required additional acquisitions given the variance in planting densities and planting dates in this region. In this case, accurate soybean classification required TerraSAR-X images until early August when seed development was beginning (R5 reproductive stage).

Plans for Next Growing Season

It is still uncertain, but RapidEye acquisitions will continue.

Publications

Kross, A., Lapen, D., McNairn, H., Sunohara, M., & Champagne, C. (under review). Crop response to controlled tile drainage under varying weather conditions in eastern Ontario, Canada. *Agriculture Water management.*

Angela Kross, Heather McNairn, David Lapen, Mark Sunohara, Catherine Champagne (2014). Assessment of RapidEye vegetation indices for estimation of leaf area index and biomass in corn and soybean crops. *International Journal of Applied Earth Observation and Geoinformation. (*http://dx.doi.org/10.1016/j.jag.2014.08.002).

McNairn, H., Kross, A., Lapen, D.R., Caves, R., and Shang, J. (2014). "Early Season Monitoring of Corn and Soybeans with TerraSAR-X and RADARSAT-2.", *International Journal of Applied Earth Observation and Geoinformation*, 28, pp. 252-259. doi : 10.1016/j.jag.2013.12.015. (http://dx.doi.org/10.1016/j.jag.2013.12.015).

## 8.3 Red River Watershed

Team Leader and Members: Ian Jarvis, Andrew Davidson, Heather McNairn, Jarrett Powers, Bahram Daneshfar, Catherine Champagne, Jiali Shang.

Project Objectives

The original project objectives of the site have not changed. They are:

- Crop Mapping at 30m pixel resolution
    - 2014 growing season crop inventory maps were created (30m resolution) covering all Manitoba as a part of the Agriculture and Agri-Food Canada annual EO-based national crop inventory program.
    - Developing spatial data and very accurate EO-based crop identification at 5m pixel resolution: Testing various EO-statistically-based methods and developing methodologies for highly accurate classification of target crops in different parts within the Manitoba pilot area with various levels of landform homogeneity. A journal paper is submitted for publication related to this component.
    - Testing the application of multivariate statistical methods to improve classification of pasture and forage crops from some of the annual target crops within the Manitoba pilot site. Results submitted for publication as a journal paper.
    - Testing, developing and applying geostatistical methodologies for re-allocation of target variables to the Terrestrial Monitoring sampling framework points within the prairie province based on the results of the pilot sites.
    - Developing spatial databases based on the above methods to estimate value:

1. As discrete data for the location of the samples of the Terrestrial Monitoring Framework, and depending on the variable
2. As continuous spatial data.

- Methods to accurately estimate the area of target major crops based on the stratification of the pilot sites by farming systems are being tested and developed.

- Crop Condition/Stress
  - Collected crop phenology, leaf area index, and biomass over selected fields in 2014 (Figure 54).
- Soil Moisture
  - With the addition of 3 new stations in 2014, this site currently has twelve automated in situ monitoring stations set up to capture larger scale variation in soil moisture to support calibration and validation of remotely sensed and modeled soil moisture data products. The data from these stations is collected every 15 minutes and transmitted to a central server, where it undergoes a quality control filtering before it is released for distribution.
  - Soil moisture measurements were taken at 5-cm depth weekly over two spring wheat fields, two corn fields, two canola fields and two soybean fields throughout the growing season using a Theta probe.
- Crop Residue, Tillage and Crop Cover Mapping
  - Nothing for 2014.

Site Description

- Location: Red River and Assiniboine River Basins, Manitoba (MB), Canada (see Figure 51).
- Topography: The majority of the soils in the study area are derived from lacustrine-based depositions and are very flat. The northern edge of the study area is more influenced by glacial-till deposition and has a lower relief ridge and swale topography.
- Soils: The majority of soils have a clay surface texture as a result of lacustrine deposits. Soils in the southwest region of the study area have sandier surface textures (sands-loamy sands) overlaying heavier clay deposits. Soils in the northern region are generally finer textured loams-clay loams with the occurrence of stones as a result of glacial-till deposits.
- Drainage class/irrigation: The majority of the soils are imperfect to poorly drained. A large network of surface drains is in place to allow the production of annual crops. A limited amount of irrigation exists in the area near Portage la Prairie and Carmen on lands devoted to the production of potatoes and high-value horticultural crops. Tile drainage is installed on a small percentage of land around Carmen on imperfectly drained soils that are used for high value crop production.
- Crop calendar: Early May – early June (seeding), August – early October (harvest).

- Field size: Quarter Section - 64 hectares (160 acres).

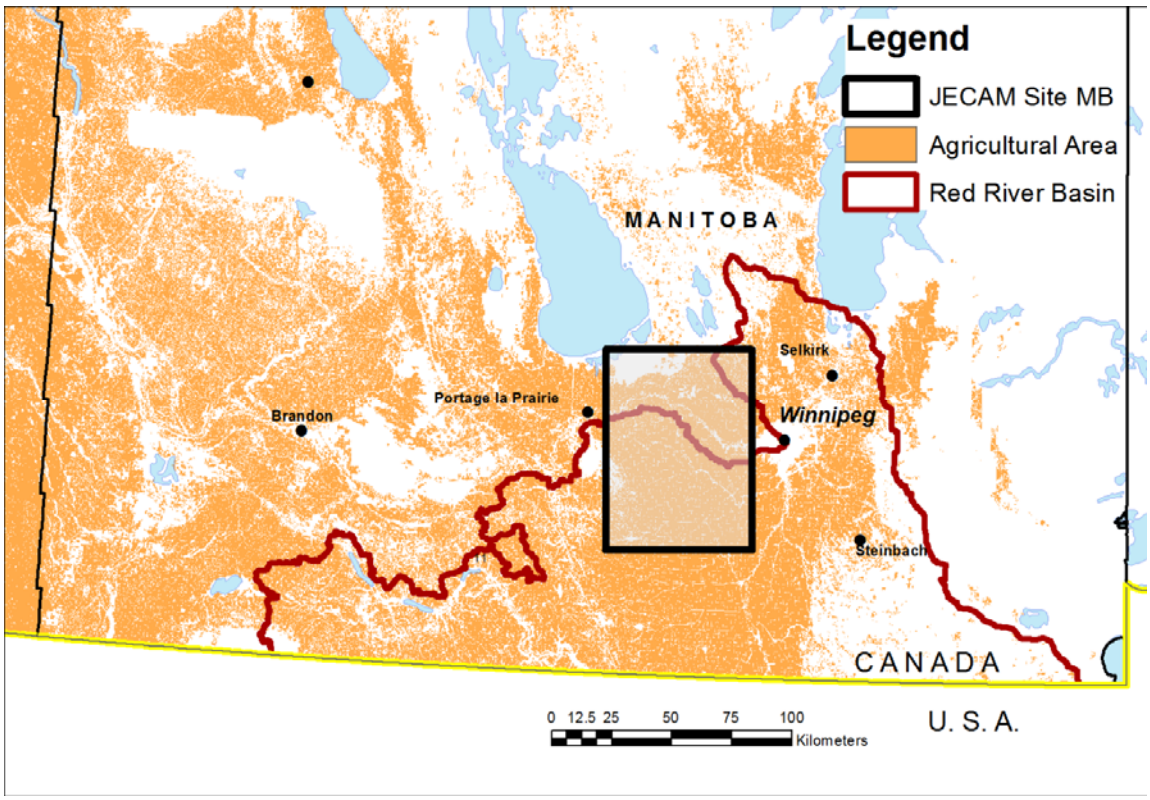


**Figure 51 Location of the JECAM Monitoring Site in Southern Manitoba, Canada**

- Climate and weather: The study area falls into the Humid Continental climate zone with cold winters and warm summers. Precipitation is distributed throughout the year with the majority of precipitation falling in the spring and summer months.
- Agricultural Crops used: Land is primarily used for the production of annual crops. Primary crops include: wheat, oats, canola, soybeans, corn. Potato production and other horticultural crops are produced near Carmen and Portage la Prairie. Conventional and minimum tillage systems are used for most annual crop production. The more marginal land in the northern areas is used for forage and pasture production.

**Figure 52 Example of the General Morphology and Landscape of the JECAM Monitoring Site in Manitoba, Canada**

EO Data Received/Used

Landsat 8, RADARSAT-2, RapidEye data were acquired during the growing season of 2014.

In situ Data

Presently there are 12 in situ soil moisture monitoring stations in the Red River basin site as indicated in Figure 53. Intensive crop biophysical parameters were measured weekly throughout the growing season in 2014 for spring wheat, corn, soybean, and canola.

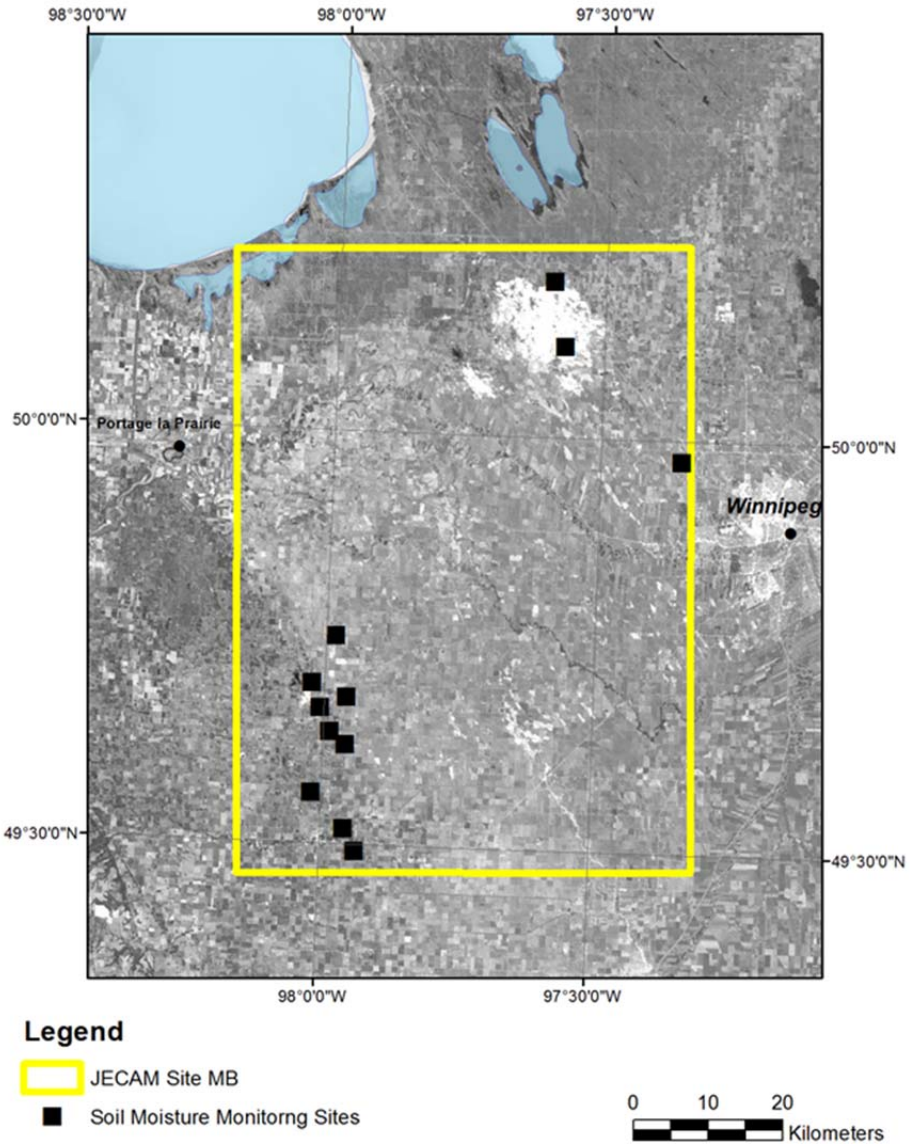


**Figure 53 Location of the 12 In situ Soil Moisture Monitoring Stations within the JECAM Monitoring Site in Southern Manitoba, Canada**

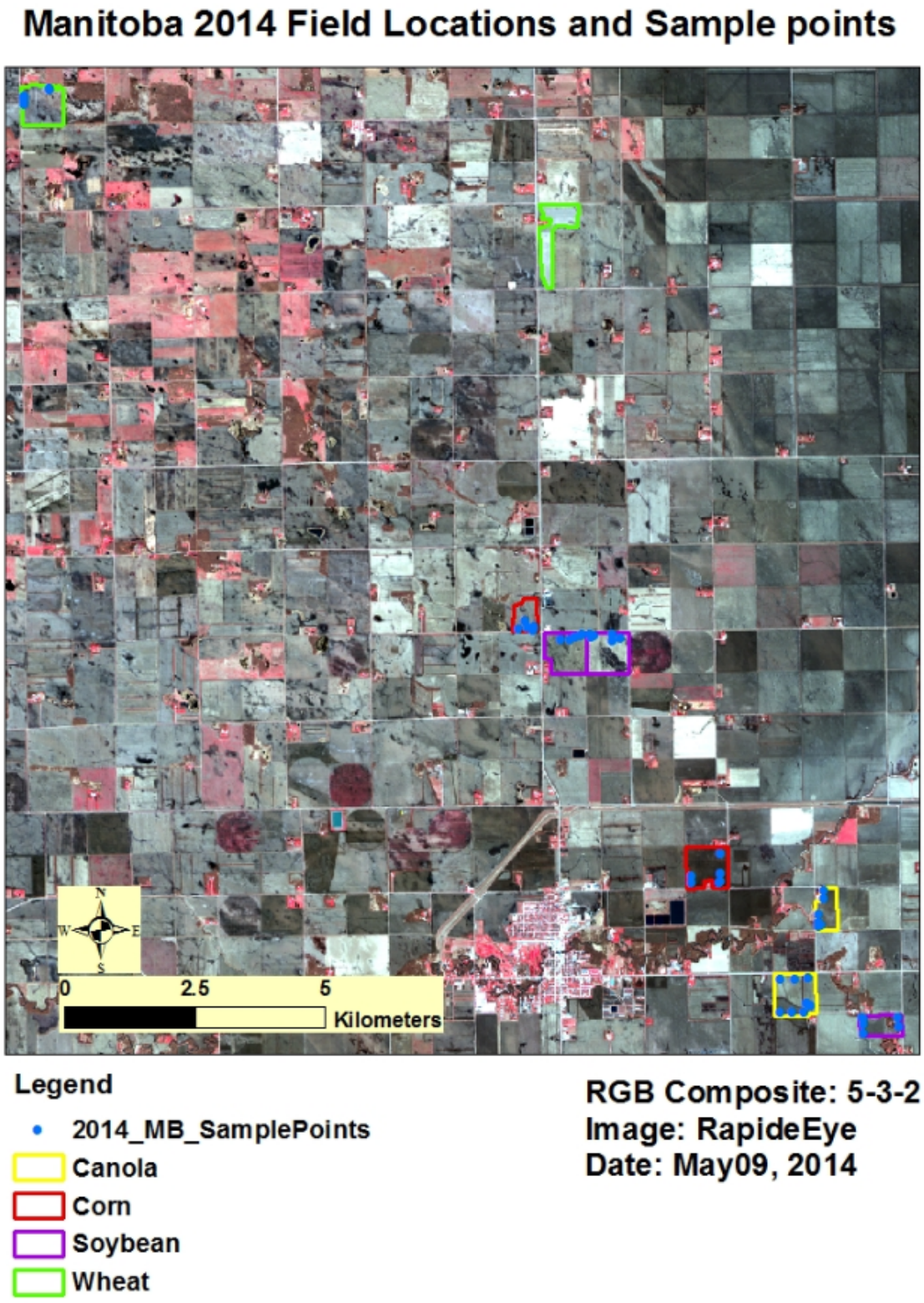


**Figure 54 Intensive Field Sampling Distribution of the JECAM Monitoring Site in Manitoba, Canada**

A crop type map (30 m resolution) was created for the whole area including the JECAM monitoring site for the 2014 growing season. Methods for accurate crop area estimation based on the annual crop inventory and crop types identified at the locations of the sampling framework of the monitoring sections are being developed.

Plans for Next Growing Season

The EO-based 2014 crop inventory map (30 m resolution) will be created for the whole agricultural area covering the JECAM monitoring area. The accuracy of crop classes is estimated to be around 85%. Field work will be done to record crop types for all fields within some of the monitoring sections located in the JECAM monitoring area. Results will be applied to develop methods for very accurate crop area estimations.

Crop conditions will be monitored at several time intervals in an area south of the JECAM monitoring site (Figure 51). Methods to derived crop condition from radar and optical satellites will be developed.

Soil moisture mapping from active and passive microwave is being piloted over this site due to the high quality soil moisture validation available.

Publications

Wiseman, G., McNairn, H., Homaayouni, S., Shang, J**.** (2014). RADARSAT-2 Polarimetric SAR Response to Crop Biomass for Agricultural Production Monitoring. IEEE Journal of Selected Topics in Applied Earth Observations and Remote Sensing, VPP (99):11.

# 9. China

## 9.1 Anhui

Team Leader and Members: Zhiyuan Pei (leader), Xiaoqian Zhang, Lin Guo, Fei Wang, Shangjie Ma, Heather McNairn, Jiali Shang, Juanying Sun.

Project Objectives

The original objectives have not changed but new ones have been added. The project objectives are:

- Crop identification and Crop Area Estimation
  - ✓ determine to what level of accuracy RADARSAT-2 can classify crops with a different cropping system in China.
  - ✓ determine whether RADARSAT-2 data alone can produce classification accuracies targeted by CAAE (overall and individual accuracies of 90%) at the early stages of the growing season.
  - ✓ develop comprehensive algorithms using RADARSAT-2 in combination with other data resources in the operational crop monitoring system.
- Crop biophysical parameters estimation
  - ✓ Leaf area index monitoring using RADARSAT-2 images at regional scale.

Site Description

- Location: Anhui Site (Chizhou), located in Middle China (30.8° N/117.6° E, Centroid). The main crops in Chizhou are Rice with one and two harvests per year, Winter Wheat, and Cotton. Other minor crops include vegetables, soybean, etc.
- Topography: Study site mainly located in flat area, and low hills around.
- Crop calendar: Early rice growth season lasts from March to June and late rice growth season lasts from July to October, while single-cropping rice growth season lasts from May to September.
- Field size: 1~6ha
- Climate and weather: Chizhou has subtropical monsoon climate. Annual average temperature is 16.5°C.

Figure 55 Photos of Chizhou, Anhui Site

EO Data Received/Used

RADARSAT-2:

- Space agency or Supplier: MDA and CSA
- Eleven RADARSAT-2 products were acquired in fine quad polarization mode during the critical rice growth stage in 2013, and 7 products in 2014. See Table 11. The FQ polarization scene swath is 25km and nominal resolution is 5.2 m*7.6 m. The processing level of the products is single look complex (SLC).

Table 11 RADARSAT-2 Data Acquired of Anhui Site

| Year | Date of pass | Incidence angle(°) | Year | Date of pass | Incidence angle(°) |
|---|---|---|---|---|---|
| 2013 | Mar 17 | 37.56 | 2014 | May 16 | 42.95 |
| | May 11 | 32.56 | | Jun 20 | 45.41 |
| | May 21 | 42.95 | | Jul 14 | 45.41 |
| | Jun 14 | 42.95 | | Aug 7 | 45.41 |
| | Jul 6 | 24.73 | | Aug 20 | 42.95 |
| | Jul 8 | 42.95 | | Aug 31 | 45.41 |
| | Jul 22 | 32.56 | | Sep 24 | 45.41 |
| | Aug 6 | 31.5 | | | |
| | Aug 19 | 42.23 | | | |
| | Sep 12 | 40.34 | | | |
| | Sep 29 | 45.41 | | | |

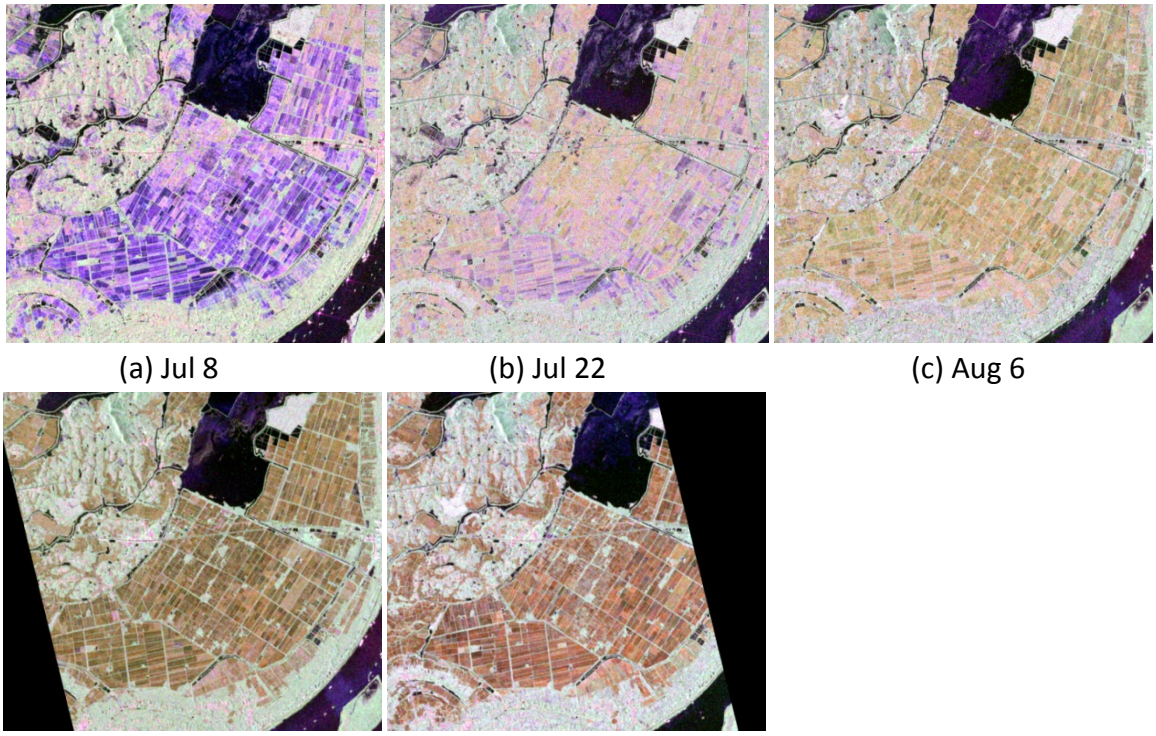

(a) Jul 8 (b) Jul 22 (c) Aug 6

(d) Aug 19 (e)Sep 12

**Figure 56 RADARSAT-2 Images of Single-crop Rice in 2013**

Figure 56 shows selected RADARSAT-2 images from 2013. Red indicates HH; green is HV and blue is VV.

In situ Data

Ten sample plots were established for measurements of rice canopy parameters like planting pattern, growing stage, seeding/transplanting date, plant height, Leaf area index (LAI), and weather conditions during key rice growing stages concurrently with the satellite pass. Hundreds of points for land cover type were collected once per season to assess the accuracy of rice identification.

**Figure 57 In situ Measurements**

Collaboration

No.

Results

*Rice leaf area index (LAI) monitoring using time-series RADARSAT-2 data*

**Figure 58 Multi-temporal LAI Distribution, 2013**

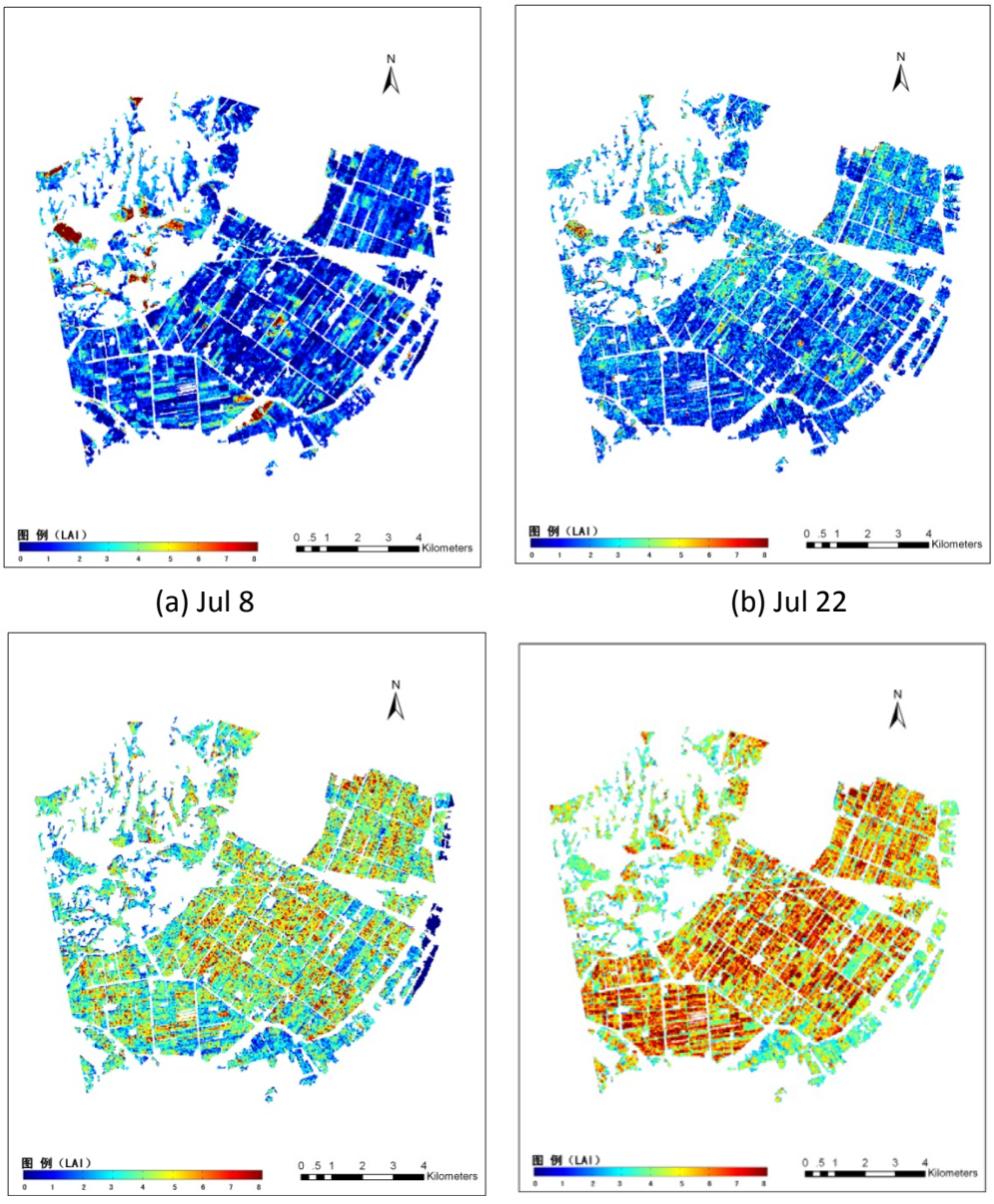


(a) Jul 8 (b) Jul 22

(c) Aug 6 (d) Aug 19

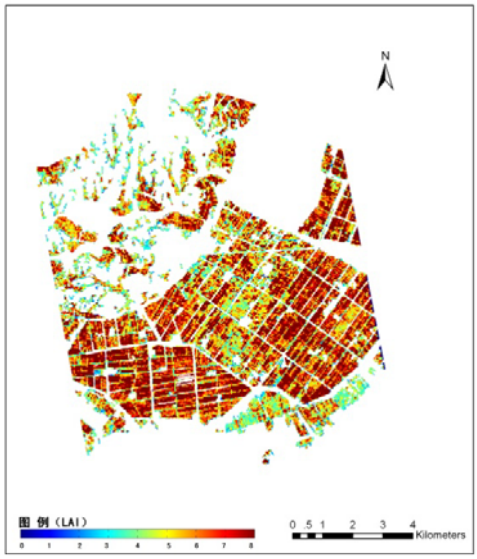


(e) Sep 12

*Rice identification*

Figure 59 shows rice identification from a RADARSAT-2 image on August 7, 2014.

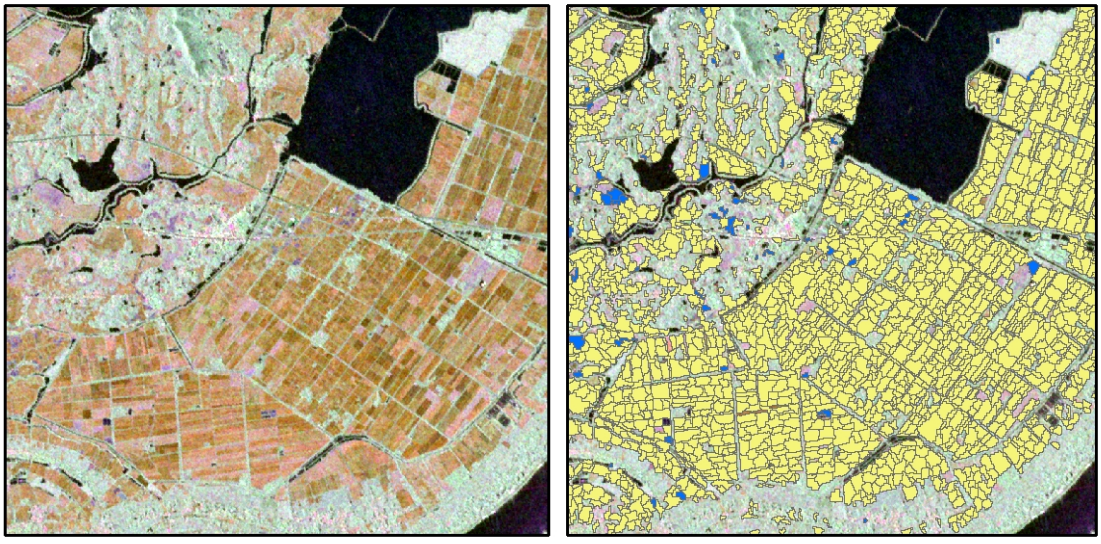

(a) original image(R:HH;G:HV;B:VV) (b) object-oriented classification


**Figure 59 Rice Identification Map Derived from RADARSAT-2 Image of Aug 7, 2014**

Plans for Next Growing Season

None yet.

Publications

No.

## 9.2 Guangdong

Note that last year, a team led by Professor Wu Bingfang reported on a site at Taishan in Guangdong province, China. This year's report is of a different site in the same province, executed by a different team.

Team Leader and Members: Zhiyuan Pei (leader), Xiaoqian Zhang, Lin Guo, Fei Wang, Shangjie Ma, Heather McNairn, Jiali Shang, Juanying Sun.

Project Objectives

The original project objectives have not changed. They are:

- Crop identification and Crop Area Estimation
  - ✓ determine to what level of accuracy RADARSAT-2 can classify crops with different cropping system in China
  - ✓ determine whether RADARSAT-2 data alone can produce classification accuracies targeted by CAAE (overall and individual accuracies of 90%) at the early stages of the growing season
  - ✓ develop comprehensive algorithms using RADARSAT-2 in combination with other data resources in the operational crop monitoring system
- Crop biophysical parameters estimation
  - o Leaf Area Index monitoring using RADARSAT-2 images at regional scale.

Site Description

- Location
  Guangdong Site (Leizhou), located in southern China (20.45° N/110.08° E, Centroid). The major crop in Leizhou site is rice with two harvests per year. Other minor crops include soybean, corn, vegetables, and aquatic plants.
- Topography
  Study site mainly located in a flat area, and low hills around.
- Drainage class/irrigation
  Almost all the rice planted regions have a good irrigation system.
- Crop calendar

The major crop is rice with two harvests per year. The early rice growth season lasts from early March to mid-late June. The late rice growth season lasts from August to November.

- Field size
  1~6ha
- Climate and weather
  Leizhou has a typical tropical climate. The average annual rainfall is above 2000mm.

**Figure 60 Photos of Leizhou (Guangdong) Site**

EO Data Received/Used

RADARSAT-2:

- Space agency or Supplier: MDA and CSA
- There are 9 RADARSAT-2 products (Table 12) in fine quad polarization mode acquired during the critical rice growth stage in 2013, and 7 products in 2014. The FQ polarization scene swath is 25km and nominal resolution is 5.2 m x 7.6 m. The processing level of the products is single look complex (SLC).

**Table 12 RADARSAT-2 Data for Leizhou, Guangdong Site**

| Year | Date of pass | Incidence angle(°) | Year | Date of pass | Incidence angle(°) |
|---|---|---|---|---|---|
| 2013 | Mar 18 | 43.79 | 2014 | Mar 25 | 45.41 |
| | Mar 30 | 45.41 | | Apr 1 | 40.34 |
| | Apr 6 | 40.34 | | Apr 30 | 43.79 |
| | Apr 30 | 40.34 | | May 24 | 43.79 |
| | May 22 | 37.56 | | Jun 17 | 43.79 |
| | May 31 | 33.6 | | Aug 16 | 45.41 |
| | Jun 15 | 37.56 | | Sep 9 | 45.41 |
| | Aug 28 | 40.34 | | | |
| | Sep 21 | 40.34 | | | |

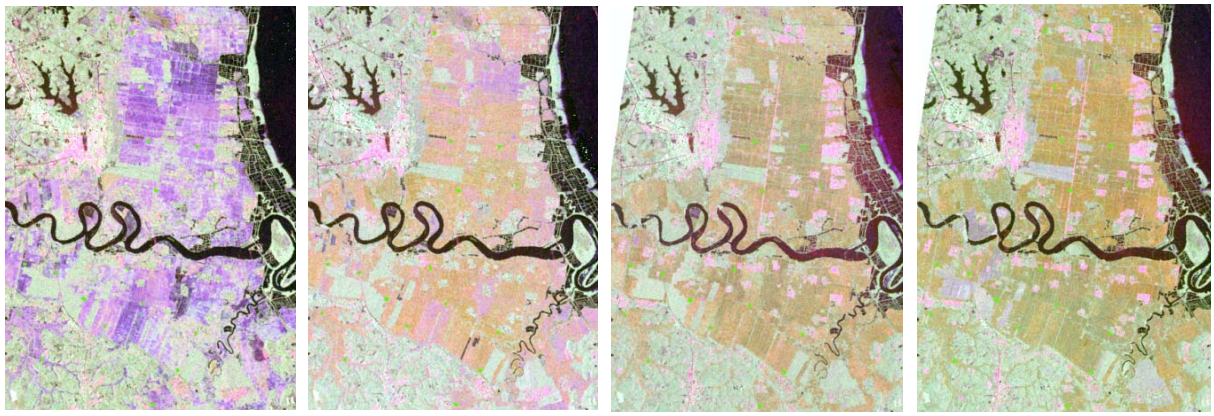

a) April 6 b) April 30 c) May 22 d) June 15

**Figure 61 RADARSAT-2 Images of Early Rice, 2013**

Figure 61 shows four RADARSAT-2 images of early rice in 2013. HH is red; HV is green; VV is blue.

In situ Data

25 sample plots (Figure 62) were established for measurements of rice canopy parameters like planting pattern, growing stage, seeding/transplanting date, plant height, Leaf area index (LAI), weather condition and digital photos during key rice growing stages concurrently with the satellite pass.

Land cover type was collected at hundreds of points once per season to assess the accuracy of rice identification.

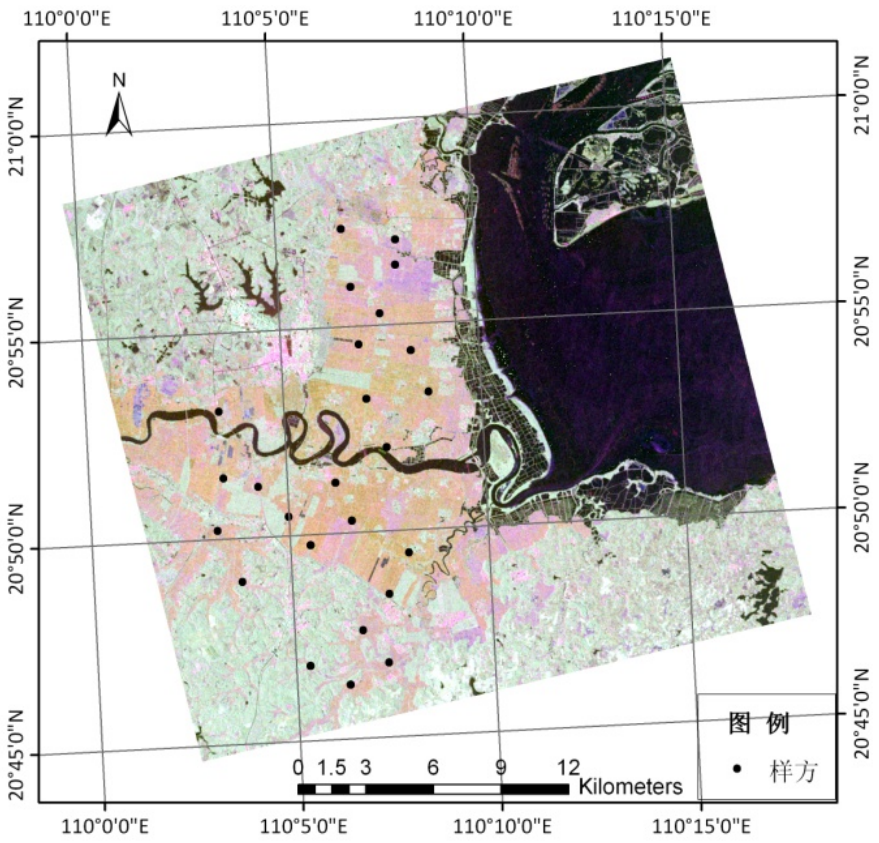


**Figure 62 Location of Sample Plots**

**Figure 63 In situ Measurements, Leizhou Site**

Collaboration

No.

Results

**Rice Leaf Area Index (LAI) Monitoring using Time-series RADARSAT-2 data**

Figure 64 shows time series backscattering coefficients and LAI value analysis.

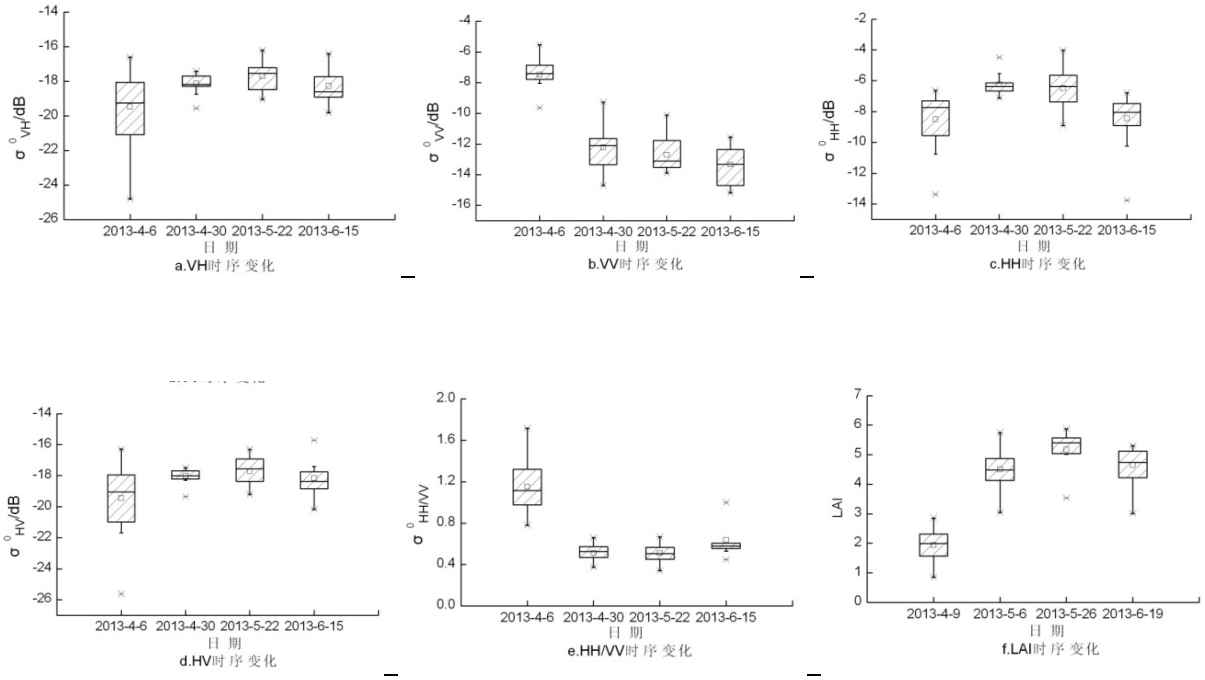


**Figure 64 Variation of Multi-temporal Backscattering Parameters and LAI Values**

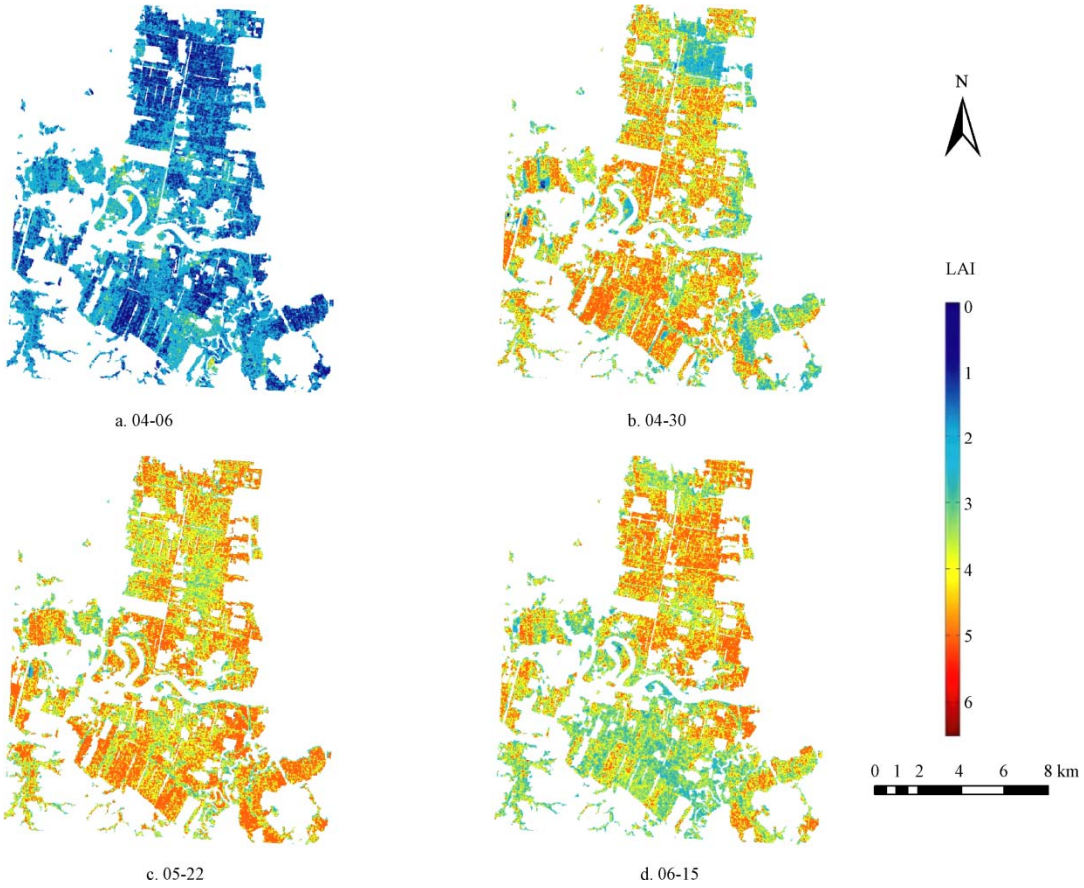


**Figure 65 Multi-temporal LAI Distribution Map in Early Rice Growth Season, 2013**

Figure 65 shows LAI mapping in the early rice growth season in 2013. Figure 66 provides validation of the results.

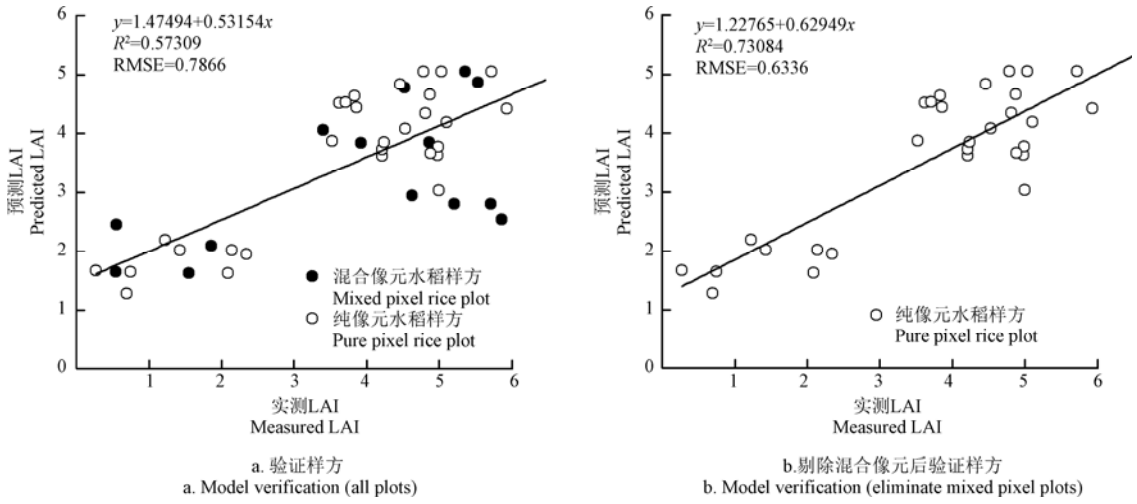


**Figure 66 Relationship between Measured LAI and Predicted LAI**

**Rice Identification**

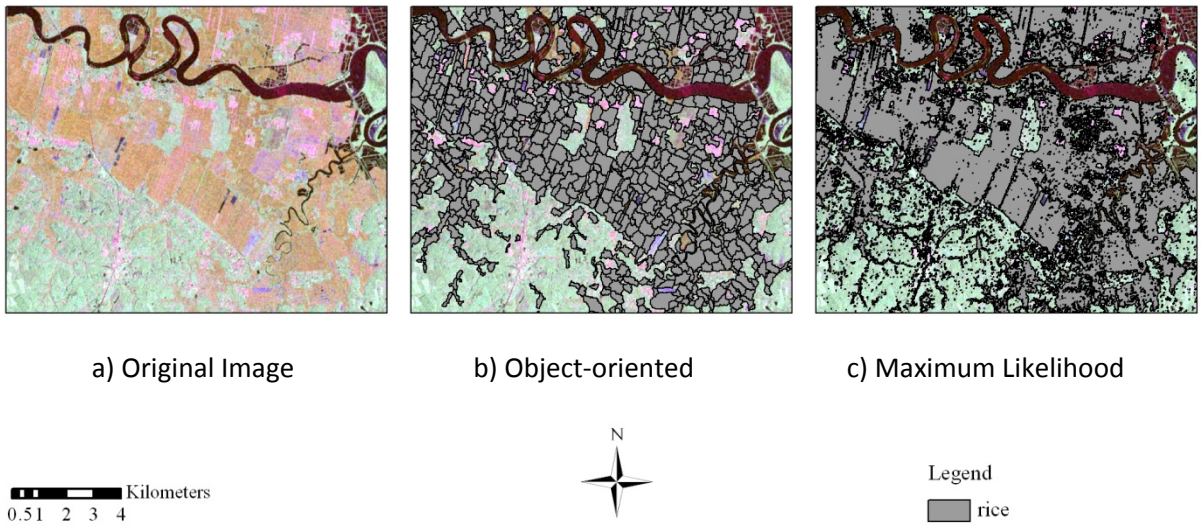


**Figure 67 Rice Identification Map Derived from RADARSAT-2 Image of 30 April 2014**

Plans for Next Growing Season

None yet.

Publications

Zhang Xiaoqian, Guo Lin, Ma Shangjie, et al. Application of rice leaf area index monitoring using time-series SAR data[J]. Transactions of the Chinese Society of Agricultural Engineering (Transactions of the CSAE), 2014, 30(13): 185—193. (in Chinese with English abstract)

## 9.3 Heilongjiang

No report received.

## 9.4 Jiangsu

Team Leader: Yun Shao

Members: Kun Li, Brian Brisco, Fengli Zhang, Long Liu, Zhi Yang, Weiguo Li

Project Objectives

The original objectives of the site have not changed. They are:

- Crop identification and Crop Area Estimation

Identify rice fields with polarimetric responses and scattering mechanisms, and estimate the rice acreage accurately.

- Crop Condition/Stress

Rice phonological stage retrieval, providing timely and accurate information about rice growth condition, in order to plan cultivation practices (irrigation, fertilization, etc.).

- Yield Prediction and Forecasting

A quantitative relationship between polarization variables and rice key parameters (biomass, LAI) will be established. Then a crop model, taking into account the variation of the time - domain and environmental stress, will be employed for rice yield prediction.

Site Description

The test site is located in Jinhu (33°15'22.33"N - 32°58'35.00"N, 118°49'39.97"E - 119° 6'51.67"E), Jiangsu Province, east of China (Figure 68). The terrain is flat, with the average altitude mostly less than 10m. The area belongs to the transition region between the subtropical and the temperate climatic zones, with four distinct seasons. The annual average temperature of the test site is about 13 to 16℃. The average precipitation is about 800 to 1200 mm every year, and more than half of the precipitation occurs from June to September. The sunshine hours can be up to 2400 every year. The soil type of this region is mostly yellow brown clay, which is favourable for rice plant development. The main paddy varieties in this area are hybrid rice (H-R) and japonica rice (J-R). There is one rice crop a year, with the growth cycle about 150 days, from early June to late October or early November.

There are two rice planting methods in the test site, transplanting and direct-seedling, which will produce two different rice field structures (Figure 69) and have a certain impact on rice yields. The size of rice field parcels is 1700 $m^2$ or so. In this study, forty-one sample plots were selected in the test site, covering twenty-nine transplanting fields and twelve direct-seedling fields. The distribution of these sample plots is shown in Figure 68. The cloud and sun symbols mean Transplant and Direct-planting Rice Fields respectively. Apart from agricultural land, the five other land cover types at the test site were forest, bare land (B-L), urban, crab ponds (C-P), and water.

**Figure 68 Location of Jiangsu Test Site and the Distribution of the Sample Plots**

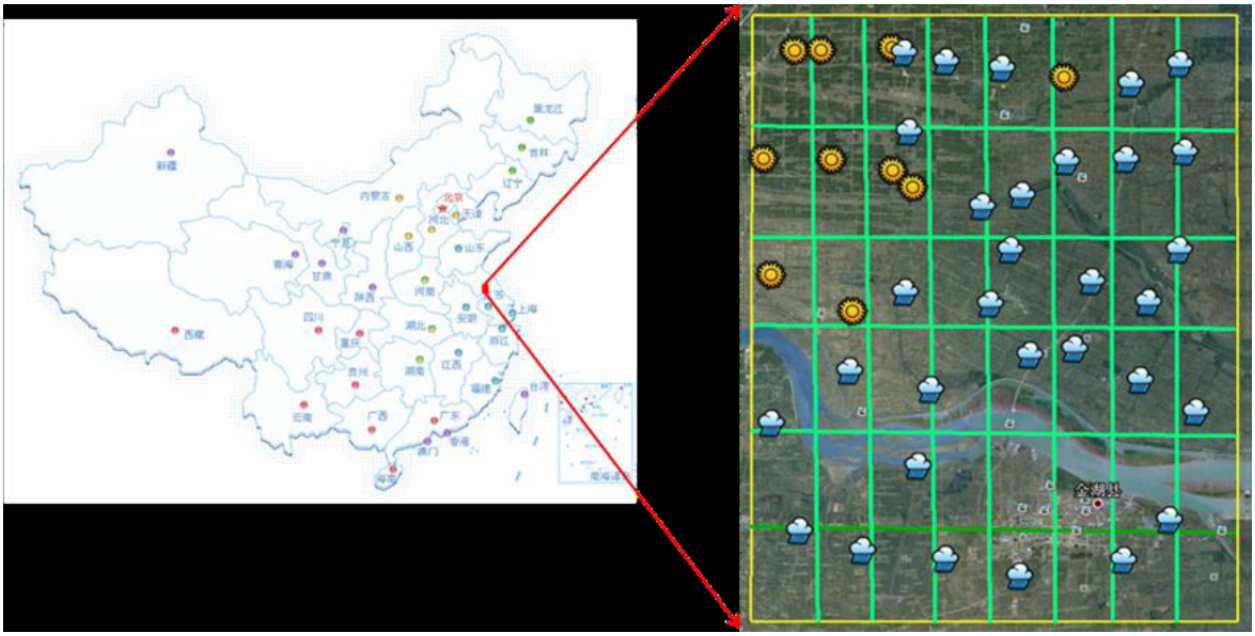

**Figure 69 Rice Fields in the Jiangsu Test Site**

(a) Transplanting (b) Direct-seedling

EO Data Received/Used

From late June to early November 2012, twelve RADARSAT-2 images were acquired, including eleven polarimetric images and one Multi-look Fine image. The details of the SAR data are displayed in Table 13. Compact polarimetry (CP) SAR data, with CTRL imaging model (T: right circular polarization, R: Horizontal and vertical polarizations) were simulated from eleven polarimetric SAR data. No more SAR data was acquired in 2013 or 2014.

| Dates | Mode | Product | Resolution (m) | | Image Size ($km^2$) | Incidence Angle ($^o$) | Look | Polarization |
|---|---|---|---|---|---|---|---|---|
| | | | Range | Azimuth | | | | |
| 6/27/2012 | FQ20W | SLC | 5.2 | 7.6 | 565 | 38.89 | 1 | HH/HV/VH/VV |
| 7/11/2012 | FQ9W | SLC | 5.2 | 7.6 | 571 | 27.53 | 1 | HH/HV/VH/VV |
| 7/21/2012 | FQ20W | SLC | 5.2 | 7.6 | 565 | 38.89 | 1 | HH/HV/VH/VV |
| 7/28/2012 | MF22W | SLC | 3.1 | 4.6 | 603 | 31.73 | 1 | HH |
| 8/4/2012 | FQ9W | SLC | 5.2 | 7.6 | 571 | 27.53 | 1 | HH/HV/VH/VV |
| 8/14/2012 | FQ20W | SLC | 5.2 | 7.6 | 565 | 38.89 | 1 | HH/HV/VH/VV |
| 8/28/2012 | FQ9W | SLC | 5.2 | 7.6 | 571 | 27.53 | 1 | HH/HV/VH/VV |
| 9/7/2012 | FQ20W | SLC | 5.2 | 7.6 | 565 | 38.89 | 1 | HH/HV/VH/VV |
| 9/21/2012 | FQ9W | SLC | 5.2 | 7.6 | 571 | 27.53 | 1 | HH/HV/VH/VV |
| 10/15/2012 | FQ9W | SLC | 5.2 | 7.6 | 571 | 27.53 | 1 | HH/HV/VH/VV |
| 10/25/2012 | FQ20W | SLC | 5.2 | 7.6 | 565 | 38.89 | 1 | HH/HV/VH/VV |
| 11/8/2012 | FQ9W | SLC | 5.2 | 7.6 | 571 | 27.53 | 1 | HH/HV/VH/VV |

**Table 13 Technical Parameters of RADARSAT-2 Data Acquired in 2012**

In situ Data

During the growing season in 2012, 12 ground campaigns were conducted (see Figure 70). No field work was conducted in 2014. We mainly concentrated on data analysis in 2014.

In 2012, field data was collected from three representative rice plants in each sample plot. The following were measured: variety, crop calendar, phenological stage, plantation geometry, plant structural information (plant height, number of leaves, leaf length and width, number of stems and of ears), plant biomass (dry and wet weight). Figure 71 displays Leaf Area Index (LAI), plant height, fresh and dry weight of transplanting rice in the whole growing season. Different symbols mean different fields. Figure 72 shows the same parameters for the 13 direct-seedling fields. Again, different symbols mean different fields.

Figure 70 Field Work - Jiangsu

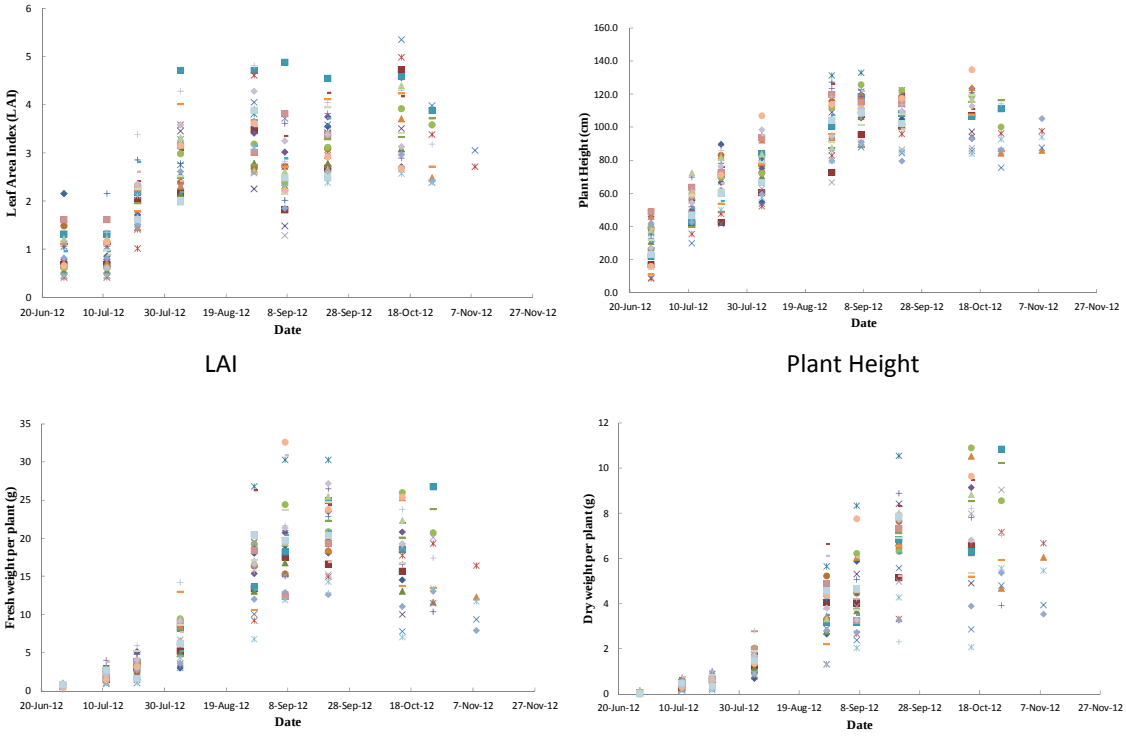


LAI Plant Height

Fresh Weight Dry Weight

Figure 71 Rice Parameters Collected from 29 Transplanting Fields during the Whole Growing Season

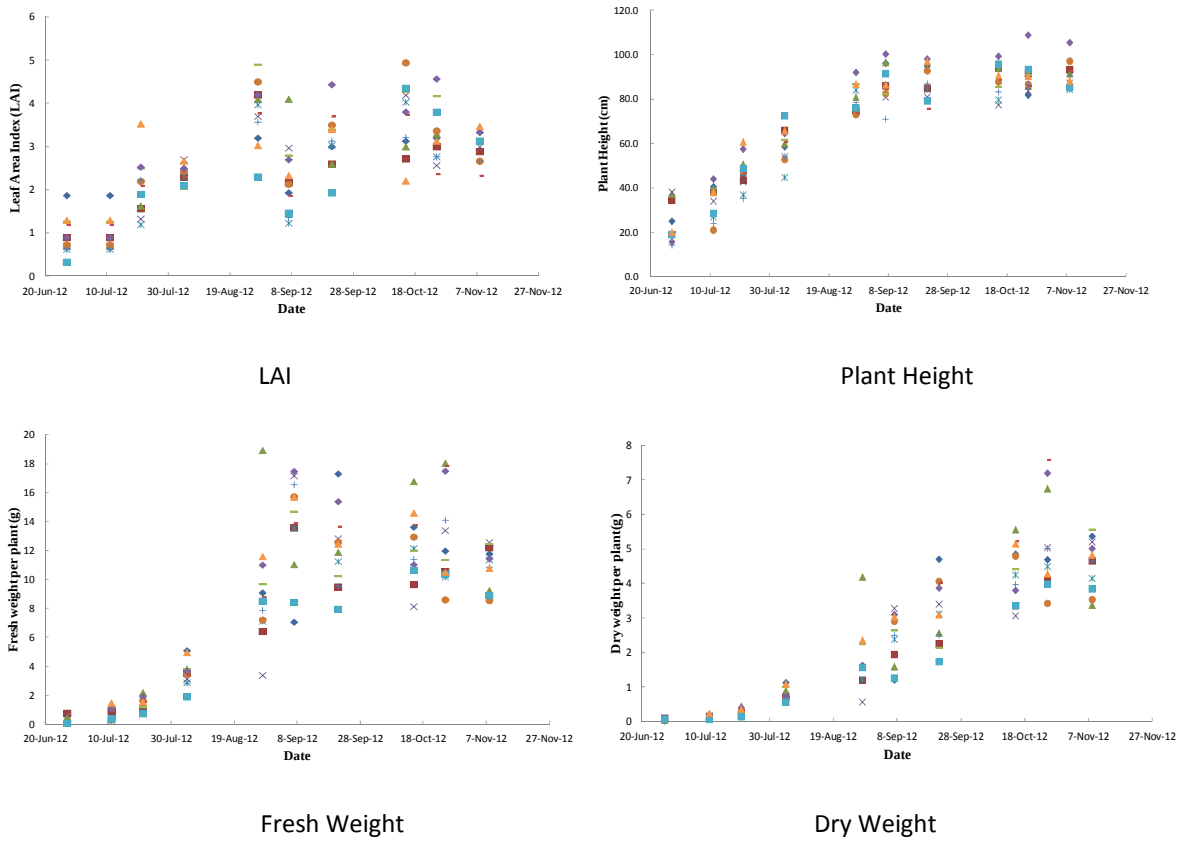


**Figure 72 Rice Parameters Collected from 13 Direct-seedling Fields during the Whole Growing Season**

## Collaboration

We have not been approached to participate in a collaborative project with other sites.

## Results

### Two Types of Rice Field Discrimination and Rice Area Estimation with CP Simulated SAR Data

To eliminate interference by forest, urban, and other land cover types, rice identification was carried out before two types of rice field discrimination. Backscatter coefficients for rice and other land covers were extracted from simulated Compact Polarimetry (CP) SAR data and analyzed. A simple threshold method using backscattering coefficients in RH/RV/RR/RL polarizations was applied for rice identification, with an accuracy of 96.72% when compared to field data. Figure 73 shows the result of rice mapping. The rice area can be calculated using the map.

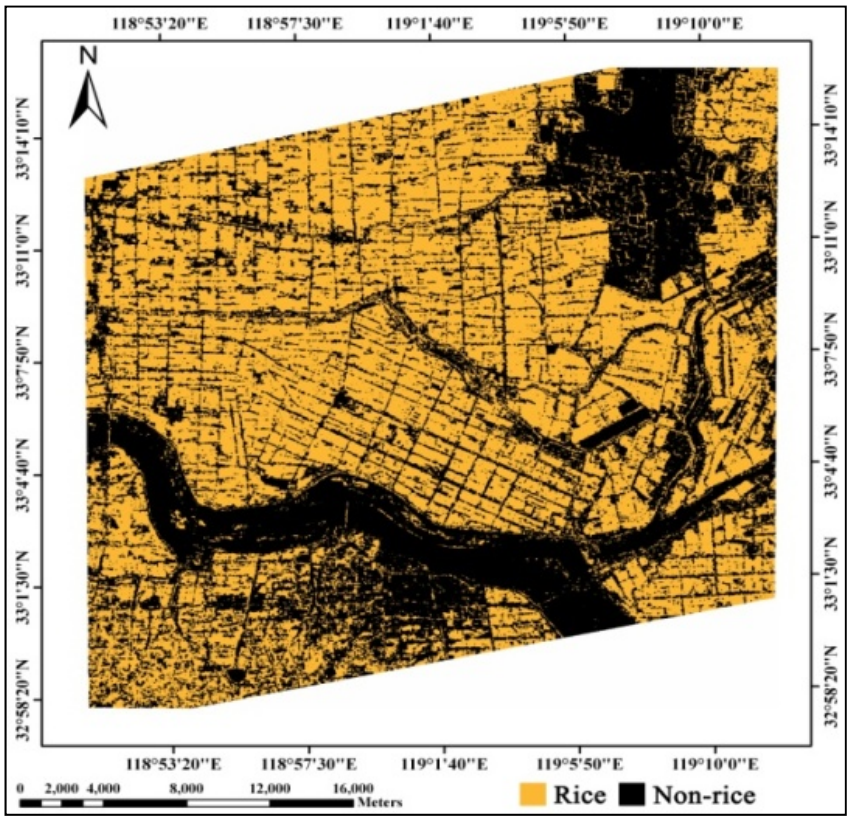


**Figure 73 Rice Mapping using Simulated CP SAR Data**

After rice identification, eleven CP parameters were investigated as the H-R and J-R evolved. It was found that the seedling stage (June 27, 2012) was the optimal phase for H-R and J-R discrimination. At this stage, the J-R plants were smaller than H-R plants because of no cultivation in the seedbed. The configurations of both rice fields were totally different owing to the differences in planting patterns. The H-R was transplanted into the fields, in regular line and row spacing about 15cm and 30cm, respectively, whereas the J-R was sown randomly. The planting density of J-R fields was greater than that of H-R fields (30–40 plants/$m^2$). Additionally, the underlying surface of H-R fields was water surface and therefore prone to specular reflection, while the underlying surface of J-R fields was a rough soil, causing stronger surface scattering. As the plants grew, the geometrical structures and features of plants in both rice fields become more similar, especially after the canopy leaves and stems were fully developed.

Figure 74 illustrates the 11 CP parameters of both rice fields on 27 June 2012. The left side (a)) shows backscattering coefficients in CP mode. The right side (b)) shows m, $\alpha_s$, $\mu$, and $\delta$. It was found that the dominant scattering at the seedling stage for H-R fields was volume and for J-R fields it was surface; the smallest scattering component for H-R fields was surface, and for J-R fields it was double bounce. Thus, the greatest difference between H-R and J-R fields was the surface scattering component, whose intensity for J-R fields was higher than H-R fields by about

5dB (Figure 74 (a)). The decision tree was applied for two types of rice field discrimination. Figure 75 shows the results of H-R and J-R discrimination.

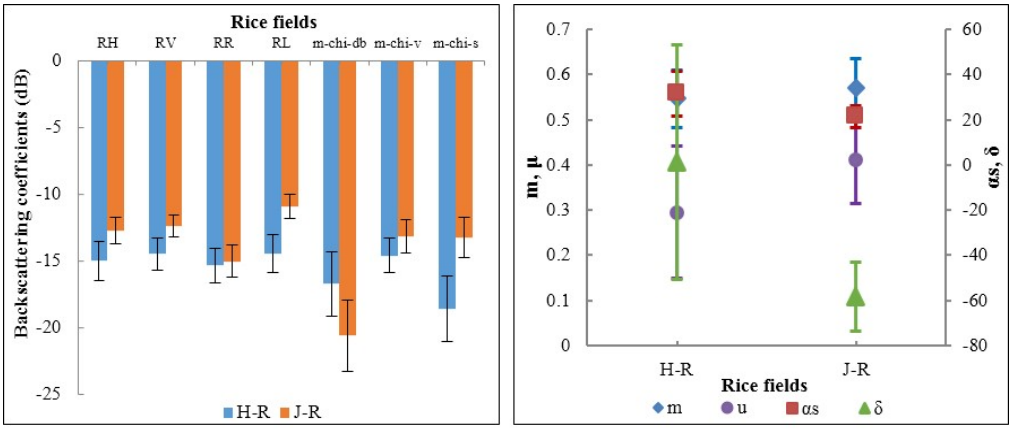


(a) (b)

**Figure 74 Amplitude Variation of 11 Parameters for H-R and J-R Fields, 27 June 2012**

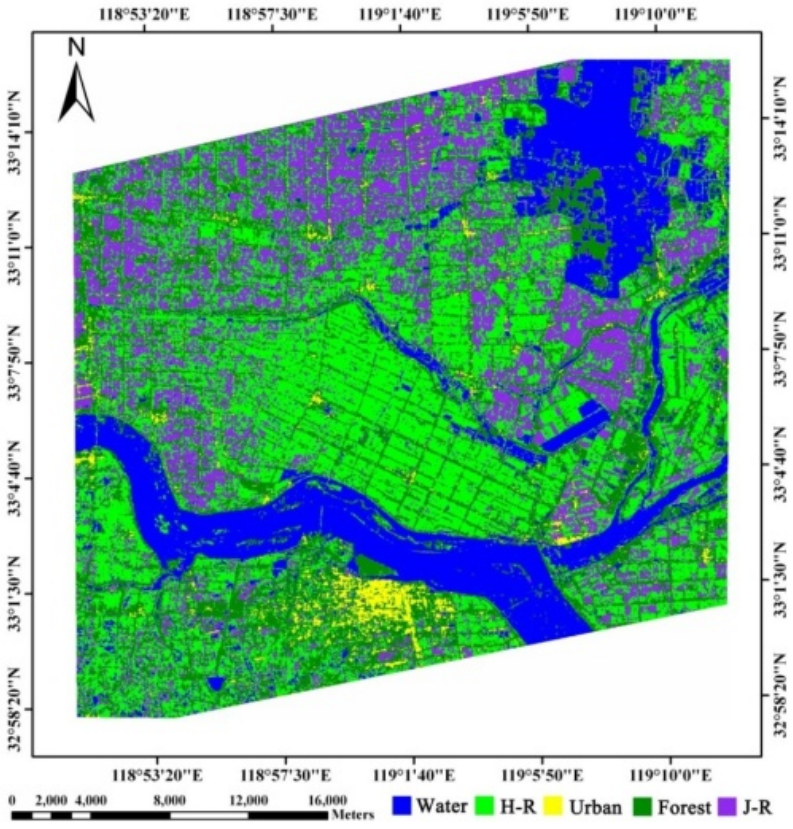


**Figure 75 H-R and J-R Discrimination with the Simulated CP Temporal Images**

**Rice Phenological Stage Retrieval**

The BBCH scale was introduced to quantify phenology of H-R and J-R and then all the field data and CP observables were represented as a function of the phenological stage. The analysis was centred on the sensitivity of the CP observables to the phenological features of rice. The decision tree algorithm was also applied for rice phenological stage retrieval. No more than four CP observables were used for retrieval of each stage (Figure 76). The stages are identified by different colours. Figure 77 shows the results of H-R and J-R of phenological stages retrieval over the image scene on each acquisition date.

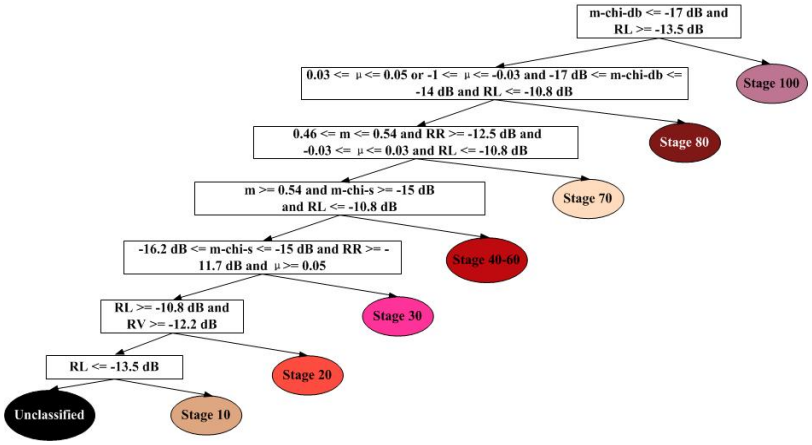


(a) H-R

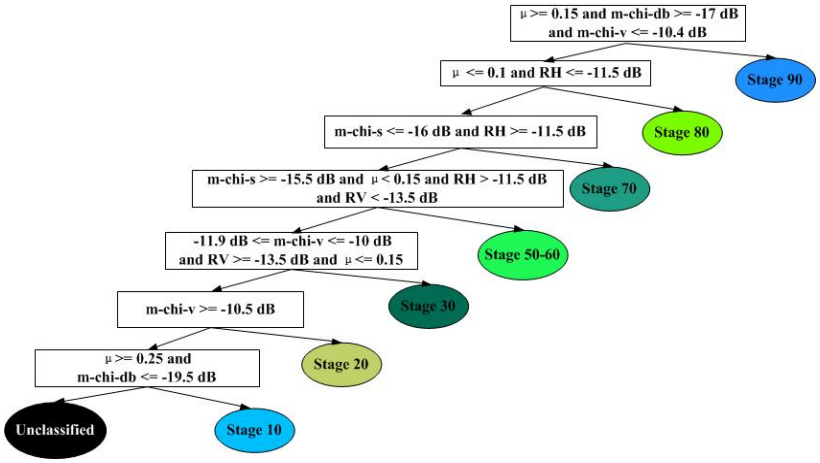


(a) J-R

**Figure 76 The Decision Trees and Appropriate Thresholds for Retrieval of Phenological Stages of H-R and J-R**

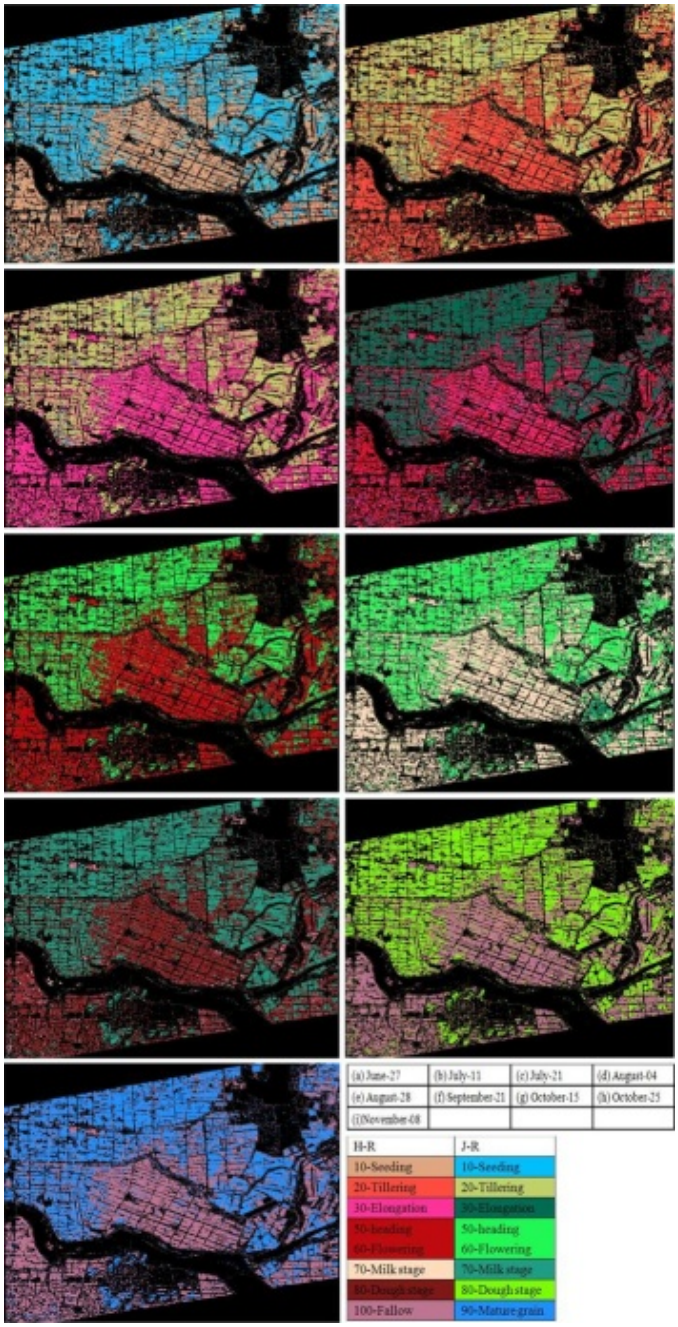


**Figure 77 Retrieval of Rice Phenological Stages on each Acquisition Date**

**Rice Yield Prediction and Forecasting**

The key problem of SAR rice yield estimation is inversion of rice parameters. The physical scattering model is crucial to analyze rice scattering mechanisms and inversion of parameters. In order to understand the physical meaning of rice backscatter, a coherent scattering model, considering the rice ear layer, using the Monte-Carlo method, was introduced for rice parameter estimation. Figure 78 shows the model structure and the simulation results.

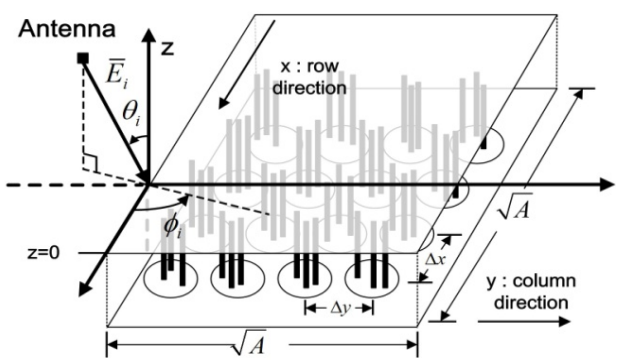


Rice fields simulation

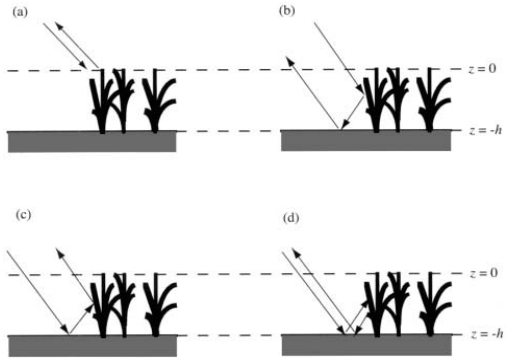


Dominant scattering mechanisms

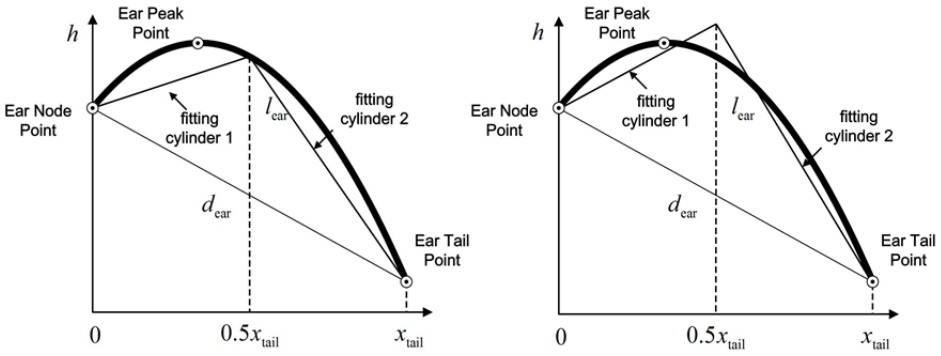


Curved rice panicle simulation

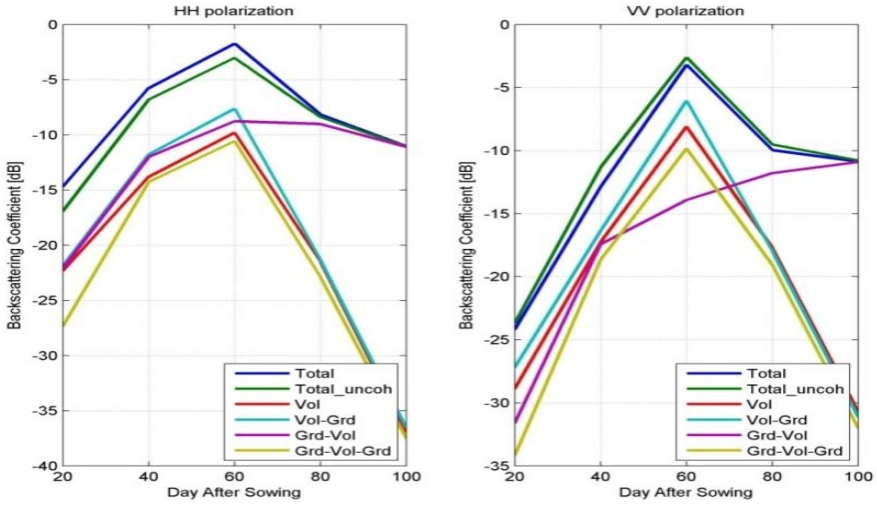


Backscattering coefficients of rice from different scattering mechanisms

**Figure 78 Monte-Carlo Model Structure and Simulation Results**

At this point, rice mapping and rice area estimation with polarimetric SAR data have been completed. The models for inversion of rice parameters (biomass, plant height) with polarimetric SAR data have been improved. However, we have not considered the influence of

environmental stress on rice yields. We will introduce environmental stress into our model in 2015.

In addition, the SAR data we've acquired in August 14,2012 (elongation or heading stage of rice), severely affected by thunderstorms, cannot be used. And we also missed rice backscatter of the milk stage. This missing data of two important stages affect the accuracy of rice parameter estimation. We will acquire new data and conduct field work in 2015 to solve the problem.

## Plans for Next Growing Season

We will improve the method of rice phenological stages retrieval methods, by using the SVM and SFS algorithms.

We plan to order RADARSAT-2 polarimetric SAR data in 2015. We also plan to acquire ALOS polarimetric data and apply for compact polarimetric data.

## Publications

Zhi Yang, Kun Li*, Long Liu, Yun Shao, Brian Brisco, and Weiguo Li. 2014. Rice Growth Monitoring using Simulated Compact Polarimetric C-band SAR. Radio Science, Vol.49, No.12, pp.1300-1315.

Long Liu*, Kun Li, Shao Yun, Pinel Nicolas, Zhi Yang, Gong Huaze, and Wang Longfei. 2015. Extension of the Monte Carlo Coherent Microwave Scattering Model to Full Stage of Rice. IEEE Geoscience and Remote Sensing Letters, Vol.12, No.5, pp.988-992.

## 9.5 Shandong

Team Leader: Bingfang Wu

Team members: Miao Zhang, Hongwei Zeng, Wentao Zou, Sheng Chang, J.K. Inkendo, Yang Zheng, Bo Chen, Mingzhao Yu, Xin Zhang

Project Objectives

The original objectives of the site have not changed. They are:

- Crop identification and Crop Area Estimation
  - Multi-configuration SAR data
- Crop Condition/Stress
  - Crop Growing Conditions Over the Growing Season
  - NDVI, NDWI, Vegetation condition index, temperature condition index, crop water stress index, etc.
- Estimation of Biophysical Variables
  - fAPAR, LAI-Radiation transfer model
- Yield Prediction and Forecasting
  - Biomass-modified CASA model
  - Harvest index
- Crop Residue Cover and Tillage Mapping
  - Crop residue cover
  - Tillage classification
- Phenological Events
  - Crop maturity date prediction
  - NDVI threshold method

Site Description

- Location
  - Top-Left

    Latitude: 37.331°N Longitude: 116.319°E
  - Bottom-Right

    Latitude: 36.331°N Longitude: 116.819°E
- Topography
  - Plain
- Soils
  - Soils in the study site are mainly alluvial soil.
- Drainage class/irrigation

- Almost all the farmlands are irrigated in the site. Irrigation water is mainly from the river or underground water.

- Crop calendar
  - Typical crop rotation is winter wheat and corn.
  - The crop calendar for winter wheat is from mid-October to early June of the next year, and for corn is from mid-June to end of September.
- Field size
  - Typical field size is 2000 - 8000 m².
- Climate and weather
  - The climatic zone is temperate, semi-arid, monsoon climate. The annual mean temperature is about 13.1°C. The annual mean precipitation is about 582 mm, concentrated from late June to September.

**Figure 79 Wheat (left) and Maize (right) Fields at China Shandong JECAM Site**

EO Data Received/Used

China Environmental Satellite (HJ-1 CCD):

- Supplier: China Centre for Resource Satellite Data and Applications (CRESDA)
- Optical
- 12 scenes of HJ-1 CCD images
- From late-March to early December, 2014
- CCD: 454-72/455-72/454-73/456-72
- Level 2 Product
- We no difficulty in acquiring HJ-1 data, nor in processing and using HJ-1 data.
- Sample locations were slightly modified from the previous year.

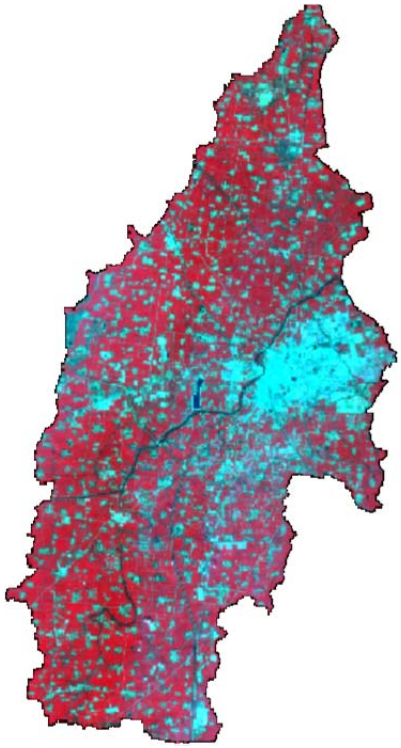

**Figure 80 HJ-1 CCD Images of China Shandong JECAM Site**

GF-1&ZY03

- China Centre for Resource Satellite Data and Applications (CRESDA)
- Optical
- 8 images
- March 20th to September 30th, 2014
- The data was provided as level 1A/2A products.
- We had some limitation in acquisition of the data.
- We had no difficulty in processing the data. However, the geo-correction of the Level 1A products was done manually using ERDAS software.

MODIS:

- Supplier: NASA
- Optical
- 46 scenes
- From 1 January 2014 to 31 December 2014
- Beam modes/ spatial resolutions: H27V05, 250m/500m/1km
- Level 2

- We had no difficulty in acquiring MODIS data, nor in processing and using MODIS data. However, the resolution is too coarse for the study site.

Proba-V

- ESA/VITO
- Optical
- 57 images
- Every five days from March 20th to December 31st, 2014
- X29Y03, 100m resolution
- Reflectance at TOC and vegetation index products
- We acquired the data through EC FP7 SIGMA project. We had no difficulty in processing and using the data.

Rapideye

- Supplier: Blackbridge
- Optical
- 4 images
- March 23rd, April 12th, May 12th, and June 12th, 2014

In situ Data

The main variables measured and instruments we are using are shown in Table 14. All the variables were measured once a month from April to September except for the following. Yield, harvest index and crop type mapping were measured once per growing season.

The biggest challenge is irritation. Sometimes, during the field observations, the farmland had just been irrigated. In this case, it is difficult to enter into the field to measure canopy variables.

**Table 14 In situ Variables and Instruments - Shandong**

| Main Variables | Instruments or Processing Method |
|---|---|
| Dry amount of above ground biomass | Oven dried and weight |
| Yield | Oven dried and weight |
| Harvest index | Calculated by yield and AGB |
| Density/canopy height | Tape measured |
| Fractional vegetation cover | Fish-eye camera |
| Crop calendar | Visual interpretation |
| Crop type mapping | Field interpretation |
| Crop type proportion | GVG instrument |
| Irrigation | Interview and record |


**Figure 81 In situ Measurements at Shandong Site**

Collaboration

We collaborated with other JECAM sites including Argentina, Ukraine, Russia, and Brazil under the SIGMA project. We shared crop type measurements in 2014 with each other and we plan to publish a paper jointly on the topic of cropland mapping.

Results

**Crop Condition Assessment with Adjusted NDVI using the Uncropped Arable Land Ratio**

Using China Environmental Satellite HJ-1 CCD images, cropped fields and uncropped fields were separated using the threshold method combined with a decision tree. A pixel-based uncropped arable land ratio (UALR) at 250m resolution was generated by spatial aggregation of the 30 m resolution cropped and uncropped arable land map. The UALR-adjusted NDVI was produced by assuming that the MODIS reflectance value for each pixel is a linear mixed signal composed of

the proportional reflectance of cropped and uncropped arable land. Crop condition monitoring results are more reliable when based on UALR-adjusted NDVI because the adjusted NDVI values exclude the influence of inter-annual variability in the cropping area. The biggest advantage of this method is that it relies only on the identification of cropped and uncropped arable land, which is much easier than identification of specific crops.

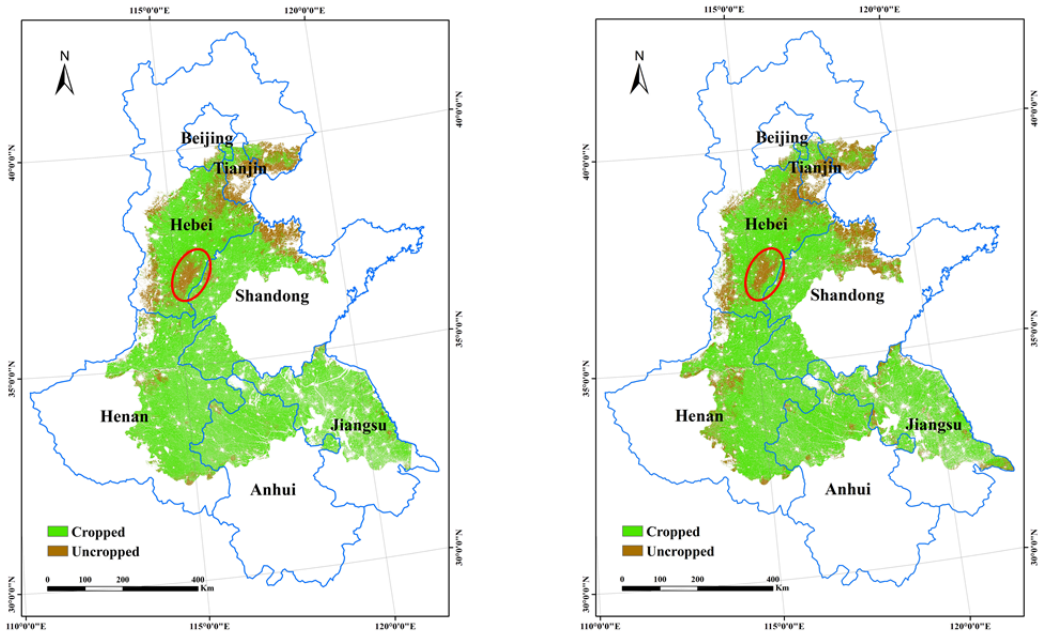


**Figure 82 Distribution of Cropped and Uncropped Arable Land for the Winter Crop Growing Season in a) 2010 and b) 2011**

The UALR-adjusted NDVI time series derived from the 16-day composite MODIS band reflectance data were used for crop condition assessment in the North China Plain (NCP). Inter-annual comparisons of UALR-adjusted NDVI for corresponding time periods and the seasonal dynamics of the UALR-adjusted NDVI time series (the NDVI profile) were employed for crop condition monitoring. NDVI profiles were developed based on the statistical average of UALR-adjusted NDVI in a particular region.

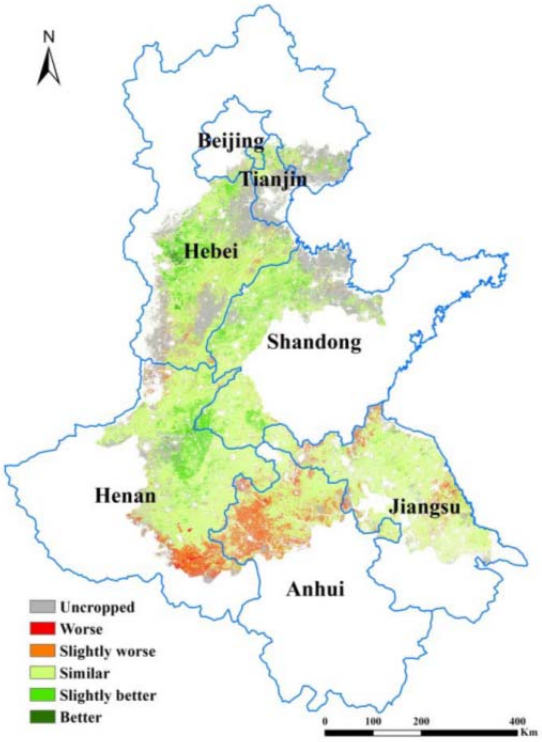


**Figure 83 Crop Condition Map of NCP UALR Adjusted NDVI for May 2011 Compared to Previous Year**

For current snapshots, two NDVI images representing comparable periods from the current and previous years are compared to identify areas where crop conditions are worse, better or similar/normal. For seasonal dynamics, a time series of NDVI images across the growing season is used to develop crop-growth profiles based on the statistical average of the NDVI (weighted for the percentage of farmland) in a region or country compared to those from previous years.

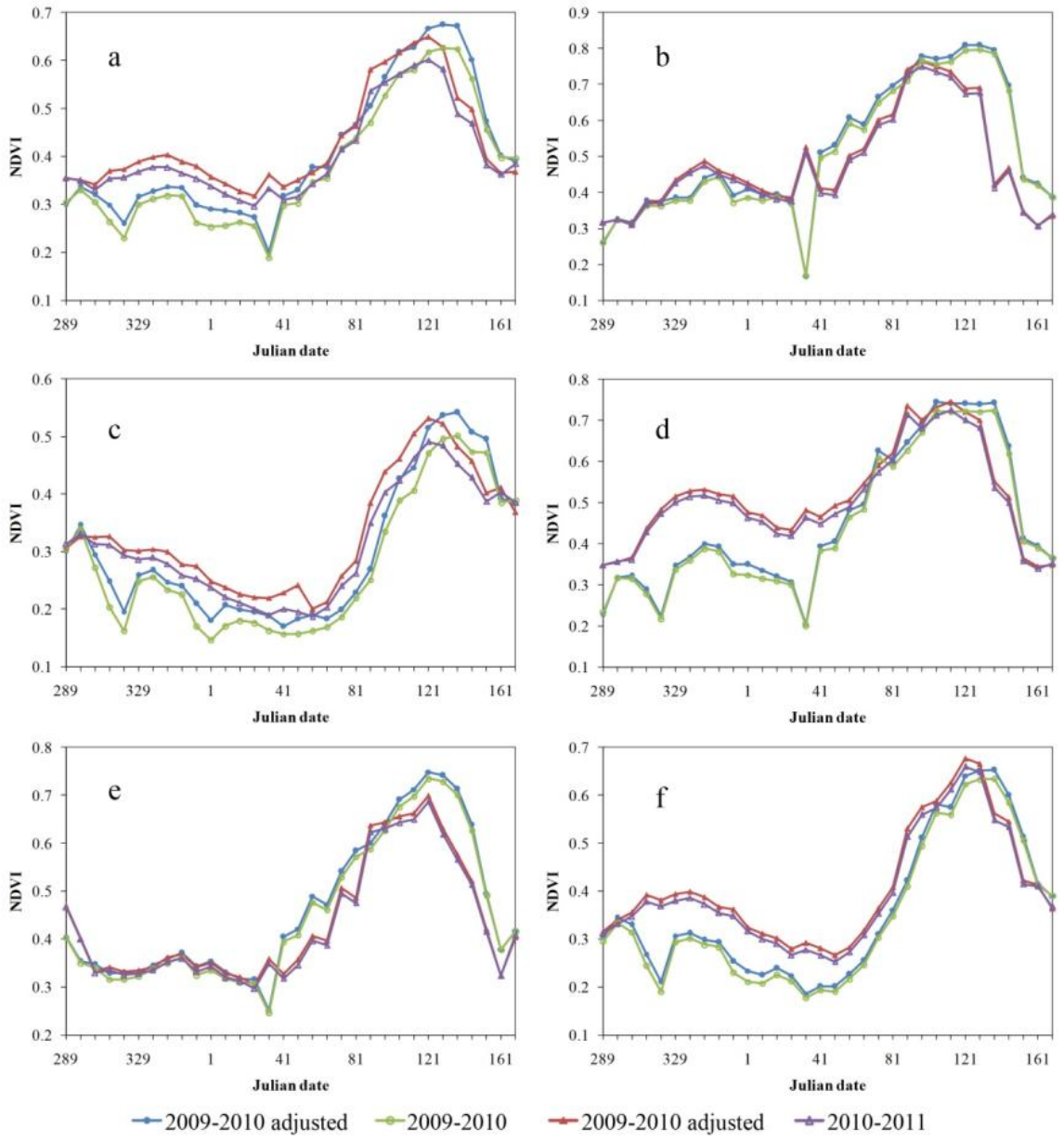


**Figure 84 Crop Growth Profiles for NCP a) and five provinces: b) Anhui, c) Hebei, d) Henan, e) Jiangsu, and f) Shandong**

Further research will focus on incorporating inter-annual variation of crop phenology into crop condition assessment. We will try to use accumulated temperature to normalize inter-annual comparisons of NDVI.

**Fraction of Absorbed Photosynthetically Active Radiation (FAPAR) Retrieval by Chlorophyll-related Vegetation Indices**

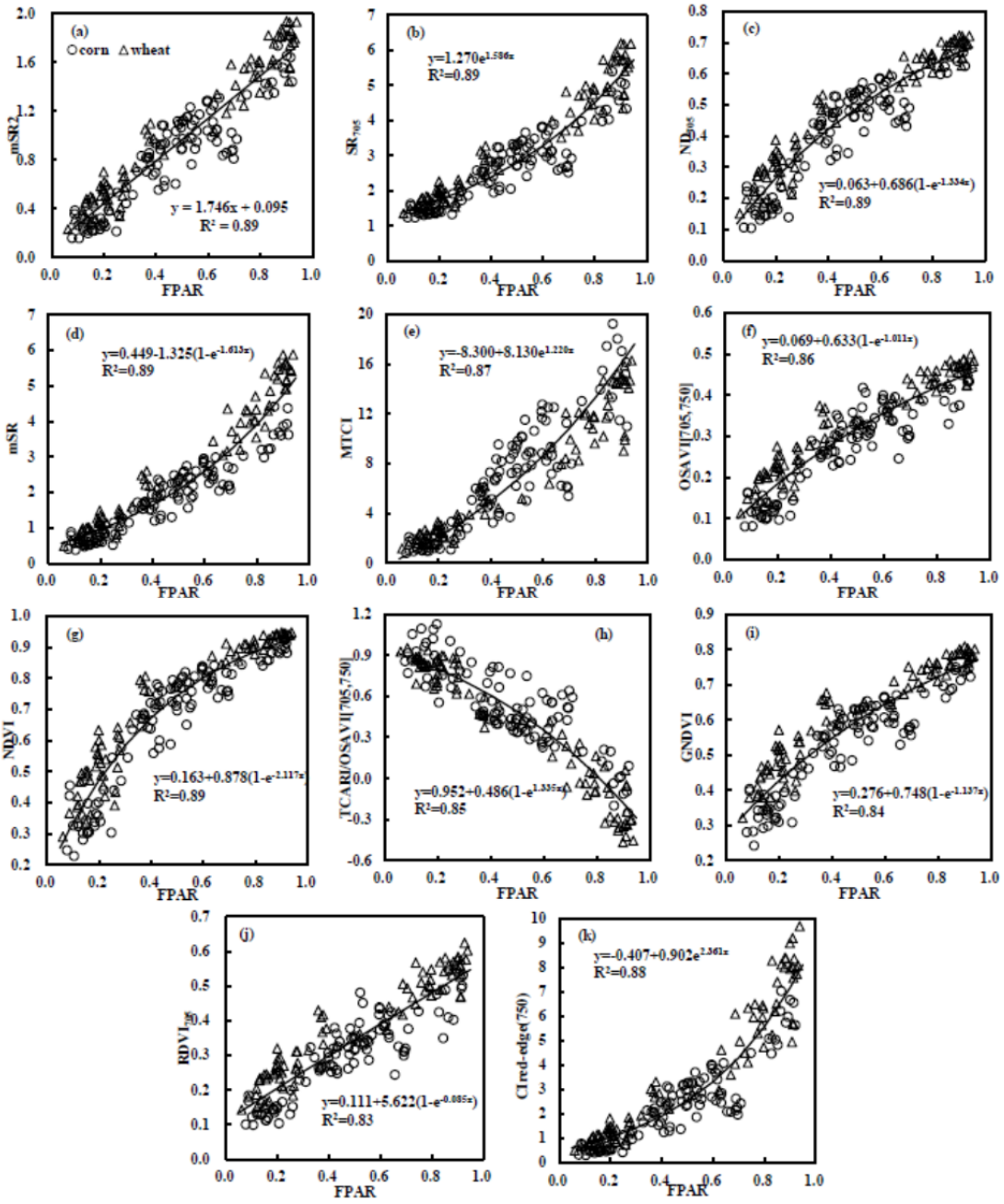


**Figure 85 Relationships between FAPAR and Vegetation Indices with a Linear Coefficient of Determination greater than 0.83**

Over the China Shandong JECAM site, chlorophyll-related vegetation indices (VIs) were selected and tested for their capability in crop FAPAR estimation using simulated Sentinel-2 data. These indices can be categorized into four classes: the ratio indices, the normalized difference indices,

the triangular area based indices, and the integrated indices. Two crops with distinctive canopy and leaf structure, wheat and corn, were studied. Regression analysis was conducted between measured FAPAR and different vegetation indices derived from Sentinel-2 reflectance simulated from field spectral measurements. At the same time, the effects of the red-edge reflectance on crop FAPAR estimation and the impact of different crop types on FAPAR estimation are explored. It was found that VIs using the near-infrared and red-edge reflectance, including the modified Simple Ratio2 (mSR2), the red-edge Simple Ratio (SR705), the Red-edge Normalized Difference Vegetation Index (ND705), MERIS terrestrial chlorophyll index (MTCI), and the Revised Optimized Soil-Adjusted Vegetation Index (OSAVI[705, 750]), were strongly correlated with FAPAR, especially in the high biomass range. Among all the indices, RDVI705 and mSR2 were more linearly correlated with FAPAR, whereas the other indices deviated slightly from a linear correlation.

When the red-edge reflectance was used, the ratio indices (e.g., mSR2 and SR705) had a stronger correlation with crop FAPAR than the normalized difference indices (e.g., ND705). Sensitivity analysis showed that mSR2 had the strongest linear correlation with FAPAR of the two crops across a growing season. Further analysis indicated that indices using the red-edge reflectance might be useful for FAPAR retrieval. Indices using the red-edge reflectance are independent of crop types. This suggests the potential for high resolution and high quality mapping of FPAR for precision farming using the Sentinel-2 data.

**Crop Area Estimation based on High Spatial and Temporal Rapideye Images**

Single multispectral imagery is often used for crop identification, but many researchers have recognized the benefits of using multi-temporal imagery within a given growing season to map agricultural crops. Four different classifiers including minimum distance, support vector machine (SVM), maximum likelihood, and spectral angle mapper (SAM) were applied to multi-temporal Rapideye images. Four cloud-free images taken on March 23$^{rd}$, April 12$^{th}$, May 12$^{th}$, and June 12$^{th}$ were used for crop classification. Independent field samples were used for classification accuracy evaluation to select one classifier for winter wheat area estimation. Also, harvested winter wheat area is extracted based on change detection of cropped and uncropped arable land map at the growing peak stage and after harvest.

Crop classification using four different classifiers shows similar distribution map of winter wheat in the Yucheng site but with great difference in north-east and south-east of the site. Validation results indicate that the SVM classifier yields best winter wheat extraction accuracy. Producer's accuracy (PA) and user's accuracy (UA) are listed below.


| | | | | |
|---|---|---|---|---|
| Producers' accuracy | 96.54% | 96.24% | 93.06% | 87.33% |
| Users' accuracy | 96.46% | 96.32% | 95.89% | 96.47% |

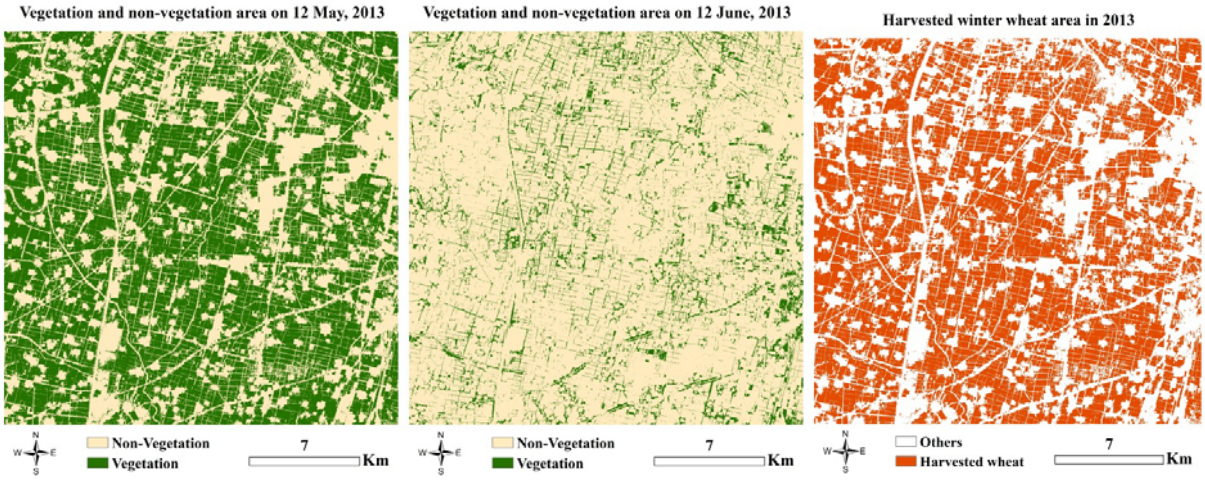


**Figure 86 Crop Area Estimation Results**

A decision tree was used to separate vegetation and non-vegetation at growing peak stage and after harvest. Validation results showed that the accuracy of identification of vegetation and non-vegetation exceeded 99%. It is assumed that the only pixels with vegetation during the peak growing stage and non-vegetation after harvest are harvested winter wheat. The change

detection method was employed to generate the harvested winter wheat map. Harvested winter wheat area is consistent with the winter wheat map based on the SVM classifier.

Plans for Next Growing Season

In 2015 and the future, we will measure same variables same as that in 2014.

In 2014, we acquired time series Proba V reflectance and vegetation index products. In 2015, we will continue the acquisition and do some analysis using that data. The JECAM coordinator already summarized the RADARSAT-2 acquisition plan over 2015.

As for the research, we will continue to focus on yield estimation. We already acquired enough data. 2015 is the time to analyze the data and summarize results in a paper.

Publications

Miao Zhang, Piccard Isabelle, Bydekerke Lieven, Bingfang Wu. Comparison of field campaigns for crop monitoring in China (Yucheng) and Europe (Belgium). Oral presentation in Global Vegetation Monitoring and Modeling workshop, February 3rd to 7th, 2014, Avignon, France.

Bingfang Wu, Jihua Meng, Qiangzi Li, Nana Yan, Xin Du, Miao Zhang, 2014. Remote sensing-based global crop monitoring: experiences with China's CropWatch system. International Journal of Digital Earth, 7(2): 113-137. DOI: 10.1080/17538947.2013.821185.

Miao Zhang, Bingfang Wu, Jihua Meng. Quantifying winter wheat residue biomass with a spectral angle index derived from China Environmental Satellite data. International Journal of Applied Earth Observation and Geoinformation, 2014, 32: 105-113.

Miao Zhang, Bingfang Wu, Jihua Meng, et al. Fallow land mapping for better crop monitoring in Huang-Huai-Hai Plain using HJ-1 CCD data[C]//IOP Conference Series: Earth and Environmental Science. IOP Publishing，2014，17(1): 012048.

Miao Zhang, Bingfang Wu, Mingzhao Yu, et al. Monthly monitoring of uncropped arable land: concepts and implementation – a case study in Argentina. Journal of Remote Sensing, accepted, 2014 (ahead of print).

Taifeng Dong, Jihua Meng, Jiali Shang, Jiangui Liu, Bingfang Wu. An evaluation of chlorophyll-related vegetation indices using simulated Sentinel-2 data for estimation of crop fraction of absorbed photosynthetically active radiation (FPAR),IEEE Journal of Selected Topics in Applied Earth Observations and Remote Sensing. DOI 10.1109/JSTARS.2015.2400134.

Taifeng Dong, Jihua Meng, Jiali Shang, Jiangui Liu, Ted Huffman, Bingfang Wu. Modified vegetation index for estimating crop fraction of absorbed photosynthetically active radiation, Submitted to International Journal of Remote Sensing, 2015.

Bingfang Wu, Miao Zhang and Yang Zheng. Crop area estimation based on high spatial and temporal Rapideye images, Presented in Sentinel-2 agriculture workshop & Sentinel-2 for Science workshop, May 2014.

# 10. France

Team Leader: Eric Ceschia

Team Members : Aurore Brut, Olivier Hagolle, Frédéric Baup, Gérard Dedieu, Jean François Dejoux, Jordi Inglada, Valérie Demarez, Benoit Coudert, Vincent Rivalland, Silvia Valero, Claire Marais-Sicre, Valérie Le Dantec, Patrick Mordelet, Milena Planells, Vincent Bustillo, Tiphaine Tallec, Jérôme Cross, Mireille Huc, Nathalie Jarosz, Bartosz Zawilski, Hervé Gibrin, Amanda Veloso, Marjorie Battude

Project Objectives

The original project objectives have not changed. They are:

- Crop identification and Crop Area Estimation
- Crop Condition/Stress
- Soil Moisture
- Yield Prediction and Forecasting
- Crop Residue, Tillage and Crop Cover Mapping
- $CO_2$ and water fluxes/budgets.

Site Description

The JECAM Test Site Name is OSR (Observatoire Spatial Régional, or Regional Space Observatory).

- Location: South west of Toulouse, France (area of study is approx 50*50 km) including 2 experimental plots (Auradé and Lamasquère Fluxnet, which are ICOS sites, installed in 2004).
- Topography: hilly for Auradé, in a valley for Lamasquère.
- Soils: clay at Auradé, clay loam at Lamasquère.
- Drainage class/irrigation: irrigation at Lamasquère when maize is grown.
- Crop calendar: depends on crops.
- Field size: around 30 ha at Auradé and 20 ha at Lamasquère.
- Climate and weather: mean annual temperature around 13 °C, mean annual precipitation around 650 mm.
- Agricultural methods used: crop rotations are winter wheat, sunflower, winter wheat, rapeseed at Auradé and maize for silage, winter wheat at Lamasquère. Auradé only receives mineral fertilizers whereas Lamasquère receives both mineral and organic fertilizers. Lamasquère is irrigated when maize is grown.

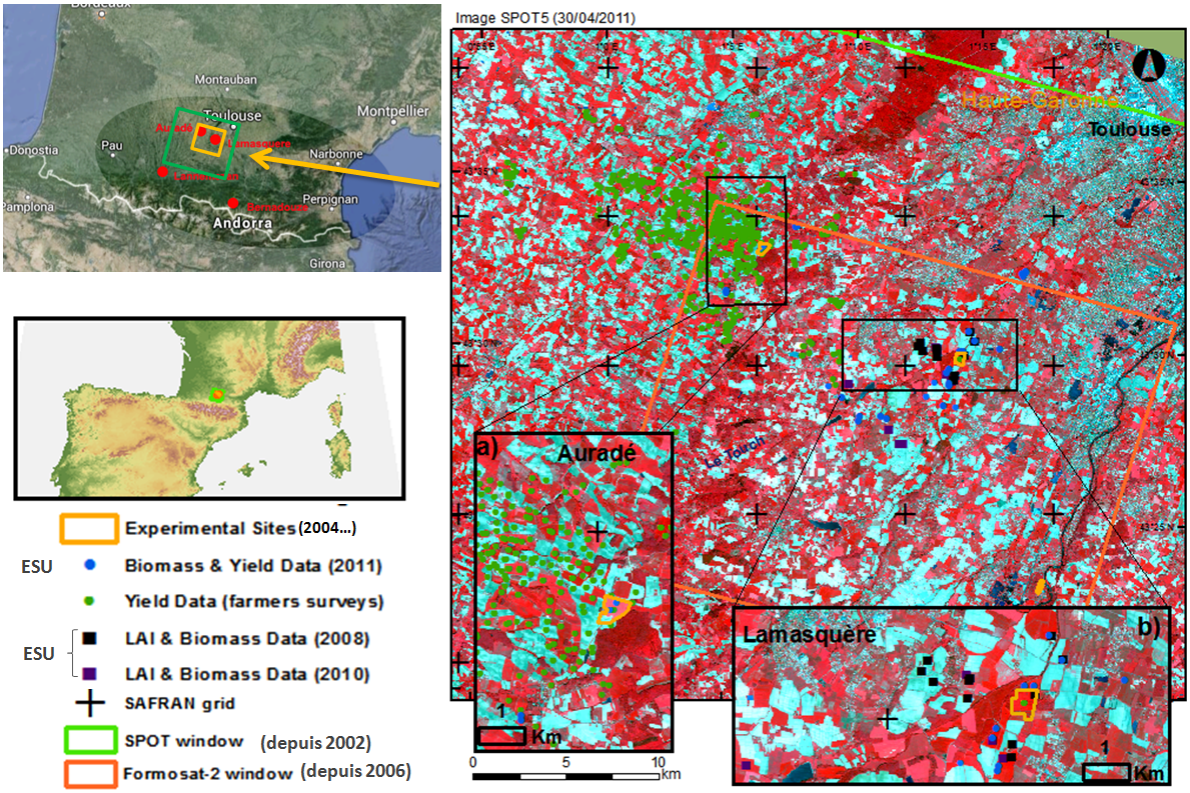


**Figure 87 OSR including the Auradé and Lamasquère Fluxnet/ICOS Sites**

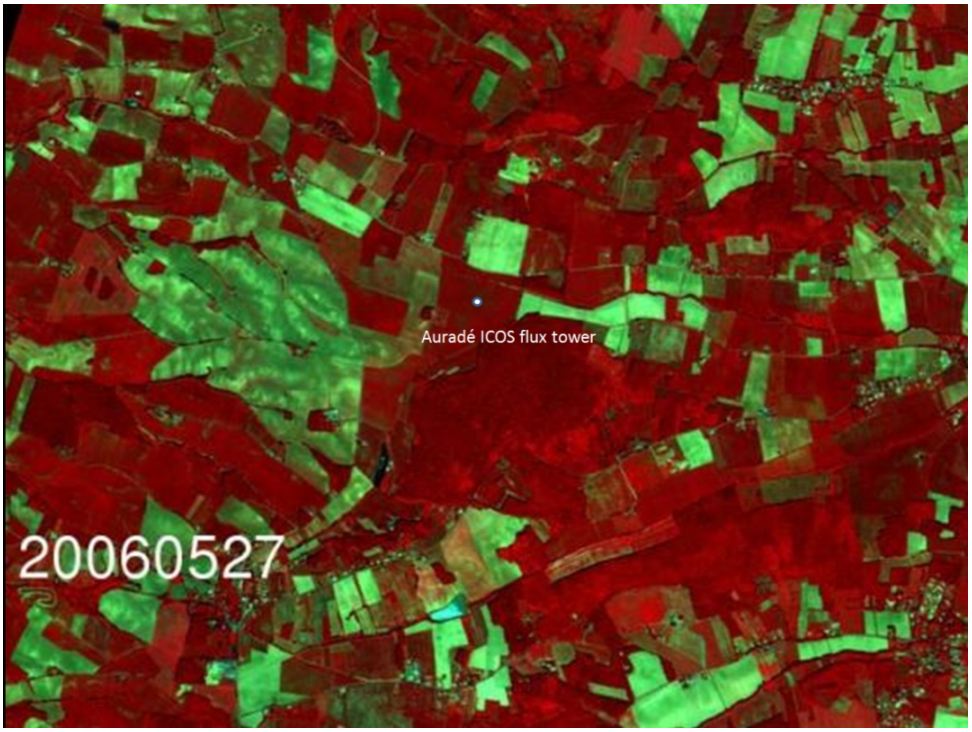


**Figure 88 Formosat-2 Image of the Area around the Auradé Site, 27 May 2006**

EO Data Received/Used

All the following images were obtained independently from the JECAM project. The TerraSAR-X data are not openly accessible but can be made available after an agreement has been signed.

**Images obtained from the CNES KALIDEOS program**

***Spot5 (optical, 10m, 2500 km²)***. 4 images (10 April; 13 September; 26 October; 21 November).

***Formosat (optical, 8m,900 km²)***. 18 between March 2nd and December 31st, 2014.

***Pléiade (optical, 2,8m,400 km²)***. 3 images in 2014.

***TerraSAR-X (SAR, X band)***. Every 11 days since April 2014.

**Images acquired through the French THEIA consortium (level 2A)**

***Landsat 8 (optical,30m ,all over the OSR footprint)***. 11 cloudfree images (February 12 to December 22)

***Sentinel-1***. First images collected over the OSR footprint in October 2014.

**Images acquired through projects in which CESBIO is involved**

***Deimos 1 (optical, 22m, 10 000 km² on average enclosing the OSR area)***. 10 images between January and October 2014.

In situ Data

Both Auradé and Lamasquère sites are ICOS sites and therefore biomass, soil humidity, meteorological, and flux measurements are standardised according to the ICOS protocols. See http://gaia.agraria.unitus.it/icos/working-groups.

In total, 135 micro-meteorological variables are recorded every 30 minutes at each site. They include air temperature and humidity, air pressure, soil temperature and humidity at 0-5, 5, 10, 30, 100 cm depth, soil heat flux at 5 cm depth, global (shortwave and longwave) and PAR incident radiation, global (shortwave and longwave) and PAR reflected radiation, albedo, transmitted PAR, diffuse PAR and global shortwave radiation, NDVI, PRI, surface temperature, soil $CO_2$ and $N_2O$ fluxes (automatic chambers), net $CO_2$, water, sensible heat fluxes by means of the eddy-covariance method.

Collaboration

The OSR site and its members are involved in

1) the Sentinel 2 agriculture project :

see: http://www.esa-sen2agri.org/SitePages/Home.aspx

**Figure 89 The Lamasquère Site Around the Micrometeorological Station**

**Figure 90 The Auradé Site Around the Micrometeorological Station**

The Sentinel-2 for Agriculture (Sen2-Agri) project has recently been launched by ESA, as a major contribution to the R&D component of the GEOGLAM initiative and to the JECAM network activities. The project will demonstrate the benefit of the Sentinel-2 mission for the agriculture domain across a range of crops and agricultural practices. The intention is to provide the international user community with validated algorithms to derive Earth Observation products relevant for crop monitoring (in particular mapping of the crop fields).

Partners of the S2-Agri project:

Agriculture and Agri-Food Canada

IFAD

ARVALIS Institut du végétal

INTA

ATIC Alberta Terrestrial Imaging Centre

جامعة شعيب الدكالي Université Chouaïb Doukkali

RADI

RCMRD

cirad LA RECHERCHE AGRONOMIQUE POUR LE DÉVELOPPEMENT

SAEOGEO SOUTH AFRICAN GROUP ON EARTH OBSERVATIONS

European Commission

Agriculture and Agri-Food Canada

International Fund for Agricultural Development

ARVALIS (Institut du vegetal), France

Instituto Nacional de Tecnologia Agropecuaria, Argentina

Alberta Terrestrial Imaging Centre, Canada

Chouaïb Doukkali University & Réseau National des Sciences et Techniques de la Géo-Information, Morocco

Institute of Remote Sensing and Digital Earth, Chinese Academy of Sciences, China

Regional Center for Mapping of Resources for Development, Kenya

Centre de cooperation Internationale en Recherche Agronomique pour le Developpement

National Earth Observation and Space Secretariat (NEOSS), South Africa

European Commission


Food and Agriculture Organization


Space Research Institute (SRI) of the National Academy of Science & State Space Agency, Ukraine


Federation of Irrigation Associations, Portugal


US Geological Survey (USGS) - Earth Resources Observation and Science (EROS)


The World Food Programme (WFP)

2) The sites are involved in several collaborative projects such as CiCC (http://www.sud-ouest.cerema.fr/projet-de-recherche-ademe-cultures-intermediaires-a875.html) and CESEC financed by the French agency ADEME, MAISEO (http://www.pole-eau.com/Les-Projets/Projets-finances/Maiseo) and REGARD (http://www.fondation-stae.net/fr/actions/projets-soutenus/?pg=2).

3) The sites are also involved in several networks such as Fluxnet (http://fluxnet.ornl.gov/) and ICOS (http://gaia.agraria.unitus.it/home). The ICOS network will be running for the next 20 years.

4) OSR is part of the French THEIA initiative (https://www.theia-land.fr/). The Theia Land Data Centre is a French national inter-agency organization designed to foster the use of images issued from the space observation of land surfaces. Theia is offering scientific communities and public policy actors a broad range of images at different scales, methods and services. They partners are potentially involved in "thematic" and / or "regional" expertise centres. The Scientific Expertise Centres are laboratories or groups of national laboratories leading research and developing innovative processes to use space data for “land surfaces” issues. The OSR is involved in 12 of them (see https://www.theia-land.fr/en/presentation/scientific-expertise-centres). The Regional CES's objectives are 1) to unite and coordinate users (scientists and public stakeholders) at regional level, and 2) to participate in community training efforts, particularly concerning added-value products developed by the thematic CES’s. The OSR is identified in THEIA as the Midi-Pyrénées CES.

5) A scientific and technical network on sunflower has been laid out from 2012 to 2017 in Toulouse (named "UMT Tournesol"). Remote sensing research and development is one of the major contributions of CESBIO to this UMT. A 3-year project has begun in 2014 on

"sunflower yield and quality prevision" also involving agricultural cooperatives. Several campaigns have been performed in 2014 by Cesbio, Cetiom and INRA (measurements of GAI, biomass and yield). In this framework, we tested different approaches to calibrate relationships between remotely sensed and in situ GAI (calibration of BVnet). Field data will be used to calibrate models like SAFYE or SUNFLO that simulated among other things biomass and yield.

Results

**Within the framework of the CICC project**: crop plots were identified on which spontaneous crop re-growth, development of weeds or seeding of cover crops occurred in 2014 in the OSR area. Because those covers are spatially very heterogeneous and because their dynamics of development are very heterogeneous too, it is difficult to distinguish those different sub-classes or the species of cover crops. Ground truths are therefore needed to classify them correctly. We are currently collecting ground truth data and we are developing some methods to map those different covers. This is a critical issue for improving spatial estimates of cropland carbon and water budgets. Figure 91 shows the importance of accounting for the effects of cover crops on net $CO_2$ fixation and carbon budgets. It shows the components of the annual net ecosystem carbon budget (NECB) for the Auradé site in 2006: on the left side, the effect of crop voluntary regrowth on the net annual $CO_2$ flux (NEP) and the carbon budget (NECB) is not considered, and on the right side when accounting for this effect. For the net ecosystem production (NEP, grey bars) and the amount of carbon exported at harvest (Cexp, white bars), the first bar of each pair represents the measurements and the information provided by the farmer, respectively, and the second bar, hatched, represents the results obtained with the SAFY-$CO_2$ model. The black bars represent the carbon imported as seeds (Cinp): the values for the left and right bars are the same since this variable cannot be estimated by the model. The green bars represent the NECB calculated from the observations (previous left bars) and from the model outputs (previous right bars).

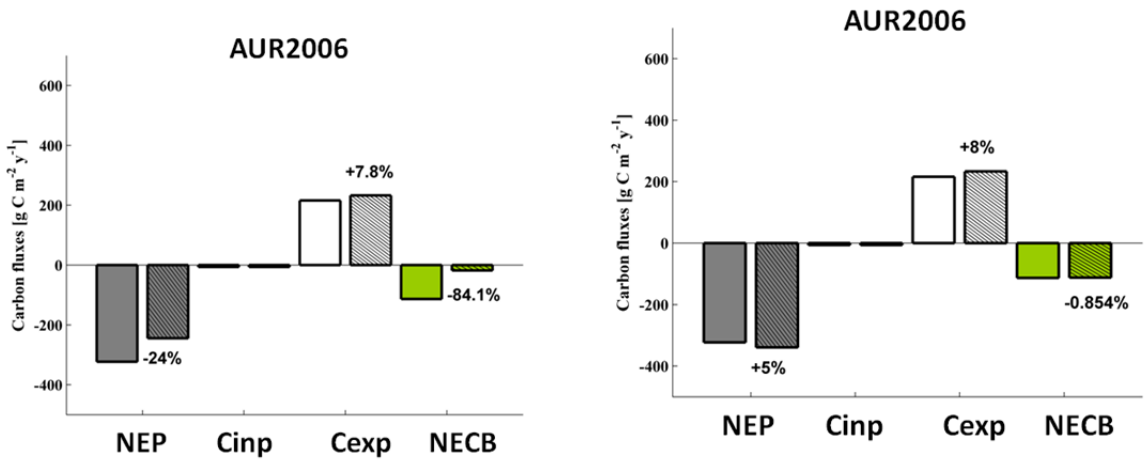


**Figure 91 Components of the Annual Net Ecosystem Carbon Budget (NECB) for Auradé in 2006**

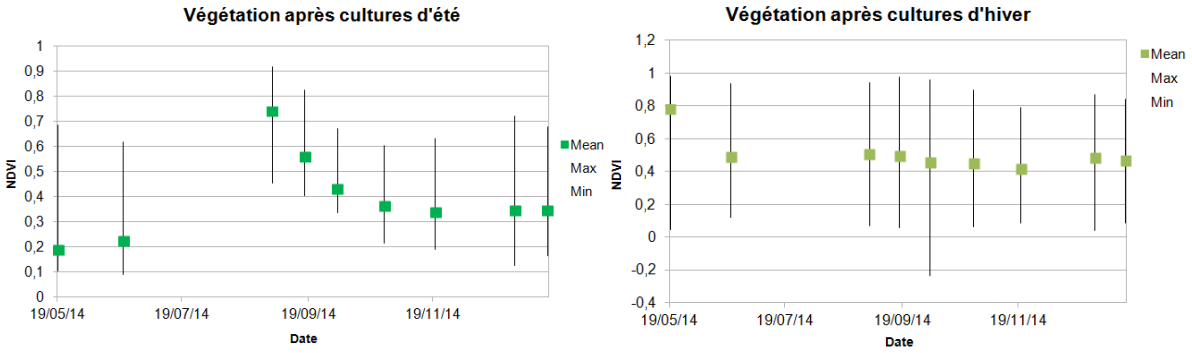


**Figure 92 NDVI Dynamics and Variability for Cover Crops after a Summer Crop (L) and after a Winter Crop (R)**

Sen2-Agri: a mask for cropland areas is being developed and tested on the OSR area (in addition to the other areas of study involved in the project).

An intensive field campaign was held in 2013 within the framework of the Calvados project financed by the CNES. Digital Hemispherical Photographs were taken during this campaign over winter wheat, maize and sunflower crops. They were then processed with the CAN-EYE software in order to estimate ground truth of GAI, FAPAR and FCOVER. The objective was to validate satellite maps of GAI, FAPAR and FCOVER produced by the BVNet tool developed by INRA in Avignon (M. Weiss and F. Baret). The main results are presented in Figure 93. (In this figure, green = winter wheat; red = maize; blue = soja; black = sunflower). The satellite images used for this project are the SPOT4, SPOT 5 and LANDSAT images.

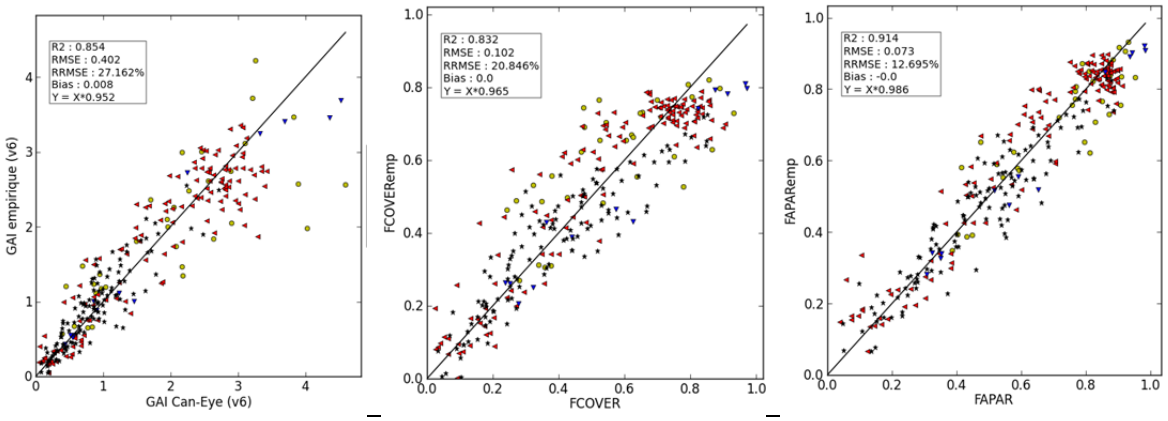


**Figure 93 Comparison of GAI, Fcover, FAPAR Estimated from Hemispherical Photographs and from the BVnet Tool for Several Crop Species**

Within the framework of the Maiseo project, water requirements and biomass production for maize were estimated using Formosat-2 Time series Data and the SAFYE simple crop model. The objective of this project is to develop of an operational tool to accurately estimate crop water requirements in order to optimize irrigation while maintaining acceptable production. For this, Formosat-2 high resolution images during 3 years (2006/2008/2012) were used to produce GAI (BVNET tool) maps that were used to calibrate the phonological parameters of the SAFYE model. In situ measurements of LAI, DAM, ET flux data, irrigation, Soil Water Content (SWC) were used to validate the model outputs.

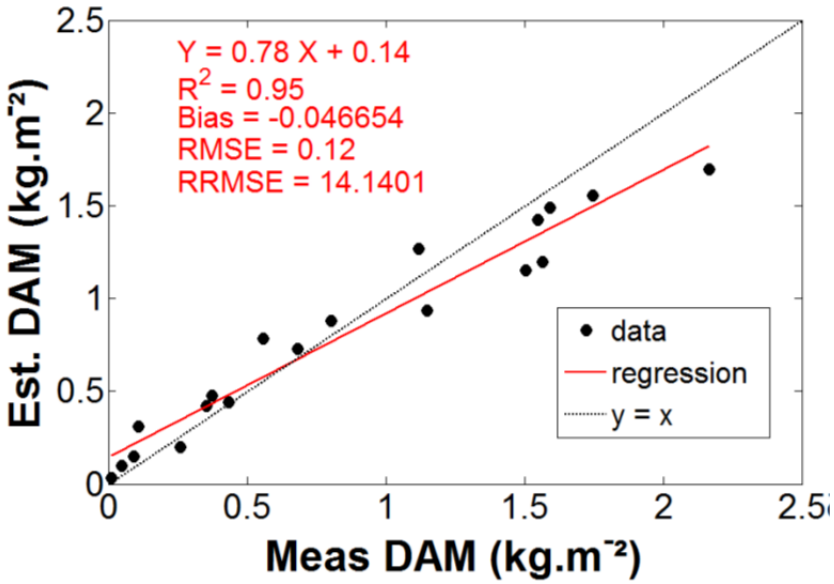


**Figure 94 Comparison of Measured (Destructive Protocol) and Estimated DAM of Maize for 2006/ 2008/ 2012**

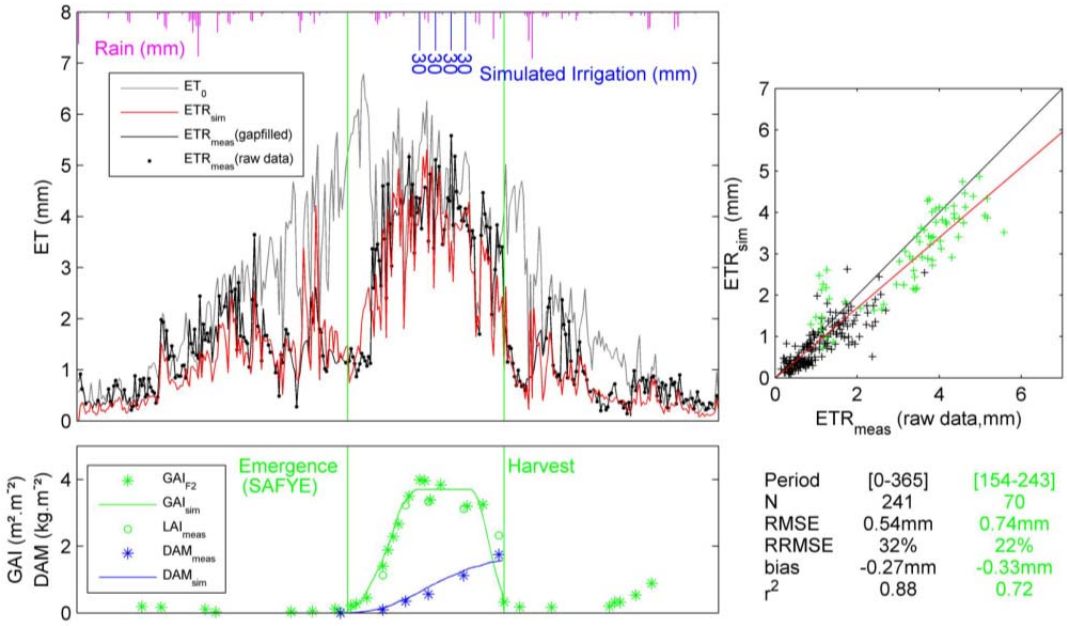


**Figure 95 Top & Right: Comparison of Simulated and Measured ETR for Maize at the Lamasquère Site in 2006 Bottom: Comparison of Simulated and Measured GAI and Biomass Time Series**

In Figure 95, the top and right show a comparison of simulated and measured ETR for maize on the Lamasquère site in 2006 (whole year (black); vegetative period (green)) with the scores associated. The bottom shows a comparison of simulated and measured GAI and biomass time series.

This simple approach, combining High Spatial and Temporal Remote sensing data with a simple crop model based mainly on efficiencies (Monteith for carbon and FAO-56 for water), resulted in good estimates of crop biomass (RRMSE = 14 %) and seasonal ETR (RRMSE2006 = 32%). We were able to describe the main processes of the plant related to the carbon and water budgets, even if errors persist mainly due to the difficulty to describe intermediate variables such as soil water content.

The model outputs will be validated using networks of in-situ sensors and water used over a large number of maize plots in the Neste watershed (southwest France), thanks to SPOT4-Take 5 2013 dataset and AROME meteorological data.

**To what extent have the project objectives been met?**

So far for the different projects in which we are involved, the project objectives have been met.

**Can this approach be called 'best practice'?**

The combination of HSTR data with a simple crop model and diverse ground data for validating different outputs of the model (GAI based upon DHP, Biomass with intensive destructive campaigns, fluxes with eddy covariance data) has proven to be an efficient approach for estimating the main components of the carbon and water budgets for croplands.

Plans for Next Growing Season

In 2015, CNES will change the SPOT 5 orbit to produce a similar set of data as the one that was produced two years ago with SPOT 4 (SPOT 4 take 5).

We anticipate ordering the same type/quantity of EO data next year.

Publications

T. Tallec, **P. Béziat**, N. Jarosz, V. Rivalland & **E. Ceschia** (2013) **Crops' water use efficiencies in temperate climate: comparison of stand, ecosystem and agronomical approaches**. *Agricultural and Forest Meteorology*, 168, 69–81.

**P. Béziat**, V. Rivalland, T. Tallec, N. Jarosz, G. Boulet, P. Gentine & **E. Ceschia** (2013) **Crop evapotranspiration partitioning and analysis of the water budget distribution for several crop species: comparison between a simple method based on marginal distribution sampling and a SVAT modeling approach**. *Agricultural and Forest Meteorology*, 177, 46– 56.

S. Luyssaert, M. Jammet, P.C. Stoy, S. Estel, J. Pongratz, **E. Ceschia**, G. Churkina, A. Don, H. Erb, **M. Ferlicoq**, B. Gielen, T. Grünwald, R.A. Houghton, K. Klumpp, A. Knohl, T. Kolb, T. Kuemmerle, T. Laurila, A. Lohila, D. Loustau, M. J. McGrath, P. Meyfroidt, E. J. Moors, K. Naudts, K. Novick, J. Otto, K. Pilegaard, C. A. Pio, S. Rambal, C. Rebmann, J. Ryder, A. E. Suyker, A. Varlagin, M. Wattenbach & A.J Dolman (2014) **Land management and land-cover change have impacts of similar magnitude on surface temperature**. *Nature Climate change*, 4, 389–393.

S. Ferrant, S. Gascoin, A. Veloso, J. Salmon-Monviola, M. Claverie, V. Rivalland, G. Dedieu, V. Demarez, E. Ceschia, J.-L. Probst, P. Durand & V. Bustillo (2014) **Agro-hydrology and multi temporal high resolution remote sensing: toward an explicit spatial processes calibration**. *Hydrol. Earth Syst. Sci*., 11, 7689-7732, doi:10.5194/hessd-11-7689-2014.

# 11. Italy Apulian Tavoliere

Team Leader and Members: Annamaria Castrignanò[1], Daniela De Benedetto[1], Domenico Ventrella[1], Anna Maria Stellacci[1], Pasquale Campi[1], Michele Rinaldi[2], Alessandro Matese[3], Piero Toscano[3], Carmen Maddaluno[2] and Massimo Mucci[2].

1- CRA-SCA Bari

2- CRA-CER Foggia

3- CNR-IBIMET Florence

Project Objectives

The main objectives of the project were to collect soil and crop data in order to:

1) validate a simulation model of water balance and crop growth;
2) implement a method by which leaf area index (LAI) can be generated from ground-truth LAI measurements using remote sensing multiband images as auxiliary variables. The lack of granted projects obliged us to simplify the sampling strategy.

Site Description

The interest of our study is focused on "Capitanata area", a plain of about 4000 km$^2$ located in the northern part of Apulia Region (south-eastern Italy). See Figure 96. This area is characterized by farms with average size up to 20 ha, and highly productive soils cultivated under intensive and irrigated regime. Winter durum wheat (Triticum durum L.) represents the main cereal crop often grown in rotations with irrigated horticultural species. Among these, processing tomato crop (Lycopersicon aesculentum Mill.) is well represented. In particular, two-year rotation (tomato-wheat) and three-year rotation (tomato-wheat-wheat) are the typical farming rotations of this important productive area.


Figure 96 Aerial Photo of Study Area

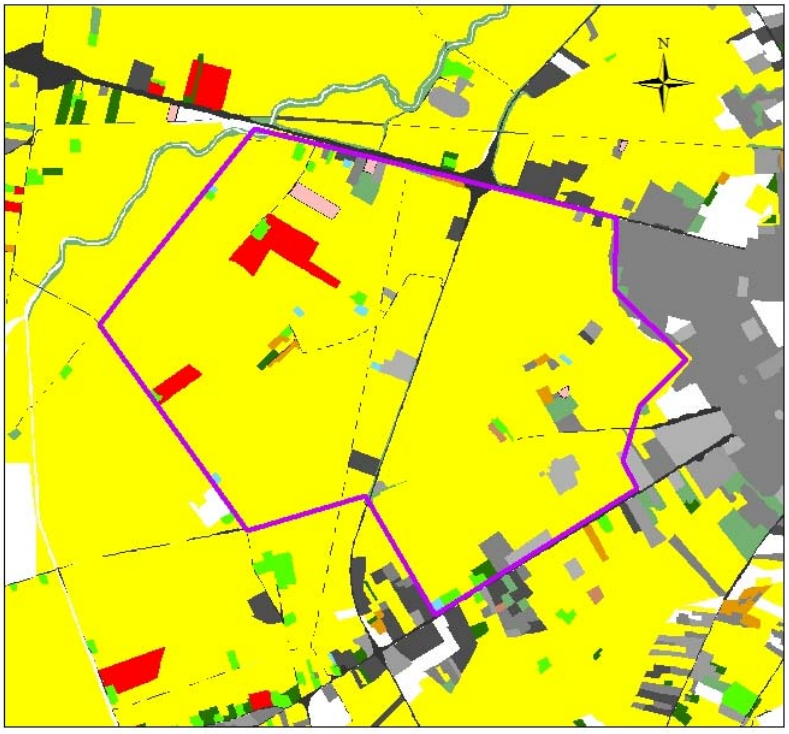


Figure 97 Land Use Map of the Surveyed Area within the Capitanata Plain

The Capitanata plain is delimited by the Apennines Chain on the west side and by Gargano Promontory on the east, and is mostly constituted by continental and fluvial sediments and some terraced marine deposits of the Pliocene and Pleistocene ages. The climate of this zone is classified as “Accentuated Thermo-Mediterranean” (UNESCO-FAO), with winter seasons characterized by temperatures that sometimes descend below 0°C and hot summers with temperature that may exceed 40°C. Annual precipitation ranges between 400 and 800 mm, mostly concentrated in the winter months. The rainiest months are October and November, while the dry period is from May to September.

In general, the soils are deep and clay with vertical behaviour, characterized by large and deep cracks in summer season under rain fed conditions. A wide part of the area is served by an irrigation consortium that fulfils the water requirements of crops with spring-summer cycle (e.g. tomato). In other parts, the irrigation for spring crops is carried out by utilizing private wells. The water table is very deep (200-300 m).

**Figure 98 Photo of Capitanata**

EO Data Received/Used

For this study we downloaded a total of 2 images (19 March 2014 and 6 May 2014) under clear sky conditions from the U.S. Geological Survey (USGS) website (http://glovis.usgs.gov, accessed on 2 February 2015). The 2 images are SR (Surface Reflectance) Landsat 8 products with a 30 m spatial resolution corresponding to the period of field activities and experimental campaign.

The vegetation indices computed in this study from LANDSAT data were: NDVI, SAVI, MSAVI, EVI, NBR, NBR2, NDMI. The normalized difference vegetation index (NDVI), the soil adjusted

vegetation index (SAVI) and the modified soil adjusted vegetation index (MSAVI) are all based on red and near infrared (NIR) bands.
Specifically, NDVI is the normalized difference between NIR and red bands. SAVI and MSAVI have been developed to take into account for changes in the soil optical properties; they contain respectively a soil brightness correction factor (L) and an inductive L function applied to maximize reduction of soil effects on the vegetation signal.
The three indices are computed as follows:

- **NDVI - Normalized difference vegetation index**

$$\mathrm{NDVI} = \frac{(NIR - red)}{(NIR + red)}$$

where NIR and red represent the reflectance in NIR and red bands, respectively.
In Landsat 8, NIR and red bands correspond to Band4 and Band5, respectively, thus the equation is: NDVI = (Band 5 – Band 4) / (Band 5 + Band 4).

- **SAVI – Soil adjusted vegetation index**

$$\mathrm{SAVI} = \frac{(NIR - red)}{(NIR + red + L)}(1 + L)$$

In Landsat 8 (L=0.5), SAVI = ((Band 5 – Band 4) / (Band 5 + Band 4 + 0.5)) * (1.5).

- **MSAVI – Modified soil adjusted vegetation index**

MSAVI= (2 * NIR + 1 – sqrt ((2 * NIR + 1)$^2$ – 8 * (NIR - R))) / 2

In Landsat 8, it corresponds to:
MSAVI = (2 * Band 5 + 1 – sqrt ((2 * Band 5 + 1)2 – 8 * (Band 5 – Band 4))) / 2.

The Enhanced Vegetation Index (**EVI**), together with the red and NIR bands, includes also a blue band. The index was developed to improve the NDVI by optimizing the vegetation signal in LAI regions using the blue reflectance, to correct for soil background signals and reduce atmospheric influences, including aerosol scattering. Specifically, it incorporates a “L” value to adjust for canopy background, “C” values as coefficients for atmospheric resistance, and values from the blue interval.

- **EVI -** Enhanced Vegetation Index

$$\mathrm{EVI} = \frac{\rho NIR - \rho red}{\rho NIR + C1 * \rho red - C2 * \rho blue + 1}$$

where 7 and 7.5 are two coefficients (C1 and C2, respectively); 1 is the soil adjustment factor (L).
In Landsat 8, EVI = (Band 5 – Band 4) / (Band 5 + 7 * Band 4 – 7.5 * Band 2 + 1).

Finally, the normalized difference moisture index (**NDMI**), and the normalized burn ratios (**NBR** and **NBR2**) consider also the short wave infrared (**SWIR**) region in order to discriminate the effect of water in the vegetation. Specifically, **NDMI** considers the **SWIR1** band (1570-1650 nm), **NBR** the **SWIR2** band (2110-2290 nm), whereas **NBR2** is calculated as a normalized ratio between the two **SWIR** bands, substituting the SWIR1 band for the **NIR** band used in **NBR** to highlight sensitivity to water in vegetation.
Equations for their computations are:

- **NDMI - Normalized difference moisture index**

$$\mathrm{NDMI} = \frac{(NIR - SWIR1)}{(NIR + SWIR1)}$$

In Landsat 8, NDMI = (Band 5 – Band 6) / (Band 5 + Band 6).

- **NBR - Normalized burn ratio**

$$\mathrm{NBR} = \frac{(NIR - SWIR2)}{(NIR + SWIR2)}$$

In Landsat 8, NBR = (Band 5 – Band 7) / (Band 5 + Band 7).

- **NBR2 - Normalized burn ratio 2**

$$\mathrm{NBR2} = \frac{(SWIR1 - SWIR2)}{(SWIR1 + SWIR2)}$$

In Landsat 8,NBR2 = (Band 6 – Band 7) / (Band 6 + Band 7).

We have also downloaded Sentinel-1 images of October 2014 that will be analyzed jointly with ground-truth data in 2015.

**References**

Masek, J.G., Vermote, E.F., Saleous, N., Wolfe, R., Hall, F.G., Huemmrich, F., Gao, F., Kutler, J., and Lim, T.K. (2006). A Landsat surface reflectance data set for North America, 1990-100, IEEE Geoscience and Remote Sensing Letters. 3:68-72.

Ren, H., Du, C., Liu, R., Qin, Q., Meng, J., Li, Z.L., Yan, G. (2014) Evaluation of Radiometric Performance for the Thermal Infrared Sensor Onboard Landsat 8, Remote Sensing 6, 12776-12788

In situ Data

**VALIDATION OF CROP MODEL**

The application of the crop growth and development model AquaCrop to durum wheat requires a series of inputs:

- Meteorological data: Daily values of maximum, minimum, dry and wet bulb temperatures, solar radiation, sunshine hours, rainfall, wind velocity and humidity (Figure 99);

**Figure 99 Photo of the Meteorological Station at the Experimental Farm of CRA-SCA**

- Physiological parameters: sowing date, number of seeds/$m^2$, various data related to phenological phases:
    - Crop development was expressed as growing degree days (GDD);
    - Canopy ground cover (CC) as a function of LAI was estimated by the following equation: CC = 1 – exp (−K•LAI); where K (extinction coefficient) was assumed to be equal to 0.65 for durum wheat;
    - The minimum effective rooting depth and the maximum effective rooting depth were set at 0.05 m and 1.2 m, respectively;
- Soil data: profile data of hydrological properties and total nitrogen content (each 2 cm in 40 layers).

**Table 15 Soil Inputs (Physical Properties)**

| Soil characteristics | Foggia |
|---|---|
| Depth (m) | 1.2 |
| Saturated hydraulic conductivity (mm $d^{-1}$) | 100 |
| Water content at field saturation (% volume) | 50 |
| Water content at field capacity (% volume) | 39 |
| Water content at wilting point (% volume) | 23 |

- Agronomic data: quality and quantity of soil profile nitrogen ($NH_4$, $NO_3$) content at the date of the start of simulation; rooting data.

These data were collected in one of the test sites cropped with durum wheat (cultivar Grecale) at the experimental CRA-SCA farm located in Foggia (41° 27' latitude N, 3° 04' longitude E) with the aim of validating the AquaCrop model for a rainfed crop in a Mediterranean area.
Durum wheat was sown on December 10th 2013. The durum wheat crop was grown using conventional agro-techniques (150 kg $ha^{-1}$ N).
For monitoring soil water status (W), capacitive probes of 0.1 m in length (Decagon devices, 10HS, USA) were installed horizontally in the soil at two depths (10 and 45 cm from the soil surface) in 2013 (Figure 100). The probes were linked to a Grillo datalogger (Tecno.El, ITA), which recorded the daily data of soil water content from February 1st to June 8th, 2014.


**Figure 100 Photos of Decagon Device**

The data of soil water status (W) were used for validation of the AquaCrop model. In particular, the measured data were compared with the output data from the model and model performance was evaluated through three statistics:

1. Model Efficiency Index (Nash and Sutcliffe, 1970), calculated with the following equation:

$$EF = 1 - \frac{\sum_{i=1}^{n} (Predicted_i - Observed_i)^2}{\sum_{i=1}^{n} (Observed_i - AvgObserved)^2}$$

where n represents the number of data pairs, i is the pair index and AvgObserved is the average of the observed data. Predicted and Observed correspond to model output and observation, respectively.

EF provides a simple index of model performance on a relative scale, where EF=1 indicates a perfect fit, EF=0 suggests that the model predictions are no better than the average, and a negative value indicates poor model performance.

2. the Relative Root Mean Square Error (RRMSE), calculated with the following equation:

$$RRMSE = \sqrt{\frac{\sum_{i=1}^{n} (P_i - O_i)^2}{n}} \cdot \frac{100}{\overline{O}}$$

where n is the number of observations, $P_i$ the value predicted by the model, $O_i$ the measured value, and $\bar{O}$ the mean of the measured values.

The validation is considered to be excellent when RRMSE is <10%, good if RRMSE is between 10 and 20%, acceptable if RRMSE is between 20 and 30%, and poor if >30% (Jamieson et al., 1991).

3. The coefficient of determination $R^2$ is defined as the squared value of the Pearson correlation coefficient and signifies the proportion of the variance of measured data explained by the model. It ranges from 0 to 1, with values close to 1 indicating a good agreement; values greater than 0.5 are considered acceptable in watershed simulations (Moriasi et al., 2007).

**References**

Allen R.G., Pereira L.S., Raes D., Smith M. (1998). Crop evapotranspiration: guidelines for computing crop water requirements. Irrigation and Drainage paper No. 56, FAO, Rome, 300 pp.

Jamieson P. D., Porter J. R., Wilson D. R., 1991. A test of the computer simulation model ARCWHEAT on wheat crops grown in New Zealand. Fields Crop Research, 27, 337-3.

Moriasi, D. N., Arnold, J. G., Liew, M. W. V., Bingner, R. L., Harmel, R. D., and Veith, T. L., 2007. Model evaluation guidelines for systematic quantification of accuracy in watershed simulations. Transactions Of The ASABE 50, 885–900

Nash J.E., Sutcliffe J.V., 1970. River flow forecasting through conceptual models part I - A discussion of principles. Journal of Hydrology, 10, 282-290.

Steduto P., Hsiao TC., Fereres E., Raes D. (2012). Crop Yield response to water - FAO Irrigation and Drainage Paper 66, Rome (Italy), 500pp.

## VALIDATION OF LANDSAT 8 SATELLITE-DERIVED LAI FROM FIELD MEASUREMENTS

Leaf area index (LAI) is one of the key biophysical variables to describe land surface processes of fundamental importance for vegetation, such as photosynthesis, transpiration and energy balance. Current spatial missions allow to estimate LAI at global scale, however product validation is needed for its reliable use. Evaluation of the product uncertainty is commonly based on direct validation, consisting in using indirect ground-truth data obtained from selected locations and time periods (Justice et al., 2000). As ground–based plot measurements are always temporally and spatially limited, the direct comparison with the satellite-derived products cannot be feasible due to spatial scale mismatch, georeferencing errors and spatial variability. Therefore, advanced methodologies must be developed (Martinez et al., 2009).

The Copernicus Global Land Service (http://land.copernicus.eu/global/) aims to continuously monitor the status of land territories and provide a series of bio-geophysical products (e.g. Albedo, LAI, FAPAR, Burnt Areas, Surface Temperature) on the status and evolution of land surface at global scale. The biophysical variables should be collected and processed according to the CEOS WGCV Land Product Validation (LPV) guidelines to be directly comparable with the medium resolution satellite product. Moreover, building a network of sites for the provision of regular and consistent ground biophysical datasets is necessary for the validation of Copernicus Global Land products. In the context of the FP7 ImagineS (2012-2016) project (http://fp7-imagines.eu/), in support of the evolution of the Global Land Service, a network of demonstration sites for the validation of Copernicus Global Land products has been established over cropland/grassland areas. The initial network has been expanded with additional sites where ground data are being collected thanks to the collaboration with other research teams involved in JECAM (http://www.jecam.org/), FLUXNET (http://fluxnet.ornl.gov/) or Environet (http://www.envir-net.org/) networks. The JECAM site of Capitanata was one of these additional sites. See Table 16 and Table 17. In Table 16, an asterisk denotes a JECAM site.

**Table 16 List of ImagineS Demonstration Sites where Ground LAI/FAPAR Measurements are Acquired**

| Site Name | Country | Latitude | Longitude | Biome |
|---|---|---|---|---|
| SouthWest(*) | France | 43.48 | 1.27 | Cropland |
| Barrax | Spain | 39.03 | -2.07 | Cropland |
| Tula (*) | Russia | 53.08 | 37.23 | Cropland |
| Upper Tana Basin | Kenia | -0.55 | 36.48 | Cropland |
| Merguellil (*) | Tunisia | 35.75 | 10.08 | Cropland |
| Ottawa | Canada | 45.30 | -75.50 | Cropland |
| San Fernando | Chile | -34.70 | -70.96 | Cropland |
| 25 Mayo | Argentina | -37.90 | -67.73 | Crops/Shrubs |
| Yanco | Australia | -34.75 | 146.07 | Grassland |
| Córdoba | Spain | 37.78 | -4.73 | Cropland |
| La Albufera | Spain | 39.274 | -0.316 | Rice |
| Rosasco | Italy | 45.253 | 8.562 | Rice |
| Pshenichne(*) | Ukraine | 50.075 | 30.11 | Cropland |

**Table 17 Additional Sites where Ground LAI/FAPAR Measurements are Acquired and Shared with ImagineS**

| Site Name | Country | Latitude | Longitude | Biome |
|---|---|---|---|---|
| Guangdong | China | 20,87 | 110,08 | Rice |
| Belgium-France | Belgium/France | 50,65 | 5,00 | Cropland |
| Collelongo | Italy | 41,85 | 13,59 | DBF |
| SantaRosa | CostaRica | 10,84 | -85,62 | Tropical F. |
| Heilongjang Farm-Heilongjang | China | 47,65 | 133,52 | Rice |
| Utiel | Spain | 39,58 | -1,26 | Vinyeard |
| Capitanata | Italy | 41,53 | 15.63 | Cropland |

In this report, we present a methodology to derive reference LAI maps from ground-based measurements over an agricultural area mostly cropped with durum wheat within the JECAM site of Capitanata. The up-scaling field based measurements is based on multivariate geostatistical techniques and makes use of ancillary information as Landsat 8 imagery.

Based on the previous achievements mainly during the VALERI project (http://w3.avignon.inra.fr/valeri/), a guideline for running a field campaign has been established (Baret and Fernandes, 2012). These protocols have been provided to the ImagineS sites for consistent ground data acquisitions.

**References**

Baret, F., and Fernandes, R., 2012. Validation concept. ESA report. VALSE2-PR-014-INRA. 39pp.

Justice, C., Belward, A., Morisette, J., Lewis, P., Privette, J., Baret, F., 2000. Developments in the 'validation' of satellite sensor products for the study of the land surface. International Journal of Remote Sensing, 21 (17): 3383–3390.

Martinez, B., Garcia-Haro, F.J., Camacho-de Coca, F., 2009. Derivation of high-resolution leaf area index maps in support of validation activities: Application to the cropland Barrax site. Agricultural and forest meteorology, 149: 130-145.

Field Measurements

Leaf area index (LAI) is defined as the total one-sided leaf area per unit ground surface area ($m^2$ $m^{-2}$). LAI was measured with LAI-2000 Plant Canopy Analyzer (LI-COR, 1992 Lincoln, NE, USA) (Figure 101) which uses a fish-eye lens with a hemispheric field of view (± 45°). The detector is composed of five concentric rings (sensitive to radiation in the 320-490 nm range). Each ring responds over a different range of zenith angles and radiation is thus azimuthally integrated.
The measurements were collected in one sensor mode using a 45° view cap, in clear sky condition, to avoid interferences from users' shadow.
This equipment measures LAI in a non-destructive way, by means of gap fraction, using above and below canopy light measurements.

**Figure 101 Equipment for LAI Measurements**

LAI was measured in 30 experimental sampling units (ESU) of 10m by 10m size within a polygon of about 3 km by 3 km size (Figure 102). In the figure, the ESUs are the yellow and red pins in the 3km x 3km area (yellow line); the other lines enclose CRA property. For each ESU, the measurement was performed once above the canopy, to obtain reference values, and four times below the canopy, before being averaged out. The four measurements were carried out at the corners of 10m x 10m squares, whose centre georeferenced was used as representative of the ESU where the measurement were performed. The standard error of the four LAI measurements is also given in the instrument output.

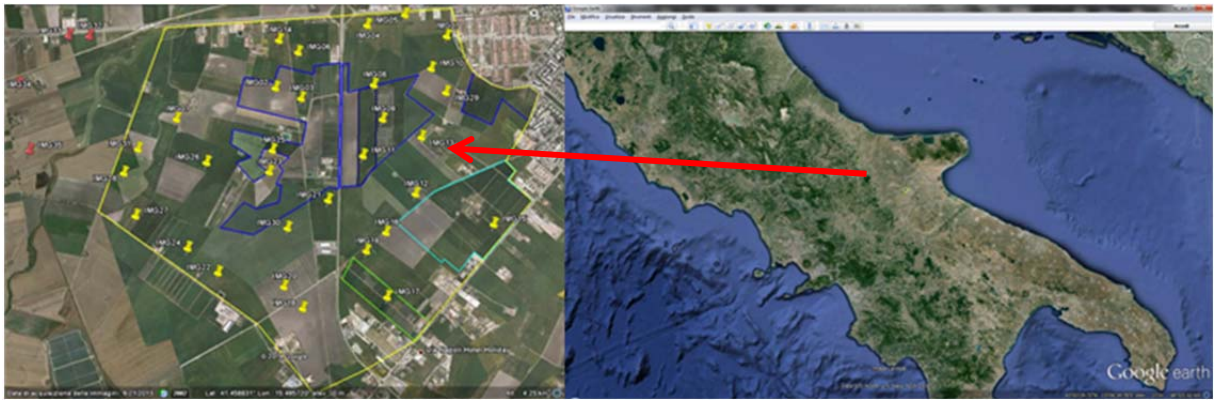


**Figure 102 Left: Location of ESUs Right: Location of the Area in Southern Italy**

**PAR**

The photosynthetic active radiation (PAR) of the surveyed area was estimated using the following equation:

**IPAR**

The intercepted PAR (iPAR) was estimated with the formula (Rinaldi and Garofalo, 2011), where *IE* is the interception efficiency of the canopy, calculated with Beer's law, as:

$$IE = 1 - e^{(k*LAI_d*Cf)}$$

$$Cf = 0.75 + (0.25) * \left(1 - e^{(-0.35*LAI_d)}\right)$$

The two surveys were carried out on March 18-20 2014 and on May 9-13 May 2014. At the first date, 35 fields were monitored: 1 of bare soil, 1 of artichoke (Figure 103 a), 4 of field beans (Figure 103 b) and 29 of durum wheat (Figure 103 c and d). The wheat crop was at elongation stage (Figure 103 d).

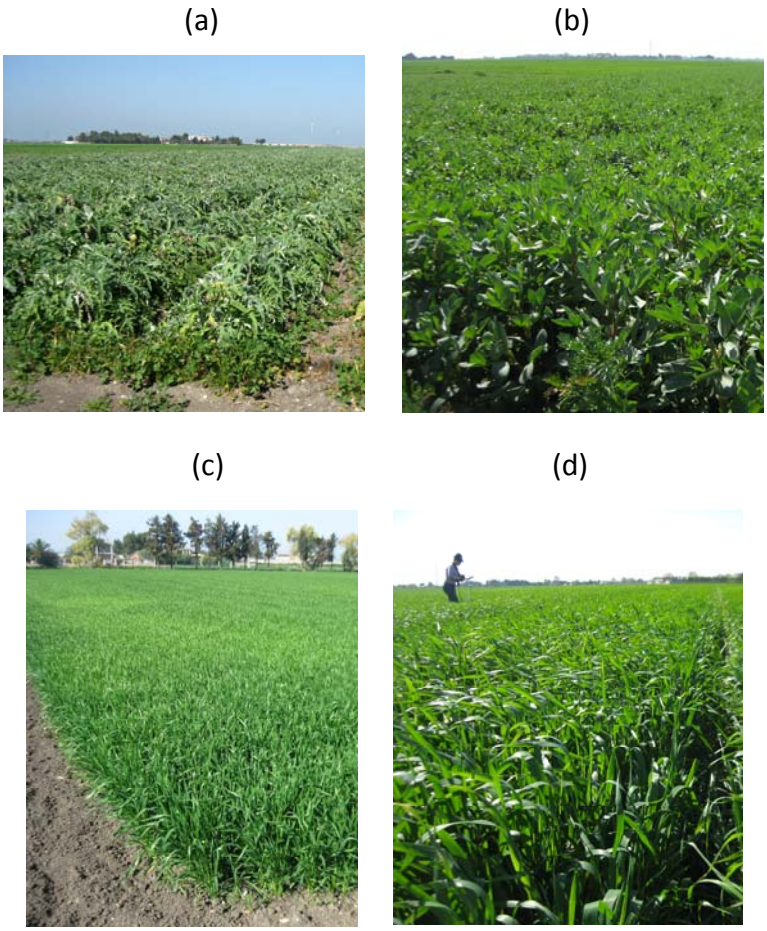


**Figure 103 Fields in March 2014: a) Artichoke, b) Field Beans, c) and d) Wheat**

At the second date, 31 fields were monitored, 1 of bare soil, 1 of artichoke, 4 of field beans and 25 of durum wheat. The wheat was at milk maturity stage (Figure 104).

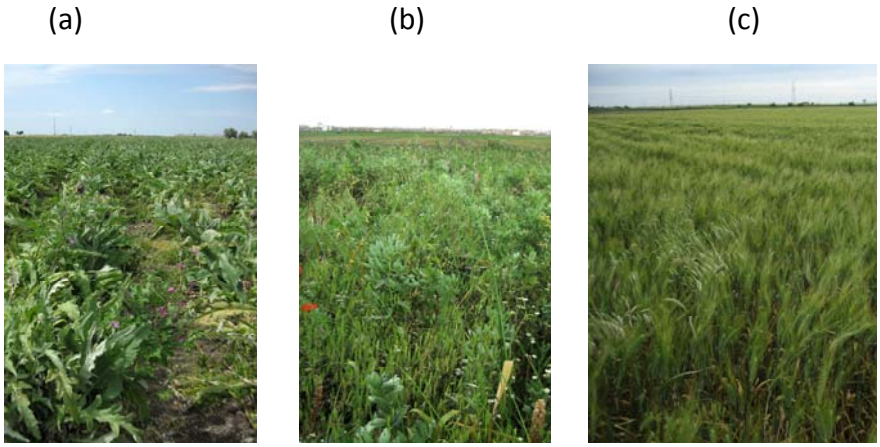


**Figure 104 Fields in May 2014: a) Artichoke, b) Field Beans, c) Wheat**

The sampling area is located in the middle of **Capitanata** plain and has a flat topography (average altitude 90 m above sea level). The surveyed area is mostly characterized by small-

medium farms of 20-ha size on average, intensively cultivated under an irrigation regime. Winter durum wheat (*Triticum durum* Desf.) represents the main cereal crop (about 70% of field crop area) often grown in rotations with irrigated horticultural species, mainly processing tomato crop (*Lycopersicon aesculentum* Mill.).

According to the local crop management scheduling, durum wheat is usually sown between November and the end of December and harvested in mid June. Another annual main crop of the region is sugar beets (sown in autumn and harvested in July), whereas permanent crops with a significant presence in the area are vineyards and olive trees.

**References**

Lang A.R.G., 1986. Leaf area and average leaf angle from transmittance of direct sunlight. Australian Journal of Botany. 34: 349-355

Lang, A.R.G., 1987. Simplified estimate of leaf area index from transmittance of the sun's beam. Agricultural and Forest Meteorology. 41: 179-186

Nilson T. 1971. A theoretical analysis of the frequency of gaps in plant stands. Agricultural Meteorology 8, 25-38

Rinaldi, M., Garofalo, P., 2011. Radiation-use efficiency of irrigated biomass sorghum in a Mediterranean environment. Crop Pasture and Science, 62:830-839.

*Up-scaling approach*

A way of integrating secondary finer-resolution information in primary sparse variable modeling is collocated cokriging, where the contribution of the secondary variable to cokriging estimate relies only on the cross-correlation between the two variables (Goovaerts, 1997). The approach is quite similar to ordinary cokriging with the only difference in the neighbourhood search. As using all secondary exhaustive information contained within the neighbourhood may lead to an intractable solution due to too much information, the initial solution of collocated cokriging was to use the single secondary value co-located at the target grid node. In ordinary cokriging, the weights attached to the secondary variable must add up to zero, therefore, if only one data value is used, its single weight is zero. The original technique was then extended so that the secondary variable is used at the target location and also at all the locations where the primary variable is defined within the neighbourhood. This solution has generally produced more reliable and stable results (Castrignanò et al., 2009; Castrignanò et al., 2012). The modified version, also referred to as “Multi-Collocated Cokriging” (MCCO) in the literature (Rivoirard, 2001) is less precise than full cokriging, because it does not use all the auxiliary information contained within the neighbourhood, so it requires much less computer time. However, because the co-located secondary datum tends to screen the influence of more distant secondary data, there is actually little loss of information. Differently than original technique of collocated cokriging, in this new version the influence of the secondary variable on the primary

variable is explicitly taken into account through the estimation of both the direct secondary variable variogram and the cross-variogram.

To perform multivariate geostatistical analysis on LAI data measured on the fields jointly with Landsat 8 data, the Remote Sensing multispectral data were collocated into the file containing the sparse LAI measurements by migrating the RS data to the location, up to a maximum distance of 30 m equal to the size of Landsat 8 pixel. The approach, different from ordinary cokriging, can advantageously utilize all the exhaustive secondary information recorded at the nodes of the interpolation grid of LAI and then upscale the sparse point measurements to a fine spatial scale.

An important requirement is to evaluate the quality of the product obtained from Remote Sensing images. In particular, it is important to derive a quality assessment index of the image to highlight areas on the LAI maps with unreliable LAI estimates, due to the technique of interpolation/extrapolation and/or sampling strategy.

To assess estimation uncertainty, the Confidence Interval (CI) was calculated. The CI reflects the inability to exactly define an unknown value and uncertainty increases with its magnitude. Calculation of CI is based on the following equation:

CI = Upper Limit – Lower Limit

where Upper and Lower limits are usually defined in terms of Standard Deviation (SD):

Upper Limit = Estimate+1.96 SD and Lower limit= Estimate – 1.96 SD (defining 95% Confidence Limits). The CI is then linked to the probability that the unknown value lies within a given range. The calculation of CI requires that the input sample data be normally distributed, otherwise they must be converted into Gaussian values. The Gaussian values are then multicollocated cokriged and the Gaussian cokriging variance is determined. Finally the Gaussian estimates and their corresponding upper and lower limits are back-transformed into the raw values. In order to make the values comparable, the relative CI was calculated by dividing by the corresponding LAI estimation and assumed as a quality index of LAI product.

**Reference**

Castrignanò, A., Costantini, E., Barbetti, R., Sollitto, D., (2009). Accounting for extensive topographic and pedologic secondary information to improve soil mapping. Catena 77: 28-38.

Castrignanò A., Wong M.T.F., Stelluti M., De Benedetto D., Sollitto D., (2012). Use of EMI, gamma-ray emission and GPS height as multi-sensor data for soil characterization. Geoderma, 175-176: 78–89.

Goovaerts P., (1997). Geostatistics for natural resources evaluation. Oxford Univ Press, New York.

Rivoirard J., (2001). Which models for collocated cokriging? Math. Geol., 33: 117–131.

**Collaboration**

We were contacted by Dr. Consuelo Latorre from EOLAB, to support the validation work of Copernicus Global Land products based on SPOT5, by using the ground data collected at the Italian JECAM site. Our team decided to accept the invitation, therefore on-the-ground measurements of LAI were carried out from spring 2014 to 2015 and are described in this report. However, since the SPOT5 were not made available by EOLAB, we decided to download the free images of LANDSAT 8, though at a coarser scale. Therefore, the size of ESU (10 m) was not suitable for LANDSAT 8, because it was planned for SPOT5 imaging.

We were also invited by dr. Fabio Vescovi of the GHP14011 – EducEO project to work voluntarily in the Pilot1 Project, which proposes the combined use of the crop data, collected by the farmers, and products derived from Sentinel1imagery. The project aims at establishing reciprocal education and information exchange between the Academic and farmers' communities. In the longer term, this activity will lead to the routine use of Sentinel-1 products to monitor the crops, help forecast the yields and provide a long term validation of Sentinel-1products. We received the first Sentinel-1 images in October 2014 and are going to use them in relation with ground-truth data and yield maps.

Results

Figure 105 and Table 18 show the results of the validation test of AquaCrop Model for durum wheat.

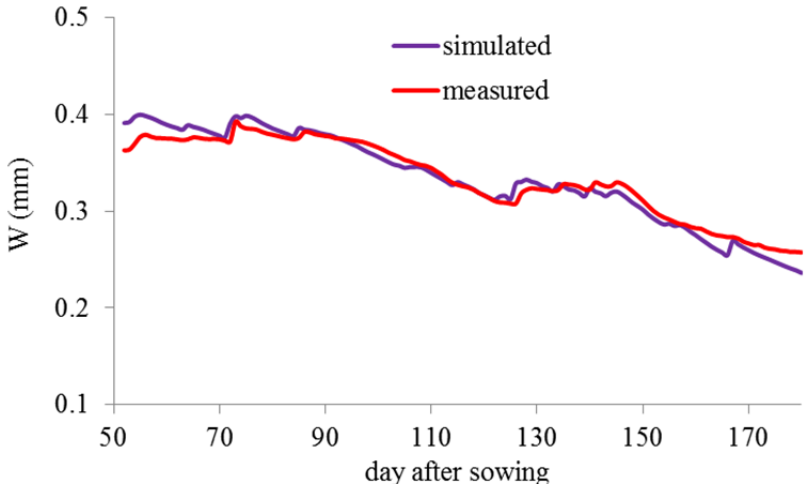


**Figure 105 Measured and Simulated Soil Water Content in AquaCrop Validation Test**

**Table 18 Results of the Validation Test of AquaCrop for Durum Wheat**

| RRMSE (%) | EF | $R^2$ |
|---|---|---|
| 3.1 | 0.93 | 0.97 |

Figure 105 shows the paths of soil water content (W) measured and simulated by the AquaCrop model during the 2014 season of durum wheat. The two lines appear to follow the same trend, with slight differences between them. However, to make the comparison more objective, the RRMSE in %, efficiency index and $R^2$ statistics were calculated (Table 18) and their values show that the model adequately simulates the soil water content at a daily scale. In particular, RRMSE is less than 10% (excellent performance), and EF and $R^2$ are quite close to 1. The very promising results of this validation encourage us to extend the application of the model to other sites of the surveyed area, previously described, where the inputs required by the model will be available. The upscaling of soil water and yield prediction will be performed by using the approach of multicollocated cokring, with fine-scale remote sensing images as auxiliary information, previously described.

Table 19 and Figure 106 show the basic statistics and the histogram distributions of the two LAI data sets measured with LICOR LAI-2000 at the two dates.

**Table 19 Descriptive Statistics of LAI Measured in March and May 2014**

| VARIABLE | Count | Minimum | Maximum | Mean | Std. Dev | Variance | Skewness | Kurtosis |
|---|---|---|---|---|---|---|---|---|
| LAI_March | 34 | 0.65 | 6.14 | 2.51 | 1.57 | 2.46 | 0.92 | 3.01 |
| LAI_May | 30 | 0.59 | 5.77 | 3.78 | 1.18 | 1.40 | -0.41 | 3.03 |

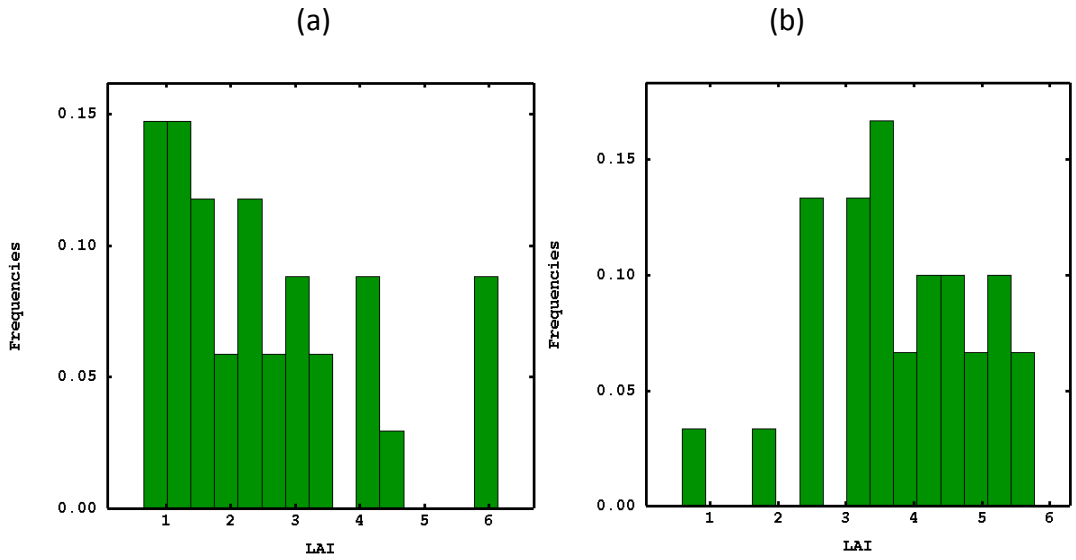


**Figure 106 Histogram Distributions of LAI Measured in March (a) and May (b)**

Whereas the distribution of March was positively skewned, the one of May was slightly negatively skewed with one outlier having a low value. Moreover, there was an increase of the mean value from March to May. The observed departures from a normal distribution may be due to the heterogeneity of the data sets including different types of crops not equally sampled owing to the prevalence of durum wheat (Figure 107).

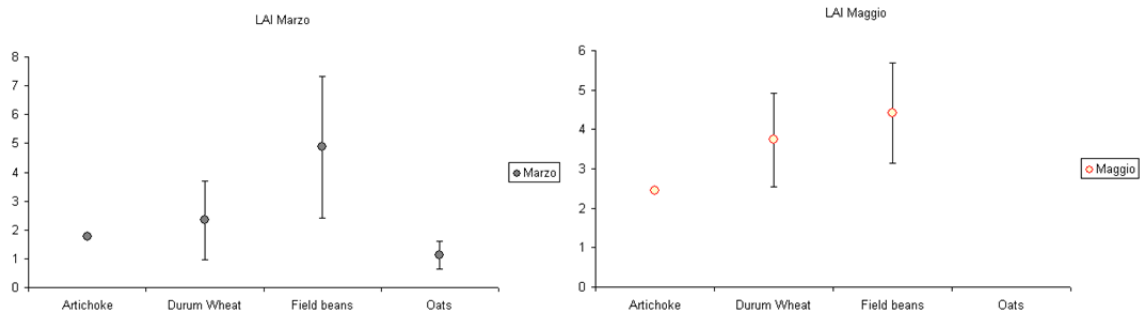


**Figure 107 Mean and Standard Deviation of Measured LAI by Crop Type in March and May**

From the previous considerations and in order to produce an assessment of LAI estimation uncertainty, the sample data were Gaussian transformed before applying multivariate geostatistical techniques with the LANDSAT-8 multiband images as auxiliary, exhaustive information.

In Figure 108 and Figure 109, the reflectance imagines of the individual Landsat-8 bands and the estimated LAI maps at the two selected dates (19 March and 6 May 2014) are displayed using an isofrequency color scale. As a common characteristic of the radiometric images, they essentially reproduce the partition of the intensively cropped area into the agricultural fields. A comparison between radiometric and estimated LAI maps results in a general high consistency: low values of reflectance in the visible (Coastal aerosol, Blue, Green, Red) and SWIR bands and high values of NIR band correspond to high values of LAI, as was expected. Conversely, high values of emittance in the thermal infrared bands (hot spots or stress areas) correspond to low canopy cover. The maps of thermal infrared bands are more smoothed due to the coarser resolution (100 meters).

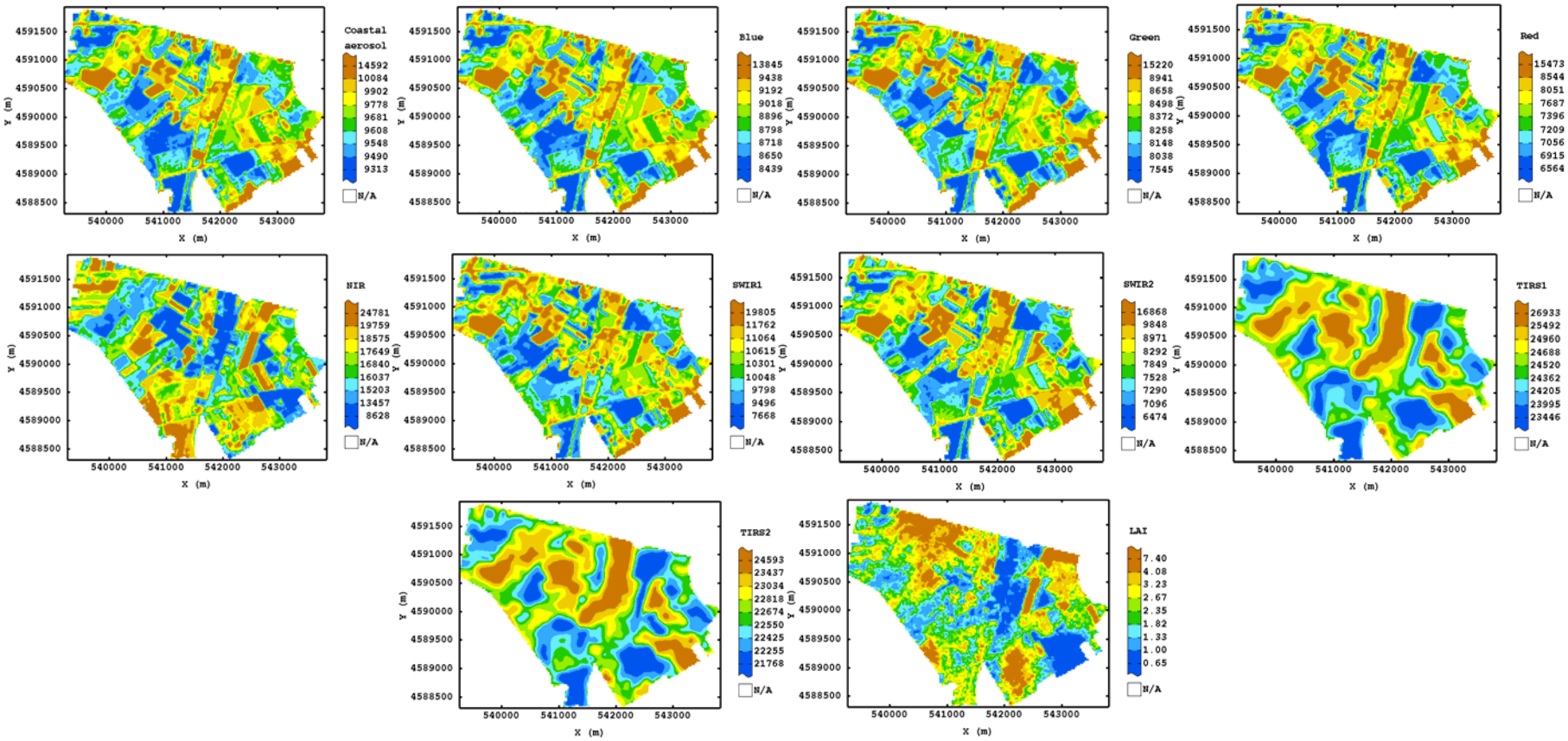


**Figure 108 Maps of the Coastal, Blue, Green, Red, NIR, SWIR and TIR Bands of Landsat-8 and LAI on 19 March 2014**

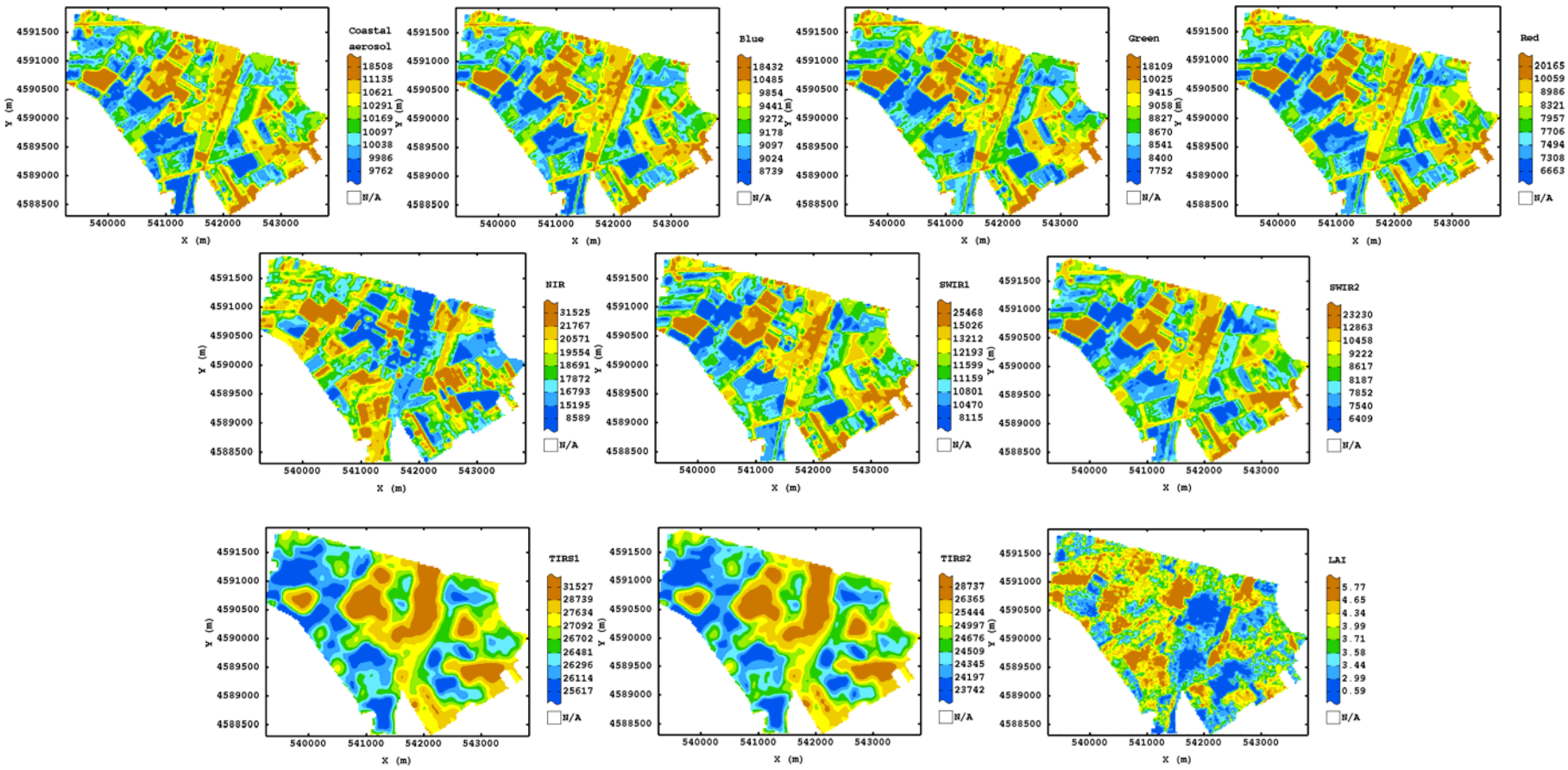


**Figure 109 Maps of the Coastal, Blue, Green, Red, NIR, SWIR and TIR Bands of Landsat-8 and LAI on 6 May 2014**

In order to make the comparison between multiband Landsat imagines and the estimated LAI map more objective, two sets of scattergram plots, using LAI as reference variable, were obtained and displayed in Figure 110 and Figure 111 for the two dates. The graphs also show the conditional expectation curve and the standard deviation of this curve. The diagrams confirm the type of relationships previously observed in a visual inspection of the relationship of LAI and NIR (positive) and the thermal bands (negative). Moreover, a wider dispersion around the conditional expected curve is observed in the diagrams of May. It is worth underlining that the more significant relationships between LAI and the individual band reflectance are not linear, which prevents us from using multivariate linear regression as the up-scaling method. Further, OLS regression does not take into account spatial correlation, which is expected to occur in fine-scale imaging.

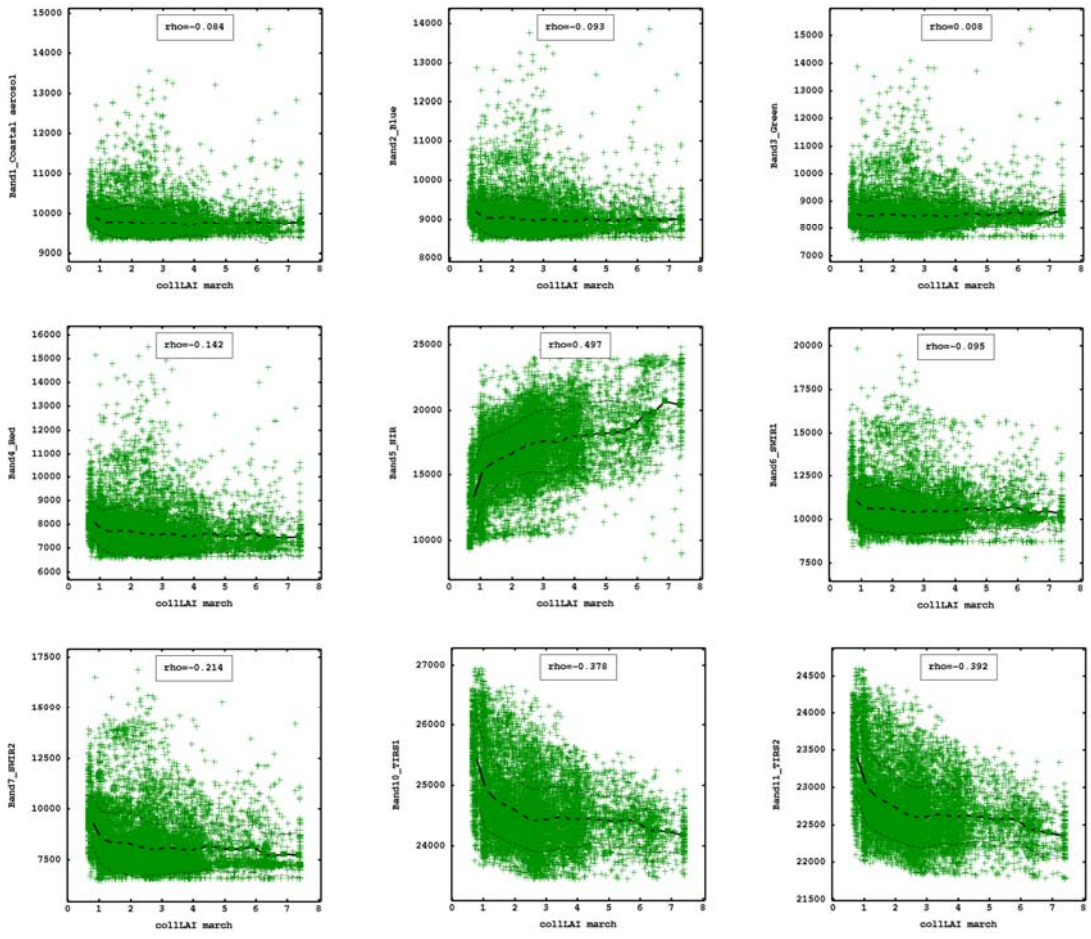


**Figure 110 Scatter Diagrams of Estimated LAI and all Landsat-8 Bands, 19 March 2014**

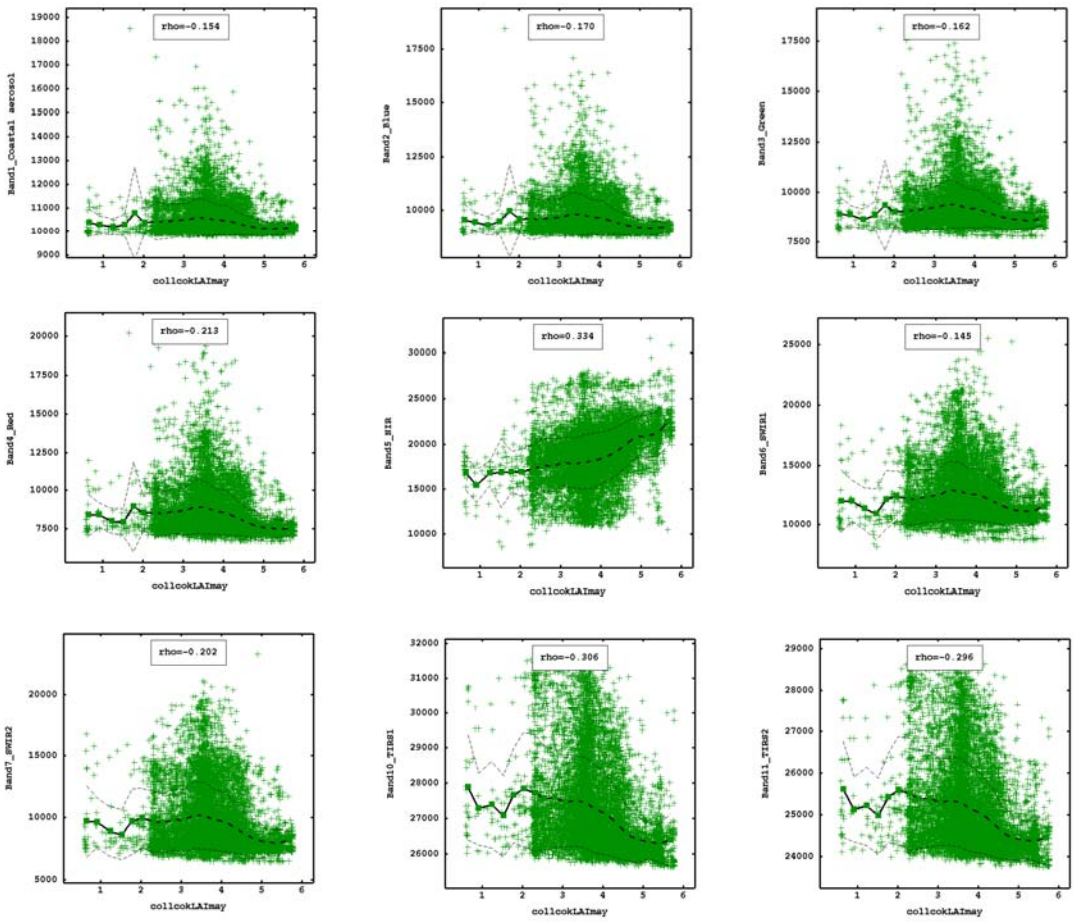


**Figure 111 Scatter Diagrams of Estimated LAI and all Landsat-8 Bands, 6 May 2014**

Figure 112 shows the quality images derived from the LAI estimator for the two dates with the locations of the sample data points superimposed. Pixels located near the samples are attributed a quality index of about 40-50% but, as the distance increases, the uncertainty becomes too great. The poor results are probably due to the too coarse sampling, with large areas without any ground-truth data of LAI.

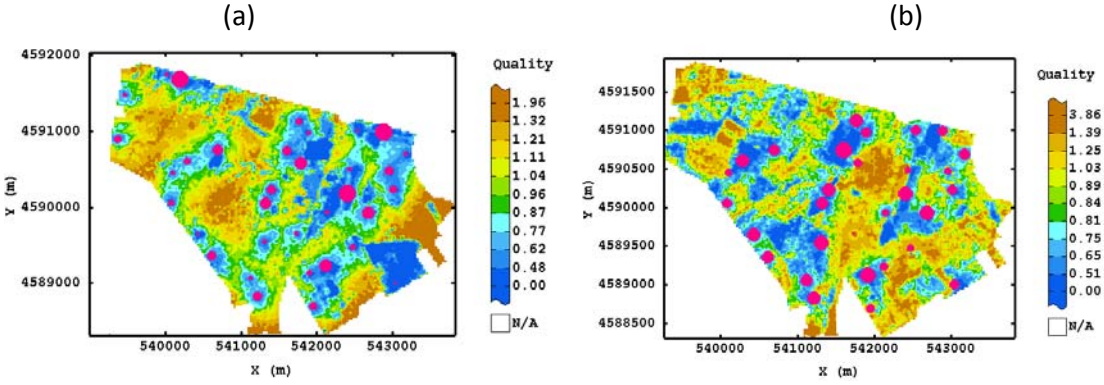


**Figure 112 Quality Maps for (a) March 2014 and (b) May 2014 with Observation Points**

In Figure 113 and Figure 114, the vegetation computed indices (VIs) are reported for the two selected dates (19 March and 6 May 2014). For each date, the spatial patterns of the

different groups of VIs (NDVI, SAVI and MSAVI; EVI; NDMI, NBR and NBR2) look very consistent. Specifically, from visual inspection of the maps and from comparison of the two dates, it seems possible to distinguish:

1. uncropped areas, characterized by very low values of all VIs at both dates;
2. small areas devoted to permanent crops (artichoke and asparagus), with high values of VIs observed at both dates;
3. areas cultivated with annual autumn and winter cycle crops (mainly wheat), where it is possible to record an increase in canopy cover between the two dates, as shown by the variation in the values of VIs;
4. areas cultivated with spring and summer cycle crops (mainly processing tomato and brassicaceae), where it is possible to record a canopy cover only in May, as shown by the variation in the values of Vis (low values in March and high values in May).

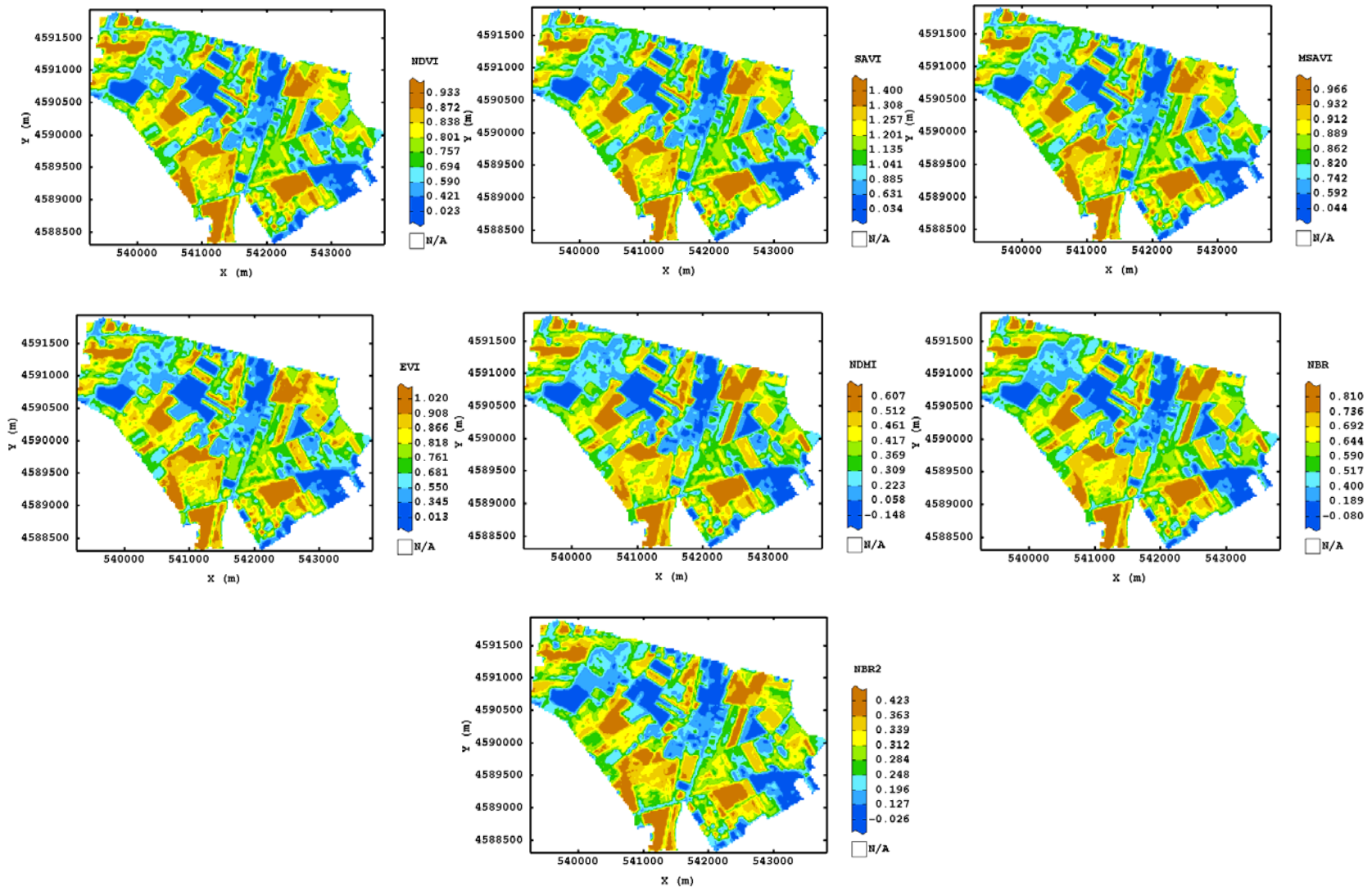


**Figure 113 Maps of Vegetation Indices Computed from Landsat-8 Bands, 19 March 2014**

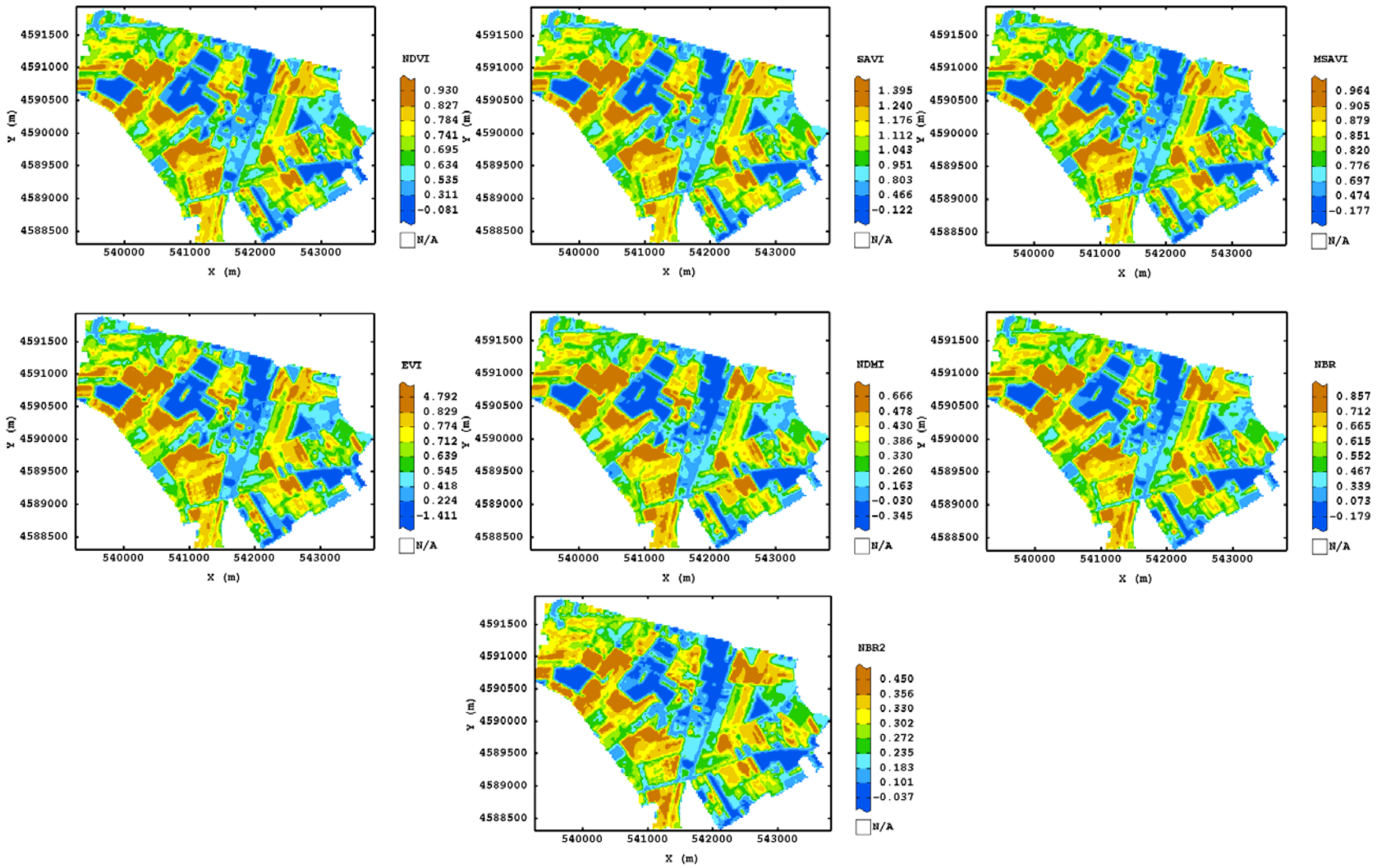


**Figure 114 Maps of Vegetation Indices Computed from Landsat-8 Bands, 6 May 2014**

Plans for Next Growing Season

Given the promising results of the AcquaCrop model validation, we plan to apply the model to other sites within the survey polygon, where durum wheat is cultivated to predict soil water content and gain yield. We also plan to continue the collection of LAI measurements according to the guidelines of IMAGINES project, to produce the high resolution maps of LAI based on fine-scale remote sensing images (SPOT5). However, we realize that the sampling strategy needs to improve according to a stratified random sampling, consisting of breaking the total area into subunits corresponding to the different land uses. Above all, in order to get an accurate characterization of the LAI heterogeneity found in the study area, it is critical to increase the number of ESUs and the number of replicated measurements (10-12) per each ESU. However, the realization of such plans of measurements, in support of validation activities, is conditional on getting funds for EO projects.

For the next crop year (2014-2015), we will also investigate the capabilities of the Sentinel-1 data of going valuable information on LAI, crop health and production potential. We will compare measurements and yield data with the Sentinel-1 images acquired at different time steps across the growing season. An analysis of pre-harvest Sentinel-1 data, field campaign data and post-harvest yield data will be performed to assess the feasibility of generating yield forecasts.

Publications

Balenzano A., Satalino G., Iacobellis V., Gioia A., Manfreda S., Rinaldi M., De Vita P., Miglietta F.,Toscano P., Annicchiarico G., Mattia F., 2014. A ground network for SAR-derived soil moisture product calibration, validation and exploitation in Southern Italy. Geoscience and Remote Sensing Symposium (IGARSS), 2014 IEEE International, 13-18 July, Quebec, Canada, 3382-3385. DOI 10.1109/IGARSS.2014.6947206.

Buttafuoco G., Castrignanò A., Matese A. Toscano P., 2014. Using geostatistical data fusion techniques and MODIS data to upscale simulated wheat yield, Abstract B33C-0182 presented at 2014 Fall Meeting, AGU, San Francisco, Calif., 15-19 Dec.

Camacho F., Lacaze R., Latorre C., Baret F., De la Cruz F., Demarez V., Di Bella C., Fang H., García-Haro J., Gonzalez M. P., Kussul N., López-Baeza E., Mattar C., Nestola E., Pattey E., Piccard I., Rudiger C., Savin I., Sanchez - Azofeifa A., Boschetti M., Bossio D., Weiss M., Castrignanò A., Zribi M., 2014. A Network of Sites for Ground Biophysical Measurements in support of Copernicus Global Land Product Validation. Proceeding of **4th International Symposium** on RAQRS**, 22-26 September 2014**.

Castaldi F., Casa R., Castrignanò A., Pascucci S., Palombo A. & Pignatti S., 2014. Estimation of soil properties at the field scale from satellite data: a comparison between spatial and non-spatial techniques. European Journal of Soil Science, 65, 842–851.

Rinaldi M., He Z., 2014. Decision Support Systems to Manage Irrigation in Agriculture. In Donald Sparks, Donald Sparks, editors, UK: Academic Press: Advances in Agronomy, 123:229-280.

## 12. Madagascar

Team Leaders: Valentine Lebourgeois and Agnès Bégué (Cirad UMR TETIS)

Team Members: Jacqueline Rakotoarisoa and Fidiniaina Ramahandry Andriandrahona (FOFIFA - National Center of Applied Research for Rural Development, Madagascar); Elodie Vintrou, Eric Scopel, Julie Dusserre (Cirad UR AIDA).

Project Objectives

The original project objectives have not changed. They are:

- Crop identification and Crop Area Estimation
- Yield Prediction and Forecasting.

This work aims at testing the potential of the future mission SENTINEL-2 to map croplands in a region of Madagascar characterized by small size fields, fragmented farmland and frequent cloud cover. The overall objective of this research is to provide new products from the future satellite mission, based on existing (SPOT) or recent (PLEIADES) missions to support early warning systems for food security. This preparatory work is conducted in two steps: (i) mapping of different cropping systems from multisource data (SPOT time series, very high resolution PLEIADES images, DEM, ground data) and data mining methods and (ii) estimation of agricultural production (phenological transition dates, yield).

Site Description

- Location: Antsirabe Region (60*60 km)
- Topography: The study site is located in a mid-altitude region characterized by presence of many hills.
- Soils: Clayey texture .
- Drainage class/irrigation : Middle.
- Crop calendar: Main cropping season from October to April.
- Field size: Mean field size 0.03 ha.
- Climate and weather: Tropical climate of altitude.
- Agricultural methods used: Manual Tillage / Hoeing / Fertilization with manure more or less mixed with ashes (few NPK inputs due to availability and cost) / Irrigation on terraces or basins, rain fed crops on the hills.

(a) (b)

**Figure 115 Irrigated Rice Fields (a) in a Basin, (b) Cultivated on Terraces**

**Figure 116 Rain fed Rice and Associated Maize**

**Figure 117 Agricultural Landscape Mainly Composed of Rice and Maize**

EO Data Received/Used

SPOT

- Space agency or Supplier: ASTRIUM - SPOT Image via SEAS-OI satellite receiving station.
- Optical
- Number of scenes: 26 images (60*60 km)
- Range of dates: October - June
- Beam modes/ incidence angles/ spatial resolution: Multispectral / incidence angles: between -31 and + 31 / 10 - 20 meters resolution
- Processing level:
    - SEAS-OI images: Delivered in level 1A then manually orthorectified and converted to top of atmosphere reflectance

Landsat-8

- Space agency or Supplier
  USGS

- Optical/SAR
  Optical
- Number of scenes
  11 images (subsets of 60*60 km)
- Range of dates
  October - June
- Beam modes/ incidence angles/ spatial resolutions
  Multispectral / incidence angles: variable / 15 meters pansharpenned.
- Processing level
  Orthorectified and converted to top of atmosphere reflectance manually

DEIMOS

- Space agency or Supplier
  Deimos Imaging
- Optical/SAR
  Optical
- Number of scenes
  3 images (subsets of 60*60 km)
- Range of dates
  November 2013 to January 2014
- Beam modes/ incidence angles/ spatial resolutions
  Multispectral / incidence angles: variable / 20 meters
- Processing level
  Orthorectified and converted to top of atmosphere reflectance manually

PLEIADES

- Space agency or Supplier: ASTRIUM - SPOT Image via CNES ISIS program
- Optical
- Number of scenes: 9 images covering 3 600 km²
- Range of dates: mid February – end of March (maximum of the growing season)
- Beam modes/ incidence angles/ spatial resolutions: Bundle (50 cm Pan + 2m 4-Band Colour) / standard incidence angle (30°)
- Processing level: Ortho.

In Figure 118, the black parts represent masked clouds.

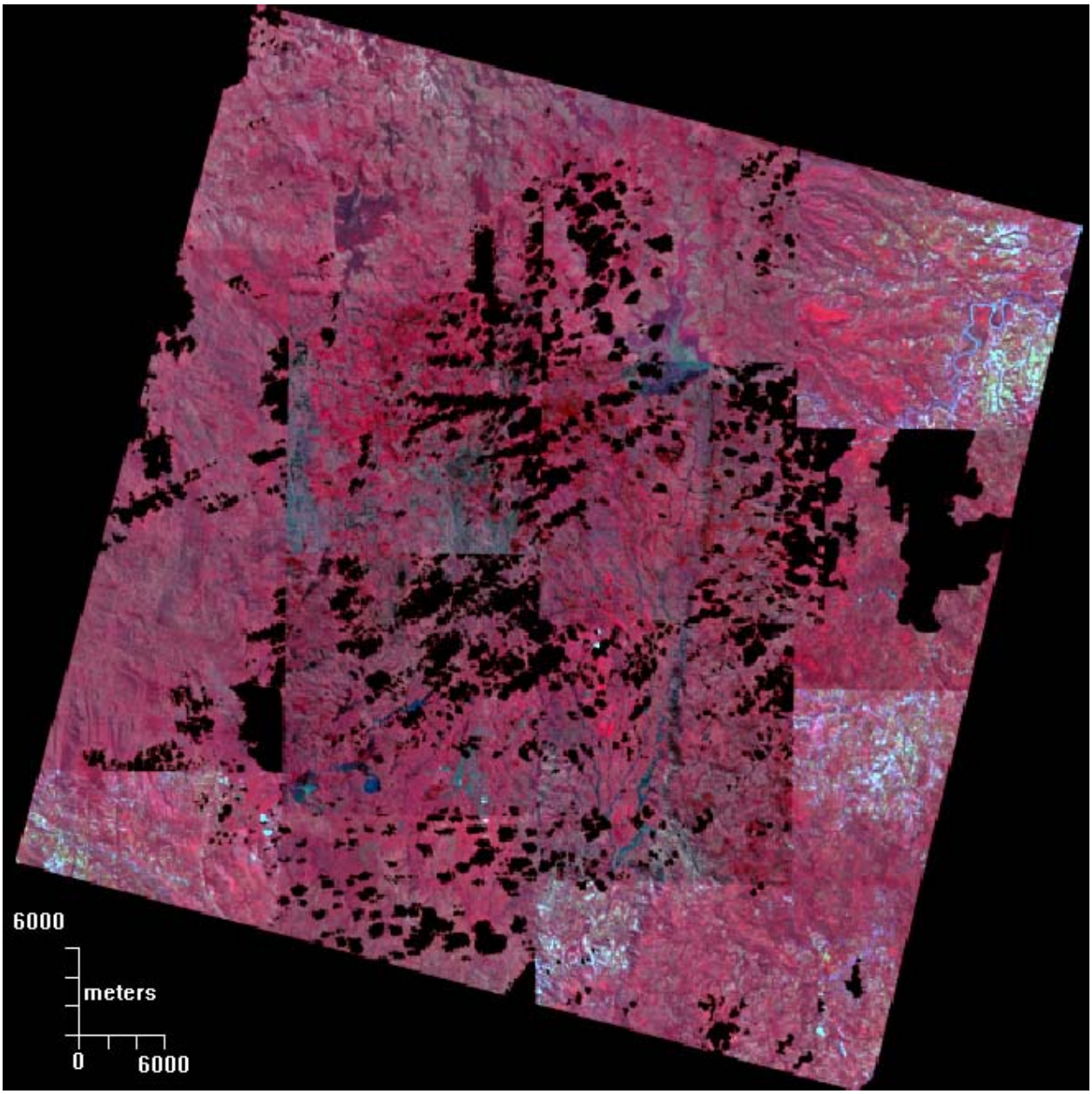




**Figure 118 Mosaic of PLEIADES Scenes Acquired in February and March 2014**

In situ Data

**Data Collected for Crop Characterization**

Field surveys were conducted in the study zone during the growing peak (end of February) of the 2013-2014 cropping seasons in order to characterize the main cropping systems. A total of 1125 GPS waypoints (851 cropped and 274 non-cropped) were registered in the study area, chosen according to their accessibility and to be as well representative of the existing cropping

systems as possible. The data gathered during the field surveys concerned farmers' practices (type of crop, use of fertilizers and irrigation). GPS waypoints were also registered on different types of natural vegetation to obtain data on the non-crop class.

**Data Collected for Estimate of Crop Production**

During 2013 harvest season, about 130 rice fields were sampled in order to obtain information on the farmers' practices (cultivar, planting date, irrigation, fertilization, harvest date) and the yield (dry biomass, grain yield on two plots of 1m² inside the field).


**Figure 119 Ground Measurements of Rice Yield**

Collaboration

We have not been approached to participate in a collaborative project with other sites.

Results

A classification method using Random Forest algorithm is currently being processed and involves three main steps:

i. satellite-derived and environmental metrics are calculated for the 1125 plots corresponding to the ground samples,
ii. the Random Forest algorithm finds the frequent “rules” of cropped and non-cropped plots (level 1) and of main crops (level 2),
iii. these frequent rules are used by the Random Forest algorithm and thanks to its attributes, each plot used as validation is affected to “crop” or “non-crop” class at level 1 and main crops at level 2.

The contribution of groups of metrics, such as spectral, textural, and spatial ones but also the contribution of the Pleiades very high resolution metrics is also analyzed.

Intermediary results are encouraging with an overall accuracy of 93% for level 1 (crop / non-crop) and 75% for level 2 (main crops).

Work on estimation of rice crop production is in progress. Due to the small size of cultivated fields, compared to the spatial resolution of satellite images (10 – 20 m), the temporal signal (NDVI) extracted for each sampled plot needs to be analyzed in order to isolate only plots having a pure temporal signal. This signal will be used for estimating crop phenological transition dates and yield.

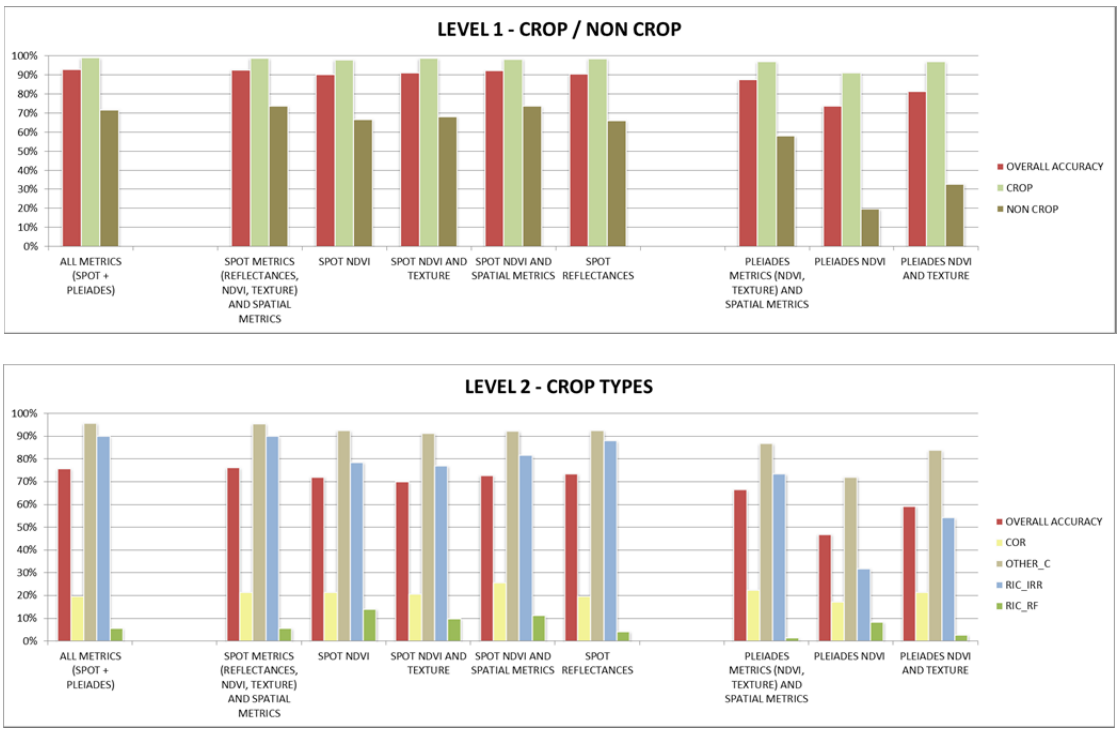


**Figure 120 Accuracy of Classes and Overall Classification of Random Forest Run (Intermediary Results)**

The results obtained meet 60% of the project objectives as the part on cultivated area and crop characterization is almost finished and work on estimation of crop production is in progress.

Plans for Next Growing Season

Next growing season, we plan to maintain the current approach. We anticipate ordering the same type/quantity of EO data next year.

Publications

Vintrou, E., Lebourgeois, V., Bégué, A., Ienco, D., Teisseire, M., Todoroff, P., Ramahandry Andriandrahona, F., 2014. Crop mapping in complex landscape by multi-source data mining and remote sensing for food security, Sentinel-2 for Science Workshop, 20-22 May, Frascati, Italie, 8 p.

## 13. Mali

No report received.

## 14. Mexico

No report received.

## 15. Morocco

Team Leaders: Lionel Jarlan (lionel.jarlan@cesbio.cnes.fr) and Saïd Khabba (khabba@uca.ac.ma)

Team Member: (JECAM correspondent) Michel LE PAGE (michel.lepage@cesbio.cnes.fr)

Project Objectives

The original project objectives have not changed. They are:

- Crop identification and Crop Area Estimation: Landcover maps at medium scale resolution from NDVI time series using either a thresholding algorithm, or an off-the-shelf algorithm for supervised classifications.
- Crop Condition/Stress: Methodological developments for the estimation and monitoring of surface states with multi-sensor, multi-spectral remote sensing of surfaces.
    - Evapotranspiration from infrared thermal and visible data (FAO-56, energy budget approach).
- Soil Moisture: High resolution soil moisture, by disaggregation of SMOS satellite measurements based on thermal and visible data (Merlin et al., 2009, 2012, 2013).
- Yield Prediction and Forecasting: A PhD thesis is working on the forecasting of wheat yield at the plot level using empirical relations. At the regional level, through statistical analysis of different types of optical and micro-wave remote sensing, combined with climate data, different dynamic prediction models of vegetation cover and cereal yields have been proposed (Jarlan et al. , 2013, Mangiarotti et al., 2013)
- Others: Two main research areas are considered. The first is to better understand the integrated hydrological functioning across the watershed and to develop tools (digital platform modeling fed by satellite and ground observation) to predict the evolution of resources. The first focus is developed with strong scientific dynamics around the following points: (1) Modeling and analysis of the functioning of the

main water flow (recharging process water, surface flows and particularly evapotranspiration, energy balance of the snow cover). In this context, we compare various approaches of evapotranspiration estimates with the level of complexity and the application for irrigation management. (2) Integrated modeling including conceptual and mechanistic modeling. (3) Satellite data assimilation into surface models. The second area focuses on the regional dimension of the problem of environmental hydro resources in the Mediterranean, and the need to produce indicators at this level in particular exploiting the remote sensing data. This area is developed around the following: (1) Methodological developments for the estimation and monitoring of surface states with multi-sensor, multi-spectral remote sensing of surfaces and (2) the characterization of indicators for better understanding of hydrological functioning. The work deals with predictability and the modeling of inter-annual variability.

Site Description

The watershed is located in the Tensift region of Marrakech in Morocco (Figure 121). Covering an area of about 20,000 km², it is composed of 3 hydrological parts. South of the basin, the northern slopes of the Atlas are well-watered and have snow (up to 600 mm / year). Peaking at over 4,000 m, these mountains are the water tower of the Haouz plain. In the center, a vast plain, characterized by a semi-arid climate (rainfall 250 mm / year), and where the water flows are predominantly vertical except for wadis and water infrastructures. The main irrigated areas are located in the central and eastern part (2000 km²) and rain fed cereals are grown on the rest of the plain. Wheat is the main crop with over 80% of acreage in wheat, followed by olive trees which occupy about 13% of the plain, and the remainder is occupied by citrus, apricot, market gardens, vineyards, fodder. These proportions change significantly in the irrigated area where tree crops dominate. In the north, the small chain of arid mountains "Jbilets" has, as far as we know, little influence on the hydrological cycle in the region.

Two test sites are considered for JECAM:

- The R3 sector is a 3000 ha area with flood irrigation on demand located 40 km east of Marrakech. The main crop is Winter Wheat. The other crops, representing less than 20% of the cultivated area, are sugar beets, olive trees, etc. The soil texture is mainly Clay Loam. The growing season of winter wheat is December-June, sugar beets from November to june, and olive groves are evergreen with latency during the summer. The whole site has been under study since 2002 and benefited from several remote sensing campaigns with optical (SPOT, Landsat, Formosat), thermal (Aster, Landsat), and SAR (ASAR) satellite time series.

- The Agafay plantation is a mandarin orchard located 20 km east of Marrakech which occupies 500 ha. The plantation benefits from drip irrigation. The soil texture is loam. Mandarin trees are evergreen with latency during the summer. The site has been monitored since 2006 with an eddy covariance system, soil temperature and humidity sensors, and flux meters. Sapflow measurements have been conducted for separation of evaporation and transpiration.

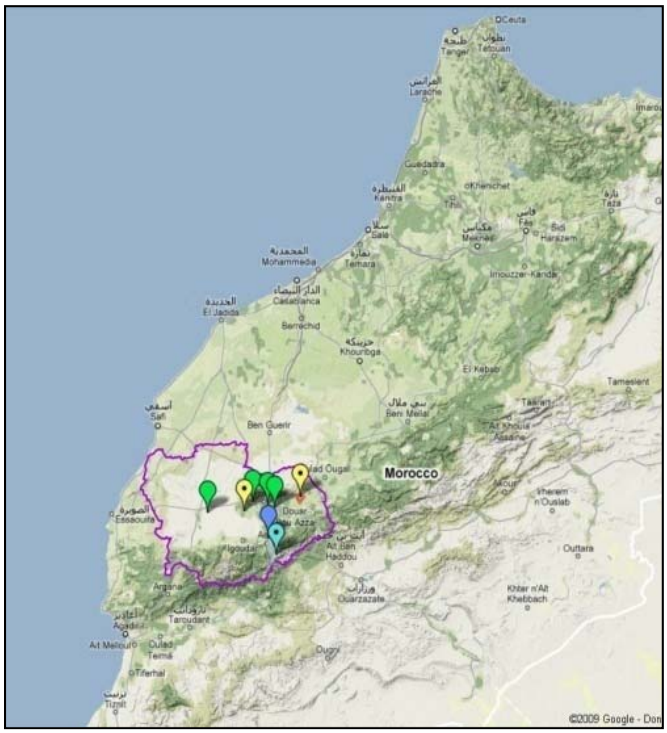


**Figure 121 Location of the Tensift Watershed in Morocco**

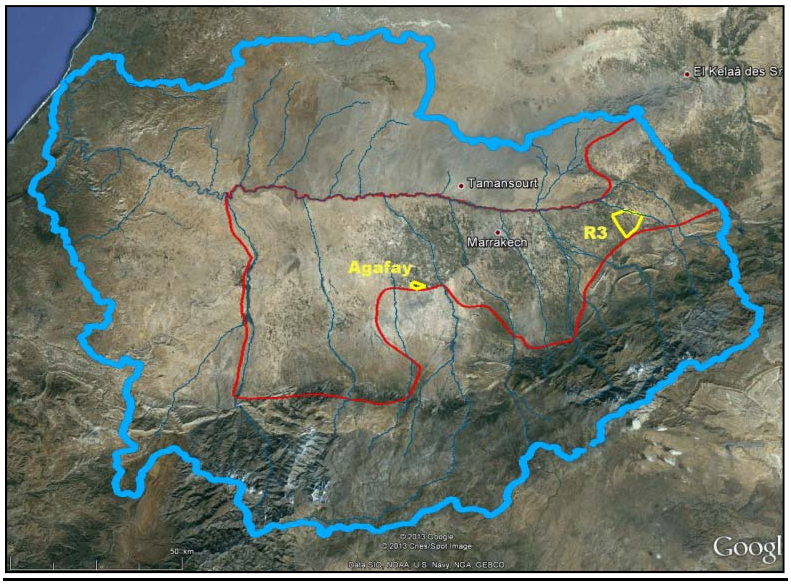


**Figure 122 Location of the Haouz Plain (red) and the Two Sites (yellow) in the Tensift Watershed (blue)**

**Figure 123 A Wheat Field in the Haouz Plain of Marrakech, with the High Atlas Mountain in the Background**

EO Data Received/Used

We have not received any EO through JECAM. The process of acquiring imagery through JECAM is unclear. The EO images used during 2014 are shown in Table 20.

| | **Supplier** | **Optical/SAR** | **Number of scenes** | **Range of dates** | **Processing level** | **Challenge ordering** | **Challenge Using** |
|---|---|---|---|---|---|---|---|
| ASTER | NASA/JSS | Optical (VIS/NIR/TIR) | 4 over R3 | April-may | Land surface temperature and VIS/NIR reflectance | DAR proposal; 70 euros per product and per scene | |
| Landsat-8 | USGS | Optical (TIR) | 2 over R3 | April-May | Brightness temperatures | none | Requires atmospheric corrections |

**Table 20 EO Images Used during 2014**

In situ Data

See Table 21.

**Table 21 In situ Data for Tensift, Morocco Site**

| Group | Parameter | Instrument | Acquisition mode | Sampling | Site | Period(s) |
|---|---|---|---|---|---|---|
| **Vegetation** | Fraction cover, LAI, Biomass | Hemi-photo | O | 10 days | R3 | Field campaigns<br>2003, 2004, 2006,2012, 2013, 2014 |
| | | Destructive cut | | Annual | Agafay | |
| | Yield (wheat) | Survey | O | Annual | R3 | |
| **Land cover And Agricultural practices** | Land cover | Survey | O | Annual | R3+ Agafay | 2002, 2004,2006<br>2010- 2015 |
| | | Remote sensing | A | Annual | R3+ Agafay | 2001-… |
| | Plowing<br>Sowing | Survey | O | Agricultural Season | R3 | Since 2006 |
| | Irrigation | Survey | O | By water turn | R3 | 2002, 2006, 2008-... |
| | | | | Drip (daily) | Agafay | 2006-... |
| **Water and Energy Budget** | Rn | Radiometer | A | 30 min. | Intensive sites (table) | |
| | G | Flux plates | | | | |
| | H | Turbulent fluxes | | | | |
| | LE | | | | | |
| | Vertical profiles of temperature | | | | | |
| | Vertical profiles of humidity | Reflectrometry probes | | | | |
| | Surface humidity | Capacitive probes | O | 1-7 days | | |

| Group | Parameter | Instrument | Acquisition mode | Sampling | Site | Period(s) |
|---|---|---|---|---|---|---|
| | Water fluxes | Fluxmeter | A | 30 min. | R3 | |
| **Weather** | P | Weather station | A | 30 min. - 1hr | 15 stations (Figure 123) | |
| | U | | | | | |
| | RH | | | | | |
| | Ra | | | | | |
| | R0 | | | | | |
| | Rain | | | | | |
| | Rain | Pluviometer | O | Daily | 36 pluvios | From the 60's for some pluviome-ters |
| **In Situ remote sensing measure-ments** | Réflectance / NDVI | Cropscan | O | 15 days | R3, wheat | Field campaign |
| | Ts | Thermoradio-meter | A | 30 min. | Intensive sites (table) | |
| | Optical depth and water vapor | CIMEL photometer | A | 15 min. | Saada | 2004-... |

## Collaboration

The International Joint Laboratory TREMA associates several partners from the research and academic sector (University Cady Ayad of Marrakech, Moroccan Center of Energy and Nuclear Sciences, Moroccan National Meteo Center, French Laboratory CESBIO) as well as decision makers (Basin Agency of the Tensift River, Regional Office of Agriculture). The LMI TREMA works in close collaboration with the "Merguellil team" in Tunisia, which is also a JECAM site (CESBIO and G-EAU labs, Tunisian Insitute of Agronomy). The Tensift site is part of the S2-AGRI project financed by the European Space Agency.

Results

Two PhD Theses were defended this year on the topic of agriculture and irrigation:

- S. BELAQZIZ: A decision support approach for the management of a gravity irrigation system: multi-agent modeling, remote sensing and optimization evolutionary algorithm.
- M.H. KHARROU: Contribution of remote sensing to analyze the performance of irrigation systems in semi-arid area.

Two other PhD theses are under preparation:

- Crop condition and stress with Remote sensing-FAO-56 method and Tseb: Phd of A Diarra began in 2013.
- Yield prediction: Phd of J. Toumi began in 2013 (Toumi et al 2015 submitted).

Whereas future sensors in the visible and near infrared bands like Sentinel-2 (Drusch et al. 2012) to be launched in 2015 will provide combined high spatial and high temporal resolution, operational soil moisture products are currently derived from radiometers or radars operating in the microwave domain with a spatial resolution above 10 km. Consequently, efforts have been put on the disaggregation of soil moisture products derived from microwave radiometers such as SMOS (Soil Moisture and Ocean Salinity, Kerr et al. 2010). As an example, the downscaled data set presented below is obtained from the disaggregation of 40 km resolution SMOS soil moisture at 1 km resolution using MODIS (MODerate resolution Imaging Spectroradiometer) data and DISPATCH (DISaggregation based on Physical And Theoretical scale Change ; Merlin et al., 2013) methodology. The on-going validation of DISPATCH at 1 km resolution in the Tensift catchment is especially challenging due to i) potentially strong topographic effects on MODIS temperature and ii) the presence of crop irrigation at a scale (typically 3-4 ha) much smaller than the target downscaling resolution. These conditions are however particularly suitable to develop performance metrics for downscaling methods since DISPATCH is expected to cover a large range of performances with possible significant errors in the output data relative to in situ measurements. Merlin et al. (2015) defined a new metric named $G_{DOWN}$ to specifically assess the overall gain achieved at high resolution by disaggregation, relatively independent from uncertainties in low resolution observation, and from the representativeness of localized in situ measurements at the target downscaling resolution. The performance metric was tested during a 4-year period by comparing 1 km

resolution DISPATCH data with the soil moisture measurements collected at 6 stations in central Morocco. The new metric was found to be consistently correlated (correlation coefficient ranging from 0.5 to 0.8) with the disaggregation gain in time series correlation, mean bias and bias in the variance. In contrast, the traditional root mean square difference between disaggregation output and in situ measurements was poorly correlated (correlation coefficient of about 0.0) with the disaggregation gain in terms of both time series correlation and bias in the variance. As the first metric dedicated to soil moisture downscaling methods, $G_{DOWN}$ is expected to be very useful in comparing different disaggregation methods applied to various low resolution soil moisture data including AMSR, SMOS and SMAP products.

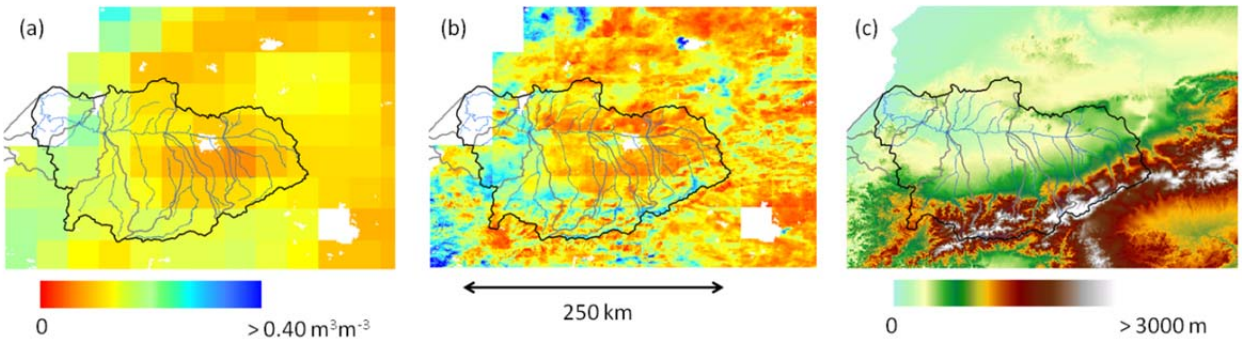


**Figure 124 SMOS Soil Moisture on 5 October 2013 (a) at Original Resolution (b) 1 km DISPATCH Data (c) 1 km DEM**

Among the considerable variety of existing approaches to estimate ET from remote sensing data, the most widely used approach is to force the FAO-56 method (Allen et al., 1998, 2005) with NDVI data (Bausch and Neale, 1989). However, the FAO-NDVI method is not sufficient to accurately estimate water consumption, especially when soil evaporation and stress under full vegetation cover conditions occur as highlighted by Er-Raki et al. (2007). Within this context, Chirouze et al. (2014) compared several approaches based on thermal imagery that should be better suited for evapotranspiration estimates under stressed conditions. Those approaches, either solving the surface energy budget at the pixel scale or assuming that complete stress conditions (from unstressed to fully stressed) are present in a remote sensing image, provide snapshot estimates of evapotranspiration at the time of the satellite overpass. This work highlights the good performance of the TSEB model for evapotranspiration estimate. TSEB has been further evaluated in different crop conditions by Bigeard et al. (2015, submitted to HESS)

and Diarra et al. (2013). At the same time, a consistent and unifying interpretation of the image-based approaches in Moran et al. (1994) and in Roerink et al. (2000) was proposed. The monosource surface energy balance model (SEB-1S) estimates the evaporative fraction (defined as the ratio of evapotranspiration to the available energy) from satellite data composed of surface temperature, a vegetation index (e.g. NDVI) and surface albedo, resulting in accurate evapotranspiration estimates at 100 m resolution (Merlin 2013). Recently, Stefan et al. 2015 have integrated a soil energy balance model into the image-based approach to improve the robustness of SEB-1S when applied to low resolution (MODIS like) data. As a step further, the SEB-1S approach was extended to a multi-source representation of agricultural fields (Merlin et al. 2014). The main originality of SEB-4S (four source surface energy balance model) is to explicitly separate the energy and water fluxes of unstressed green (photosynthetically active) vegetation, non-transpiring green vegetation, senescent vegetation and bare soil. SEB-4S has hence potential to better characterize the portion of evapotranspiration unusable for crop productivity (soil evaporation) and the crop water need (via the plant transpiration) from satellite images solely. Its modeling structure is also well adapted for integrating into the future the near-surface soil moisture retrieved from microwave data, as a further constraint on the evaporation/transpiration partitioning.

Plans for Next Growing Season

In 2015, the SPOT5-TAKE5 experiment will take place. We will focus on three aspects:

- Estimation of evapotranspiration of tree crops over a mountainous area. The experiment will associate the use of scintillometry, eddy-correlation, and high resolution optical imagery at high repetitivity with SPOT5-Take5.
- The partitioning of evapotranspiration of the vegetation into evaporation and transpiration by combining temperatures from ASTER and reflectancies form SPOT5.
- A third experiment aims to take advantage of the high repetitivity of SPOT5-Take5 to estimate the volumes of water infiltrated into the aquifer within a river flooding.

Publications

Articles

1. Belaqziz, S., S. Mangiarotti, M. Le Page, S. Khabba, S. Er-Raki, T. Agouti, L. Drapeau, M.H. Kharrou, M. El Adnani, and L. Jarlan. 2014. “Irrigation Scheduling of a Classical Gravity Network Based on the Covariance Matrix Adaptation – Evolutionary Strategy Algorithm.” Computers and Electronics in Agriculture 102: 64–72.
2. Jarlan, L, J Abaoui, B Duchemin, A Ouldbba, Y M Tourre, S Khabba, M Le Page, R Balaghi, A Mokssit, and G Chehbouni. 2014. “Linkages between Common Wheat Yields and Climate in

Morocco (1982-2008).” International journal of biometeorology 2014, 58 (7), p. 1489-1502. ISSN 0020-7128

3. Le Page M., Jihad Toumi , Saïd Khabba, Olivier Hagolle, Adrien Tavernier,M. Hakim Kharrou, Salah Er-Raki, Mireille Huc , Mohamed Kasbani , Abdelilah El Moutamanni, Mohamed Yousfi and Lionel Jarlan, A Life-Size and Near Real-Time Test of Irrigation Scheduling with a Sentinel-2 Like Time Series (SPOT4-Take5) in Morocco, Remote Sensing, 2014, 6, 11182-11203; doi:10.3390/rs61111182.
4. Merlin, Olivier, Yoann Malbéteau, Youness Notfi, Stefan Bacon, and Salah Er-raki. 2015. “Performance Metrics for Soil Moisture Downscaling Methods : Application to DISPATCH Data in Central Morocco.” Remote Sensing, minor revision
5. Merlin, Olivier, Jonas Chirouze, Albert Olioso, Lionel Jarlan, Ghani Chehbouni, and Gilles Boulet. 2014. “An Image-Based Four-Source Surface Energy Balance Model to Estimate Crop Evapotranspiration from Solar Reflectance/thermal Emission Data (SEB-4S).” AGRICULTURAL AND FOREST METEOROLOGY 184: 188–203.
6. Mangiarotti, S., L. Drapeau, and C. Letellier. 2014. “Two Chaotic Models for Cereal Crops Cycles Observed from Satellite in Northern Morocco.” Chaos: An Interdisciplinary Journal of Non linear Science 24: 023130
7. Toumi, J., Er-Raki, S., Ezzahar, J., Khabba, S., Jarlan, L. 2015. Calibration and Validation of the Aquacrop model for estimating evapotranspiration and grain yields of winter wheat in semi-arid region of Tensift Al-Haouz (Marrakech, Morocco): application to manage water irrigation. Agricultural and Water Management, en revision.
8. Vivien G. Stefan, Olivier Merlin, Salah Er-Raki, Maria-José Escorihuela, and Said Khabba, 2015. Consistency between in situ, model-derived and image-based soil temperature endmembers: towards a robust data-based model for multi-resolution monitoring of crop evapotranspiration. Submitted to Hydrol. Earth Syst. Sci.

Conferences

9. Le Page M., Khabba S., Simonneaux V., Belaqziz S., Kharrou M.H., Er-Rak S., Berjamy B., Fakir Y., Duchemin B., Boulet G., Mougenot B., Lili Chaabane Z., Hagolle O., Chehbouni G., Jarlan L. 2014. Remote Sensing Time Series for Water Management of Irrigated Areas in Semi-Arid Regions. *Sentinel-2 for Science Workshop, 20 - 22 May 2014, Frascati, Italy*
10. Er-Raki, S., Khabba, S., Ezzahar, J., Jarlan, L., Chehbouni, G. 2014. Using the Heat Balance Method to measure sap flow (Transpiration) of olives and Citrus Orchards in Semi-Arid Region of Morocco. *7th International Conference on Thermal Engineering: Theory and Applications, May 6-8, 2014, Marrakesh-Morocco.*
11. Khabba, S., Er-Raki, S., Le Page, M., Hamaoui, A., Jarlan, L. 2014. Evapotranspiration of an orange orchard in the semi-arid conditions: Calibration and validation of the Penman-Monteith Model. *7th International Conference on Thermal Engineering: Theory and Applications, May 6-8, 2014, Marrakesh-Morocco.*
12. Diarra, A., Jarlan, L., Er-Raki, S., Khabba, S., Le Page, M. 2014. Using the Two Source Energy Balance (TSEB) approach for estimating latent heat flux of irrigated crops in semi-

arid area of Marrakech (Morocco). *7th International Conference on Thermal Engineering: Theory and Applications, May 6-8, 2014, Marrakesh-Morocco.*

13. Toumi, J., Le Page, M., Er-Raki, S., Khabba, S., Ezzahar, J., Tavarnier, A., El Moutamanni, A., Kharrou, M.H., Hagolle, O., Jarlan, L. Simulations of water and energy fluxes of Winter Wheat into Soil-Plant-Atmosphere in semi-arid region: test of SAMIR software in the context of the SPOT4-Take5 experiment*. 7th International Conference on Thermal Engineering: Theory and Applications, May 6-8, 2014, Marrakesh-Morocco.*
14. Toumi, J., Le Page, M., Er-Raki, S., Khabba, S., Tavarnier, A., Kharrou, M.H., Belaqziz, S., Ezzahar, J., Jarlan, L. 2014. Potentialités de l'imagerie satellitaire pour le pilotage de l'irrigation en conditions réelles: Test du logiciel SAMIR pour une culture du blé dans la région Tensift Al Haouz/Marrakech. *Journées Méditerranéens des Systèmes d'Informations de l'Eau. 20- 21 Mars, Rabat, Maroc*.
15. L. Jarlan, S. Khabba, M. Le Page, S. Er-Raki, L. Hanich, Y. Fakir, S. Mangiarotti, J. Ezzahar, M.H. Kharrou, B. Berjamy, O. Merlin, A. Saaïdi, S. Gascoin, A. Boudhar, M. Leblanc, G. Boulet, A. Benkaddour, J. Abaoui, V. Simonneaux, F. Driouech, S. Belaqziz, G. Bigeard, G. Boulet, F. Raibi, J. Chirouze, B. Coudert, L. Drapeau, M. El Adnani, A. El Fazziki, O. Hagolle, N. Laftouhi, A. El Mandour, A. Marchane, A. Diarra, G. Aouade, J. Toumi, Y. Hajhouji, P. Fanise, H. Ibouh, N. Filali, B. Mougenot, H. Marah, A. Mokssit, Y. Kerr, G. Chehbouni. 2014. Remote Sensing of Water Resources in the semi-arid Mediterranean areas: The Joint International Laboratory TREMA. *4th International Symposium Recent Advances in Quantitative Remote Sensing Torrent (Valencia), Spain, 22-26 September 2014.*
16. Mroos K., Baroni G., Er-Raki S., Francke T., Khabba S., Jarlan L., Hanich L., Oswald S.E., 2014. Assessment of the soil water balance by the combination of cosmic ray neutron sensing and eddy covariance technique in an irrigated citrus orchard (Marrakesh, Morocco). *European Geosciences Union General Assembly, Vienna, Austria 27 April – 02 May 2014.*
17. Leblanc M., Gascoin S., Le Page M., Fakir Y., Hanich L., Khabba S., Jarlan L., Leblanc S., Leduc C., 2014. Intensification of groundwater use in the Mediterranean region observed at different scales. *European Geosciences Union General Assembly, Vienna, Austria 27 April – 02 May 2014.*
18. Merlin O., Y. Malbéteau, V. Stefan, S. Er−Raki, M. J. Escorihuela, S. Gascoin, S. Khabba, V. Le Dantec, C. Mattar, B. Molero, C. Rüdiger, L. Jarlan, Thermal Infrared: key integrator of multi−spectral/multi−resolution data for surface energy water balance studies in semi−arid regions, Recent Advances in Quantitative Remote Sensing, Valencia, Spain, Sept.

# 16. Paraguay

No report received.

# 17. Russia

## 17.1 Stavropol

Team Leader: Dr. Sergey Antonov, Stavropol Research Institute for Agriculture (SRIA), Stavropol

Contact person**:** Dr. Nina Ladonina, Space Research Institute (IKI), Moscow

Team members**:** Dr. Sergey Bartalev, Dr. Dmitry Plotnikov, Dr. Vladimir Tolpyn, Evgeny Samofal

Project Objectives

The original objectives have not changed. They are:

- Land-use and crop types mapping
- Crop biophysical parameters assessment
- Crop yield assessment
- Near real-time crop conditions assessment and stress detection
- Environmental impact of agricultural activity assessment.

Site Description

Stavropol Kray is situated in the South of the European part of Russia mainly in steppe and semi-desert zones. More than 80% of total region area (5.8 million ha) is covered by agricultural lands, of which 4 million ha are arable lands, and of that, 2.1 million ha are under cereals (the main crop is winter wheat). The gross grain harvest in Stavropol Kray in average is about 7 million tons, and grain yield is 3.3 ton/ha.

Stavropol test site has area of 66000 sq. km. It was organized in 2014 by the Stavropol Research Institute of Agriculture and Space Research Institute to conduct research aimed to develop remote sensing methods for annual land use and crop type mapping and yield assessment at the regional level.

The site consists of two levels: regional (Stavropol Kray) and local (experimental fields), which are different in functional assignment and frequency of measurement of biophysical and chemical parameters.

- Regional level corresponds to the entire Stavropol Kray and is focused on the R&D component of satellite data based land use and crop type mapping;

- Local level corresponds to a set of experimental fields and is focused on the R&D component of crops biophysical parameter assessment.

**Location**

| | | | |
|---|---|---|---|
| **Site Extent** | | **Centroid:** | 45.0, 43.2 |
| **Top left:** | 46.3, 40.7 | **Bottom Right:** | 43.5, 45.8 |
| **Core zone of 10 x 10 km**<br>**Top left:** | 42.1, 45.2 | **Bottom Right:** | 42.2, 45.1 |

The location of Stavropol test site is shown in Figure 125 (regional level) and Figure 126 (local level).


**Figure 125 Stavropol Kray in Russia**

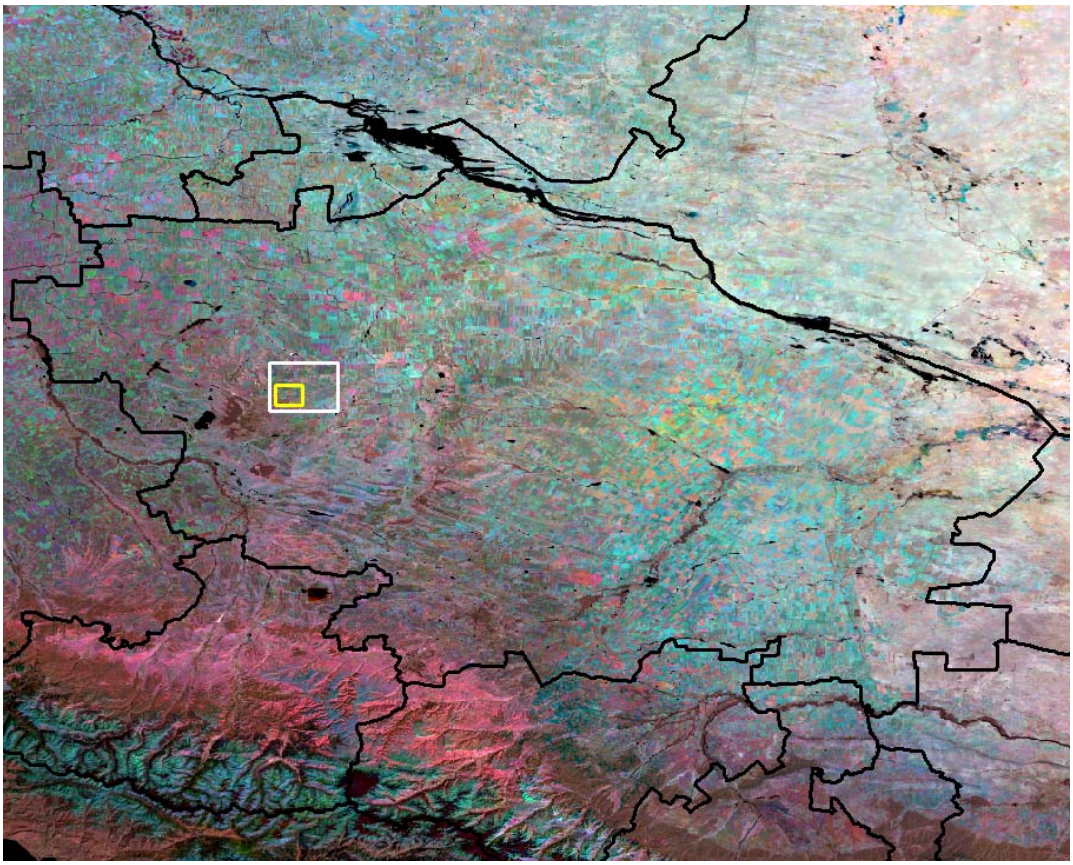

Figure 126 Location of 25 x 25 km JECAM Site with Nested Zone of 10 x 10 km

**Topography:** The landscape is mostly flat with slopes ranging from 0% to 2%; and near 15% of the territory is hilly with slopes of more than 2%. So the potential risk of wind (95%) and water (82%) erosion is high; the joint manifestation of both types of erosion has effected more than 77% of the kray territory.

**Soils**: The dominant soils are chestnut soils (3.54 million ha) and chernozems (3.15 million ha). Large areas are affected by salinity of various degrees with chloride-sulphate, sulphate and sulphate-chloride types of salinity.

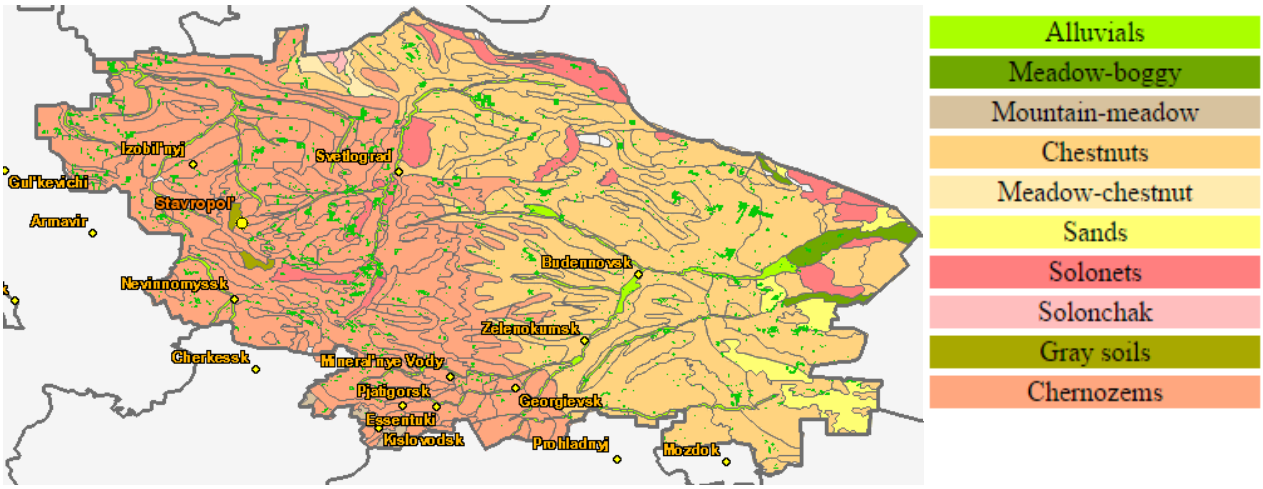


**Figure 127 Soil Map of Stavropol Kray**

**Drainage class/irrigation:** Soil drainage ranges from poor to well drained.

**Crop calendar:** September-July - winter crops; April-October - spring and summer crops.

**Field size:** typically 30 - 130 ha.

**Climate and weather:** Climate is unsustainable moisturizing with a temperate-continental type (see Figure 128).

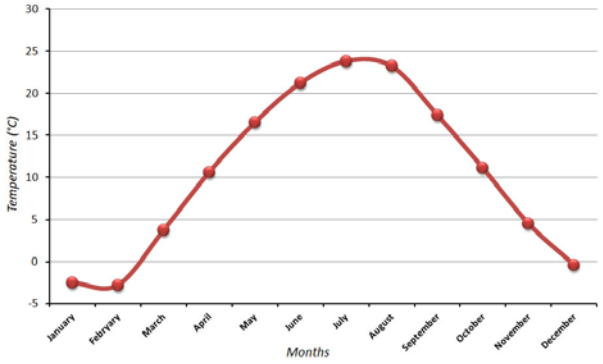


Temperature, °C

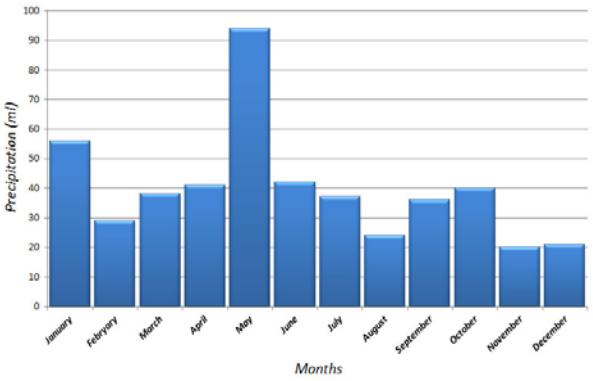


Precipitation, ml

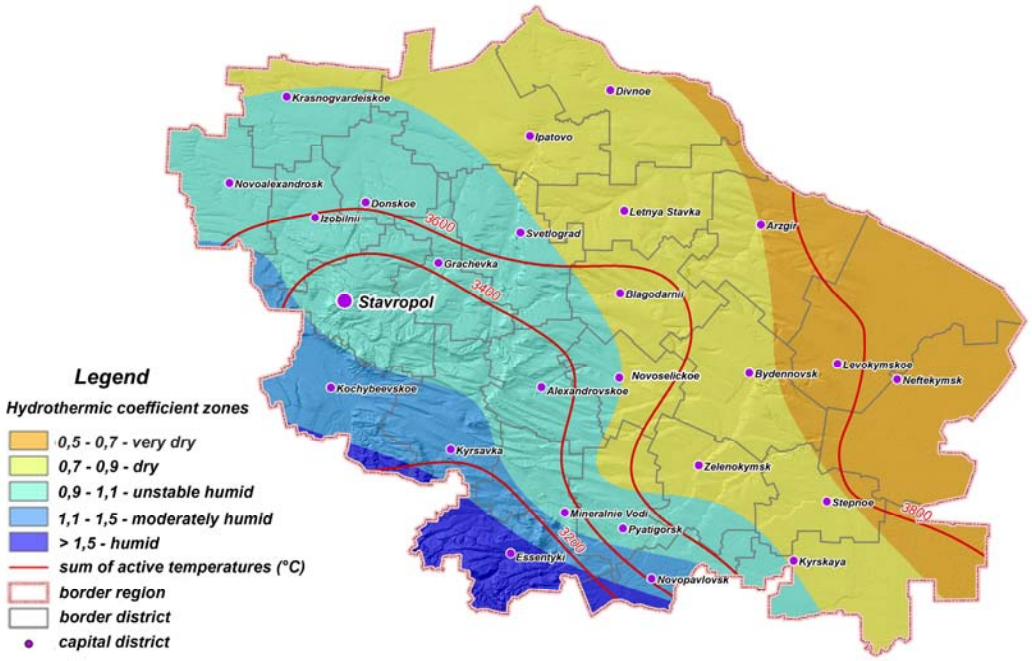


**Figure 128 Agro-climatic Conditions of the Stavropol Kray**

**Agricultural methods used:** Crop types are spring/winter wheat, spring/winter barley, peas, soybean, sunflower, winter rapeseed, perennial grasses. Typical crop rotation is: fallow/peas – winter wheat – winter rapeseed - winter wheat. Farming methods are no-till and tillage-based.

Figure 129 Photographs of Stavropol Site

EO Data Received/Used

Table 22 EO Data Used in Stavropol

| EO sensor | Data product | Time period covered and updating mode |
|---|---|---|
| MODIS | MOD09 standard product | 2000 – ongoing, automatic daily download from NASA Lan Processes Distributed Active Archive Center (LP DAAC) https://lpdaac.usgs.gov/about/citing_lp_daac_and_data |
| Landsat | Level 1T standard product | 2008 – ongoing, a day of data became available, automatic download from U.S. Geological Survey (USGS) http://earthexplorer.usgs.gov/ |
| DEIMOS | L1T orthorectified product | 2010 – ongoing, download from DEIMOS as soon as data available |

In situ Data

The following types of ground data were collected:

- **Data on crop types** was collected during field surveys along the roads. By July 2014 the information on crop location was gathered for 498 fields. The crops and numbers of fields over 25 ha (in parentheses) are as follows: winter wheat (100), sunflower (75), corn (75), winter barley (55), linen (50), spring barley (45), winter rape (40), annual grasses (40), perennial grasses (30), soybean (30), peas (20).
- **Meteo data** have been received daily from meteo-stations (temperature, humidity, precipitation, solar radiation, wind);
- **Phenological events and management practice** - information on crop calendar was collected along with surveys on data crop types and biophysical parameter measurements;
- **Biophysical parameters** (LAI, Bioproductivity);
- **Soil parameters**: moisture, humus, NPK.

Collaboration

We participate in a EU FP7 collaborative project "Stimulation Innovation for Global Monitoring of Agriculture and its Impact on the Environment in support of GEOGLAM (SIGMA)".

Results

The results achieved in 2014 are presented bellow:

**1. Land use and crop mapping**

Land use and crop mapping were conducted using **Information system VEGA-GEOGLAM** (www.vega.geoglam.ru). The VEGA-GEOGLAM provides access to daily updated satellite data and in-situ data over the JECAM sites, along with tools for integrated on-line data analysis. VEGA-GEOGLAM is focused at facilitating agricultural land and crop state analysis using time-series vegetation indices based on seasonal and multi-annual dynamics at every single point or user-specified polygons. Figure 130 demonstrates access to NDVI multi-annual time-series data aggregated at user defined polygons (field limits).

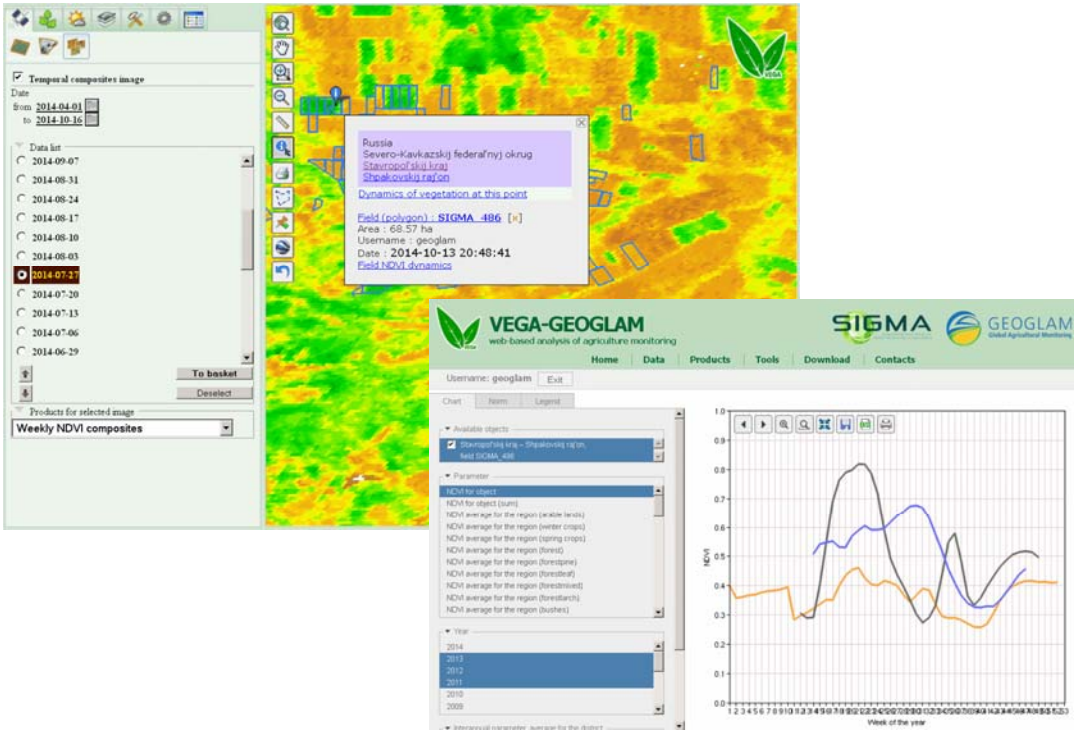


**Figure 130 Example of Land Use and Crop Type Identification Using VEGA-GEOGLAM EO Data Analysis Tools**

VEGA-GEOGLAM provides access to high resolution data (e.g. Landsat, DEIMOS) and to MODIS data along with various derived products. The service performs automated pre-processing of MODIS and Landsat satellite data with daily updates.

Both EO and in situ data can be jointly analyzed in the system. Crop identification ground research was the basis for land cover classification training. Figure 131 shows examples of (a) unsupervised and (b) supervised classification.

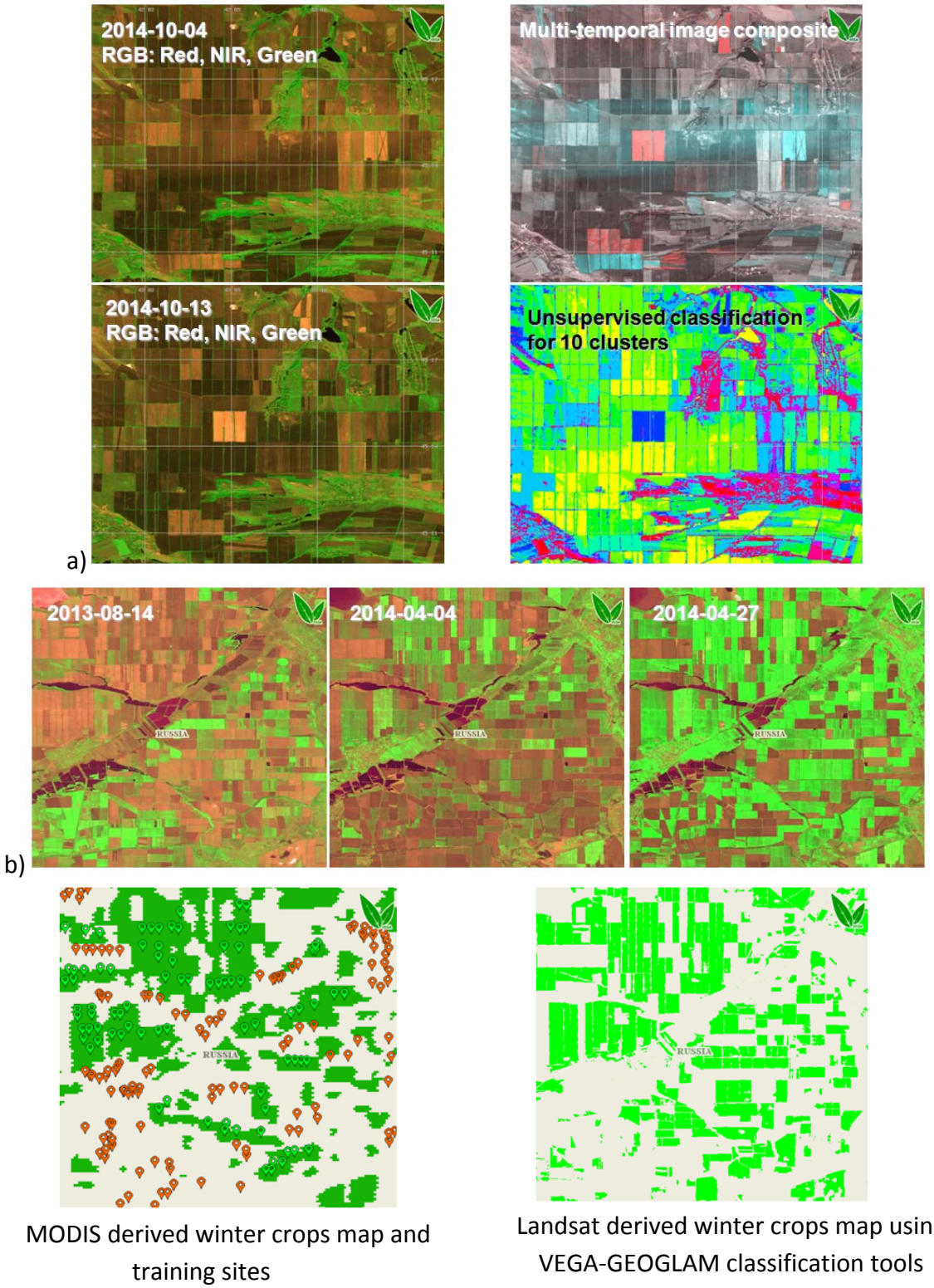


MODIS derived winter crops map and training sites

Landsat derived winter crops map using VEGA-GEOGLAM classification tools

**Figure 131 Example of Winter Crop Mapping using VEGA-GEOGLAM EO Data Analysis Tools**

Using the VEGA-GEOGLAM tools, we define land use and crop types, as well as integrate into the system other ground collected data. The time-series of Landsat-8 images was used to provide **crop classification**.

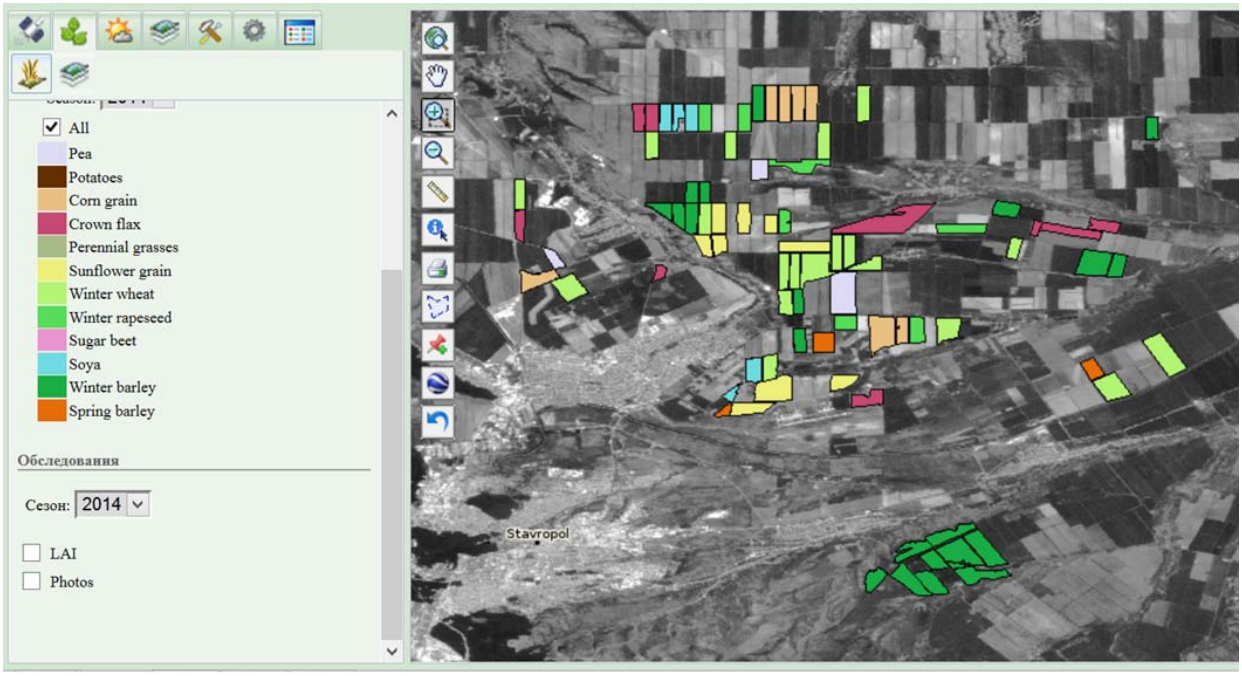


**Figure 132 In situ Sampling Data on Crop Types**

Maps on arable land, winter crops and clean fallow are produced annually. For example, thematic maps for 2014 are shown in Figure 133 and Figure 134.

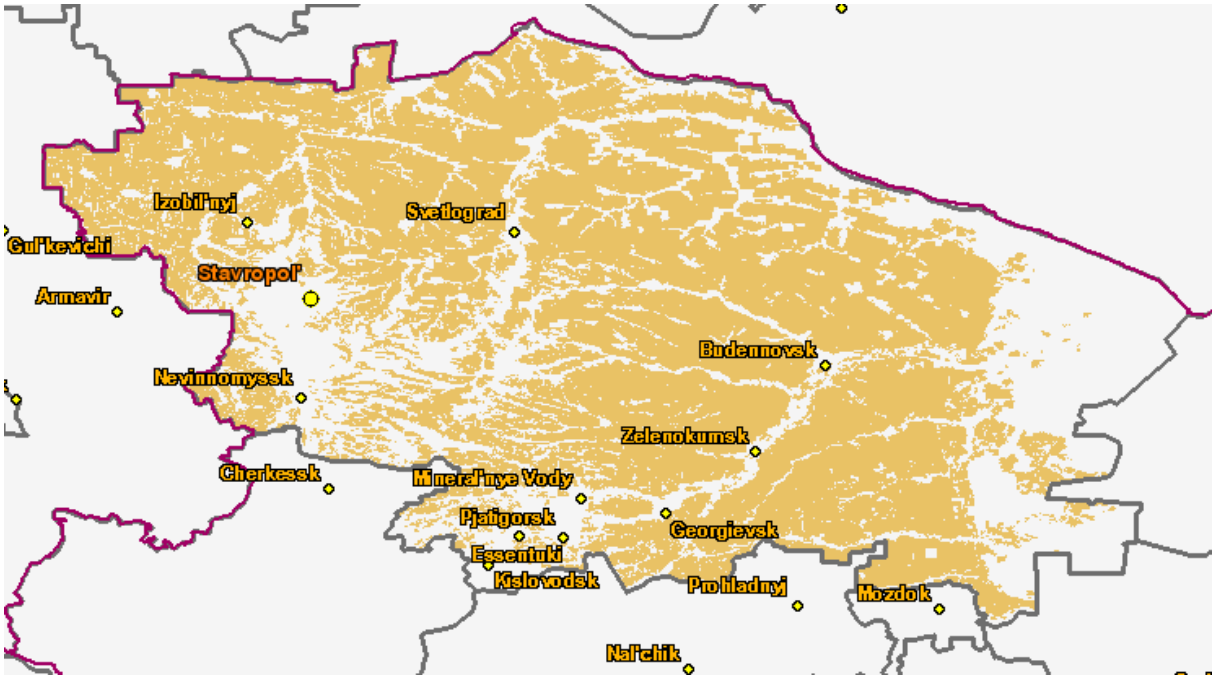


**Figure 133 Arable Land Map Derived from MODIS and Landsat Data, 2014**

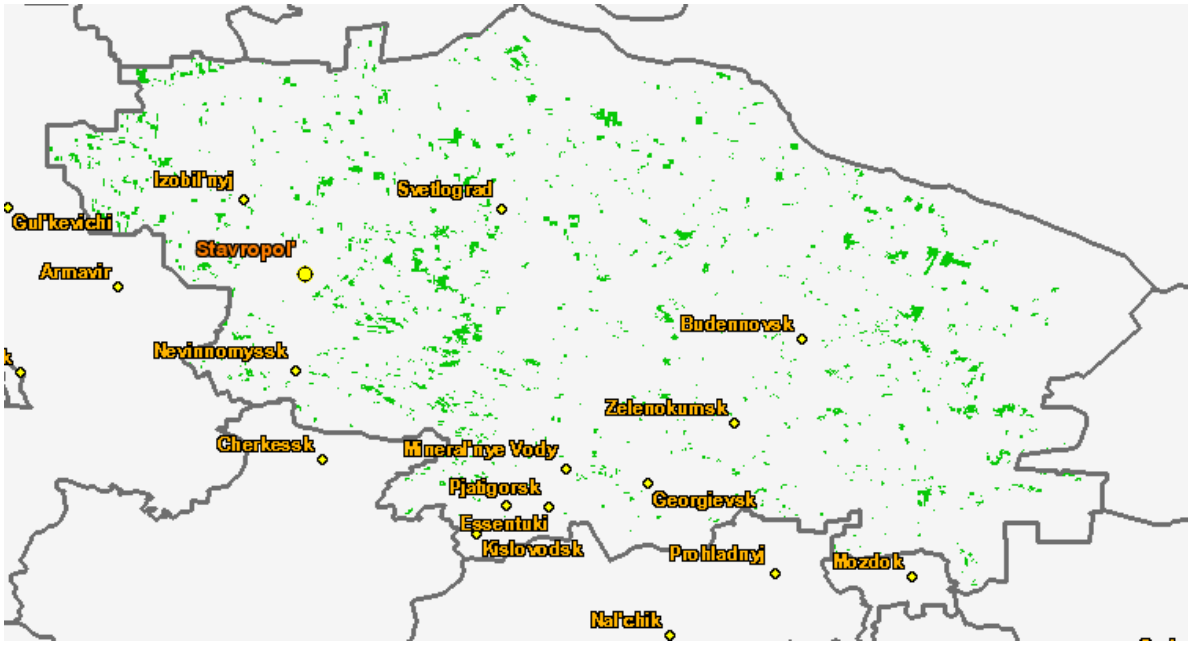


**Figure 134 Winter Crop Map Derived from MODIS Data, 2014-2015**

The VEGA-GEOGLAM system is used for analysis of satellite data for global monitoring of agricultural production and yield forecast in the framework of the **GEOGLAM Crop Monitor**.

**2. Biophysical parameters**

**LAI** measurements on the ground were collected with a Nikon D3100 Body camera with Sigma Nikon AF 4.5 mm F/2.8 EX DC Circular Fisheye HSM lens. This fisheye lens has a APS-C size sensor that ensures full circular view in the image. The GPS model Flama FL-GPS-N2 for Nikon D3100 stores the date/time with the image. All points of measurement of projective cover were located inside a field, in 30-50 meters from the edge. The distance between the points was more than 50-60 meters; totally at least 10 points were measured on the field.

**Figure 135 Taking LAI Measurements**

The scheme of LAI observations (Figure 136) and diagrams based on field studies results (Figure 137 and Figure 138) are shown below.

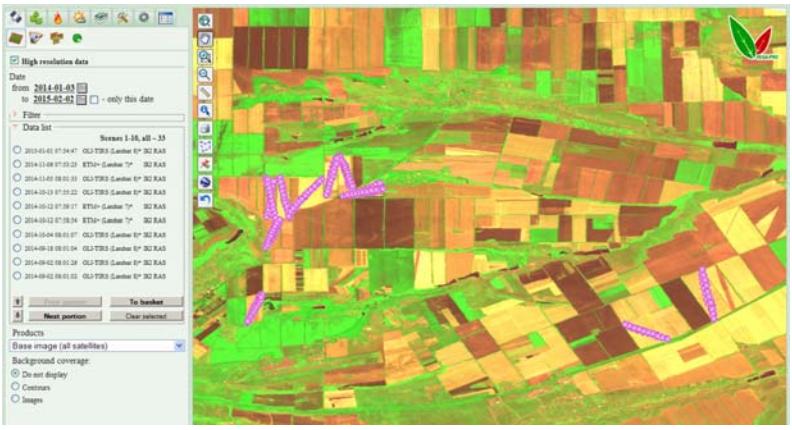

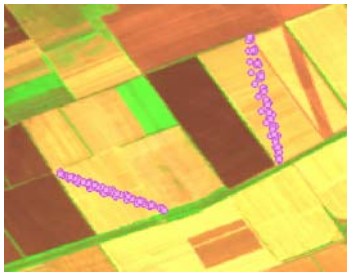

LAI observations

Sample of the photo made with Fish-Eye lens

**Figure 136 Ground Collected LAI Data**

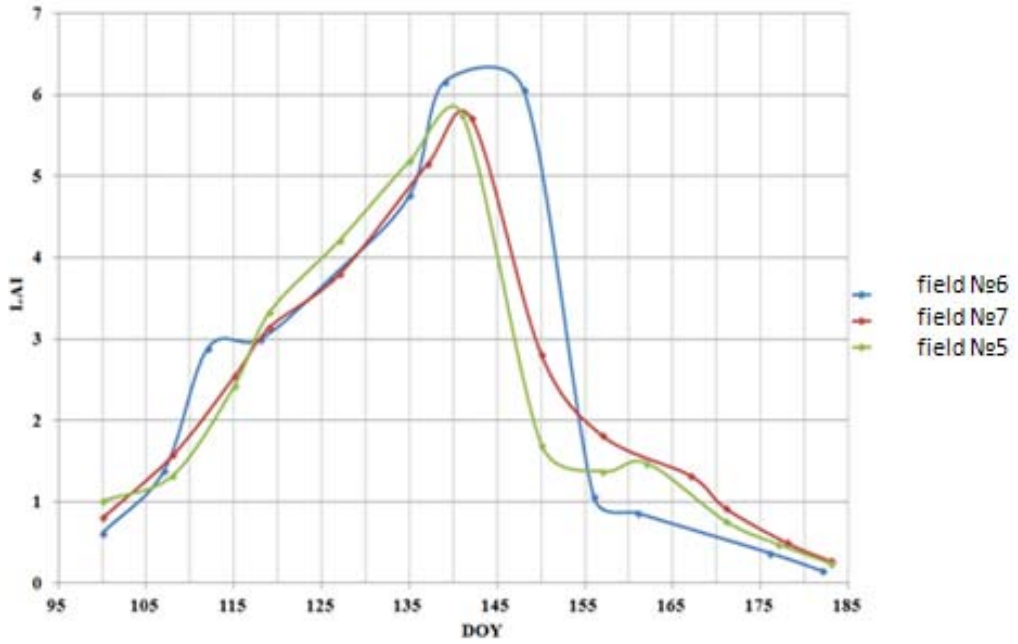


**Figure 137 LAI Time Series**

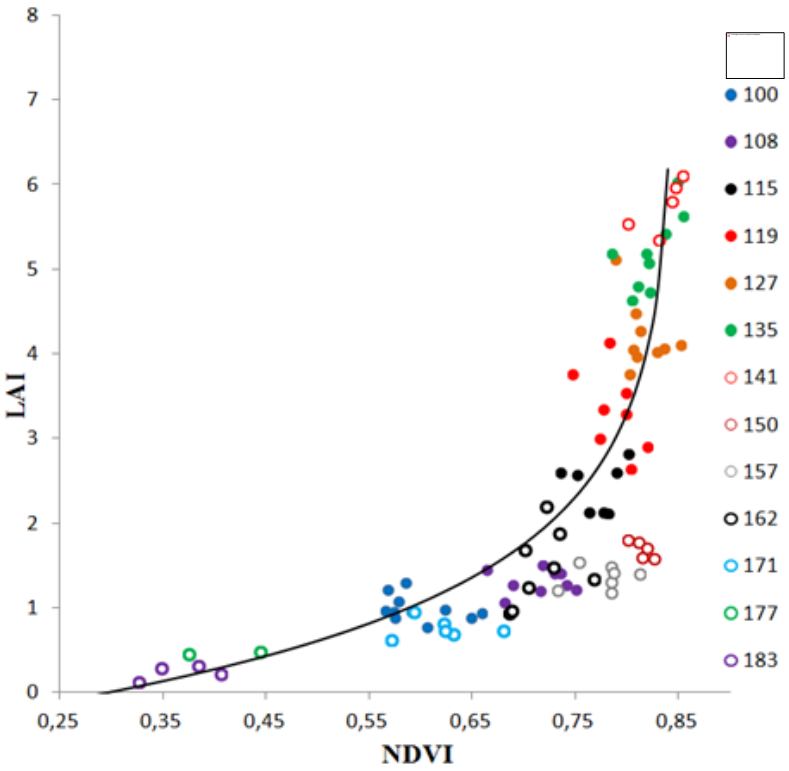


Figure 138 LAI-NDVI Relation

The logarithmic relationship between LAI and NDVI has been investigated. The best achieved determination coefficient has been found to be about 0.84.

**Biological and bunker assessment** Data on crop yield by administrative districts of Stavropol Kray (regional level) have been collected for the last five years. Local level data on crop yield was collected for 13 fields.

**Soil and Agronomic data** We determined the physico-chemical properties of soils on selected fields and compiled maps of NPK in the soil. The scheme below illustrates mapping of soil parameters.

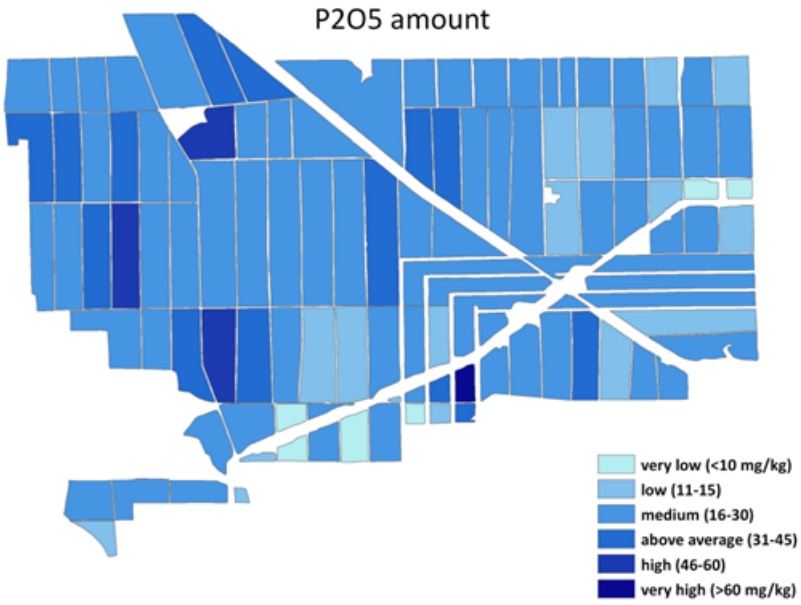


**Figure 139 Map of P2O5 Levels in the Soil**

### 3. Field passport

A summary of the available VEGA-GEOGLAM remote sensing, in-situ and meteorological data is integrated in a field passport, which also provides tools for editing of in-situ data by corresponding users (Figure 140).

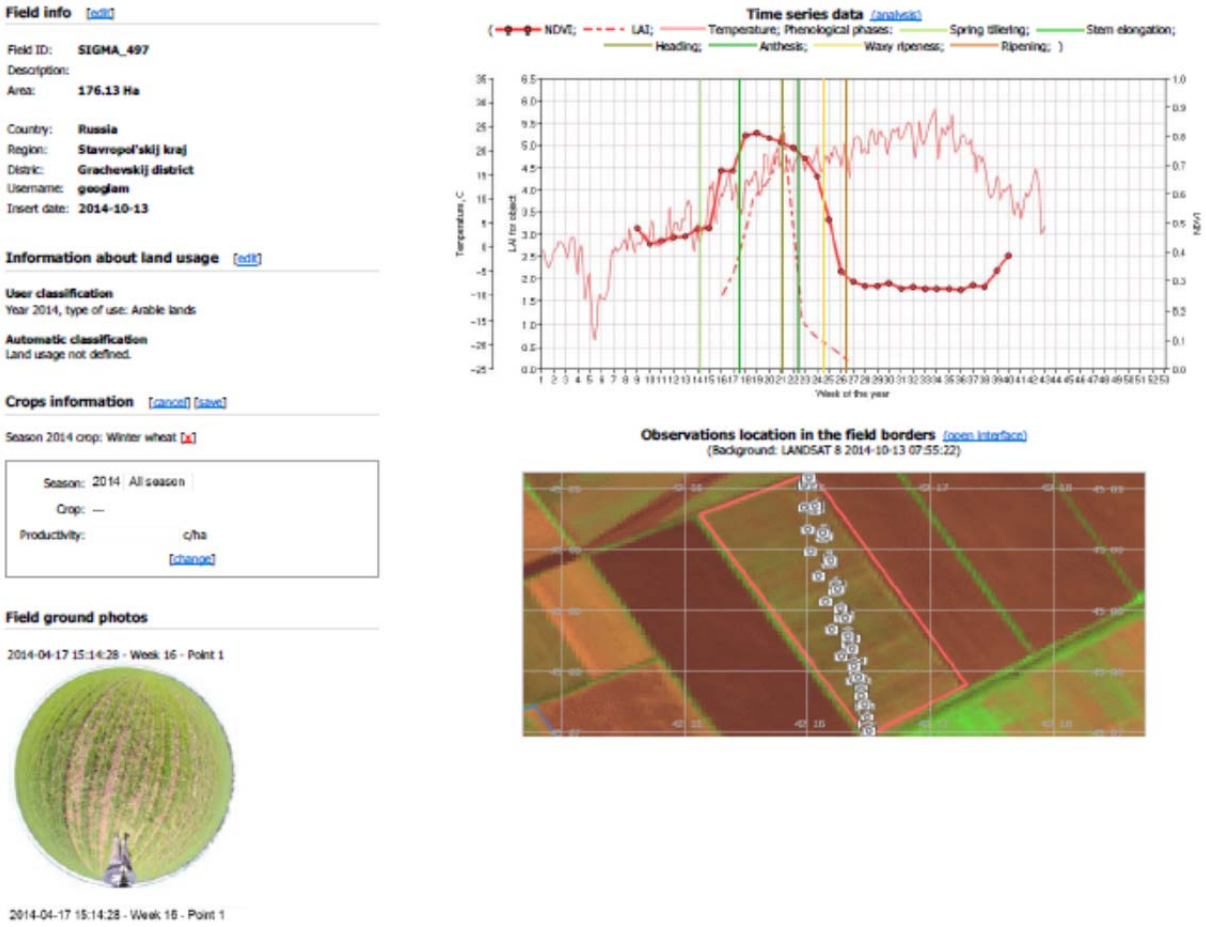


**Figure 140 Field Passport Summary of VEGA-GEOGLAM Data**

Plans for Next Growing Season

Next growing season, we will maintain the current approach. The project objectives for 2014 were met; activities will be continued in 2015.

The VEGA-GEOGLAM system was introduced during the SIGMA annual progress meeting in China (Beijing, 22-25 October 2014).

The field data collection and analysis were performed using well-known and proven "best practice" approaches.

## Publications

Results have been presented during the following meetings.

**Twelfth Annual All-Russian Open Conference "Actual Problems in Remote Sensing of the Earth from Space" (Russia, Moscow, 10-14 November 2014)**:

- Antonov S., Ladonina N., Plotnikov D., Bartalev S. "Organization of the JECAM test site in Stavropol kray for the development of methods for satellite monitoring of agriculture (Stavropol Reaserch Institute for Agriculture, IKI);

**Workshop on "The Eurasian wheat belt:future perspectives on regional and international food security" (Turkey, Istanbul, 20-22 May 2014)**

- Ladonina N. Environmental and abiotic challenges

**SIGMA annual progress meeting (China, Beijing, 22-25October 2014)**

- Bartalev S. "VEGA-GEOGLAM: web-based to and in-situ data analysis facility"

## 17.2 Tula

Team Leader: Igor Savin

Team Members: Yuri Verniuk, Igor Kim, Arseny Jogolev, Viktor Nagorny.

Project Objectives

The original project objectives have not changed. We are working on the following:

1. Winter crop identification early in a season based on MODIS data
2. Monitoring of soil moisture in rooting layer and in ploughed horizon based on MODIS data
3. Winter crop phenological development based on MODIS and Landsat data.
4. Monitoring of soil erosion based on Landsat data.

Site Description

- Location: The site is located in the south of the Tula region of Russia (Plavsk district).
- Topography: The territory is characterized by slightly undulated plane, dissected by small river valleys.
- Soils: The dominant soil is chernozem with silty-clay texture and high humus content. The soil is eroded on the slopes.
- Drainage class/irrigation: The soil is moderately drained. Irrigation is absent.
- Crop calendar: Winter crops are sown in September. The flowering is at the end of May, harvesting in July.
- Field size: Typical field size is near 100 hectares.

- Climate and weather: The climate is temperate with moderately cold winter (air temperature is near -10°C) and warm summer (air temperature is near +25°C). Amount of precipitation is near 450 mm per year.

EO Data Received/Used

We used only MODIS and Landsat data, which were downloaded from the USGS Global Visualization web site (http://glovis.usgs.gov/). We use daily MODIS data for the year, and all available Landsat scenes. Additionally we have received a number of scenes of HYPERION. All scenes were acquired at 6 dates close to the dates of field visits. Of these scenes only 2 were cloud-free (Figure 141).

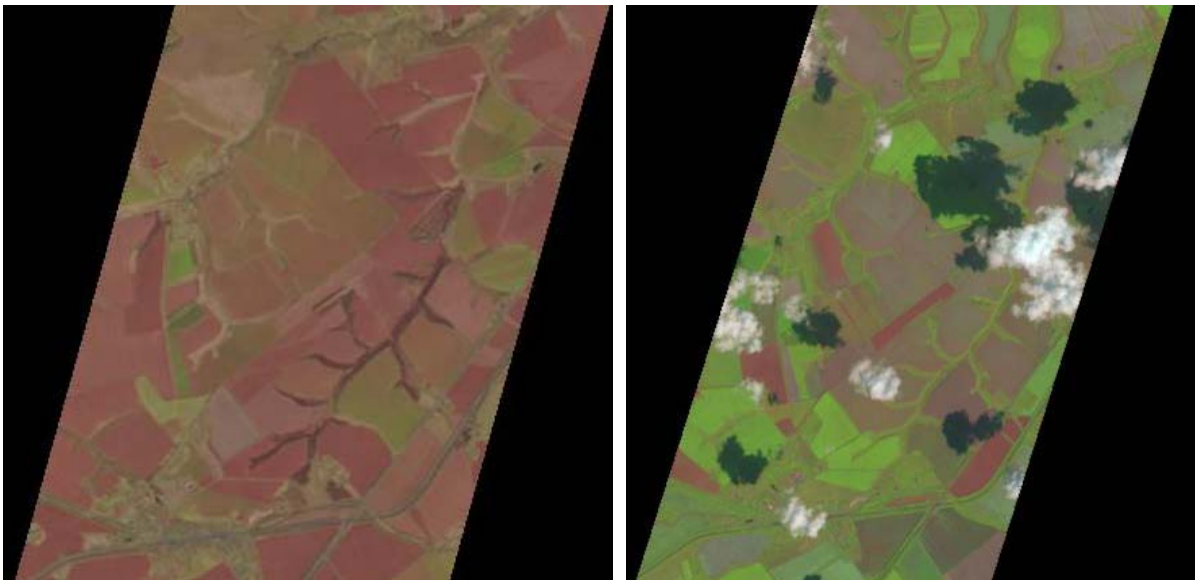

a) b)

**Figure 141 HYPERION Colour Composites (a) 24 Apr 2014 (b) 27 Jul 2014**

In situ Data

We made the following in situ observations:

- Crop type: Discrimination among crop types in georeferenced plots (nearly 20 plots). Frequency: once per crop season.
- Crop status was defined one time per month using hemispherical photo analysis.
- Soil moisture content: Measurements in selected georeferenced representative points. Frequency: before crop sowing, in the middle of the season, after crop harvesting (nearly 30 points).
- Crop phenology: Visual determination of phenological states. Frequency: each month during the growing season (nearly 20 plots).

- Soil erosion status (soil humus content): Samples were collected in selected georeferenced representative points and humus content was analyzed in the laboratory. Frequency: once in the year, after the harvest (nearly 30 samples).

**Figure 142 Typical Landscape of the Russian JECAM Site (Tula)**

**Figure 143 Winter Wheat Emergence**

Figure 144 Winter Wheat Mid-season

Figure 145 Winter Wheat after Harvest

Figure 146 Collection of Soil Samples


Figure 147 Crop Status Assessment

Collaboration

We have not been approached to participate in a collaborative project with other sites.

Results

We have collected field data and tried to use them to elaborate the method for winter crop identification and monitoring based on MODIS, Landsat and HYPERION. The data are still under analysis. We don't plan to modify the project objectives.

The analysis of the winter crop mask which was created based on MODIS shows that it cannot be used for winter crop acreage assessment due to the pixel size being too big (Figure 148, MODIS crop mask in green) and wrong detection of fields with winter wheat.

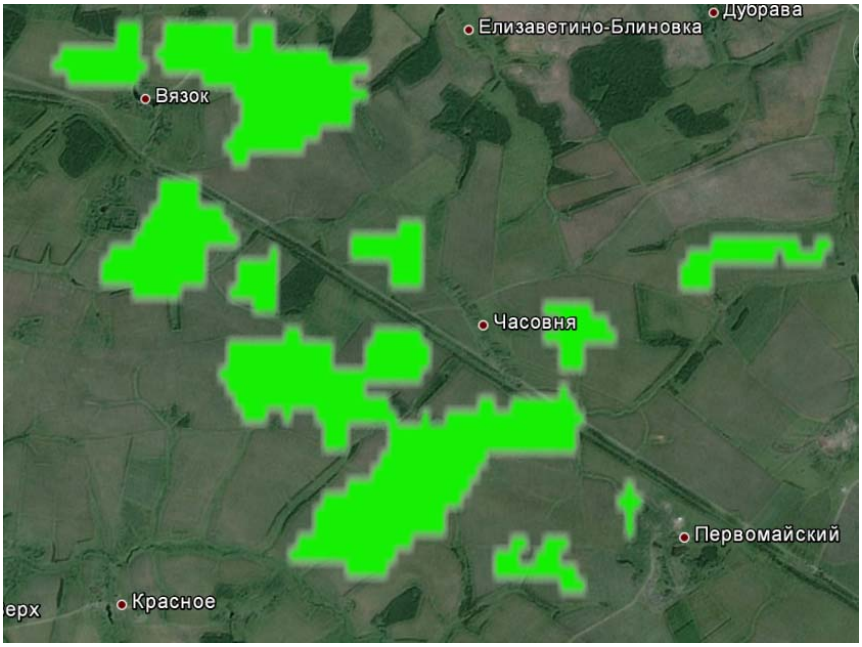


**Figure 148 Winter Wheat Crop Mask (MODIS) and Real Field Boundaries**

Plans for Next Growing Season

We plan to pay more attention on usage of HYPERION data in combination with a field spectroradiometer.

We anticipate ordering the same type/quantity of EO data next year. We plan to order HYPERION data (3-4 times per growing season) and high resolution data for crop heterogeneity analysis within crop plots.

Publications

We published a peer-reviewed paper in Russian:

*Савин И.Ю., Вернюк Ю.И., Исаев В.А.* **ОПЕРАТИВНЫЙ СПУТНИКОВЫЙ МОНИТОРИНГ ПОСЕВОВ //** Вестник Российской академии сельскохозяйственных наук. 2014. № 1. С. 22-23.

(Savin I., Verniuk Yu., Isaev V. Operative satellite based crop monitoring // Reports of Russian Academy of Agricultural Sciences. 2014. № 1. pp. 22-23.)

# 18. Saudi Arabia

No report received.

# 19. Senegal (Bambey)

Team Leader and Members: Valérie Soti (CIRAD)

## Project Objectives

The original objectives of our site have not changed. They are:

- Crop identification and acreage estimation: millet, groundnuts and maize
- Soil moisture: Joor and Deck soils
- Crop biophysical variables: NDVI
- Yield Prediction and Forecasting
- Other: Delineation and identification of trees and shrubby vegetation.

## Site Description

- Location :

**Top-Left**
Latitude: 14.819407°
Longitude: -16.660269°
**Top-Right**
Latitude: 14.819419°
Longitude: -16.468938°
**Bottom-Left**
Latitude: 14.624525°
Longitude: -16.661012°
**Bottom-Right**
Latitude: 14.625431°
Longitude: -16.468897°

- Crop Types: Millet, Groundnuts and Maize
- Typical Crop Rotation: Millet and Groundnuts
- Topography: low slope, 30 m mean elevation
- Soils: Ferruginous tropical sandy soils (Joor and Deck soils)
- Drainage class/irrigation: Very poorly drained; no irrigation
- Irrigation Infrastructure: Wells and forages

- Crop calendar: July to the end of October
- Field size 15 m x 15 m
- Climate and weather: sub-Saharan climate with a wet season from September to November and a dry season from December to August.
- Agricultural methods used: low level mechanization dominated by draft animals and manual labour.

EO Data Used

- CNES (ISIS Program)
- Optical: Pléiades satellite image
- 3 scenes (ISIS Program)
- 2013/16/01; 2014/12/31 and 2014/10/2014 (ISIS Program acquisition)
- Incidence angles : 7° (2013/16/01): 7.5° (2013/12/31) and 6° (2014/10/30)
- Spatial resolutions: 2 m in XS, and 0.5 m in pan
- Ortho level correction

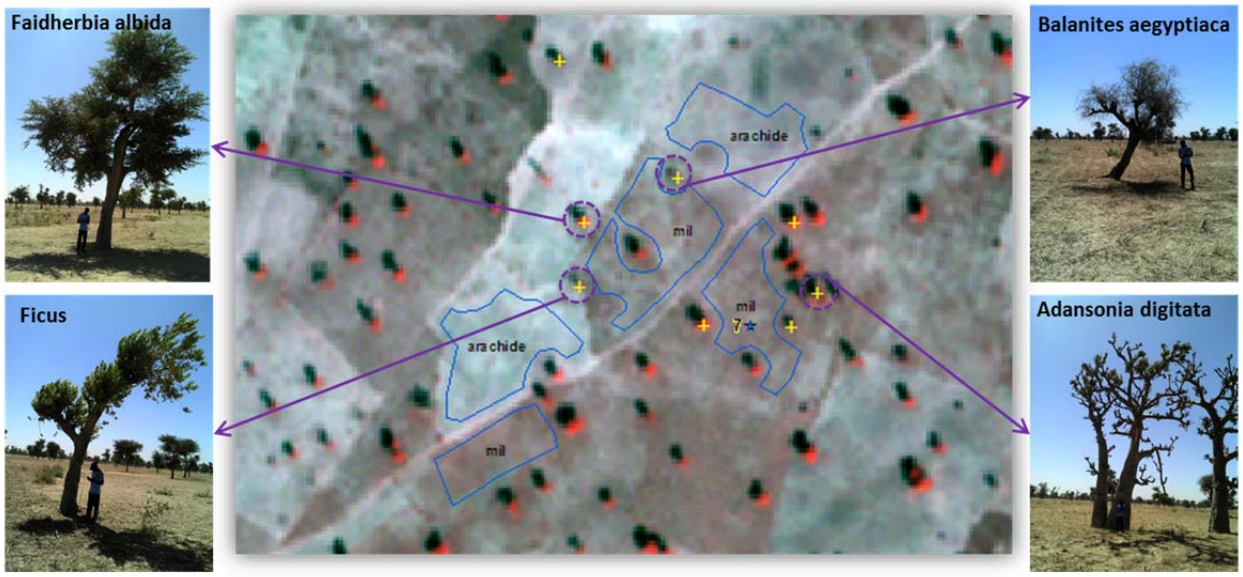


**Figure 149 Pléiades Image Showing Different Tree Species in Bambey Study Area**

In situ Data

In Senegal, field surveys were conducted during February 2013, 2014 during the dry season when trees are leafy, and in September 2014 corresponding to the crop growing season. More than 1000 trees and 1500 crops were identified (Figure 150) by species, size, density, height,

phenoloical activity, geolocated using a global positioning system (GPS), and then integrated into a GIS database.

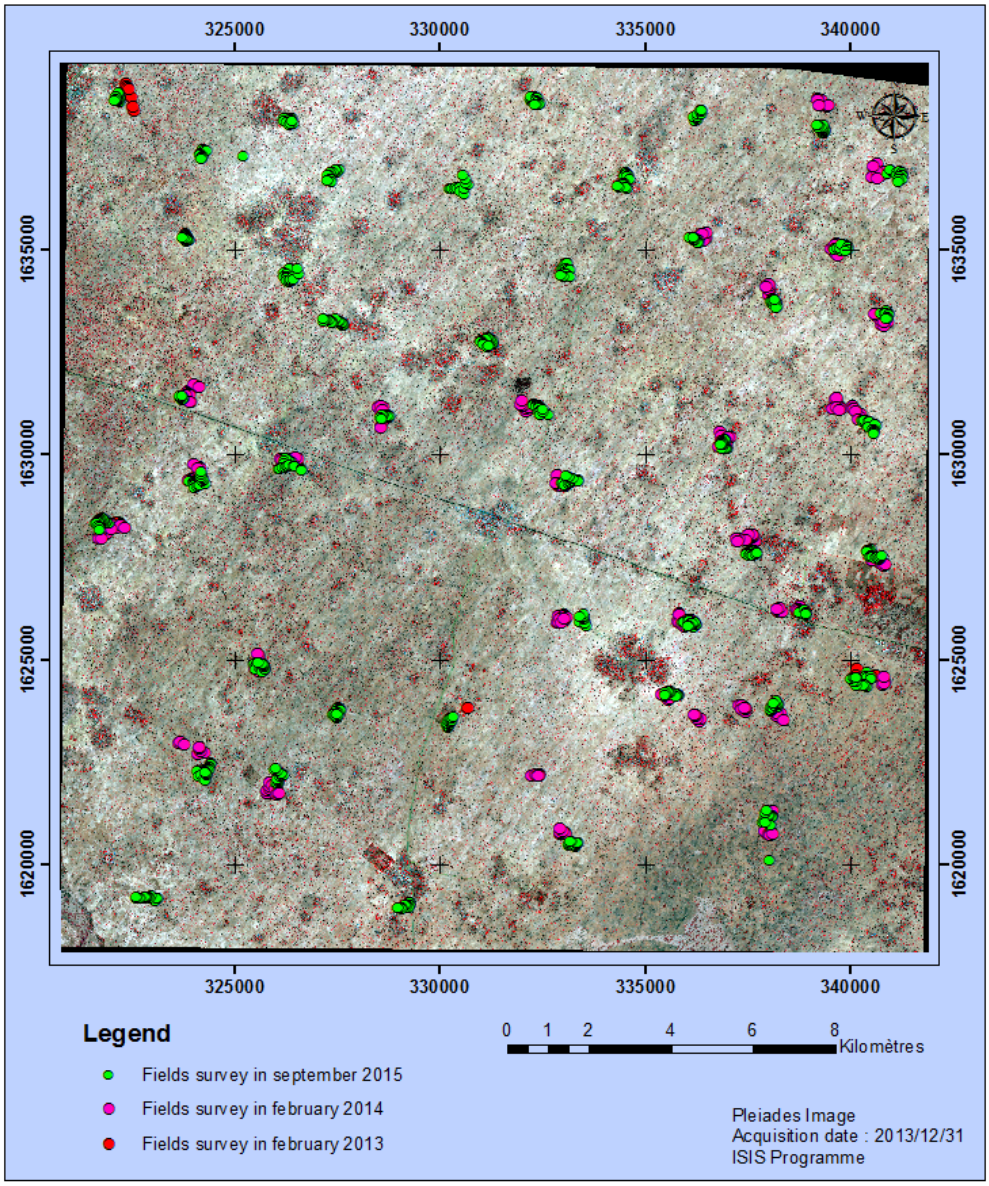


**Figure 150 Field Surveys Conducted in 2013 - 2014**

Collaboration

The first results and image acquisition have been initiated within the framework of the TRECS, RECOR and SAFSE Projects which are ongoing. The partners in these projects are the CSE (Centre de Suivi Ecologique) of Dakar (Senegal) for field data collection and image processing, the ISRA Agronomic institute and the Biopass/IRD laboratory located in Dakar for insect field data collection and identification; the French IRSTEA research center of Montpellier (France) for developing radar image processing methods for cropping surveys; and the Cirad for spatial

analysis and modeling to identify landscape management that enhances natural regulation of millet and groundnuts insect pests.

Results

Within the framework of the TRECS, SAFSE and RECOR projects, studies using Pléiades images showed limits for tree species identification, except for Azadirachta indica species which were 100 % correctly located. Concerning the crop mapping, millet and groundnuts were correctly classified at 80% and showed some confusion with bare soil and fallow lands classes. These results are due to the high heterogeneity of the vegetation cover and Chlorophyllian activity, the presence of sandy soil and the small crop plot size.

Because of the low trees identification results, we grouped all trees in a single class called "Natural Vegetation" and we produced a land cover map with 6 classes (Figure 151).

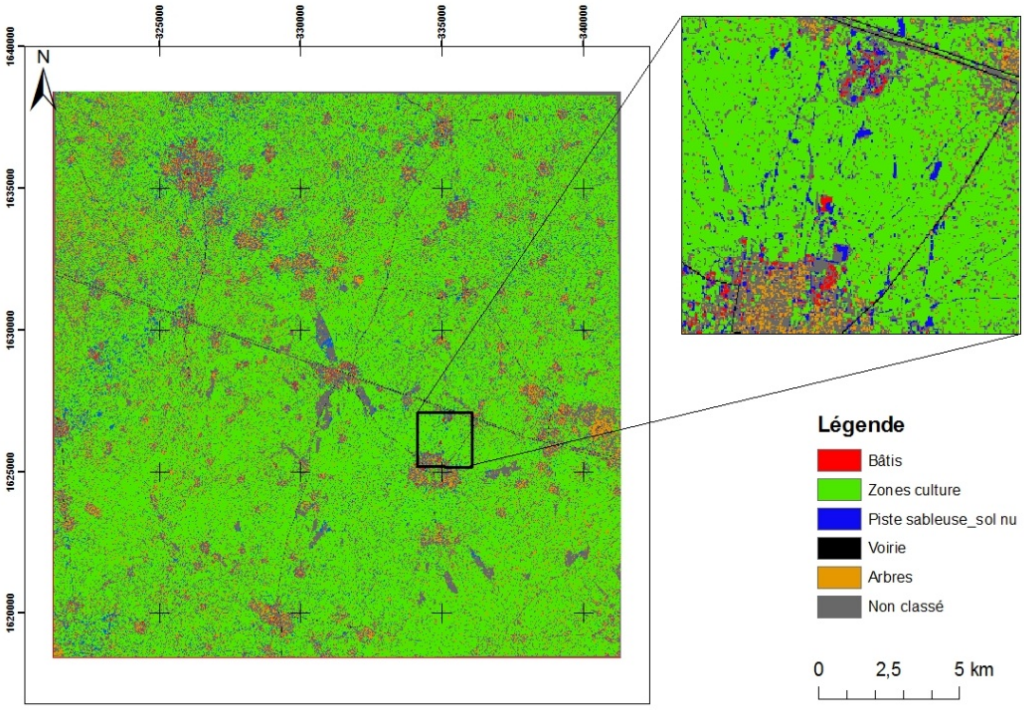


**Figure 151 Land Cover Map of Bambey Study Area**

Plans for Next Growing Season

To build on these first results in the near future, and especially to improve the identification of trees, we plan to use satellite images with a richness of bands and a high revisit time, such as WorldView3 (8 bands) or Venus (12 bands) sensors, during the dry season when trees are leafy. Also, to improve crop identification, we aim to test TerraSAR-X scenes during the rainy season, corresponding to the crop growing season.

Publications

Ndao B. (Cirad/CSE), Thiaw I. (Cirad/CSE), Soti V. (Cirad/ CSE)Apport des images Pléiades pour la caractérisation d'un parc agroforestier dans la zone de Bambey (Région de Diourbel/ Sénégal) - – International congress : XIII$^{e}$ journées du Réseau Télédétection du 17 au 19 Février 2015, Dakar, Senegal.

Soti V. (Cirad, CSE), Billand C. (Cirad), Thiaw I. (Cirad/CSE), Lelong C. (Cirad), Brevault T. (Cirad), Thiaw C. (ISRA, CNRA) Apport de la très haute résolution spatiale à l'élaboration d'un protocole d'échantillonnage spatial pour l'étude de l'effet du paysage sur la régulation naturelle des ravageurs du mil dans la zone de Dangalma au Sénégal. - International congress : XIII$^{e}$ journées du Réseau Télédétection du 17 au 19 Février 2015, Dakar (Senegal).

Brévault T., Renou A., Vayssières J.F., Amadji G.L., Assogba Komlan F., Diallo M.D., De Bon H., Diarra K., Hamadoun A., Huat J., Marnotte P., Menozzi P., Prudent P., Rey J.Y., Sall D., Silvie P., Simon S., Sinzogan A., Soti V., Tamo M., Clouvel P. 2014. DIVECOSYS: Bringing together researchers to design ecologically-based pest management for small-scale farming systems in West Africa. Crop protection, 66 : 53-60.

Ndao B : « Systèmes agroforestiers en zone sèche et régulation naturelle des insectes ravageurs des cultures : réalisation d'une carte d'occupation du sol dans la zone arachidière de Bambey au Sénégal » Master2 report- Janvier 2015.

# 20. South Africa (Free State)

Team Leader and Members:

| | | |
|---|---|---|
| Terry Newby | tnewby@csir.co.za | NEOSS |
| Wiltrud Du Randt | pdurand@mweb.co.za | ARC |
| George Chirima | ChirimaJ@arc.agric.za | ARC |
| Fannie Ferreira | Fanie.Ferreira@geoterraimage.com | GTI (pty) Ltd. |
| Celeste Dekker | Celeste@arc.agric.za | ARC |
| Johan Malherbe | Johan@arc.agric.za | ARC |
| Nicky Knox | nknox@sansa.org.za | SANSA (now Uni. Namibia) |
| Rona Beukes | RonaB@nda.agric.za | DAFF |
| NicoleneThiebaut | ThiebautN@arc.agric.za | ARC |
| Scott Sinclair | sinclaird@ukzn.ac.za | UKZN |
| Jeanine Engelbrecht | JEngelbrecht@csir.co.za | CSIR |
| Eugene du Preez | eugene.dupreez@siq.co.za | SiQ (pty) Ltd. |
| Jaco Kemp | jkemp@sun.ac.za | University of Stellenbosch |
| Adeline Ngie | adelinengie@gmail.com | University of Johannesburg |
| Johan Vermeulen | johanver36@gmail.com | University of Johannesburg |
| Roselyne Ishimwe | ishiroste@gmail.com | University of Johannesburg |

Project Objectives

The original project objectives have not changed. They are:

- Crop identification and Crop Area Estimation

  During the year a number of researchers from the SA-GEO Agricultural Community of Practice focused their research on crop type mapping.

  Spot 4 take 5 imagery was used and simple curve fitting and least squares fitting models where applied based on NDVI and EVI time series. (Knox et al 2014) The calibration and

validation samples were based upon the National Crop Estimate Committee annual aerial samples. 16 cloud free BOA Spot4-Take 5 scenes acquired between 31 Jan and 15 Jun 2013 were used for the modeling.

A study by Ishimwe et.al (2014) on identifying crop types using Landsat 8 Thermal infrared bands was carried out. Brightness temperatures where used to differentiate crops such as soya, maize sorghum sunflower and natural grasslands.

Ngie et al, (2014) investigated the use hyperspectral spectrometry for discriminating maize cultivars grown in the Free State.

The "Producer Independent Crop Estimation System" (PICES) continued to be operational over the JECAM site (and the whole of South Africa). The system is operated for the Ministry of Agriculture by a private / public consortium and a continual improvement approach is adopted for the system. Once the above mentioned research reaches conclusion, the methodologies will be incorporated into the PICES system.

- Crop condition/ stress

  The monthly UMLINDI bulletin is produced from climate data and course resolution remote sensing imagery (MODIS, Spot Vegetation, Proba V) and covers the JECAM site. It reflects the past month's growing conditions, sources of stress, soil moisture and current crop condition.

  (see: http://www.arc.agric.za/Pages/Home.aspx)

- Soil moisture

  Soil moisture is modeled at 3-hourly time-steps and updated monthly for South Africa and includes the JECAM site. This is semi-operational and work is currently underway to fully operationalize this monitoring (see http://sahg.ukzn.ac.za/soil_moisture for example results - operational outputs will be available shortly). The soil moisture status is reflected in the ARC-ISCW UMLINDI Bulletin when available. The data reflects the Soil Saturation Index (SSI), which is defined as the percentage saturation of the soil store in the TOPKAPI hydrological model. The model uses satellite derived rainfall (TRMM 3B42RT) and incoming solar radiation (LSA-SAF DSSF) in addition to inputs from the SA Weather Service's NWP model (Unified model). The modeling is intended to represent the mean soil moisture state in the root zone. Further information from: sinclaird@ukzn.ac.za

- Yield prediction and forecasting

  Durand et al (2014) has applied the QUAD –UI tool and the DSAT model to datasets from the Free State to investigate the feasibility of assessing climate change impacts on maize production at district level in the Province. A maize crop field level land cover was developed using satellite imagery. The producer independent crop estimate survey (PICES) and crop type classification results were used as model input and verification data. This approach honours the scale of a homogeneous plot at which the crop model (DSSAT) was developed, but takes into account district level yield variation as the whole population of maize fields within a district is modeled. Crop management such as row spacing, plant population and planting dates were derived from objective yield surveys based on a point sampling frame and associated with the fields proportionally to their occurrence. GIS and pedo-transfer functions were used to derive soil profile descriptions for each field based on land types. Fertilization was based on the average modeled 50 year yield potential of each field. Crop model applications related to climate prediction depend critically on the assumption that the models can capture the year-to-year pattern of response to climate variability. The objective of the study was to test whether the approach of using a field level crop land cover could be used to simulate past (1980-2010) and future (5 General Circulation Models (GCMs) for the time period 2040-2070, with Representative Concentration Pathway (RCP) 8.5 and CO2 of 571 ppm) maize productivity, using the DSSAT crop model, and then summarizing to either quinary catchment or district level. The approach was tested within three districts of the Free State province of South Africa.

  Knox et al (2014) analyzed a small data set obtained through the GrainSA co-operative from a farmer practicing precision agriculture in the region of the Spot4-Take5 acquisition area. The farmer provided hardcopies of the maize yields recorded during harvesting at the time of the Spot4-Take5 acquisition period. His yields were correlated with estimated yields based on the Spot4 Take 5 Imagery.

  Thiebaut et all (2014) used forward regression analysis on noisy course resolution 2007 NDVI datase in an attempt to model yield. The yield data for the Free State from the operational national crop estimates system was used as verification.

- Others: Weed Discrimination

  Vermeulen (2014) investigated the possibility of detecting weed infestations in maize fields in the Free State province using hypespectral remote sensing. He collected and analyzed spectra from a variety of weeds and of maize to determine the most suitable

bands for weed discrimination. Attention was given to the red edge inflection points of Maize and the selected weeds.

Site Description

See www.JECAM.org for the site description.

EO Data Received/Used

For multi-temporal monitoring through earth observation data over the 2 sites, the archived and operational datasets, available for MODIS TERRA, Proba V and SPOT VEGETATION are utilized. The following shows some of the recent earth observation data, for which the entire time series have been made available for the area (including the 2 sub sites).

Figure 152 shows the time series of NDVIs from MODIS, as a seasonal curve compared to the long term average, as well as the rainfall for the year compared to the long term mean (source: UMLINDI Newsletter Feb 2015, www.arc.agric.za).

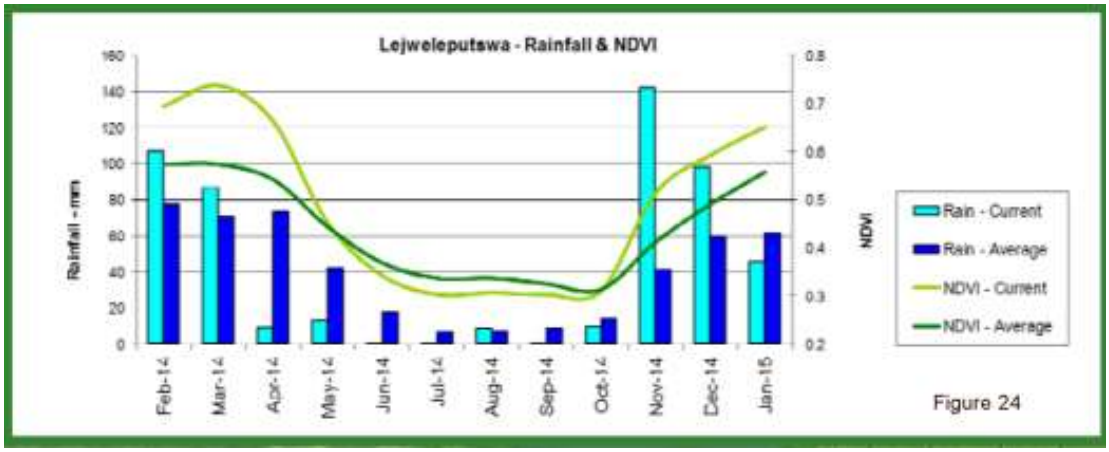


**Figure 152 Rainfall and NDVI Graphs of a Major Maize Producing District Municipality in the Free State**

SPOT VEG decadal NDVI

- Space agency or Supplier: Devcocast
- Optical
- Number of scenes: 1 per Africa
- Range of dates: Every 10 days
- Spatial resolution: 1000 m
- Processing level: NDVI completed product

MODIS 16-day NDVI

- Space agency or Supplier: Nasa Reverb-Echo
- Optical
- Number of scenes: 4 per SA.
- Range of dates: Monthly, and every 16 days
- Spatial resolution: 250-l000 m
- Processing level: Q1

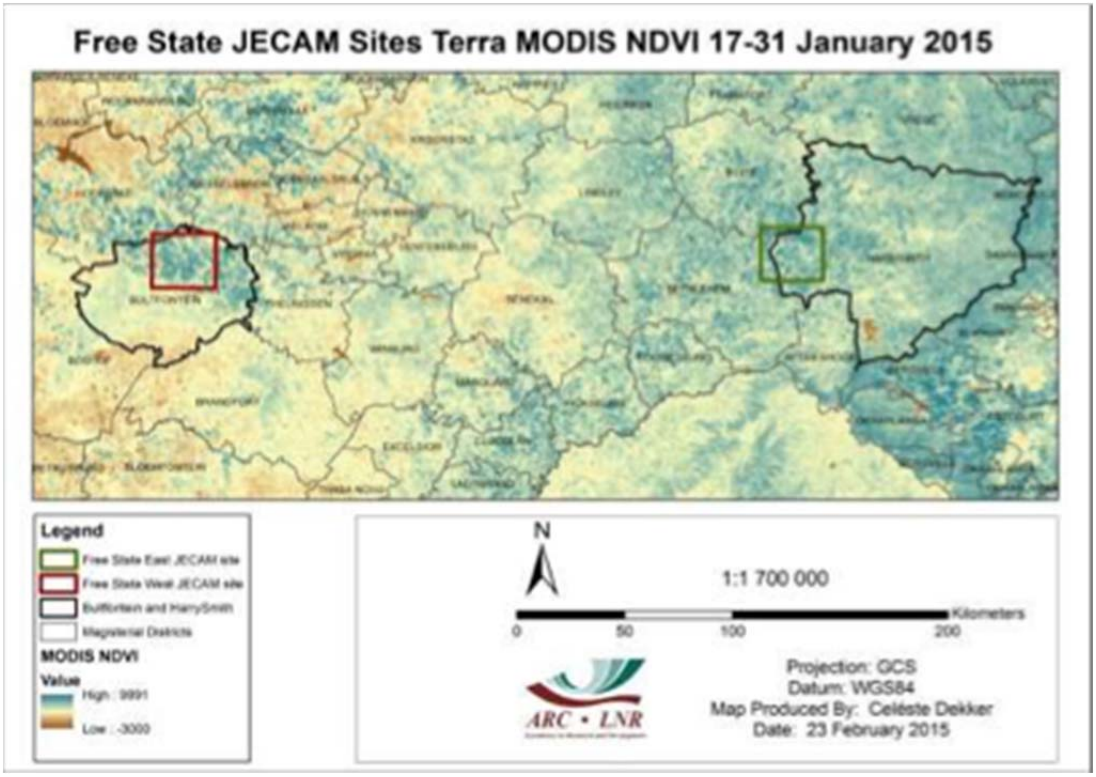


Figure 153 MODIS NDVI Data for 17-31 Jan 2015

Proba V Imagery

- Space Agency Supplier: ESA Earth Watch programme □
- Optical/SAR - Optical □
- Number of scenes - Daily □
- Range of dates – 2014 □
- Spatial resolution – 1Km □
- Processing level - □
- Challenges, if any, in ordering and acquiring the data - No □
- Challenges, if any, in processing and using the data - No □

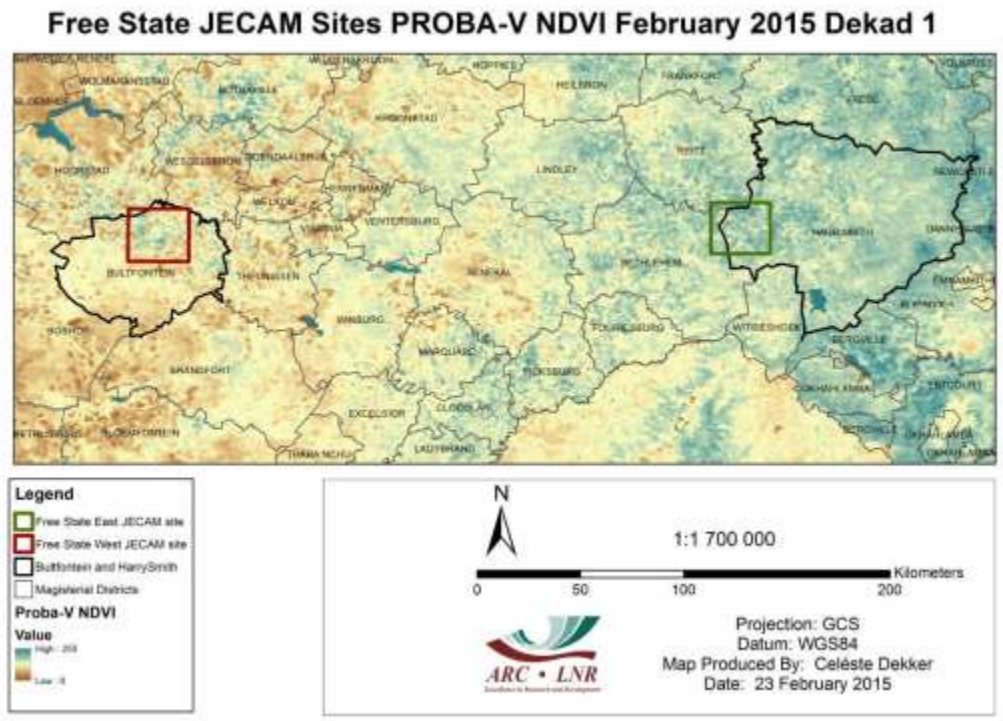


**Figure 154 Proba V NDVI for 1-10 Feb 2015**

SPOT 5 Imagery

- Space agency or Supplier - South African National Space Agency (SANSA) 
- Optical/SAR - Optical 
- Number of scenes - Spot5: 54 x Multispectral (10m) & 54 x PanMerge (2.5m) 
- Range of dates – 01 Jan 2013 – 31 Dec 2014 (National Mosaic) 
- Spatial resolutions - Multispectral (10m) & PanMerge (2.5m) 
- Processing level - Level 3 - Ortho-rectified 
- Challenges, if any, in ordering and acquiring the data - No 
- Challenges, if any, in processing and using the data - No 

Landsat 8-OLI 

3 Landsat scenes from April-June 2013 were used in crop type identification. 

Spot 4 Take 5 Imagery 

- Supplier: ESA 
- Optical: MS
- No of Scenes: 16

- Dates: 31 Jan 2013 – 15 Jun 2013

In situ Data

Weather station data from the automatic weather station network of the ARC-ISCW have been collected at/near each of the 2 sub-sites. Data were collected for the following elements:

- Temperature
- Humidity
- Rainfall
- Solar Radiation
- Wind
- Potential evapotranspiration (Derived).

The stations are at Bultfontein (western site) and Harrismith (eastern site).

**Figure 155 Automatic Weather Station near Bultfontein**

The time series of available data from the ARC-ISCW weather stations close to the sites are shown for the current summer rainfall season (starting in July 2014) in Figure 156 and Figure 157.

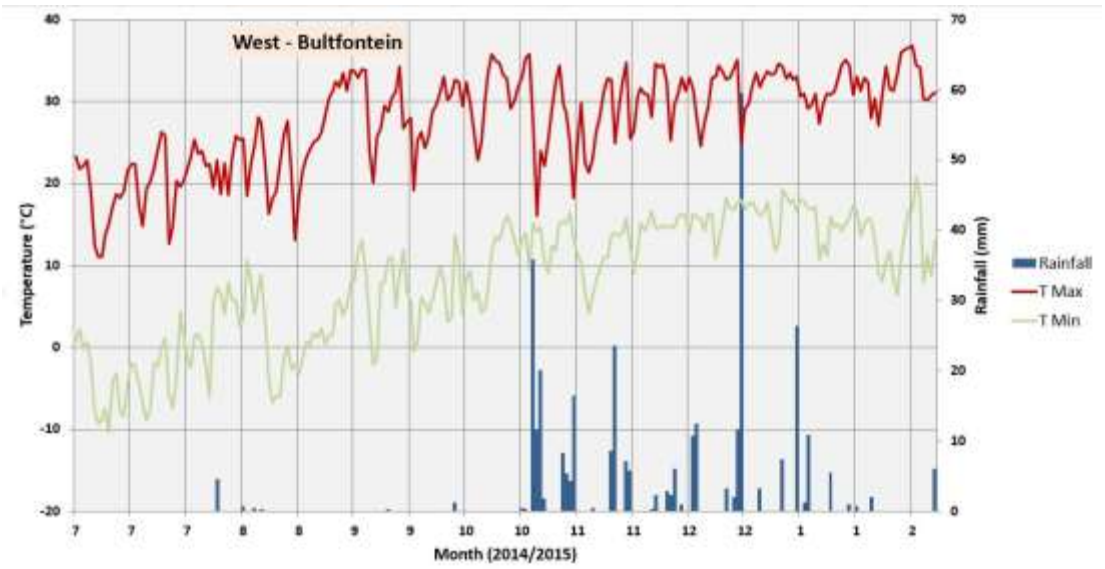


**Figure 156 Time Series Graphs of Climate Parameters (July 2014-Feb 2015) (Bultfontein)**

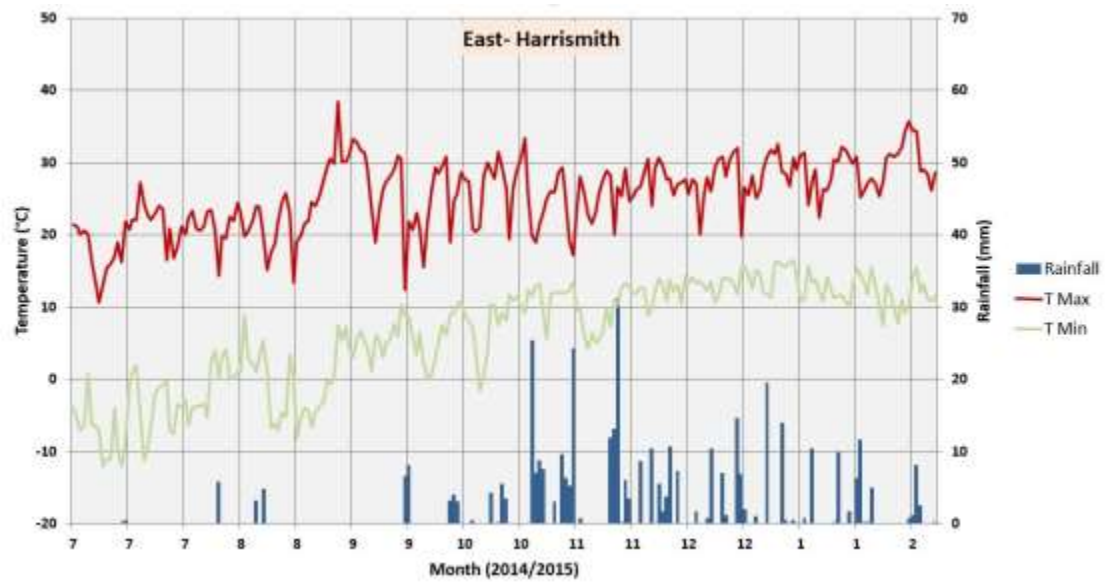


**Figure 157 Time Series Graphs of Climate Parameters (July 2014-Feb 2015) (Harrismith)**

Spatialization of rainfall data from the ARC climate station network is depicted in the following figures (Figure 158 and Figure 159).

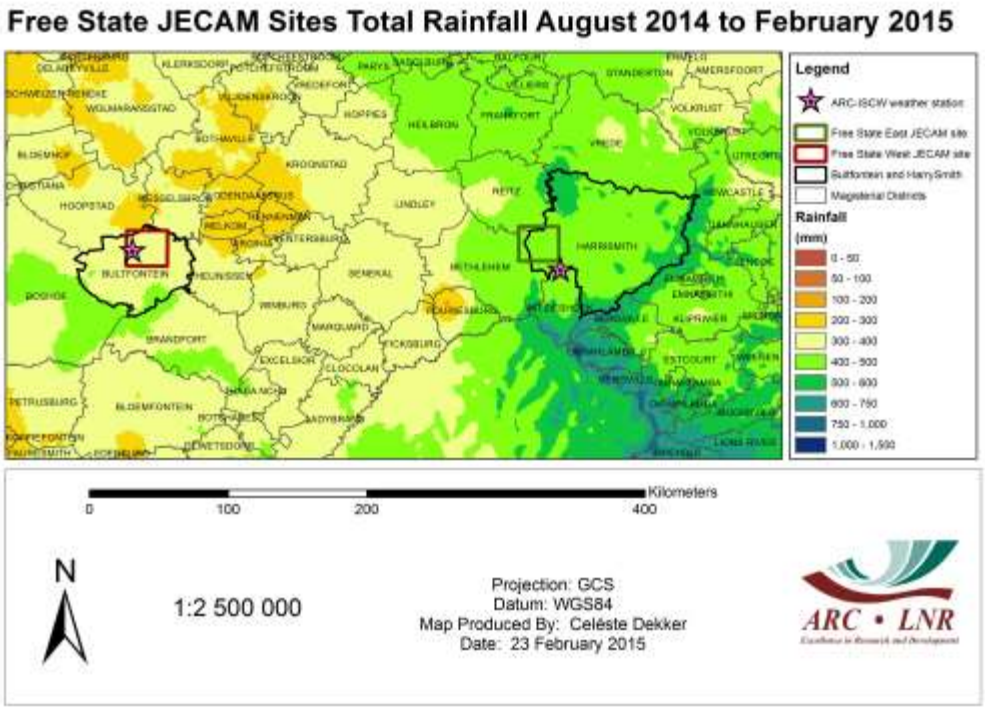


Figure 158 Total Rainfall August 2014 - February 2015

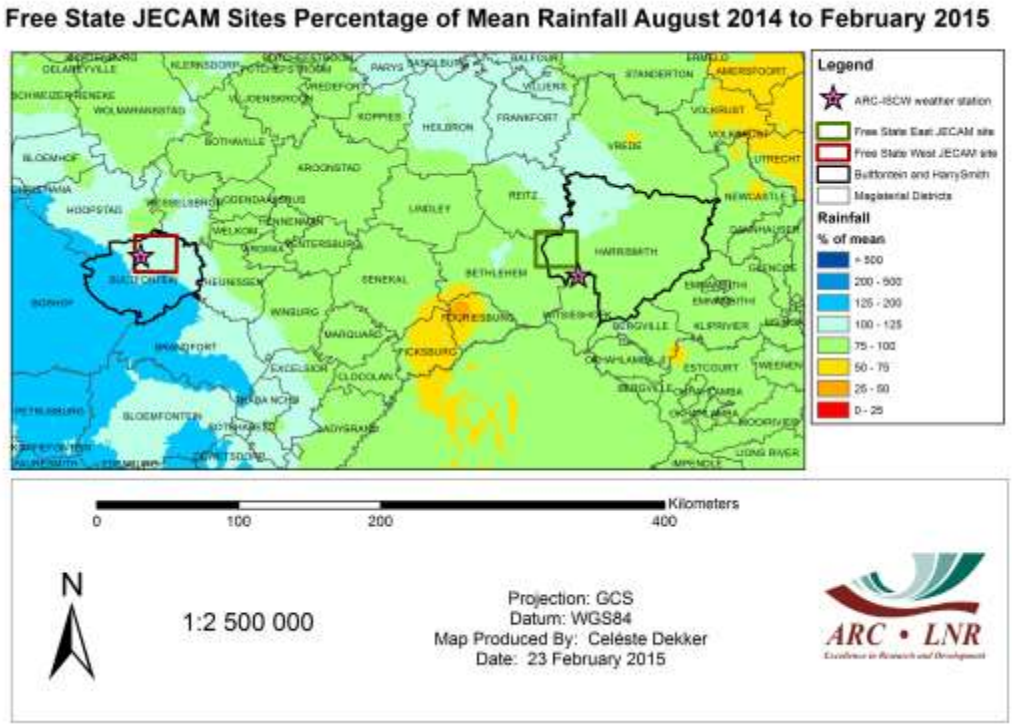


Figure 159 Percentage of Mean Rainfall August 2014 - February 2015

**Precision Farming Harvest Data**

A small set of data from a farmer using yield monitors on his harvester was made available to the research team.

**Field Based Yield Data**

In field yield estimate data is collected from around 300 randomly selected points for the winter (wheat) and summer (maize) provincial yield estimate. These points have a geo location and a yield estimate as well as some ancillary data such as row width, weed condition and variety. The data is embargoed in season and is only released after the season has concluded.

Collaboration

Our collaboration status is shown in Table 23.

| Collaboration Partner Contact Person | Subject | Status |
|---|---|---|
| Discussion on data sharing relating to the IMAGENS project is underway and a MOA between University of Stellenbosch and Université catholique de Louvain (Belgium) is in process of being finalized. | Exchange of Radar data and in-situ field data | MOA being finalized. |

**Table 23 Collaboration with South African JECAM Site**

Results

**Crop identification and Crop Area Estimation**

The analysis of the multispectral Spot 4 take 5 data acquired over the Bothaville district investigated crop type modeling. The crop type modeling focused on 5 primary crop/land cover types: Maize, Sunflower, Soy beans, Pasture, Fallow.

Results showed poor agreement between the time series and the different crop types. This is most likely due to the time frame of the acquired images that missed the start of the growing season. The current models applied included the post harvest, but this should be removed from the modeling to capture only the crop growth season. Figure 160 shows the results of the discrimination between the various crops.

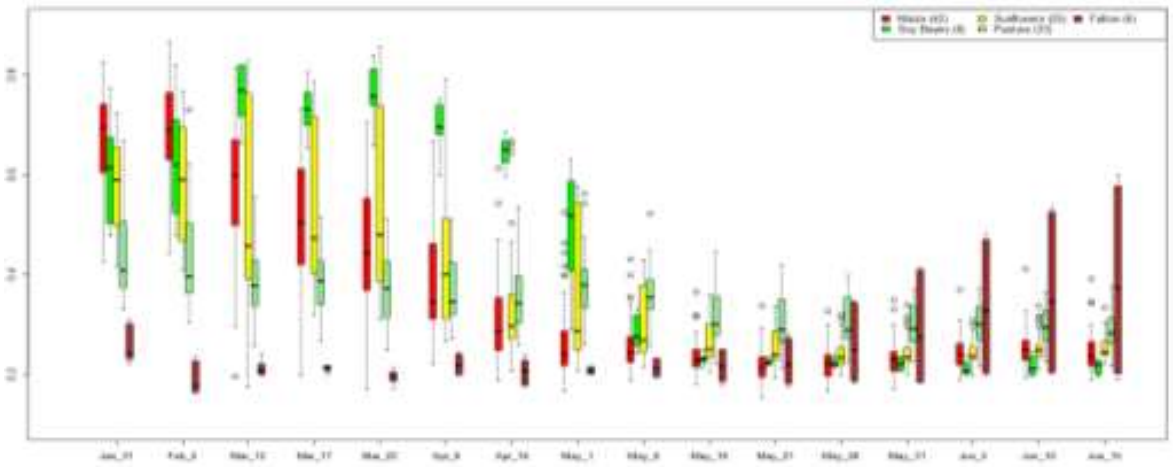

Figure 160 Plot showing NDVI Values of Different Crops over the Acquisition Period

a)

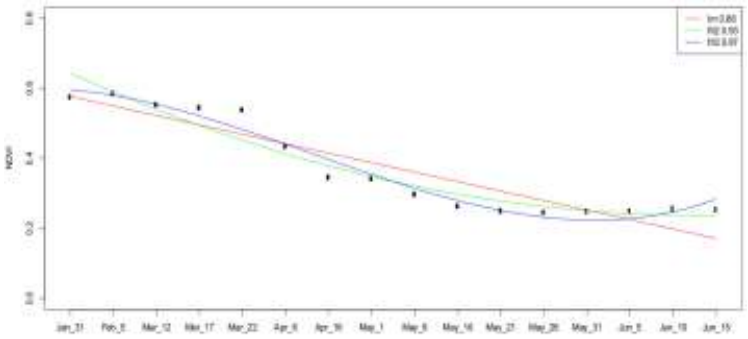

b)

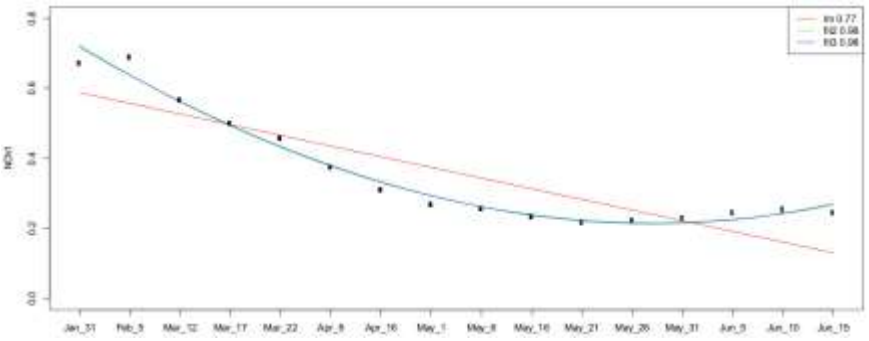

Figure 161 Sunflower (a) and Maize (b) Curves Modeled using Least Squares Fitting

While the curves in Figure 161 fitted well, the models were unable to predict on the validation data set and resulted in large prediction errors and misclassification of the 5 crop classes.

The study by Ishimwe et al (2014) where they investigated the use of Landsat thermal imagery for crop discrimination found that there is a statistical and spectral significant difference

between grass and other crops as well as between sorghum and other crops (soybeans, sunflower and maize). However maize, soybean and sunflower could not be differentiated based on their brightness temperature. The similarity in the brightness temperature of the inseparable crop type pairs (soybeans, maize and sunflower) were attributed to their quantitative similarity of physiochemical composition (such as C3 plants, carotenoids, steroids and xanthophylls) that are involved in crop energy absorption and balance. In addition maize, soybeans and sunflower have similar composition of chlorophyll molecules (I and II).

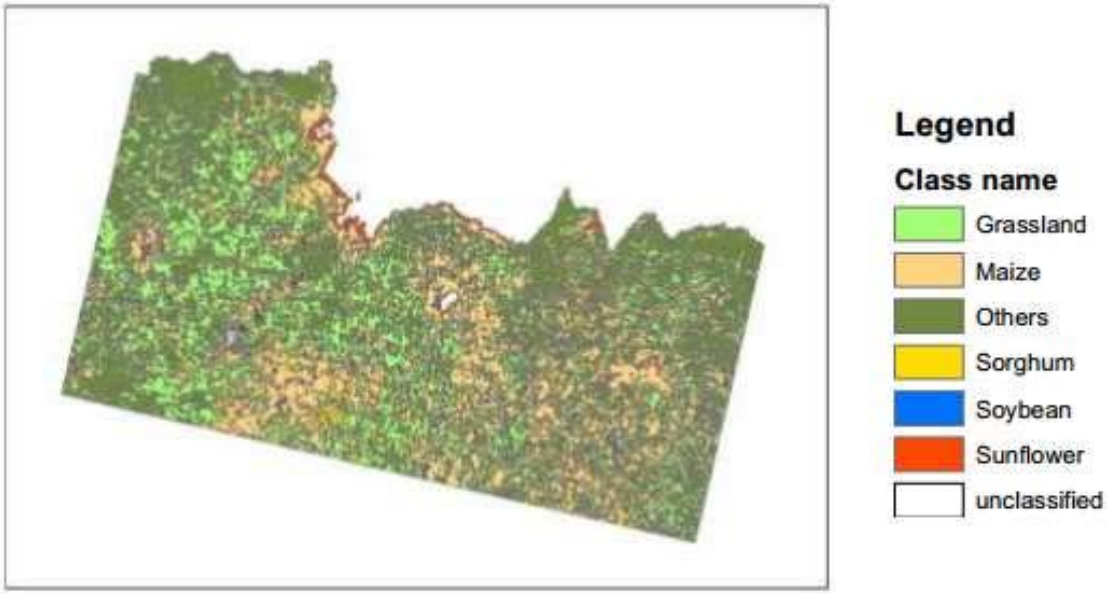


**Figure 162 Crop Type Map for an Area in the Free State Derived from Landsat-8 Thermal Imagery**

They concluded that brightness temperature of different crop types contain sufficient information to discriminate different crop types. The results of the study (Figure 162) showed that 75% of crop types under study were statistically and spectrally different based on their brightness temperature. Further, freely available Landsat-8 imagery can be used as an initial no-cost image to monitor agricultural land use in order to generate a crop-specific temporal record and to gather information on crop productivity.

The work by Ngie et al (2014) where they investigated the feasibility of hyperspectrally (Figure 163) discriminating maize cultivars indicated successful separation of the cultivars from spectral measurements at foliar level. They speculated on the possibility of integrating these hyperspectral measurements with space borne hyperspectral imagery for automated discrimination of various cultivars on field level.

Figure 163 Collecting Spectra in Field

**Maize / Weed Discrimination**

Vermeulen (2014) in his study (Figure 164) on using spectra to discriminate weeds from maize found that maize may be spectrally distinguished from all of the weed-species in the study area based on leaf-level hyperspectral reflectance at specific wavelength-ranges throughout the VIS, NIR and SWIR regions of the electromagnetic spectrum, however the unique characterization of weed-species in the study area based on leaf-level reflectance is not possible for all species, and where it is possible, it is highly wavelength-specific and would require high spectral resolution hyperspectral data. The wavelength-regions most suitable for the spectral characterization of


Figure 164 Study Area in which Maize and Weeds were Discriminated Spectrally

maize-crops and weed species in the study area are: 418nm – 438nm, 517nm – 530nm, and 566nm – 170nm in the visible wavelengths; 693nm – 718nm in the Red-Edge region, 1 138nm –

1 331nm in the NIR-region, and 1 496nm – 1 596nm and 2 097nm – 2 320nm in the SWIR-region. Certain species appeared to show a high level of spectral separation based on SWIR-reflectance at leaf-level. The addition of strategically placed spectral bands to high spatial resolution multispectral sensors improves the overall potential for the spectral discrimination of weed-species, especially in the SWIR wavelength region.

**Yield Estimation**

The work by Durand et al (2014) on modeling yield for assessing the impacts of climate change on production showed that by using GIS, all the climate, soil and management inputs required to run the crop model for each field could be collated and exported to Excel as input to the QUAD- UI. This tool allows for the wrapped assembly of large amounts of crop model runs required for climate change studies. Field level simulations showed the advantage that they can be summarized to different levels such as, farms, quinary catchments or districts (Figure 165). The results can easily be presented in a table or graph, because of the existing link to a GIS in map format.


**Figure 165 The Three Districts used in the Climate Change Impact Study**

Linking satellite imagery, surveying and crop modeling can be used as an alternative to household survey to assess impacts of climate change on maize production at field to district level in South Africa.

Knox et al (2014) initial attempts to model the yield (Figure 166) showed an agreement of approximately 50%. This modeling can undoubtedly be improved if the digital version of the yields were obtained thus having better geo-referencing between the yield dataset and the acquired images. Discussions with the farmer are ongoing to try to obtain the digital data.

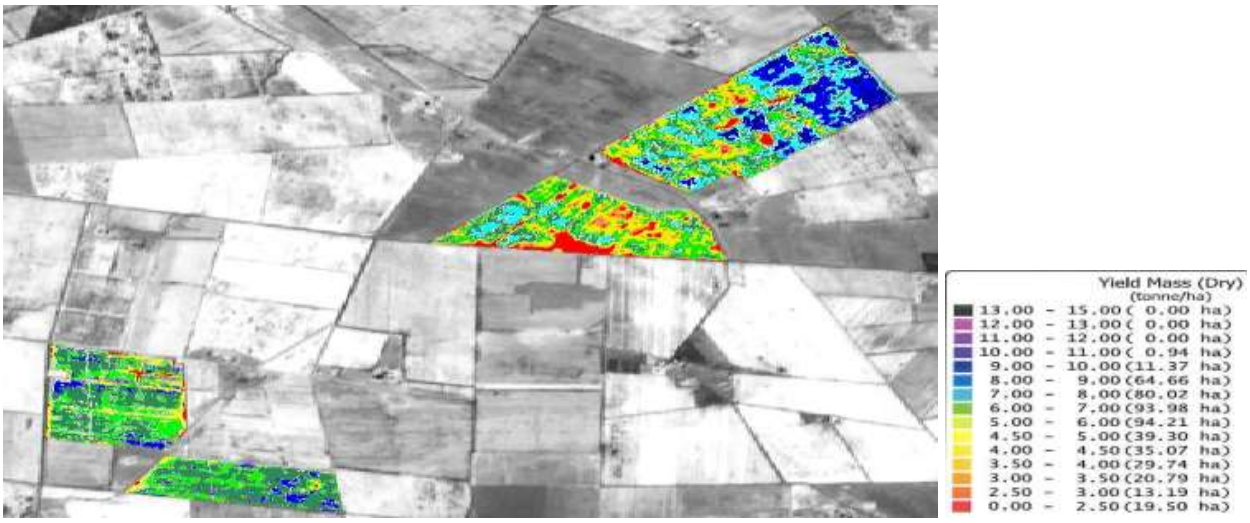


**Figure 166 The Screen Digitized Yield Overlaid on an Acquired Spot4 Scene**

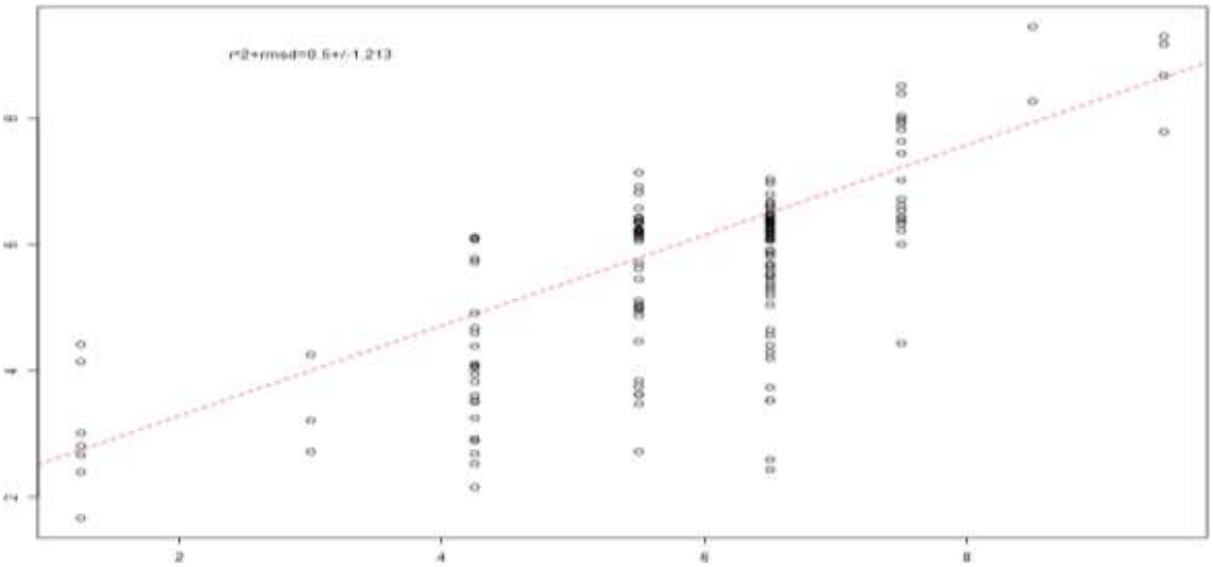

**Figure 167 Plot of the Validation Outcome Obtained from the Random Forest Model Applied to Predict Maize Yield**

Thiebaut et al (2014) found that forward regression analysis with a good sample size gave a reasonable estimation of yield but that co-linearity constrained the results. The introduction of a set of more independent variables would improve the estimation.

Operational System Results

The estimates of the operational system, after discussion modification and verification by the national Crop Estimates Committee confirmed the area planted in maize and estimated final production as at 24 September 2014 (end of season) are reflected in Table 24.

| JECAM SITE | Area planted | | | Final Estimate (24 Sept 2014) | | |
|---|---|---|---|---|---|---|
| | 2014 | | | 2014 | | |
| | White (Ha) | Yellow (Ha) | Total (Ha) | White Tons | Yellow Tons | Total Tons |
| Free State | 730,000 | 465,000 | 1,195,000 | 3,759,500 | 2,511,000 | 6,270,500 |

**Table 24 Area and Production Estimates for Free State Maize 2014 Production Year**

The estimated area planted in wheat and expected production as at January 2015 (end of season) are reflected in Table 25.

| JECAM Site | Area planted (Ha) | 6th Forecast (Tons) (27 Jan 2015) |
|---|---|---|
| Free State | 69,500 | 271,050 |

**Table 25 Area and Production Estimates for Free State Wheat 2014 Production Year**

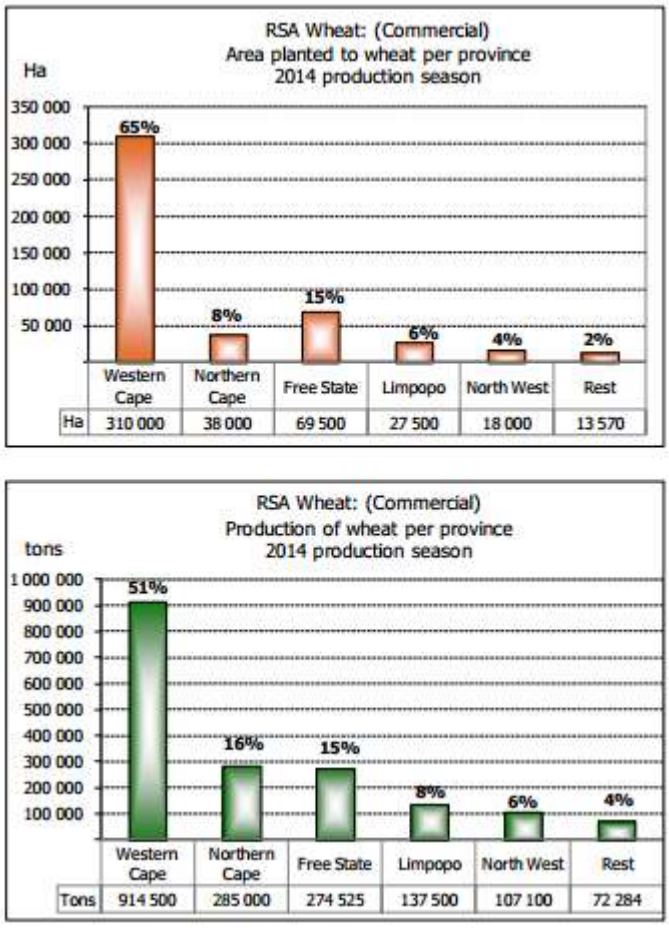


Placing the wheat area and production in national context, the Free State in the production year 2014 planted 15% of the country's wheat area (69,500 Ha) and produced 15% of the country's wheat (274,525 tons) (Figure 168).

The Free State JECAM site is used as an indicator of the grain production in South Africa. The methodologies developed and tested are incorporated into the operational crop estimation and monitoring system. A continual improvement approach is adopted and as new methodologies emerge, these are incorporated. This results in an operational system that is continually updated and is at the cutting edge of technology. The research team regards the system as being based on current best practices.

**Figure 168 Wheat Production of the Free State in the National Perspective**

Plans for Next Growing Season

The SA GEO Agricultural Community of Practice will continue research activities at the JECAM site. The location of the sub site for the collection of SPOT 5 Take 5 data has been shifted to accommodate the wheat growing area in the Free State. This was done so as to accommodate the collection time of the imagery as it coincides with the wheat growing season more than with the maize growing season.

The preliminary estimate (27 Jan 2015) of the area planted to maize in the Free State is 712,000 Ha white maize and 500,000 Ha yellow maize, totaling 1,212,000 Ha.

Publications

Durand, W., Beletze, Y., Cammarano, D, Crespo, O, Nhemachens, C., Walker, S., Tesfuhuney, W., Teweldemdin, M., Gamedze, M., Gwimbi, P., Mpuisang, T., Bonolo, P. Jonas, J., 2014. Integrated Assessment of Impacts of Projected Climate Change on Maize Production in the Southern Africa. Poster presentation ASA, CSSA, & SSSA international Annual meeting, Long Beach California, 31 October to 6 November 2014.

Durand, W., Ferreria, F., du Toit, D.L., Crespo, O, Beletze, Y., 2014. Linking satellite imagery, surveying and crop modeling to assess impacts of climate change on maize production at district level in South Africa. Poster presentation ASA, CSSA, & SSSA international Annual meeting, Long Beach California, 31 October to 6 November 2014.

Durand W., Determining of Present and Projected Future Maize Yields over South Africa using Field Scale Crop Modelling. Unpublished report to prof. Schulze. University of KZN.

Durand, W., 2014. Climate change and Adaptation. Stakeholder meeting. Grand Palm Hotel, Gaborone, Botswana. 24 June 2014.

Durand, W., 2014. Climate change and Adaptation. Stakeholder meeting. Maseru Sun, Maseru, Botswana. 23 June 2014.

Durand, W., 2014. National Climate Change Adaption Stakeholder Consultation Workshop. Stakeholder meeting. Agricultural Research Council, 1134 Park Street, Hatfield Pretoria. 9 September 2014. [M103/40]

Ishimwe, R., AbuThaleb, K., Ahmed, F., & A. Ngie, 2014; Identifying Crops using Landsat 8 Thermal Infrared Bands. Peer reviewed paper presented at AARSE 2014, Johannesburg, South Africa. (http://www.aarse2014.co.za/assets/1.roselyne_subm_id_78.pdf) sited 13 Feb 2015

Knox, N.M, L.T. Tsoeleng, C. Adjorolo, and T. Newby. Crop type & yield mapping: Preparatory study for Sentinel 2. Oral Presentation at Sentinel 2 for Science Workshop, Frascati, Italy, May 2014.

Ngie, A., Ahmed, F., AbuTaleb, K., Ishimwe, R., 2014; Discrimination of Maize Cultivars Using Hyperspectral remote Sensing. Peer reviewed paper presented at AARSE 2014, Johannesburg, South Africa. (http://www.aarse2014.co.za/assets/3.a_ngie_subm_id_202.pdf) sited 13 Feb 2015

Thiebaut, N. M., Steffens, F.E. & Frost, C. (2014) An investigation for the most accurate model in Forward Regression Analysis by using an example of noisy data. Poster presented at the 25th International Biometry congress (03 July 2014), Florence, Italy.

Vermeulen, J. 2014; An investigation into the potential application of hyperspectral remote sensing for weed detection in maize crops in the Free State Province of South Africa. Paper presented at AARSE 2014, Johannesburg, South Africa.

(http://www.aarse2014.co.za/assets/2.j_vermeulen_subm_id_278.pdf.) sited 13 Feb 2015

## 21. Taiwan

No report received.

## 22. Tanzania

No report received.

## 23. Tunisia

Team Leader and Members: Vincent Simonneaux, Mehrez Zribi, Gilles Boulet, Bernard Mougenot, Pascal Fanise, Zohra Lili Chabaane.

Project Objectives

The original project objectives of the site have not changed. They are:

- Crop identification and Crop Area Estimation: Crops types are discriminated using multitemporal NDVI data. Empirical algorithms have been implemented for each year, and we intend to develop a more general and robust method. Information about land cover type is required to parameterize the models used (ET, Biomass, etc.).
- Crop Condition/Stress : Our main goal is to monitor crop consumption and irrigation requirements using the coupling of FAO-56 method and NDVI time series (see Results section). Crop water budget is useful operational information at plot scale (farmers) and at perimeter scale (irrigation managers). This type of product is also a valuable input for watershed integrated modeling, aimed at basin scale management, including groundwater. Crop water stress is monitored using thermal image processing, and the results are aimed at being assimilated in the crop water budget model (see below).
- Soil Moisture: Soil moisture is the primary objective tackled using microwave data, relying on ground measurements for cal/val purposes. This type of information may also be input into the crop water budget model.
- Yield Prediction and Forecasting: Yield prediction is done using empirical relationships with remotely sensed indices.
- Crop Residue, Tillage and Crop Cover Mapping: We don't study residues nor tillage (although this was done some years ago). Crop cover mapping is related to 'Crop identification and Crop Area Estimation' above.

Site Description

- Location

  Top left Latitude: N35° 42' 20"

  Longitude: E9° 41' 45"

  Bottom right Latitude: N35° 23’

  Longitude: E10° 07’

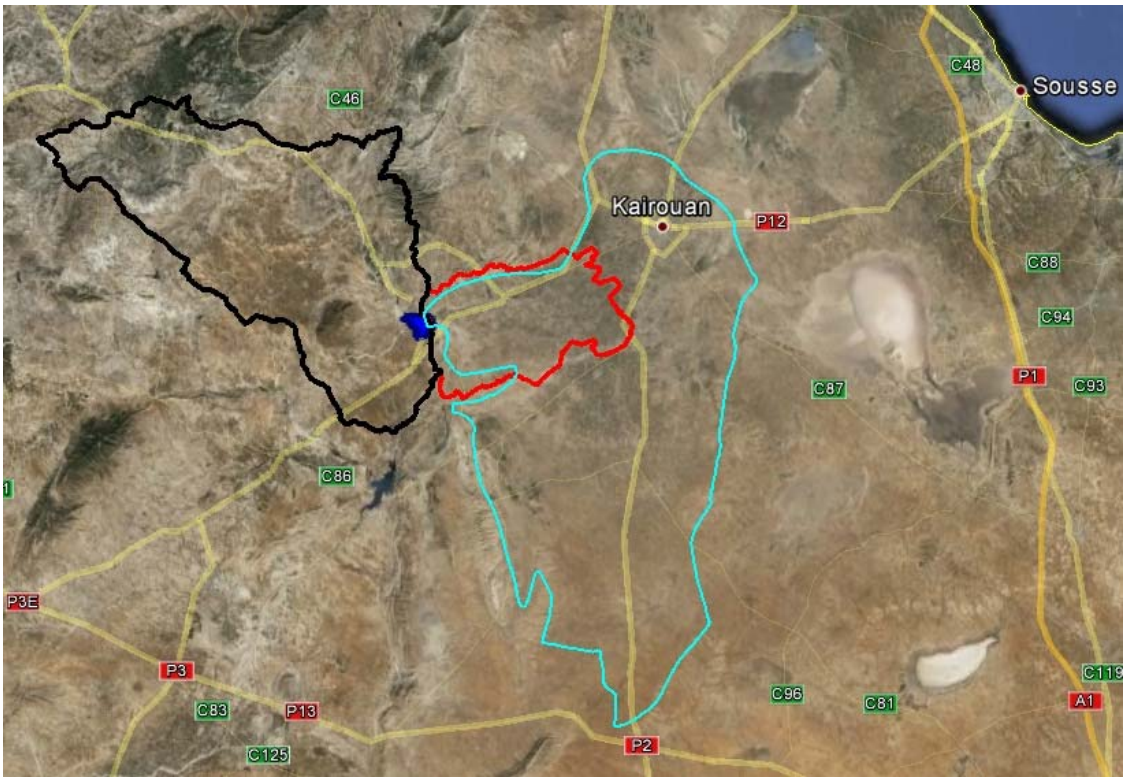


**Figure 169 Tunisia Merguellil Site**

The site is shown in Figure 169. The boundary of the upper watershed is in black, in red the boundary of the irrigated area, and in cyan the boundary of the aquifer.

- Topography: Alluvial plain.
- Soils: Variable texture, from fine sand to clay-loam.
- Drainage class/irrigation: Well drained soils.
- Crop calendar: See Table 26.
- Field size: Typically 1 to 4 ha.
- Climate and weather: Semi-arid mediterranean climate, rainfall around 250 mm/y, ET0 around 1500 mm/year.

| | Jan | Feb | Mar | Apr | May | Jun | Jul | Aug | Sep | Oct | Nov | Dec |
|---|---|---|---|---|---|---|---|---|---|---|---|---|
| Melon early | | Plough | Plant | | | Harvest | | | | | | |
| Melon | | | Plough | Plant | | Harvest | Harvest | | | | | |
| Watermelon | | | | | Plough | Plant | | | | Harvest | | |
| Tomato | | | | | Plough | Plant | | | | Harvest | | |
| Chili pepper | | | | | | Plant | | | Harvest | | | |
| Tomato late | | | | | | | | Plough | Plant | | Harvest | |
| Chili pepper late | | | | | | | | Plough | Plant | | Harvest | |
| Broad bean | Harvest | Harvest | Harvest | | | | | | Sow | | | |
| Olive trees | Prune | | | | | | | | | Harvest | Harvest | Prune |
| Almond trees | | | | | | Harvest | | | | | | |
| Oat | | | | | Harvest | | | | | Plough | Sow | |
| Barley (dry cultivation) | | | | | Harvest | | | | | | Plough | Sow |
| Wheat (dry) | Sow | | | | | Harvest | | | | | | Plough |
| Forage | | | | Harvest | | | | | | | | |
| Cattle pasture | | | | | | | | | | | | |

**Table 26 Merguellil, Tunisia Crop Calendar**

- Agricultural methods used: Dry cereals and olive cultivation; Irrigation for cereals, vegetables and some fruit trees (apple, peach, etc.).

EO Data Received/Used

Although the project acquired images from various sensors (see Table 27 below), only Landsat-7 and 8 images can be considered to have been acquired in the framework of JECAM.

| Sensor | # Images | Optical /SAR | Supplier | Pixel Size | Proc. Level | Challenges Ordering | Challenges Processing |
|---|---|---|---|---|---|---|---|
| SPOT-5 | 7 | Optical | SPOT Image/ CNES | 10 | 1A | Specific offer for French Labs (ISIS Action) | Problem of getting atmospheric parameters. Global server (H20, aerosols, ozone) are a significant advance but local photometer is better |
| Landsat-7 | 10 | Optical | JECAM/ USGS | 30 | Radiance | | Not yet processed |
| Landsat-8 | 19 | Optical | JECAM/ USGS | 30 | TOA ref | | Processed using the MAACS chain prototype (designed for 2A level for THEIA) |
| TerraSAR -X | 5 | SAR | DLR | 2 | Dual polarization | | |

**Table 27 Tunisia Site EO Data Ordered**

**Figure 170 (L) Flux Tower in Irrigated Barley (R) Well and Pipe for Irrigation**

In situ Data

- Crop identification ground campaigns for land cover classification training. Two campaigns: 150 plots in April, 60 plots in June.
- Soil roughness observation on bare soil plots for SAR images processing validation.
- Vegetation traits (LAI, fraction cover, biomass) collected of wheat and olive trees.
- Three permanent meteorological stations (including temperature, humidity, wind speed, net radiation, rainfall).
- Two Flux stations on irrigated pepper (May-November 2014) and rainfed olive orchard (1/01 – 31/12/2014).
- One X-LAS scintillometer transect (2 km) starting spring 2013 (area-averaged surface heat fluxes).
- Soil moisture probes with automatic acquisition (5 sites on dry cultivation) + campaigns for soil surface moisture (20 sites).
- Surveys of monthly irrigation volumes at the perimeter scale + daily irrigation volumes at farm scale for about 30 private farms.

Collaboration

The CESBIO Lab in Toulouse has two sites in north Africa (this site and the Marrakech site, also in JECAM) which are continuously communicating and are answering jointly to some calls. They are both involved in a joint project called AMETHYST funded by the French research agency (ANR). We also benefit from funding of student exchanges between Tunisia, Morocco, Algeria and France (PHC program).

Results

**Crop Water Budget Monitoring**

Remote sensing has long been used for computing evapotranspiration estimates, which is an input for crop water balance monitoring. Up to now, only medium and low resolution data (e.g. MODIS) are available on regular basis to monitor cultivated areas. However, the increasing availability of high resolution high repetitivity VIS-NIR remote sensing, like the forthcoming Sentinel-2 mission to be launched in 2015, offers unprecedented opportunity to improve this monitoring.

Methods for computing evapotranspiration (ET) using remote sensing belong basically to two broad families, either using thermal remote sensing used to solve the energy budget of the surface, or using SVAT modeling forced by remotely sensed information of vegetation properties (e.g. fraction cover, leaf area index, crop coefficients...). The latter group includes the coupling of the dual crop coefficient method described in FAO paper 56 (Allen, 1998) with NDVI time series providing spatialized estimates of the fraction cover (fc) and the basal crop coefficient (Kcb). We developed in previous works the SAMIR tool implementing this method using high resolution image times series (SPOT, Landsat, FORMOSAT and forthcoming Venus and Sentinel-2).

Instantaneous estimates of evapotranspiration

Thermal data (MODIS, ASTER, Landsat) have been used to derive actual evapotranspiration estimates (ETR). The methods have been improved by constraining ETR with potential values and using specific formalism for senescent vegetation. These algorithms have been validated for cereals (Boulet et al., 2014) and are under work for trees (rainfed and irrigated olive trees). Considering the importance of sparse coverages in the study area, a special focus has been put on the comparison of single versus dual source models (homogeneous crop or juxtaposition of bare soil and vegetation). Single source models show better results on simple crops like wheat.

Estimates of irrigation volumes

In this study, water consumption of regional crops was estimated with the SAMIR software (Satellite of Monitoring Irrigation). The main objective of this work is to assess the operationality and accuracy of SAMIR at plot and perimeter scales, when several land use types (winter cereals, summer vegetables...), irrigation and agricultural practices are intertwined in a given landscape, including complex canopies such as sparse orchards.

The FAO-56 method relies on the so-called “reference evapotranspiration” (ET0), which is the evapotranspiration of a well-watered short grass, and can be computed using the Penman-Monteith equation. The ET of any actual vegetation is then obtained by simply multiplying ET0 by coefficients accounting for vegetation transpiration limited by the actual amount of active vegetation (Kcb), a stress coefficient accounting for water availability in the soil (Ks) and a coefficient accounting for soil evaporation (Ke), also accounting for soil surface water content. The key input of remote sensing, the vegetation index (e.g. NDVI), can be related to crop coefficients by linear relations. Conversely, a shortcoming of the method is the lack of information about the actual soil water status, linked to irrigation inputs. Opposite to rainfall, irrigation inputs cannot be known exhaustively on large areas, thus the necessity to simulate irrigation inputs based on assumed rules reproducing the farmer’s behaviour (when, how much…).

Meteorological ground stations were used to compute the reference evapotranspiration and get the rainfall depths. Two image time series have been acquired for the 2008-2009 and 2012-2013 hydrological years over the site. For 2012-2013, the series was a mix of classical SPOT5 images acquired through ordering and SPOT4 images acquired from February to June through the SPOT4-Take5 experiment achieved at the end of life of the SPOT4 satellite (http://www.cesbio.ups-tlse.fr/multitemp/?page_id=406). The SPOT5 images were manually corrected first using the 6S Algorithm for atmospheric correction, then adjusted using invariant objects located on the scene, based on visual observation of the images. The SPOT4 images were corrected using the MAACS algorithm designed in CESBIO to process time series of constant looking angle images (in prevision of Sentinel-2 mission), then they were also improved using invariants. From these time series, a Normalized Difference Vegetation Index (NDVI) profile was generated for each pixel.

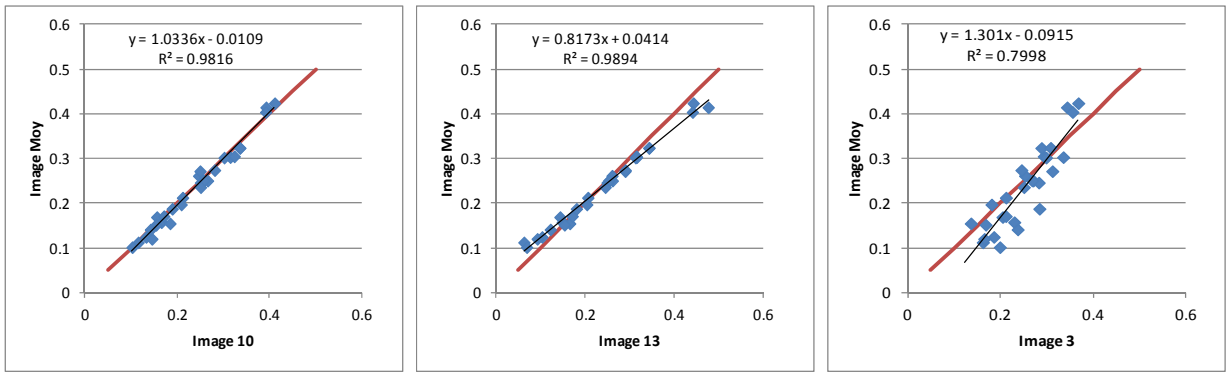


**Figure 171 Relative Correction of the SPOT5 Time Series**

In Figure 171, each date (X) is plotted regarding the average of the time series (Y) for 30 pseudo-invariant objects identified on the image. Three examples of results are shown: (a) good agreement between the date and the average, (b) significant bias for this date requiring correction, (c) problem of haze requiring (elimination of the date).

SAMIR was first calibrated based on ground measurements of evapotranspiration achieved using eddy-correlation devices installed on irrigated wheat and barley plots. After calibration, the model was run to spatialize irrigation over the whole area and a validation was done using cumulated seasonal water volumes obtained from ground survey at both plot and perimeter scales. The results show that although determination of model parameters was successful at plot scale, irrigation rules required an additional calibration which was achieved at perimeter scale (Saadi, 2015). In Figure 172, one campaign equals one perimeter in one season.

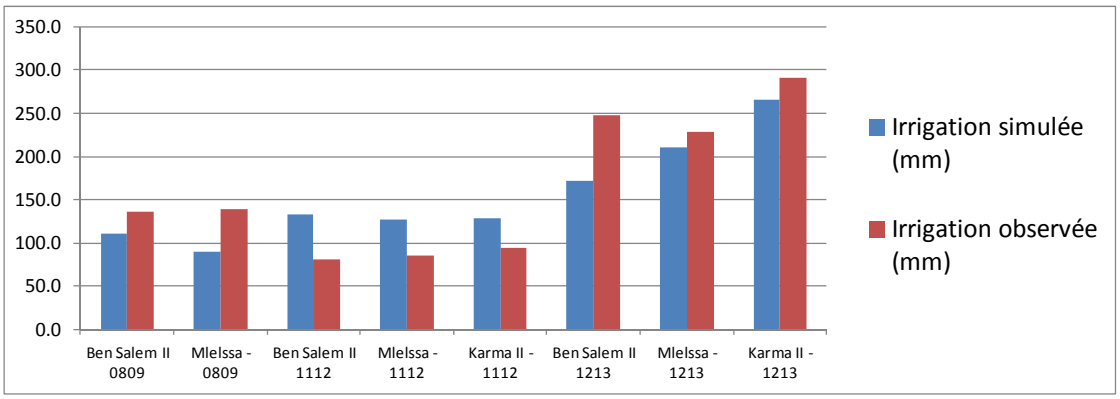


**Figure 172 Comparison between Observed Seasonal Irrigation Depth and Irrigation Depth Simulated using SAMIR for Eight Campaigns**

**Soil Water Content Monitoring**

Soil water monitoring using microwave data has been studied at various scales, from 1km to 2m. We present here the results on the JECAM site. A sensitivity analysis has been conducted on TerraSAR-X and COSMO-Skymed (X band) images regarding soil roughness and water content. This analysis is based on images acquired during three month in winter (Nov 2013-Jan 2014) and simultaneous ground observations on 15 bare soil plots. Relations have been established between standard deviation of roughness high and a new SAR image parameter, Zg (Zribi, 2014a,b). Other backscattering schemes (IEM, Dubois, IEM-Baghdadi) have been validated on this data (Gorrab et al., 2015).

**Yield Estimates**

Wheat yields have been forecasted based on optical data (VIS-NIR) two months before harvest (Chahbi et al., 2014). This analysis is based on a three year database including satellite data and ground observations on a set of 30 wheat and barley plots. A second approach was successfully tested using the vegetation model SAFY (Simple Algorithm For Yield estimates, Duchemin et al., 2008), using as input remotely sensed LAI estimates (from VIS-NIR high resolution data) to calibrate an efficient model simulating biomass and yield.

Plans for Next Growing Season

A time series of SPOT5 images is currently being acquired until March 2015 (and of SPOT5 commercial service) and the SPOT5-Take5 experiment (led by CNES) will allow following on these acquisitions every 5 days from 1/04/2015 to 31/08/2015. This dataset will be processed using the same methods as previous years (with the SAMIR tool) in order to validate the model on large areas. These repetitions will be useful considering the complexity of the area regarding the vegetation cycles. We intend also to be able to tackle the use of medium resolution time

series (MODIS, MOD13Q1 products) and thermal data (Landsat-8) to improve the soil water compartment control.

We anticipate ordering the same type/quantity of EO data next year.

Publications

**Articles**

Amri, R., Zribi, M., Lili-Chabaane, Z., C. Szczypta, J. C. Calvet, G. Boulet, 2014, FAO-56 dual approach combined with multi-sensor remote sensing for regional evapotranspiration estimations, Remote Sens. 6(6), 5387-5406; doi:10.3390/rs6065387

Chahbi, A., Zribi, M., Lili-Chabaane, Z., Duchemin, B., Shabou, M., Mougenot, B., Boulet, G., 2014, Estimation of the dynamics and yields of cereals in a semi-arid area using remote sensing and the SAFY growth model, International journal of Remote Sensing, 35:3, 1004-1028.

Zribi, M., Gorrab, A., Baghdadi, N., Lili-Chabaane, Z., Mougenot, B., 2014a, Influence of radar frequency on the relationship between bare surface soil moisture vertical profile and radar backscatter, IEEE Geoscience and Remote Sensing Letters, 11(4) 848 - 852 10.1109/LGRS.2013.2279893.

Zribi, M., Gorrab, A., and Baghdadi, N., 2014b, A new soil roughness parameter for the modeling of radar backscattering over bare soil, Remote Sensing of Environment, 152, 62-73.

Gorrab, A., M. Zribi, Nicolas Baghdadi, Bernard Mougenot and Zohra Lili Chabaane, 2015, Potential of X- band TerraSAR-X and COSMO-SkyMed SAR data for the assessment of physical soil parameters, Remote Sensing, 7(1), 747-766.

Saadi, S., Simonneaux, V., Boulet, G., Lili Chabaane, Z., et al. Monitoring irrigation consumption using high resolution high repetitivity image times series. Aplication to the Kairouan area (Tunisia). Submitted to Remote Sensing special issue “SPOT4-Take5 experiment”.

**Conferences**

Amri, R., M. Zribi, Z. Lili-Chabaane, B. Duchemin, Gruhier, G., Analysis of vegetation dynamics and persistent behavior in a North Africa semi-arid region, using SPOT VEGETATION NDVI data, Global Vegetation Monitoring and Modeling GV2M, Avignon France 3-7 février 2014.

Amri, M. Zribi, Z. Lili-Chabaane, C. Szczypta, J. C. Calvet , G. Boulet, FAO-56 dual approach combined with multi-sensor remote sensing for regional evapotranspiration estimations, IEEE International conference on Advanced Technologies for Signal and Image Processing, ATSIP, 17-19 march 2014 Sousse, Tunisia.

Chahbi, A., M. Zribi, Z., Lili-Chabaane, B. Duchemin, B. Mougenot, Analysis of optical remote sensing potential for yields of cereals estimation, IEEE International conference on Advanced Technologies for Signal and Image Processing, ATSIP, 17-19 march 2014 Sousse, Tunisia.

Chahbi, A., Zribi, M., Lili-Chabaane, Z., Duchemin, B., Mougenot, B., Early forecasting of cereals yields in a semi arid area using spot/hrv images and the agro-meteorological model «SAFY». Global Vegetation Monitoring and Modeling GV2M, Avignon France 3-7 février 2014.

Gorrab, A., Zribi, M., N. Baghdadi, Z. Lili-Chabaane, B. Mougenot, Influence of radar frequency on the relationship between bare surface soil moisture vertical profile and radar backscatter, IEEE International conference on Advanced Technologies for Signal and Image Processing, ATSIP, 17-19 march 2014 Sousse, Tunisia.

Gorrab A., Zribi M., Baghdadi N., Lili-Chabaane Z., and Mougenot B., 2014. X-band TERRASAR-X and COSMO-SKYMED SAR data for bare soil parameters estimation. International Geoscience and Remote Sensing Symposium 2014 (IGARSS 2014), 13 - 18 July 2014, Quebec, Canada.

Gorrab A., Zribi M., Baghdadi N., Mougenot B., and Lili-Chabaane Z., 2014. Potential of X-band SAR data from TerraSAR-X and COSMO-SkyMed sensors to retrieve physical soil properties. 4th International Symposium on Recent Advances in Quantitative Remote Sensing (RAQRS'IV), 22-26 September 2014, Torrent, Valencia, Spain.

Zribi, M., Gorrab, A., Baghdadi, N., A new Zg roughness parameter for improving backscattering analysis over bare soils, International Geoscience and Remote Sensing Symposium 2014 (IGARSS 2014), 13 - 18 July 2014, Quebec, Canada.

Zribi M., Gorrab A., and Baghdadi N., 2014. Roughness and vertical moisture heterogeneities introduction to improve soil moisture estimation with radar remote sensing. 4th International Symposium on Recent Advances in Quantitative Remote Sensing (RAQRS'IV), 22-26 September 2014, Torrent, Valencia, Spain.

Zribi M., Kotti F., Gorrab A., Amri R., Baghdadi N., Mougenot B., Lili-Chabaane Z., and Boulet G., 2014. Operational soil moisture mapping using multitemporal ASAR/Wide Swath ENVISAT data. 4th International Symposium on Recent Advances in Quantitative Remote Sensing (RAQRS'IV), 22-26 September 2014, Torrent, Valencia, Spain.

Boulet G., Mougenot B., Lili-Chabaane Z, Fanise P., Olioso A., Bahir, M., Rivalland V., Jarlan L; Coudert B. and Lagouarde, J.-P., 2014. Total and component evapotranspiration retrieval performances of a single- pixel energy balance model over agricultural crops RAQRS'IV, Valencia, Spain.

Saadi S., Simonneaux V., Boulet G., Lili Chabaane Z., Mougenot B., Fanise P., Ayari H., Zribi M., 2014, Monitoring crop water budget and irrigation consumption using high and low resolution NDVI image time series. Calibration and validation in the Kairouan plain (Tunisia), 4th International Symposium, Recent Advances in Quantitative Remote Sensing, September 22-26, Torrent, Spain;

Mougenot B., Touhami N., Lili Chabaane Z., Boulet G., Simonneaux V., Zribi M., 2014, Trees detection for water resources management in irrigated and rainfed arid and semi-arid agricultural areas, April 1-3, 2014, PLEIADES DAYS, Toulouse.

# 24. Ukraine

Team leader: Prof. Nataliia Kussul, Deputy Director, Space Research Institute NASU-SSAU

Team Members: Prof. Andrii Shelestov, Senior Researcher, Integration-Plus Ltd.;Dr. Sergii Skakun, Senior Researcher, Integration-Plus Ltd.;Dr. Andrii Kolotii, Space Research Institute NASU-SSAU;Ruslan Basarab, Director, Integration-Plus Ltd.;Andrii Mironov, PhD Student, Space Research Institute NASU-SSAU; Bohdan Yailymov, PhD Student, Space Research Institute NASU-SSAU.

Project Objectives

The original objectives have not changed.

- Crop identification and Crop Area Estimation
- Crop Condition/Stress
- Yield Prediction and Forecasting.

Site Description

The main activities in 2014 were carried out for the JECAM test site in Kyiv region.

- Location

  The site consists of two parts:

  - the whole Kyiv region (28,000 sq. km) intended for crop mapping and acreage estimation;
  - intensive observation sub-site (25x15 sq. km) indented for crop biophysical parameters estimation. This sub-site consists of a research farm of the National University of Life and Environmental Sciences of Ukraine where intensive in-situ measurements are being collected.

The latitude and longitude of the site and sub-site are given in Table 28. The map of the site is shown in Figure 173.

### Table 28: Geographical Coordinates of the Ukraine Test Sites

| **Kyiv** | | |
|---|---|---|
| **Centroid** | | Latitude: 50.355<br>Longitude: 30.715 |
| **Site Extent** | **Top left** | Latitude: 51.54<br>Longitude: 29.26 |
| | **Bottom right** | Latitude: 49.17<br>Longitude: 32.17 |
| **Sub-site for Intensive Observation (Pshenichne research farm of NULESU).** | | |
| **Centroid** | | Latitude: 50.075<br>Longitude: 30.11 |
| **Site Extent** | **Top left** | Latitude: 50.14<br>Longitude: 29.96 |
| | **Bottom right** | Latitude: 50.01<br>Longitude: 30.26 |

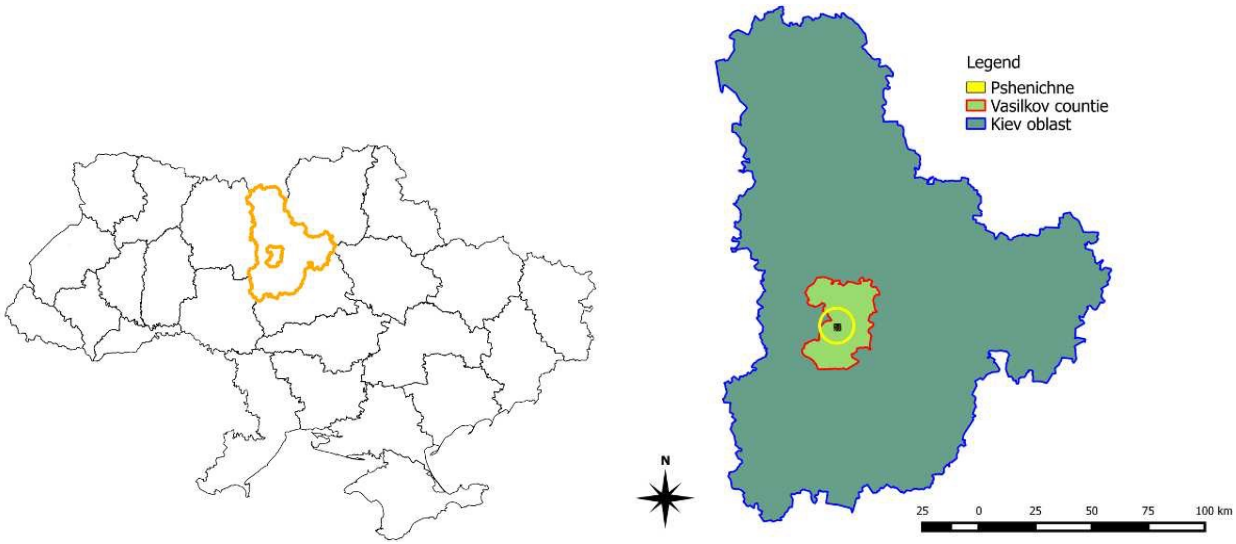


### Figure 173 Administrative Map of Ukraine and Location of Kyiv Region

For winter wheat yield forecasting, the whole territory of Ukraine was considered. Forecasting was done at oblast level. An oblast is a sub-national administrative unit that corresponds to the NUTS2 level of the Nomenclature of Territorial Units for Statistics (NUTS) of the European Union.

- Topography: The landscape is mostly flat with slopes ranging from 0% to 2%. Near 10% of the territory is hilly with slopes about 2-5%.
- Soils: The soils of the cultivated land are mainly different kinds of chernozems.
- Drainage class/irrigation: Soil drainage ranges from poor to well-drained. Irrigation infrastructure is limited. About 6% of the territory is drained (1700 $km^2$). About 4% (1200 $km^2$) of the territory is used for irrigated agriculture.
- Crop calendar: The crop calendar is September-July for winter crops, and April-October for spring and summer crops.
- Field size: Typical field size is 30-250 ha.
- Climate and weather: The climatic zone is humid continental.
- Agricultural methods used: Crop types include winter wheat, winter rapeseed, spring barley, maize, soy beans, sunflower, sugar beets and vegetables. Due to the relatively large number of major crops and other factors, there is no a typical simple crop rotation in this region. Most producers use different crop rotations depending on specialization.

**Figure 174 Rapeseed, 21 March 2014**

**Figure 175 Winter Wheat, 12 June 20124**

EO Data Received/Used

Landsat-8

- Space agency or Supplier: USGS
- Optical
- Number of scenes: 6
- Range of dates: 3 April 2014, 6 June 2014, 8 July 2014, 10 September 2014, 12 October 2014, 28 October 2014
- Spatial resolution: 30 m
- Processing level: L1
- Challenges, if any, in ordering and acquiring the data: No challenges.
- Challenges, if any, in processing and using the data: No challenges.

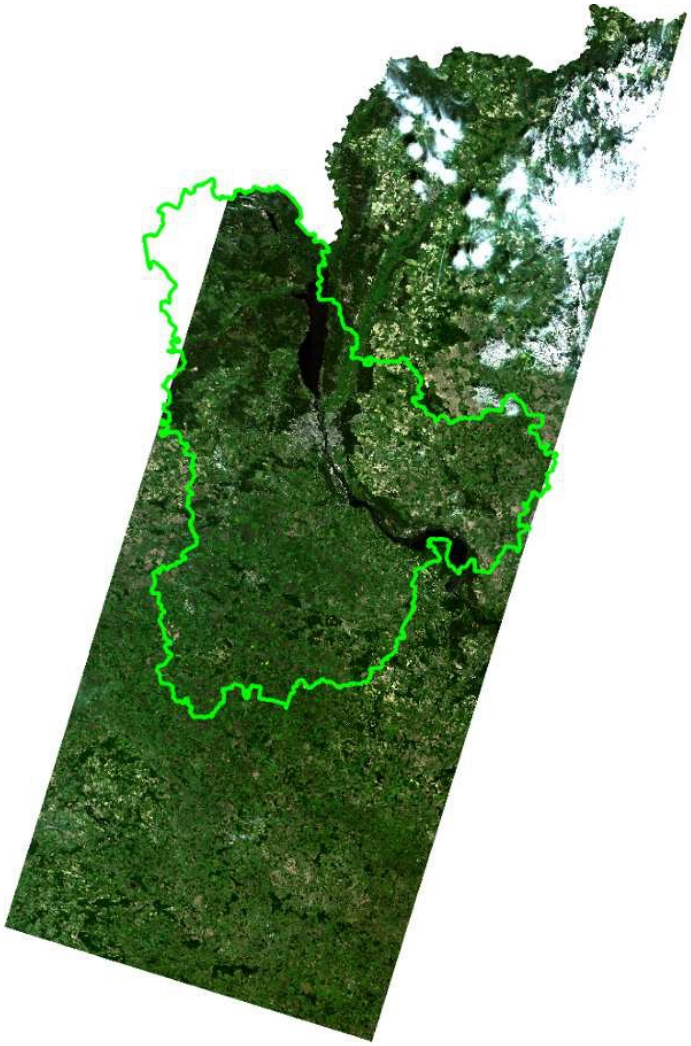

**Figure 176 Landsat-8 Image Acquired on 6 June 2014**

Proba-V

- Space agency or Supplier: VITO/ESA 
- Optical 
- Number of scenes: 7 
- Range of dates: 5 April 2014, 18 April 2014, 25 May 2014, 30 June 2014, 1 August 2014, 6 September 2014, 15 September 2014 
- Spatial resolution: 100 m 
- Processing level: L1 
- Challenges, if any, in ordering and acquiring the data: No challenges.
- Challenges, if any, in processing and using the data: No challenges.

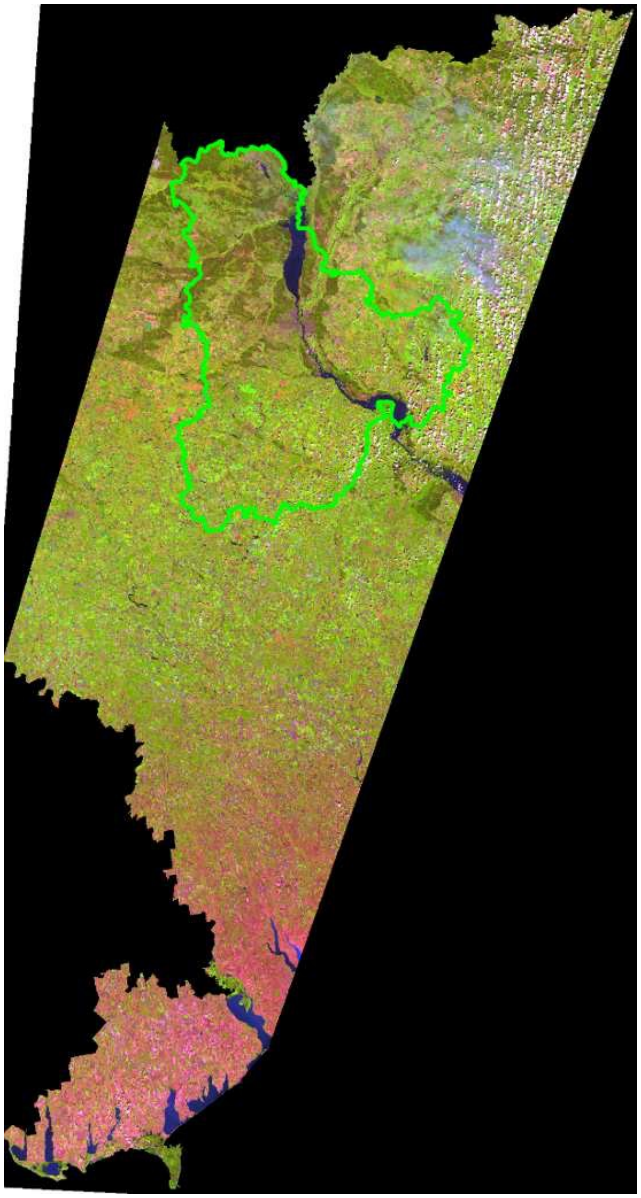

**Figure 177 Proba-V Image Acquired on 30 June 2014**

In situ Data

Two types of ground data were collected:

- Along the roads to collect data on crop types
- Sample (point) observations on biophysical parameters using VALERI protocol.

**Along the roads**

About 420 fields were observed with major crop classes (Figure 178). The observations were made in March 2014 for collecting information on winter and spring crops and in June 2014 for summer crops.

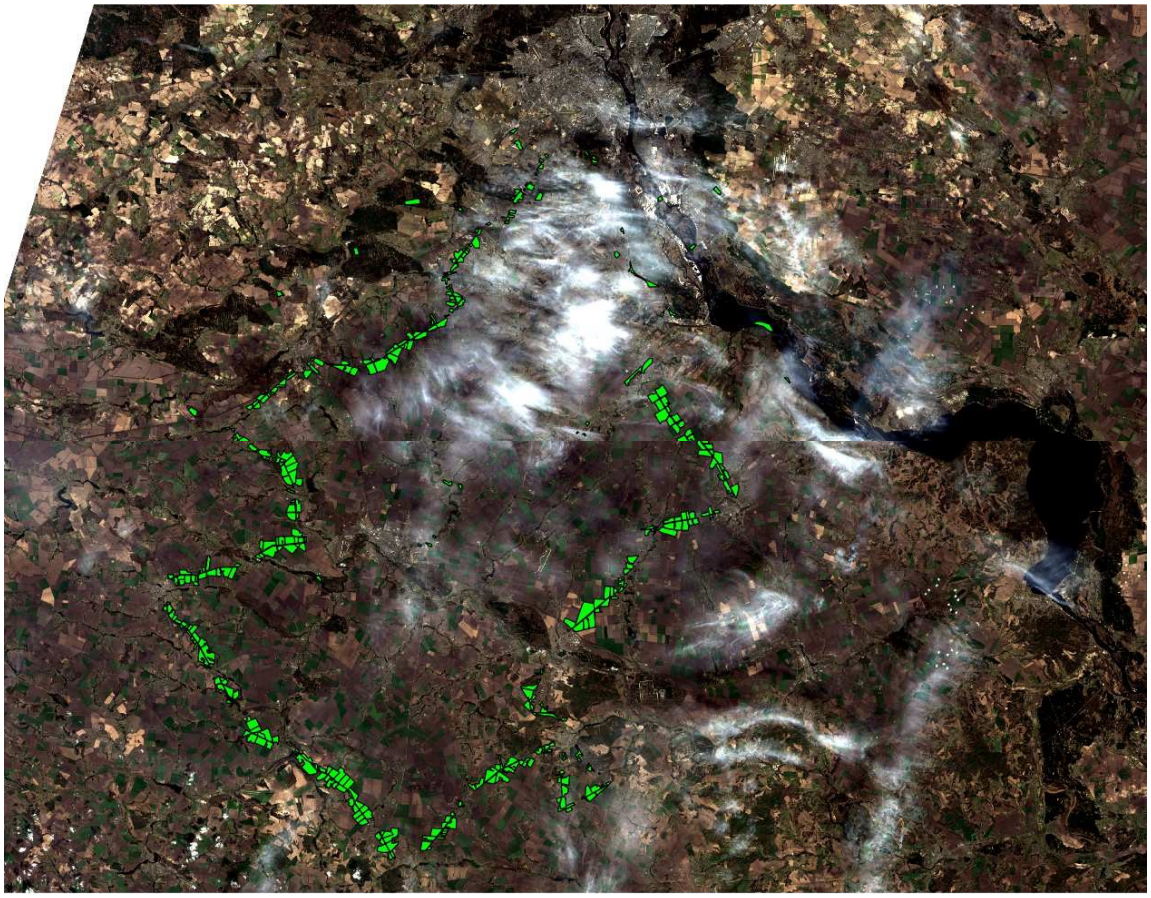

**Figure 178 Samples taken on 21 March 2014 overlaid on Landsat-8 Image Acquired on 3 April 2014**

**Observations of biophysical parameters**

Three field campaigns to characterize the vegetation biophysical parameters at the Pshenichne test site were carried out:

- First campaign: 12 June 2014.
- Second campaign: 31 July 2014.

Digital Hemispheric Photographs (DHP) images were acquired with a NIKON D70 camera. Hemispherical photos allow the calculation of LAI and FCOVER measuring gap fraction through an extreme wide-angle camera lens (i.e. 180º) (Weiss et al., 2004). The hemispherical images

acquired during the field campaign are processed with the CAN-EYE software (http://www.avignon.inra.fr/can_eye) to derive LAI, FAPAR and FCOVER.

The in situ biophysical values were used for producing LAI, FCOVER and FAPAR maps from optical satellite images, and provide cross-validation, and validation of global remote sensing products.

Collaboration

We participate in the following collaborative projects:

1. EU FP7 project “Stimulating Innovation for Global Monitoring of Agriculture and its Impact on the Environment in support of GEOGLAM” (SIGMA). Participation as project partner.
2. EU FP7 project “Implementation of Multi-scale Agricultural Indicators Exploiting Sentinels” (ImagineS). Providing ground observations for validation of EO products.
3. ESA Sentinel-2 for Agriculture. Participation as a “Product Developer” in 2014.

Results

**Crop Mapping**

Early stage winter crops mapping for Kyiv oblast (area 28,000 km2) using Landsat-8 (3 April) and Proba-V (5 April) in 2014.

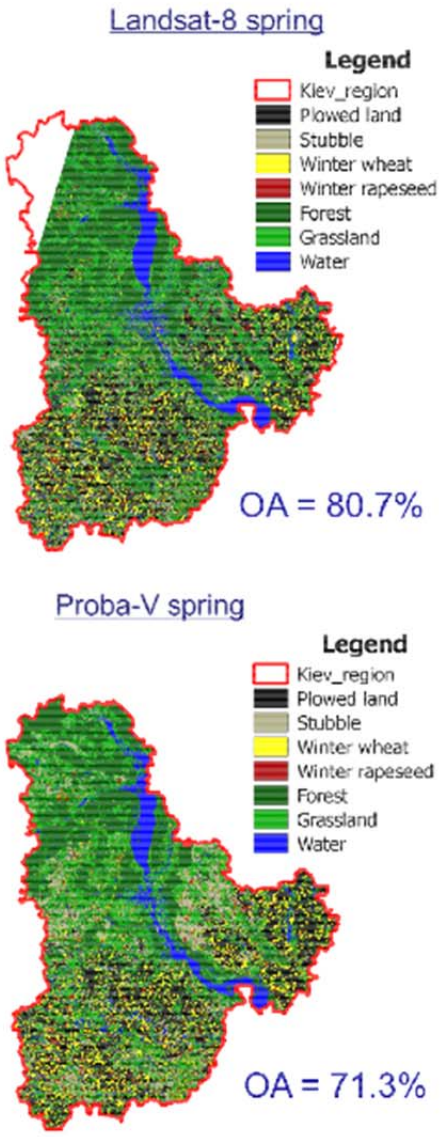


**Figure 179 Early Stage Winter Crops Mapping using Landsat-8 (3 April) and Proba-V (5 April) in 2014**

In 2014, activities were also continued for the exploring feasibility of RADARSAT-2 for crop mapping in Ukraine. We used images that were acquired for the 2013 season. Different combinations of optical and SAR imagery were used for the experiment.

The first set of experiments was conducted in order to assess efficiency of using a committee of MLPs for classification of multi-temporal SAR and optical images. Table 29 shows the comparison of overall classification accuracy and Kappa coefficient for classification with SAR and optical images using a committee of neural networks and the best single neural network.

| # | Input | Committee | | Best Single NN | |
|---|---|---|---|---|---|
| | | OA, % | Kappa | OA, % | Kappa |
| 1 | Landsat-8 + FQ8W + FQ20W | 90.10 | 0.875 | 89.18 | 0.864 |
| 2 | Landsat-8 | 86.01 | 0.824 | 84.07 | 0.800 |
| 3 | Landsat-8 + FQ8W | 87.54 | 0.843 | 87.45 | 0.842 |
| 4 | Landsat-8 + FQ20W | 88.08 | 0.850 | 87.97 | 0.849 |
| 5 | FQ8W + FQ20W | 84.07 | 0.801 | 83.32 | 0.792 |
| 6 | FQ8W | 71.78 | 0.654 | 71.18 | 0.648 |
| 7 | FQ20W | 76.99 | 0.715 | 76.30 | 0.706 |
| 8 | Landsat-8 + (VV + VH) | 88.62 | 0.857 | 87.44 | 0.842 |
| 9 | Landsat-8 + (HH + HV) | 88.99 | 0.862 | 88.43 | 0.855 |
| 10 | VV + VH | 80.71 | 0.761 | 80.09 | 0.747 |
| 11 | HH + HV | 81.07 | 0.765 | 80.12 | 0.753 |
| 12 | Landsat-8 + FQ8W + FQ20W (until 06.08.13) | 87.74 | 0.846 | 86.62 | 0.834 |
| 13 | FQ8W + FQ20W (until 06.08.13) | 74.33 | 0.683 | 73.35 | 0.671 |

**Table 29 Comparison of Overall Classification Accuracy and Kappa Coefficient**

For all cases, a committee of 10 MLPs was used with the number of hidden neurons ranging from 10 to 100. The use of committee allowed us to increase OA from +0.09% up to +1.94% comparing to the single best MLP with average being +0.79%. Addition of all multi-temporal RADARSAT-2 images to Landsat-8 images increased OA by +4.09%, +2.61%, +2.98% for all polarizations VV+VH+HH, dual polarizations VV+VH and HH+HV, respectively. Addition of SAR images acquired under steeper angle (Landsat-8+FQ8W) increased OA by +1.53% while addition of SAR images under shallow angle (Landsat-8+FQ20W) increased OA by +2.07%. Among dual polarization, slightly better performance was obtained for HH+HV polarization compared to VV+VH. Therefore, in all cases OA was improved when adding SAR images to the optical ones.

As for the crop specific accuracies, the following results were achieved.

*Winter wheat:* The best results were obtained for combination Landsat-8+FQ20W (PA=98.5%, UA=98.4%). In general, this crop was reliably identified (with PA and UA more than 85%) for all combinations but FQ8W. More importantly, using only SAR images (all polarizations VV+VH+HH and dual polarizations VV+VH or HH+HV) it was possible to surpass 85% accuracy. This suggests

that optical images can be easily substituted by SAR for winter wheat classification in case of cloud cover.

*Winter rapeseed:* As with winter wheat, winter rapeseed was in general reliably classified by both optical and SAR images. PA was the highest for HH+HV combination (92.8%) while UA was the highest for Landsat-8+FQ20W combination (98%). Landsat-8 alone was able to discriminate rapeseed due to the availability of images during the rapeseed flowering stage (on May 02 and 18). Addition of SAR images to optical images was substantial only for the Landsat-8+FQ20W combination where UA was improved by +1.8%. Using SAR images alone, it was possible to achieve both PA and UA more than 85% only for VV+VH combination (88.2% and 87.8% respectively), while for other combinations, UA was always lower than 85%.

*Spring crops:* Discrimination of spring crops (mainly barley) using the available set of satellite imagery failed to produce reasonable performance for this type of crops. The main confusion of this class was with winter wheat (class 2) and other cereals (class 9). The reasons for this are as follows. When collecting ground data, it was impossible to discriminate winter crops from spring crops in the fields. Therefore, all wheat samples were assigned winter wheat class (since proportion of spring wheat is small), and all barley samples were assigned spring crops class (since proportion of winter barley is small). Unfortunately, reliable satellite data (including coarse resolution MODIS) for the autumn period of 2012 were not available due to strong cloud contamination. Confusion with other cereals can be explained by almost the same vegetation cycle of spring barley with other cereals produced in the region, namely with rye and oats. For example, combining spring crops and other cereals classes for all data sets (Landsat-8+FQ8W+FQ20W) would improve accuracy for spring crop class from PA=48.8% and UA=71.7% to PA=82.2% and UA=90.65%.

*Maize:* When adding all SAR images to the optical ones, PA and UA improved by +2.2% and +6.2%, respectively. In general, maize was reliably identified (with PA and UA more than 85%) for all combinations but FQ20W and FQ8W+FQ20W (up to 06.08.2013). SAR images alone were able to provide reliable classification of maize for all polarizations and dual polarization combinations with PA and UA exceeding 90% accuracy. As to the observation angle, better results were achieved for steeper angle (FQ8W, PA=85.8% and 95.1%) than for shallow angle (FQ20W, PA=83.9% and 87.1%). Optical images were critical in providing early season maps in August as PA and UA were 95.5% and 91.8% respectively for combination of Landsat-8 and RADARSAT-2 images, and 82.8% and 87.7% for RADARSAT-2 images only.

*Sugar beets:* The impact of using SAR images for discriminating sugar beet was in general limited. The gains of adding SAR images to the optical ones were +2.9% and -4.4% for PA and UA, respectively. The use of SAR images alone yielded PA=88.5% and UA=51.6% which was lower than for optical images alone PA=95.7% and UA=70.4%. Considerably better performance

was observed for shallow angle (FQ20W) than for steeper angle (FQ8W): PA=89.9% and UA=61.4% against PA=41.5% and UA=26.7%. One reason that might contribute to the poor discrimination of this crop was that only 8 fields of sugar beets were available from ground survey.

*Sunflower:* The gains of adding SAR images to the optical ones were +6.6% and +25.9% for PA and UA, respectively. Moreover, SAR images alone provided better accuracies than optical images alone: PA=66.4% and UA=84.7% against PA=62.3% and UA=67.3%. All three polarizations and both steeper and shallow observation angles were important in providing the best performance of SAR images.

*Soybeans:* The gains of adding SAR images to the optical ones were +16.2% and +1.7% for PA and UA, respectively. The use of SAR images alone yielded PA=71.4% (+5.5% comparing to the optical images only) and UA=83.7% (-3.9%). Better performance was achieved for steeper observation angle (FQ8W). Among dual polarizations, higher accuracies were obtained for HH+HV polarizations than for VV+VH.

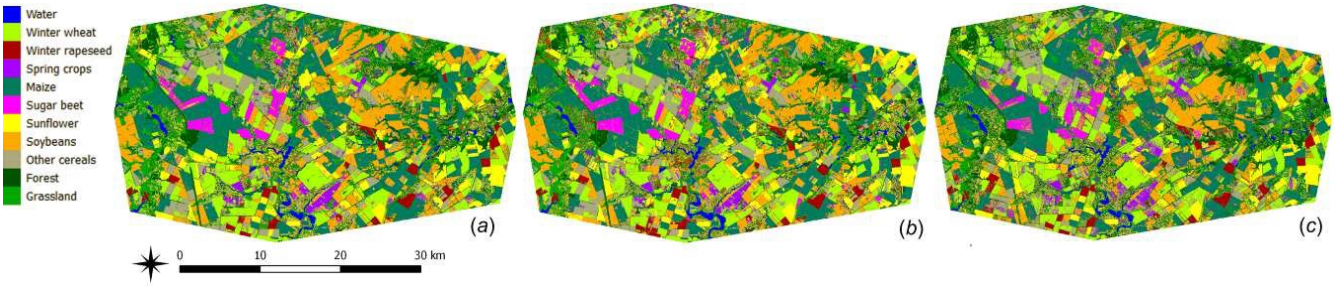


**Figure 180 Final Classification Maps (a) Using all Landsat-8 and RADARSAT-2 Data (b) Landsat-8 Images Only (c) RADARSAT-2 Images Only**

Retrieval of Biophysical Parameters

Relationships between satellite derived NDVI values and ground measurements of biophysical parameters are built using linear and exponential models and the best model (in terms of RC) is selected. It should also be noted that for all cases, the models are significant (F-statistics are greater than critical values), and NDVI parameters are statistically significant, which is confirmed by the p-value. Scatter-plots between ground observations and estimates using EO-based NDVI show good correlation for LAI, FAPAR and FCOVER with points distributed along the 1:1 line (up to R2=0.92). However, for the first campaign in 2013, the NDVI-based estimates present less variability than the ground observations.

The following criteria are used to compare biophysical parameters derived from different satellite images: root mean square error (RMSE), mean absolute error (MAE), and mean and standard deviation of biophysical parameters. These values are computed for the 3 km x 3 km

Pshenichne site. The obtained results show that there is a good correspondence between biophysical parameters derived from different satellites (Landsat-8, SPOT-4, RapidEye, SPOT-5). When comparing different biophysical maps, the average R2 is 0.54; average RMSE for LAI is 0.6; average RMSE for FAPAR is 0.14; and average RMSE for FCOVER is 0.12. Therefore, it indicates that biophysical maps from different satellites at different spatial resolution can be mutually used for continuous monitoring of crop state.

| | | *First campaign* | | *Second campaign* | | *Third campaign* | |
|---|---|---|---|---|---|---|---|
| | | *Mean* | *STD* | *Mean* | *STD* | *Mean* | *STD* |
| Landsat-8 | LAIeff | 0.398 | 0.387 | 1.227 | 0.424 | 2.236 | 0.671 |
| SPOT-4 | LAIeff | 0.486 | 0.340 | 1.200 | 0.394 | | |
| SPOT-5 * | LAIeff | 0.482 | 0.595 | 1.418 | 0.508 | | |
| RapidEye | LAIeff | 0.506 | 0.413 | 1.223 | 0.443 | | |
| Landsat-8 | LAI | 0.513 | 0.565 | 1.724 | 0.569 | 3.296 | 0.847 |
| SPOT-4 | LAI | 0.592 | 0.432 | 1.695 | 0.534 | | |
| SPOT-5 * | LAI | 0.670 | 0.876 | 2.142 | 0.856 | | |
| RapidEye | LAI | 0.879 | 0.895 | 1.729 | 0.608 | | |
| Landsat-8 | FAPAR | 0.237 | 0.154 | 0.562 | 0.132 | 0.782 | 0.110 |
| SPOT-4 | FAPAR | 0.347 | 0.239 | 0.557 | 0.127 | | |
| SPOT-5 * | FAPAR | 0.288 | 0.239 | 0.592 | 0.144 | | |
| RapidEye | FAPAR | 0.321 | 0.228 | 0.562 | 0.145 | | |
| Landsat-8 | FCOVER | 0.188 | 0.111 | 0.422 | 0.060 | 0.627 | 0.107 |
| SPOT-4 | FCOVER | 0.295 | 0.205 | 0.417 | 0.052 | | |
| SPOT-5 * | FCOVER | 0.232 | 0.220 | 0.449 | 0.089 | | |
| RapidEye | FCOVER | 0.269 | 0.195 | 0.419 | 0.061 | | |

**Table 30 Comparison of Biophysical Parameters derived from Different Remote Sensing Sensors (2013)**

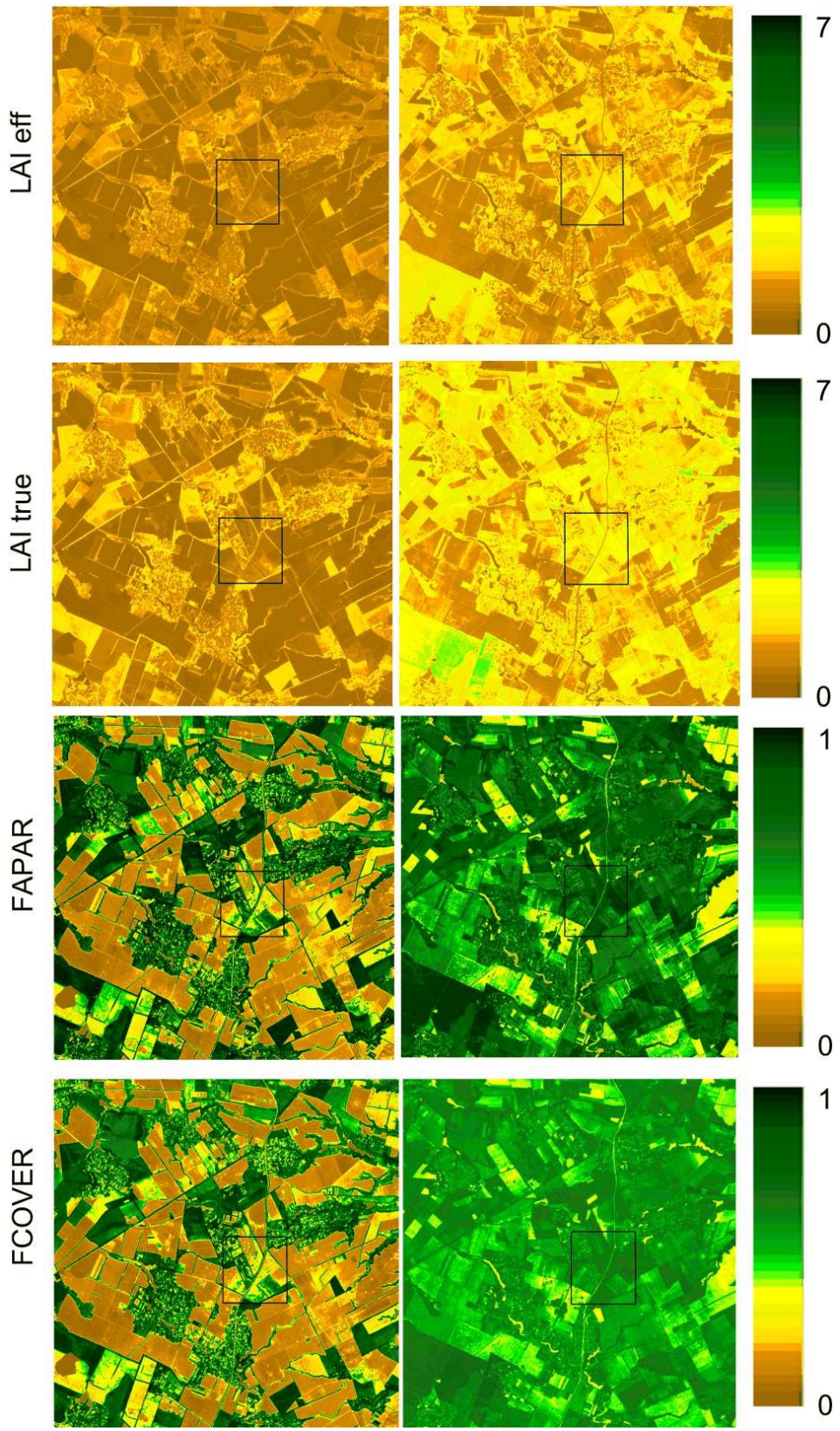


**Figure 181 Biophysical Maps of the Pshenichne Site using SPOT-4 Images (L) First campaign May 2013 (R) Second Campaign June 2013**

**Winter wheat yield forecasting**

In 2014, different biophysical parameters were explored as predictors in empirical-based regression models. It was found that VHI and FAPAR values taken in April–May provided the minimum error value when comparing to the official statistics, thus enabling forecasts 2-3 months prior to harvest. This corresponds to the results derived from the cross-validation (LOOCV) procedure for the NDVI, VHI and FAPAR time series.

The best timing for making reliable yield forecasts is nearly the same as it was for the NDVI-based approach (±16 days) – for most of the crop-production regions of Ukraine.

The most accurate predictions for 2011 were achieved using the VHI-based approach with the RMSE value of 0.51 t $ha^{-1}$ (performance of FAPAR- and NDVI-based approaches was 0.52 t $ha^{-1}$ and 0.63 t $ha^{-1}$). At the same time, the most accurate predictions for 2012 and 2013 were achieved using the FAPAR-based approach with the RMSE value of 0.56 t $ha^{-1}$ (performance of VHI-based and NDVI-based approaches were 0.7 t $ha^{-1}$ and 0.68 t $ha^{-1}$, respectively) for 2012 and 0.41 t $ha^{-1}$ (performance of VHI-based and NDVI-based approaches were 0.59 t $ha^{-1}$ and 0.58 t $ha^{-1}$, respectively) for 2013. These results are summarized in Table 31.

| | | 2010 | 2011 | 2012 | 2013 |
|---|---|---|---|---|---|
| **NDVI** | **rmse, t $ha^{-1}$** | 0.82 | 0.62 | 0.68 | 0.58 |
| | **mean, t $ha^{-1}$** | 0.68 | -0.37 | -0.34 | -0.2 |
| **VHI** | **rmse, t $ha^{-1}$** | 0.63 | 0.51 | 0.70 | 0.59 |
| | **mean, t $ha^{-1}$** | 0.55 | -0.38 | -0.36 | -0.21 |
| **FAPAR** | **rmse, t $ha^{-1}$** | 0.89 | 0.52 | 0.56 | 0.41 |
| | **mean, t $ha^{-1}$** | 0.76 | -0.21 | -0.05 | -0.08 |

**Table 31 Efficiency Estimation of Different Satellite Data Usage for Winter Wheat Yield Forecasting in Ukraine**

Therefore, we can conclude that performance of empirical regression models based on satellite data with biophysical variables (such as VHI and FAPAR) is approximately 20% (from 16% to 23% on different data sources) more accurate (on datasets available at the moment) compared to the NDVI approach when producing winter wheat yield forecasts at oblast level in Ukraine 2–3 months prior to harvest. The consistency of selection of informational features for modeling

was checked by independent methods and got nearly the same result for the time series of parameters that was used.

**To what extent have the project objectives been met?**

In 2014, all project objectives have been met. Crop maps were produced based on Landsat-8 (a continuation from 2013) and new images from Proba-V. Proba-V provides very good performance in terms of coverage and spatial resolution for the Ukrainian landscape. A new set of features, namely biophysical parameters FAPAR and VHI, was explored and compared to the established NDVI approach and showed promising results and better performance.

**Can this approach be called 'best practice'?**

We think that both approaches on crop mapping and winter wheat forecasting could be considered as best practices. For dealing with missing data due to clouds and shadows in Proba-V images, we applied the same approach as for Landsat-8 images. The crop yield forecasting methodology was extended for biophysical parameters as features that represent more adequate and better approach then NDVI-based.

Plans for Next Growing Season

Next year, we plan to continue the same approach, and order the same type/quantity of EO data. In addition, we plan to acquire more RADARSAT-2 data, and continue the Take5 initiative.

Publications

1. Gallego F.J., Kussul N., Skakun S., Kravchenko O., Shelestov A., and Kussul O., (2014) "Efficiency assessment of using satellite data for crop area estimation in Ukraine", *International Journal of Applied Earth Observation and Geoinformation*, Vol. 29, pp. 22–30. (http://dx.doi.org/10.1016/j.jag.2013.12.013)
2. Kussul, N.; Skakun, S.; Shelestov, A.; Kussul, O., "The use of satellite SAR imagery to crop classification in Ukraine within JECAM project," *2014 IEEE International Geoscience and Remote Sensing Symposium (IGARSS)*, pp.1497-1500, 13-18 July 2014. doi: 10.1109/IGARSS.2014.6946721
3. Kussul, N.; Kolotii, A.; Skakun, S.; Shelestov, A.; Kussul, O.; Oliynuk, T., "Efficiency estimation of different satellite data usage for winter wheat yield forecasting in Ukraine," *2014 IEEE International Geoscience and Remote Sensing Symposium (IGARSS),* pp. 5080-5082, 13-18 July 2014. doi: 10.1109/IGARSS.2014.6947639.

Presentations:

1. Shelestov, “JECAM test site in Ukraine”, *S2 Agri 1st User Workshop*, 19 May 2014, Rome, Italy.

2. N. Kussul, “Efficiency estimation of different satellite data usage for winter wheat yield forecasting in Ukraine”, *IGARSS 2014*, 13-18 July 2014, Quebec City, Canada. 
3. N. Kussul, “The Use of Satellite SAR Imagery to Crop Classification in Ukraine within JECAM Project”, *IGARSS 2014*, 13-18 July 2014, Quebec City, Canada. 
4. N. Kussul, “JECAM Site Ukraine”, *JECAM/GEOGLAM Science Meeting, 21 – 23 July 2014*, Ottawa, Canada. 
5. N. Kussul, “Restoration of Missing Data due to Clouds on Optical Satellite Imagery Using Neural Networks”, *Sentinel-2 for Science Workshop*, May 22, 2014, ESA/ESRIN, Frascati, Italy. 
6. N. Kussul, “JECAM Site Ukraine: Agricultural Issues and Remote Sensing Solutions”, *SIGMA workshop/training on Agricultural Productivity Assessment (WP4),* 15-24 September 2014, Wageningen, The Netherlands. 

# 25. Uruguay

No report received.

# 26. U.S.A.

## 26.1 Iowa

Team Leader and Members: Michael Cosh, USDA-ARS-HRSL, Joe Alfieri, USDA-ARS-HRSL, Martha Anderson, USDA-ARS-HRSL, Craig Daughtry, USDA-ARS-HRSL, Bill Kustas, USDA-ARS-HRSL, John Prueger, USDA-ARS-NLAE, Ali Sadeghi, USDA-ARS-HRSL, Mark Tomer, USDA-ARS-NLAE

Project Objectives

The original project objectives for our site have not changed.

- Crop identification and Crop Area Estimation

  Crop area estimation was conducted via the USDA Farm Service Agency and National Agricultural Statistical Service programs for the South Fork. This is an operational product.

- Crop Condition/Stress

  As part of a remote sensing project, the evaporative stress index (ESI) is being computed on a 10 km resolution for the continental U.S. This is available from http://hrsl.arsusda.gov/drought/. This is operational.

- Soil Moisture

  Currently there are 20 stations collecting soil moisture and soil temperature data in the domain. http://hrsl.arsusda.gov/southfork/.

- Crop Residue, Tillage and Crop Cover Mapping

  Assessments of crop residue amount are in the process of being analyzed for publication on methodologies for estimation.

Site Description

- Location: South Fork, Iowa (Hardin and Hamilton Counties, Iowa, USA). See Figure 182.
- Topography: Flat
- Soils: Clay Loam
- Drainage class/irrigation: Poorly drained, installed drainage tiles, limited irrigation.
- Crop calendar: April/May Planting, September/October Harvest
- Field size: 800 m by 800 m
- Climate and weather: Temperate/Humid
- Agricultural methods used: Corn and Soybean, no-till and tilled.

EO Data Received/Used

AWIFS data was received for five dates in April to Sept 2014.

In situ Data

There are currently 20 in situ soil moisture stations collecting soil moisture, soil temperature and precipitation data in the South Fork Region, shown in Figure 182. Fifteen USDA stations are labelled SF01-SF15. NASA operated stations are labelled NA01-NA05. In addition, during the spring and fall, in situ crop residue studies were conducted to estimate residue amounts via field measures and roadside surveys. A collection of validation data points were collected during the summer of 2014 which will help to calibrate the in situ network for satellite comparisons.

Collaboration

Mr. Sujay Dutta of IRS has received data on land cover type for the past 10 years for comparison to AWIFS data per the agreement with JECAM.

Results

The majority of the work in this domain is research in progress with no substantial conclusions yet. Data collection and infrastructure improvement are the primary tasks.

Plans for Next Growing Season

We will continue to measure crop residue and will be performing soil moisture validation on the newly installed network.

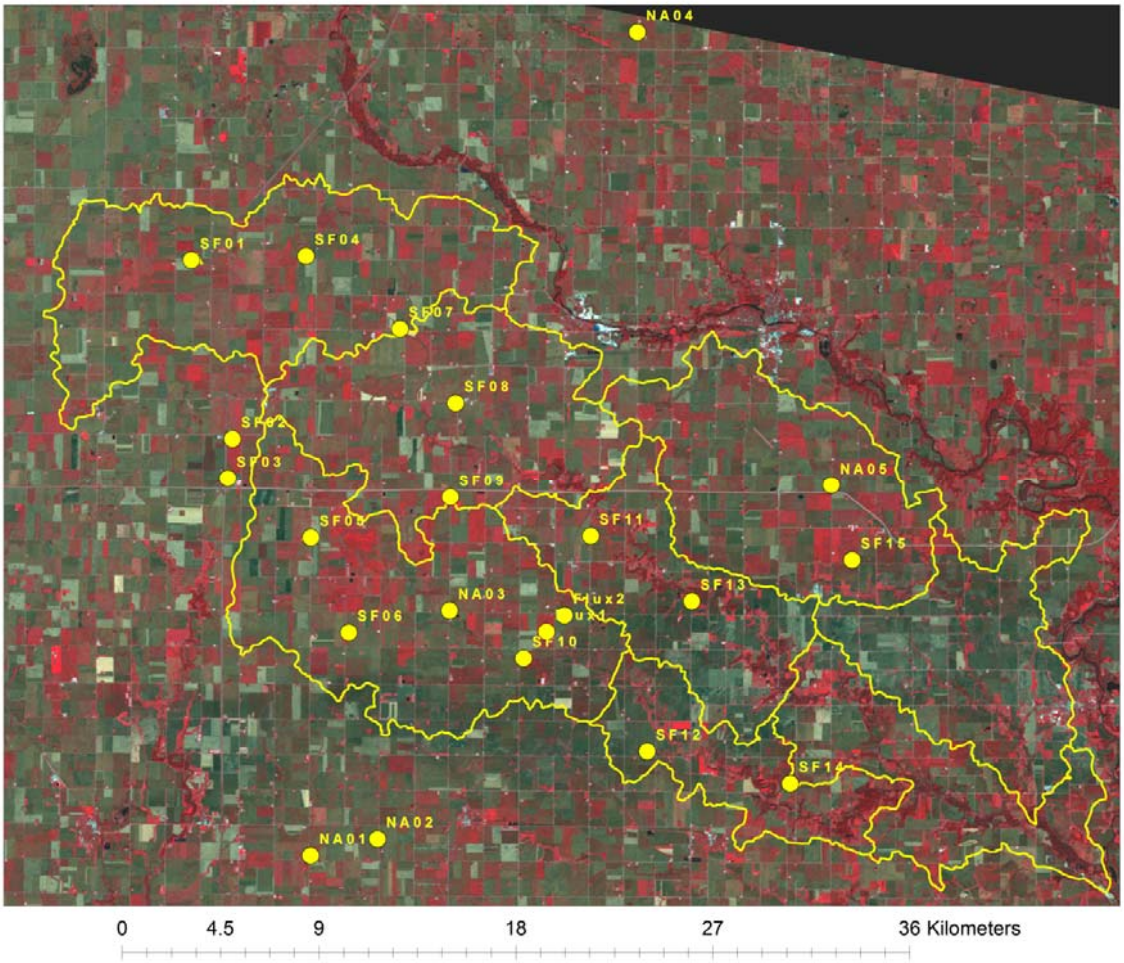


**Figure 182 Plot of the Network at South Fork**

**Figure 183 Example of a Network Site, Next to a Corn Field**

Publications

Rondinelli, W. J., Hornbuckle, B., Patton, J. C., Cosh, M.H., Walker, V. A., Carr, B. D., Logsdon, S. D. 2014. Different rates of soil drying after rainfall are observed by the SMOS satellite and the South Fork In Situ Soil Moisture Network, Journal of Hydrometeorology, in press.

Coopersmith, E., Cosh, M.H., Petersen, Walter, Prueger, J.H., Niemeier, James J. 2014. Multi-Scale Soil Moisture Model Calibration and Validation: An ARS Watershed On the South Fork of the Iowa River Journal of Hydrometeorology, in press.

## 26.2 Oklahoma

No report received.